Isolation and Characterisation of Bacterial Exopolysaccharides Produced by *Lactobacillus delbrueckii* subsp. *bulgaricus* NCFB 2483 and *Sphingomonas elodea* ATCC 31461

Massey University

A thesis presented in partial fulfilment of the requirements for the degree of

Doctor of Philosophy

in

Food Technology

at Massey University, Palmerston North,

New Zealand.

Kelvin Kim Tha Goh

2004

Massey University
COLLEGE OF SCIENCES

INSTITUTE OF FOOD, NUTRITION
AND HUMAN HEALTH
Te Kura Hangarau o
Kai-oranga-ā-tāngata
Private Bag 11 222
Palmerston North
New Zealand
T 64 6 350 4336
F 64 6 350 5657
www.massey.ac.nz

CERTIFICATE OF REGULATORY COMPLIANCE

This is to certify that the research carried out in the Doctoral Thesis entitled

Isolation and Characterisation of Bacterial Exopolysaccharides Produced by *Lactobacillus delbrueckii* subsp. *bulgaricus* NCFB 2483 and *Sphingomonas elodea* ATCC 31461
in the Institute of Food, Nutrition and Human Health at Massey University, New Zealand:

(a) is the original work of the candidate, except as indicated by appropriate attribution in the text and/or in the acknowledgements;

(b) that the text, excluding appendices/annexes, does not exceed 100,000 words;

(c) all the ethical requirements applicable to this study have been complied with as required by Massey University, other organisations and/or committees N.A which had a particular association with this study, and relevant legislation.

Please insert Ethical Authorisation code(s) here: (if applicable) _____

Candidate's Name:
Kelvin Kim Tha Goh

Signature: Goh

Date: 30 July 2004

Supervisor's Name:
Professor Harjinder Singh

Signature: Harjinder Singh

Date: 30 July 2004

Massey University
COLLEGE OF SCIENCES

INSTITUTE OF FOOD, NUTRITION
AND HUMAN HEALTH
Te Kura Hangarau o
Kai-oranga-ā-tāngata
Private Bag 11 222
Palmerston North
New Zealand
T 64 6 350 4336
F 64 6 350 5657
www.massey.ac.nz

SUPERVISOR'S DECLARATION

This is to certify that the research carried out for the Doctoral thesis entitled "Isolation and Characterisation of Bacterial Exopolysaccharides Produced by *Lactobacillus delbrueckii* subsp. *bulgaricus* NCFB 2483 and *Sphingomonas elodea* ATCC 31461" was done by Kelvin Kim Tha Goh in the Institute of Food, Nutrition and Human Health, Massey University, Palmerston North, New Zealand. The thesis material has not been used in part or in whole for any other qualification, and I confirm that the candidate has pursued the course of study in accordance with the requirements of the Massey University regulations.

Supervisor's Name

Professor Harjinder Singh

Signature

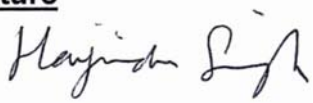

Date

30 July 2004

Massey University
COLLEGE OF SCIENCES

INSTITUTE OF FOOD, NUTRITION
AND HUMAN HEALTH
Te Kura Hangarau o
Kai-oranga-ā-tāngata
Private Bag 11 222
Palmerston North
New Zealand
T 64 6 350 4336
F 64 6 350 5657
www.massey.ac.nz

CANDIDATE'S DECLARATION

This is to certify that the research carried out for my Doctoral thesis entitled "Isolation and Characterisation of Bacterial Exopolysaccharides Produced by *Lactobacillus delbrueckii* subsp. *bulgaricus* NCFB 2483 and *Sphingomonas elodea* ATCC 31461" in the Institute of Food, Nutrition and Human Health, Massey University, Turitea campus, Palmerston North, New Zealand is my own work and that the thesis material has not been used in part or in whole for any other qualification.

Candidate's Name

Kelvin Kim Tha Goh

Signature

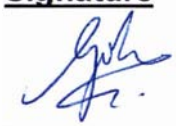

Date

30 July 2004

ABSTRACT

The aim of this study was to explore the characteristics of a non-gelling exopolysaccharide (EPS) obtained from *Lactobacillus delbrueckii* subsp. *bulgaricus* NCFB 2483 and a gelling EPS obtained from *Sphingomonas elodea* ATCC 31461 (31461). The EPSs were isolated from the two bacterial strains grown in milk permeate-based media. They were purified and then characterised using light scattering and viscometric techniques. A greater emphasis of this research was placed on 2483 EPS since its physical characteristics have not been reported to date. In the case of 31461 EPS, a model for gelation of the sodium gellan was proposed based on rheological and light scattering measurements. The rheological properties of the two EPSs were also compared with several commercial polysaccharides.

Microscopy examination of 2483 EPS was carried out using confocal laser scanning microscopy (CLSM) and scanning electron microscopy (SEM). In CLSM, the lectin SBA (from *Glycine max*) Alexa Fluor 488 conjugate was used to stain the EPS since it has affinity for galactopyranosyl residues present in 2483 EPS. The CLSM micrographs showed a random distribution of EPS aggregates in the culture medium. At high magnification, the SEM micrographs showed web-like EPS structures. These structures were formed during the critical point drying process, when the EPS, which filled the interstices and channels of the protein aggregates, dehydrated. The 2483 EPS aggregates were found to be stable at neutral or low pH (~3.9) but were disrupted at high pH (pH 8-10).

Procedures commonly used to quantify EPS from culture medium were found to be unreliable. In the development of an improved EPS assay, each of the processing steps was examined. Key improvements included the use of Flavourzyme for protein hydrolysis; optimising ethanol concentration to prevent lactose crystallisation yet allowing complete EPS precipitation; and a suitable centrifugation regime to minimise EPS loss. The improved EPS assay gave reproducible results (5% coefficient of variation).

The isolation of 2483 EPS from milk media proved to be a difficult task because of interference from non-EPS components. An effective and simple approach allowing maximum EPS recovery involved the use of a hydrolysed milk medium which was ultrafiltered (UF) to remove molecular species larger than 2.5 x 10^5 Da. The UF permeate was suitable for the growth of 2483 with an EPS yield of ~400mg/L. Two EPS fractions (namely a soluble and an insoluble fraction) were isolated by ethanol precipitation and the soluble 'ropy' fraction was further purified to achieve ~98% purity. The elemental analysis of the purified fraction revealed the presence of nitrogen (~2.7% w/w). This could be due to the interaction of some peptides (from the growth medium) with the EPS. The polysaccharide composition of the soluble EPS fraction comprised of galactose, glucose, rhamnose and mannose residues (5:1:0.6:0.5). Traces of glucosamine were also found in the fraction.

The purified fraction of 2483 EPS was characterised. Using a capillary viscometer, an intrinsic viscosity of ~2013mL/g was determined. The flow curves of the 2483 EPS solutions obtained using a rotational viscometer showed shear-thinning behaviour and an exponent value of ~0.76 (based on the Cross-type model) is typical of random coil polymers. The concentration dependence of the viscosity plot produced gradients of ~1.1 in the dilute domain and ~3.3 in the semi-dilute to concentrated domain. The coil overlap parameters at three concentration domains ($c^*[\eta], c_{cr}[\eta]$ and $c^{**}[\eta]$) were 0.55, 2.86 and 5.67 respectively. The molecular parameters of the 2483 EPS were found via static light scattering measurements to have a weight-average molar mass (M_w) of ~2 x 10^6 Da, a z-average root-mean-square radius ($\left(r_g^2\right)_z^{1/2}$) of ~165nm and a low polydispersity index (M_w/M_n ~1.15). The plot of M_w versus $\left(r_g^2\right)_z^{1/2}$ gave a gradient of approximately 0.5, which also suggested that the EPS polymer adopted a random coil conformation.

The second part of the research involved gellan gum. Two gellan samples were studied. The first gellan sample was obtained from the fermentation of *Sphingomonas elodea* ATCC 31461 using milk permeate-based medium (31461). The second sample was a commercial high acyl gellan (LT100). Both gellan samples were converted to their

sodium forms (Na-31461 and Na-LT100 gellan) using cation exchange resin and purified. The Na-gellan samples were highly sensitive to changes in Na^+ concentrations. From oscillatory measurements, it was found that the complex moduli of the two Na-gellan samples superimposed closely at a specific Na^+ concentration. The model for the conformational changes of Na-gellan molecules from a solution to a gel was proposed based on rheological and light scattering data. At very low Na^+ concentrations (<19mM, in the case of Na-LT100), Na-gellan molecules were single-stranded (M_w ~2.5 x 10^5 Da) and adopted random coil conformation (exponent value based on the Cross-type model of ~0.76). At a slightly higher Na^+ concentration (~19-24mM), Na-gellan molecules formed double-helices which led to a two-fold increase in molecular weight (M_w ~5.2 x 10^5 Da). The double-stranded molecule appeared to be stiffer (exponent value of the Cross-type model ~0.82) and the mechanical spectra (G', G'') demonstrated 'weak gel' characteristics. A further increase in the Na^+ concentration (>24mM) resulted in the formation of a gel network. The study also found that at low Na^+ concentration, both single-stranded and double-stranded Na-gellan molecules had a tendency to form aggregates under zero-shear conditions. The interactions involved in these aggregates were considered weak and transient, according to the Cox-Merz plot and light scattering data.

ACKNOWLEDGEMENTS

I would like to express my sincere gratitude to my chief supervisor, Professor Harjinder Singh for providing excellent guidance, invaluable advice, support and encouragement throughout the course of my study. I would also like to express my appreciation to Dr Derek Haisman, who with his wealth of knowledge, zest, availability and friendliness, has served as a remarkable co-supervisor. In addition, I wish to acknowledge Assoc. Professor Ian Maddox of the Institute of Technology and Engineering for providing valuable co-supervision and encouragement throughout the period of my research. My gratitude also extends to Professor Richard Archer, formerly of Fonterra Co-operative Group Limited, who never ceased to provide stimulating suggestions during our fortnightly meetings. I would also like to acknowledge Dr Vaughn Crow of Fonterra Co-operative Group Limited for helpful suggestions during the fortnightly meetings.

I am grateful to Massey University for the opportunity to pursue my doctoral study part-time while employed as a lecturer at the Institute of Food, Nutrition and Human Health. I would like to acknowledge the funding for the research from Fonterra Co-operative Group Limited and the New Zealand Foundation for Science and Technology through the Technology for Business Growth programme.

I would like to thank Dr Stephen Podzimek, Dr Adeline Lodder and Dr Michelle Chen of Wyatt Technology, USA, for their helpful suggestions in the use of the DAWN DSP via e-mail correspondence. A colleague and a friend who deserves special mention is Dr Yacine Hemar. His helpful advice in the area of rheological measurements is deeply appreciated.

Many wonderful people have assisted me in different ways with the research and completion of my doctoral thesis, and for whom I am indebted to: Ms Suzanne Bassett, Ms Michelle Curry, Mr Debjit Dey, Mr Steven Wang for providing technical help even beyond working hours; Mr Gary Radford for assisting in the operation of the UF plant and for being ever so willing to help in any way needed; Mr Byron McKillop for constructing any apparatus or tools needed for my experiments; Ms Michelle Tamehana for her patience and help with the light scattering experiments; Mr Doug Hopcroft and

Mr Raymond Bennett for assisting with processing of samples for electron microscopy; Dr Paul McJarrow for helping with the analysis of sugar composition with the Dionix; Ms Elizabeth Nickless for providing training in the operation of the confocal laser scanning microscope; Mr Peter Jeffery and Mr Bryden Zaloum who provided competent computer and software support; Ms Christine Ramsey, Ms Kathryn Tulitt, Ms Karen Pickering and Ms Yvonne Parkes for giving efficient and friendly administrative support. Mr Warwick Johnson, Mr Chris Hall, Mr Steve Glasgow, Ms Ann-Marie Jackson, Ms Felicity Jackson, Mr Michael Sahayam; Mr John Edwards; Mr Jon Palmer, Mr John Sykes and Mr Mike Stevens, all of whom have assisted me in so many ways which I deeply appreciate.

I would like to thank Mr Wong Shee Way, Mr Tang Mun Hay, Mr Jeffrey Heng, Mr Samuel Aw, Dr Ye Aiqian, Dr Rogerio Periera, Lydia Pedley, Cliff and Mary Foote for their friendship, humour and encouragements. These are only a few names, since I cannot adequately acknowledge all of the people to whom I am indebted. I hope the rest will know who they are and that I thank them very much.

Finally, I wish to acknowledge my family: mum, dad, sisters, brothers, in-laws, nephews and nieces for their prayers, love and concern.

Last, but not least, my special gratitude to my wife, Sang Mui for her love, companionship, understanding, patience and unceasing prayers. Without her support and encouragements, this thesis would not have been completed.

Above all, praise and glory to my Lord Jesus Christ, whose grace and faithfulness endure forever.

TABLE OF CONTENTS

ABSTRACT I

ACKNOWLEDGEMENTS IV

TABLE OF CONTENTS VI

CHAPTER 1 1

INTRODUCTION 1

CHAPTER 2 4

LITERATURE REVIEW 4

2.1 INTRODUCTION 4
2.2 POLYSACCHARIDES FOR FOOD APPLICATIONS 4
2.2.1 Bacterial exopolysaccharides 5
2.2.2 Exopolysaccharides from lactic acid bacteria 6
2.3 MICROSCOPY OF EPS 8
2.3.1 Transmission electron microscopy (TEM) 9
2.3.2 Scanning electron microscopy (SEM) 11
2.3.3 Confocal laser scanning microscopy (CLSM) 12
2.4 ISOLATION, PURIFICATION AND QUANTIFICATION OF EPS 14
2.5 CHARACTERISATION OF POLYSACCHARIDES 16
2.5.1 Viscosity 16
2.5.2 Intrinsic viscosity 16
2.5.3 From dilute to concentrated regime 27
2.5.4 Shear rate dependence of viscosity 31
2.5.5 Polysaccharide gels 37
2.5.6 Relationships between steady-shear and oscillatory measurements 48
2.5.7 Static light scattering 49

CHAPTER 3 63

OBSERVATION OF EXOPOLYSACCHARIDES IN CULTURE MEDIA BY CONFOCAL LASER-SCANNING AND SCANNING ELECTRON MICROSCOPIC TECHNIQUES 63

3.1 INTRODUCTION 63
3.2 MATERIALS AND METHODS 64
3.2.1 Culture media preparation 64
3.2.2 Sample preparation for confocal laser-scanning microscopy 65
3.2.3 Sample preparation for scanning electron microscopy 65
3.3 RESULTS AND DISCUSSION 67
3.3.1 Probing EPS by CLSM 67
3.3.2 Probing EPS by SEM 70
3.3.3 Effect of pH on EPS 76
3.4 CONCLUSIONS 80

CHAPTER 4 ..... **81**

DEVELOPMENT OF AN IMPROVED ASSAY FOR QUANTIFICATION OF EXOPOLYSACCHARIDES IN MILK-BASED MEDIA **81**

4.1 INTRODUCTION 81
4.2 MATERIALS AND METHODS 83
4.2.1 Fermentation of 2483 culture 83
4.2.2 Enzymes used for protein hydrolysis 83
4.2.3 Quantification of total carbohydrates 84
4.2.4 Standard curves for glucose and dextran 84
4.3 METHODOLOGY DEVELOPMENT: STAGE 1 85
4.3.1 Evaluation of existing methods for EPS determination 85
4.4 METHODOLOGY DEVELOPMENT: STAGE 2 89
4.4.1 Evaluation of EPS recovery based on added dextran 89
4.4.2 Evaluation of different enzymes for EPS recovery 94
4.4.3 Evaluation of Flavourzyme on bacterial cell integrity 96
4.5 METHODOLOGY DEVELOPMENT: STAGE 3 97
4.5.1 Recovery of EPS from media containing different percentages of RSM 97
4.5.2 Validation of the revised EPS assay 99
4.6 CONCLUSIONS 102

CHAPTER 5 ..... **103**

ISOLATION OF EXOPOLYSACCHARIDES PRODUCED BY *LACTOBACILLUS DELBRUECKII* SUBSP. *BULGARICUS* GROWN IN MILK PERMEATE-BASED MEDIUM **103**

5.1 INTRODUCTION 103
5.2 MATERIALS AND METHODS 105
5.2.1 Fermentation of 2483 culture in milk permeate-based medium 105
5.2.2 The hydrolysed milk permeate-based medium 105
5.2.3 Determination of EPS composition 106
5.3 RESULTS AND DISCUSSION 107
5.3.1 Isolation of EPS from milk permeate-based culture medium 107
5.3.2 The hydrolysed milk permeate-based culture medium 111
5.3.3 Purity of EPS 117
5.3.4 Composition of 2483 EPS 119
5.4 CONCLUSIONS 123

CHAPTER 6 ..... **124**

LIGHT SCATTERING AND VISCOMETRIC STUDIES OF PURIFIED 2483 EXOPOLYSACCHARIDES **124**

6.1 INTRODUCTION 124
6.2 MATERIALS AND METHODS 126
6.2.1 Sample preparation for static light scattering experiments 126
6.2.2 Viscometric studies of 2483 EPS 129
6.3 RESULTS AND DISCUSSION 132
6.3.1 Light scattering studies on 2483 EPS 132
6.3.2 Viscometric studies on 2483 EPS 137
6.4 CONCLUSIONS 154

CHAPTER 7 ..... **155**

ISOLATION AND CHARACTERISATION OF AN EXOPOLYSACCHARIDE PRODUCED BY *SPHINGOMONAS ELODEA* ATCC 31461 ..... **155**

7.1 INTRODUCTION 155
7.2 MATERIALS AND METHODS 157
7.2.1 Experimental samples 157
7.2.2 Fermentation, isolation and purification of 31461 gellan 157
7.2.3 Preparation of soluble gellan samples 157
7.2.4 Sample dilution and variation in ionic strength 158
7.2.5 Intrinsic viscosity determination 159
7.2.6 Steady shear and oscillatory measurements 159
7.2.7 Multi-angle Laser Light Scattering (MALLS) -batch and chromatography modes 160
7.3 RESULTS AND DISCUSSION 161
7.3.1 Commercial gellan gum (Kelcogel LT100) and 31461 gellan 161
7.3.2 Flow curves of Na-LT100, Na-31461 and xanthan solutions 162
7.3.3 Intrinsic viscosity 169
7.3.4 Concentration dependence of zero-shear viscosity 174
7.3.5 Analysis of sodium gellan molecules by static light scattering 177
7.3.6 Viscoelastic properties 188
7.3.7 Cox-Merz plot 195
7.3.8 Proposed model for the conformational changes of sodium gellan molecules 197
7.4 CONCLUSIONS 201

CHAPTER 8 ..... **203**

OVERALL CONCLUSIONS AND RECOMMENDATIONS **203**

8.1 OVERALL CONCLUSIONS 203
8.2 RECOMMENDATIONS 208

REFERENCES **211**

APPENDICES **233**

Chapter 1

INTRODUCTION

Polysaccharides possess unique physico-chemical characteristics which can be used to improve texture, quality and functionality in different food applications. Although many different polysaccharides from various sources have been isolated and applied in a wide range of food products over the last few decades, their functional properties may not be suitable in all food systems. This has sparked renewed interest in polysaccharides produced by microbial fermentation. The microbial fermentation avenue potentially creates opportunities for discovering novel polysaccharides with unique and useful functional properties. In the last decade, exopolysaccharides (EPSs) produced by lactic acid bacteria (LAB) have drawn the attention of food scientists not only for their physico-chemical properties but also because of their Generally Recognised as Safe (GRAS) status (Abbad-Andaloussi, Talbaoui, Marczak & Bonaly, 1995; Cerning, 1990, 1995; Racine, Dumont, Champagne & Morin, 1991). Hence, EPS produced by LAB can be regarded as a natural thickener. The EPS produced by LAB has been used directly *in situ* to achieve functional benefits, for example, it is used to reduce syneresis in yoghurt products. The EPS may potentially be isolated, purified and used as a functional ingredient in food systems. However, a major issue impeding commercialisation of EPS is the low yield (Cerning, 1995; Ricciardi et al., 2002). In spite of this, EPSs from LAB still present a huge potential for exploitation because of their heterogeneous macromolecular structures (Grobben, Sikkema, Smith & De Bont, 1995; van Geel-Schutten, Flesch, ten Brink, Smith & Dijkhuizen, 1998). The heterogeneity of polysaccharide structures has profound implication on the size and shape of the molecules in solution. It is the degree of space occupancy adopted by the molecule in solution, rather than the primary sequence structure, that has a major influence on the physico-chemical properties of the polysaccharide molecules. Knowledge of the conformation of polysaccharide molecules in solution and their molecular parameters is essential if their functional properties in food systems are to be well understood. (Cesaro, 1994).

To date, all reported EPSs produced by LAB are non-gelling. Polysaccharides which form gels are of equal importance in the food industry and have been used to modify and/or improve the sensory attributes of foods. At present, commercial gelling polysaccharides of bacterial origin which are GRAS-listed include only gellan gum, xanthan and curdlan. Gellan gum is an excellent gelling agent and is known to form a clear and strong gel. Research on gellan gum is relatively well-established since its discovery in the eighties (Kang, Veeder & Cottrell, 1983). However, its gelling mechanism and properties in different systems are still sustaining continual research interest.

In this research, a non-gelling polysaccharide from *Lactobacillus delbrueckii* subsp. *bulgaricus* NCFB 2483 and a gelling polysaccharide (gellan gum) from *Sphingomonas elodea* ATCC 31461 (31461) were produced by bench-scale fermentation using dairy-based media. A greater part of the research was focussed on the EPS produced by 2483 since it has not been characterised to date. In the case of the gelling EPS (gellan gum) produced by 31461, the present study investigated the physical characteristics of the EPS produced using a dairy-based medium. The laboratory-produced gellan was studied along with a commercial high-acyl gellan. The gelling mechanism of gellan in its sodium form was elucidated based on the results of the study.

Apart from the two laboratory-produced EPSs, commercial polysaccharides such as dextran, λ-carrageenan and xanthan were also examined and used for comparison. The objectives of the study were as follows:

- To examine the location and distribution of 2483 EPS in a dairy-based system using microscopy techniques (see Chapter 3).

- To develop a reliable EPS assay for quantifying EPS produced in dairy-based growth media (see Chapter 4).

- To determine the optimum conditions for 2483 EPS isolation and purification; and to ascertain the composition of the purified EPS (see Chapter 5).

- To characterise 2483 EPS using viscometric and light scattering measurements (see Chapter 6).

- To isolate and characterise sodium high acyl gellan obtained commercially and through batch fermentations using a milk permeate-based medium (see Chapter 7).

Chapter 2
LITERATURE REVIEW

2.1 Introduction

This chapter provides a comprehensive review of related studies mostly in the last 20 years up to 2004. Each section of the review was written to correspond with the subsequent chapters of the thesis. The first part of the review provides a general background on the development of polysaccharide as food ingredients. It also introduces bacterial exopolysaccharides (EPSs) as potential sources of polysaccharides with unique physico-chemical characteristics. This follows a short review on the use of different microscopy techniques and stains for EPS examinations. A brief section on EPS isolation and purification methods and the difficulties encountered by various researchers are also included. The major part of the review deals with the use of rheological techniques and various theoretical models for estimating the size, shape and conformation of polymer molecules in solution. Theory and interpretation of the viscoelastic properties of gels using small strain oscillatory measurement are discussed. In addition, a comprehensive theory on static light scattering technique and the use of various models to obtain molecular parameters such as molecular weight, root-mean-square (RMS) radius, polydispersity, etc are included in this chapter.

2.2 Polysaccharides for Food Applications

Polysaccharides are biopolymers consisting of repeat units of monosaccharide connected by glycosidic linkages. Polysaccharides have been used in the food industry as stabilisers, thickeners, gelling agents, emulsifiers and fat replacers. Some examples of the functions of polysaccharides in food formulations include the prevention of phase separation in emulsions; modification of food texture/mouthfeel; retardation of ice crystal formation in frozen foods and replacement of fats in reduced-calorie products. Food-grade polysaccharides are usually of plant, seaweed or microbial origin. Polysaccharides possess unique physico-chemical characteristics which make them suitable for use in different food applications to achieve the desired textural quality and

functionality. Some of the commercially available polysaccharides are shown in Table 2.1. In spite of the different types of polysaccharides which are available commercially, food scientists are continuing in their quest for new polysaccharides with novel and improved functional characteristics to meet the demands of the food industry and consumers.

Table 2.1 Examples of polysaccharides used in food formulations.

Source	Name
Plant (fruits, seeds, wood pulps)	Starch, Pectin, Guar Gum, Locust Bean Gum, Konjac Mannan, Gum Arabic, Carboxymethylcellulose, Microcrystalline Cellulose
Seaweed	Alginate, Carrageenan, Agar
Microbial	Xanthan, Gellan, Curdlan

2.2.1 Bacterial exopolysaccharides

The most efficient and practical means of obtaining polysaccharides with unique or improved functional characteristics can be achieved through microbial fermentation under controlled conditions. Polysaccharides that are secreted from microbial source are known as EPSs. The production of EPS is said to protect against adverse conditions such as osmotic stress, desiccation, phagocytosis, toxic compounds and bacteriophage infection (Cerning, 1995; Looijesteijn, Trapet, De Vries, Abee & Hugenholtz, 2001). However, others have suggested that the phage protection conferred by EPS may be very limited (Deveau and others 2002) and that obvious advantage of EPS to growth or survival of bacterial cells remains unclear (Broadbent and others 2003). To date, the exact functions of EPS for the bacterial cells have not been completely elucidated (Ruas-Madiedo and others 2002).

There are generally two broad groups of EPSs: homopolysaccharides and heteropolysaccharides. Homopolysaccharides contain only one type of monosaccharide, either glucose or fructose (Monsan et al., 2001). Some examples of bacterial homopolysaccharides include pullulan, levan, curdlan, dextran and cellulose. Heteropolysaccharides composed of a backbone of repeat subunits consisting more than one type of monosaccharide and may contain non-sugar organic/inorganic molecules.

The structures may be branched or linear (De Vuyst, De Vin, Vaningelgem & Degeest, 2001). Some examples of commercial bacterial heteropolysaccharides include xanthan and gellan.

Although many bacterial EPSs potentially exist, only a few have been commercialised (Sutherland, 2001). Once an EPS is recognised to possess useful functional properties and approved for use in foods, the economic benefits can become highly attractive. For example, xanthan gum, produced by the fermentation of *Xanthamonas campestris*, is now the most widely used bacterial gum in both food and non-food applications. However, commercialisation of microbial EPSs is often accompanied by a long and costly process of ensuring conformance to food safety to obtain approval from food legislators. In addition, low EPS yield, high recovery cost and sometimes inconsistent product quality can render the production process uneconomical. Xanthan gum was the first bacterial EPS to be approved by the Food and Drug Administration (FDA) for food use in the United States in 1969. This was followed by gellan gum, produced from the fermentation of *Sphingomonas elodea* (previously known as *Pseudomonas elodea*). Gellan gum obtained US FDA's approval in 1992, approximately fifteen years after it was first discovered. Gellan is marketed by Kelco as a broad spectrum gelling agent. In 1996, the US FDA approved curdlan produced by *Alcaligenes faecalis* var. *myxogenes*. While xanthan gum is used in a wide number of food applications and has been extensively studied, the applications of gellan and curdlan on the other hand, have not been fully explored in the food industry. Fundamental research into the gelling and viscoelastic behaviour of gellan has been an on-going area of interest among researchers in the last decade.

2.2.2 Exopolysaccharides from lactic acid bacteria

In most countries, labelling legislation requires that food products containing added polysaccharide such as xanthan or gellan or from other sources must be listed as a food additive. This generally does not appeal to consumers, who tend to view food additives negatively. In recent years, EPSs produced by lactic acid bacteria (LAB), *Bifidobacterium* and dairy *Propionibacterium* have drawn the attention of the food industry not only because of their viscous properties but also because of their GRAS

(Generally Recognised as Safe) status (Abbad-Andaloussi et al., 1995; Cerning, 1990, 1995; Racine et al., 1991). The EPSs from LAB may be isolated and used as a food ingredient like many commercial food hydrocolloids. Alternatively, EPSs may be produced *in situ*, in the food system to achieve the desired sensory attributes as well as functional characteristics. In some countries of the EU, where the addition of stabilisers is prohibited in yoghurt (De Vuyst & Degeest, 1999b), the 'ropy' LAB strains are used to improve/modify textural properties and to reduce syneresis (Cerning, 1995). Since LAB is naturally occurring, the inclusion of the bacterial cells and/or their by-products in food products can be considered "natural" (Ludbrook, Russell & Greig, 1997). Hence, the presence of LAB EPS in food formulations may not need to be labelled as an 'additive'.

Generally, the yield of EPS is low (typically below 500mg/L) (Cerning, 1995; Ricciardi et al., 2002). An exceptionally high EPS yield (~2350mg/L) has recently been reported (Bergmaier, Champagne, & Lacroix, 2003). The low EPS yield is probably one of the key issues impeding commercialisation. To be economically viable, the EPS production level has to be approximately 10-15g/L although a much smaller amount of EPS may be sufficient for *in situ* applications (De Vuyst & Degeest, 1999a). Many strategies have been considered to increase EPS yields. Some of these include varying medium compositions and fermentation conditions such as pH and temperature (Degeest et al., 2002; Vaningelgem, Zamfir, Adriany, & De Vuyst, 2004); chemical mutagenesis and selection (Welman, Maddox, & Archer, 2003); and the understanding at a cellular level the mechanism for EPS assembly (Broadbent et al., 2003).

Many of the EPSs produced by *lactobacilli* are heteropolysaccharides (Grobben et al., 1995; van den Berg et al., 1995; van Geel-Schutten et al., 1998) while few produced homopolysaccharides (Dunican & Seeley, 1965; Pidoux, Marshall, Zanoni & Brooker, 1990; van Geel-Schutten et al., 1998). The heteropolysaccharides produced by LAB are diverse in terms of sugar composition, each repeating subunit may consist of two (Lemoine et al., 1997) to eight (Low et al., 1998) monosaccharides. The molecular weights are typically > 1.0×10^6 Da (Cerning & Marshall, 1999), although a smaller molecular weight fraction of ~1.0×10^4 Da has been reported (Grobben et al., 1998). The EPS structures are highly variable among different strains (Cerning, 1990; Gruter,

Leeflang, Kuiper, Kamerling & Vliegenthart, 1993; Nakajima, Suzuki, Kaizu & Hirota, 1992; Stingele et al., 1999; Yamamoto, Murosaki, Yamauchi, Kato & Sone, 1994). This is because heteropolysaccharides generally have a great potential for structural variability (compared to proteins and nucleic acids) during synthesis. Variation in structures depends on monosaccharide composition, electronic charge density, type of glycosidic linkages, degree of branching, molecular weight and presence of substituted groups (Duboc & Mollet, 2001; Roberts, 1995). The heterogeneity of polysaccharide structure has profound implication on physical, biological and chemical properties, hence, providing vast opportunity for the food industry. This has brought about the search for new strains which are capable of producing EPSs with unique rheological properties (De Vuyst & Degeest, 1999b; van den Berg et al., 1993).

Interestingly, some EPSs have been reported to possess health promoting properties, for example, the modulation of the immune system (van Calsteren, Pau-Roblot, Begin & Roy, 2002), anticancer activities (Oda, Hasegawa, Komatsu, Kambe & Tsuchiya, 1983) and blood cholesterol lowering properties (Martensson et al., 2002; Nakajima, Suzuki, Kaizu, & Hirota, 1992). In addition, the viscous nature of EPS is said to improve colonisation of probiotic bacteria in the gastrointestinal tract (Duboc & Mollet, 2001). A concise review of the physiological functions of EPSs is given by (Ruas-Madiedo et al., 2002). Research in the area of polysaccharide bioactivity is currently in its infancy stage. It is envisaged that a range of EPSs from different species and strains of LAB will form a new generation of hydrocolloids (van Geel-Schutten et al., 1998) and/or potential functional food ingredients.

2.3 Microscopy of EPS

Three microscopy techniques, namely transmission electron microscopy (TEM), scanning electron microscopy (SEM) and confocal laser scanning microscopy (CLSM), which can potentially be used for the examination of EPS, are reviewed in the following sub-sections.

2.3.1 Transmission electron microscopy (TEM)

Microscopy work involved in the study of EPS produced by LAB in a fermented dairy system has not been extensive so far. One of the closely related fields that has been explored is the study of the microstructure of yogurt samples using conventional EM (Kalab & Harwalkar, 1973; Schellhaass & Morris, 1985). Transmission electron microscopy and SEM have been techniques normally employed for these studies since they can operate at high magnification and produce high resolution images. However, methods of sample preparation for electron microscopy are laborious and the quality of the image produced is highly dependent on the processing method applied to the samples. With the study of such a delicate network structure as in the fermented milk system, processing of the samples must be carried out with much care that the network structure is retained with no artefacts produced during sample preparation.

Generally, processing of a fermented milk sample for TEM involves encapsulation using agar before the fixing process (Allan-Wojtas & Kalab, 1984b). This technique helps prevent disruption and dispersion of the protein matrix during the fixation steps. A glutaraldehyde solution is used as a primary fixative to crosslink proteins at concentrations ranging from 1.4-3.5% for 1 h to approximately a week. However, it has the tendency to disperse the fermented milk (Kalab, 1979) and has been reported to cause structural change of proteins and a resultant decrease in pH (Buchheim, 1982). In the secondary fixation step, osmium tetroxide (OsO_4) is used as a heavy-metal oxidative fixative to stabilise proteins and unsaturated lipids (Kalab, Allan-Wojtas & Miller, 1995). However, an excessive amount of osmium tetroxide (> 2%) has also been found to alter the structure of the casein micelles (Allan-Wojtas & Kalab, 1984a).

Investigation using electron microscopy becomes difficult when the intent of the study is to examine the location of polysaccharides amidst the complex network of the fermented milk system. This may be complemented by other techniques such as CLSM. Foods with high polysaccharide contents are difficult to fix chemically (Kalab et al., 1995). Polysaccharides in general are not electron dense and this makes it difficult to produce images with satisfactory contrast. The use of standard fixatives (e.g. lead and uranium salts) in TEM does not reveal polysaccharides (Brooker, 1979; Skriver, Buchheim & Qvist, 1995).

The use of ruthenium red in electron microscopy to study the ultra-structure of microorganisms was first introduced by Luft (1964, 1971). It was subsequently used extensively to improve the contrast of extracellular materials associated with the cell surfaces (Brooker, 1979). Ruthenium red is a cationic dye and it reacts with acidic polysaccharides (Luft, 1971). The empirical formula for ruthenium red is given as:

$$[Ru_3O_2(NH_3)_{14}]Cl_6.4H_2O$$

and the structural formula for ruthenium red cation has been proposed by Fletcher, Greenfield, Hardy, Scargill & Woodhead (1961) and verified by Smith & Pace (1982) as:

$$[(NH_3)_5\ Ru\text{-}O\text{-}Ru(NH_3)_4\text{-}O\text{-}Ru(NH_3)_5]^{6+}$$

The ability of ruthenium red to stain a neutral polysaccharide such as dextran is not fully understood. One possible explanation is the formation of ruthenium complexes with free hydroxyl, carboxyl or sulphate groups on the monosaccharide component of the polysaccharide (Brooker, 1979; Figueroa & Silverstein, 1989). In his work, Brooker (1976, 1979) published micrographs showing good contrast of the dextran capsular layer around the cell surfaces of *Leuconostoc mesenteroides* using ruthenium red. It was reported that this surface coat is two to five times thicker than the cell wall and has fine filamentous internal structures which are thicker than the cell wall depending on the strain. Similar fibril-like structures, approximately 16nm thick, have also been examined around surfaces of *Streptococcus salivarius* (Handley, Hargreaves & Harty, 1988). In addition, Overdahl & Zottola (1991) observed ruthenium red stained outer polysaccharide layer in several strains of *Lactobacillus acidophilus.*

An essential step in applying ruthenium red stain is the exposure of the specimen to osmium tetroxide in order to impart electron density (Luft, 1971) although Cagle (1975) has suggested that the exposure to ruthenium red before the fixation step further improves the staining of EPS.

2.3.2 Scanning electron microscopy (SEM)

Scanning electron microscopy has also been used to study the microstructure of yogurt. It has been found that the fermented milk system consists of a coarse network made up of casein particles linked together in clusters or chains (Schellhaass & Morris, 1985). In a 'ropy' culture medium, Toba, Nakajima, Tobitani & Adachi (1990) showed that EPS occurs in the form of a network attaching long chains of bacterial cells to the protein matrix. The network has many void spaces. These void spaces are presumed to be occupied by the serum phase (Kalab, Allan-Wojtas & Phipps-Todd, 1983), bacterial cells and the slime secreted from the cells (Toba et al., 1990).

The preparation of a yogurt sample for SEM is described by Schellhaass & Morris (1985). It involves preparing a template of cylindrical studs (diameter: 4mm and length: 10mm) glued to the inside of a petri-dish cover. A 3% agar solution is poured 13mm deep and the template of the cylindrical studs is immersed in the agar solution. The petri-dish cover with the studs is then removed when the agar has solidified. The fermented culture can then be pipetted into the cylindrical pores and subsequently overlaid with a 3% agar. After solidification, small cubes containing the sample can be cut out of the agar. The agar cubes are then fixed in 2.5% glutaraldehyde in cacodylate buffer (pH 7.2) followed by three 5 min rinses in diluted cacodylate buffer (cacodylate/water 1:1). Secondary fixation is carried out using 1% osmium tetroxide for 1 h and is followed by three rinses of cacodylate buffer. The fixed samples are subjected to dehydration using a series of increasing concentrations of acetone (25, 40, 60, 70, 90 for 10 min each and 3 changes of 100% for 20 min each). The final dehydration step uses a critical point dryer with CO_2 (Skriver et al., 1995).

In SEM, critical point drying is the most commonly used method for yogurt type material (Kalab & Harwalkar, 1973; Schellhaass & Morris, 1985). The advantage of critical point drying is that the specimen does not pass through any phase boundary. Although this drying technique is most suitable for proteins, with fats and carbohydrates, artefacts may be formed (Skriver et al., 1995). The dried samples are fractured to expose the internal microstructure and then sputtered with gold. Due to the porous structure of the fermented milk sample, they are extremely susceptible to damage by the electron beam and examination by SEM has to be done quickly (Kalab,

1981). This type of preparation has been able to differentiate between 'ropy' and 'non-ropy' cultures but it cannot identify the location of the polysaccharides in the protein network. Ota & Fukui (1982) used similar preparation techniques by fixing the specimen in agar but fixation was carried out in a 2% osmium tetroxide in buffer solution (pH 7.2) for 2 h instead. Scanning electron micrographs of colonies of *Streptococcus mutans* show a fibrillar network interconnecting the cells and some globular particles of EPS scattered over the cell surfaces. It has however been suggested that the image produced by this method possibly gives a distorted impression of the amount of polysaccharide present (Skriver et al., 1995). Other related techniques have been explored including TEM freeze-fracturing, TEM freeze-etching, scanning tunnelling microscopy and recently atomic force microscopy (Morris, et al., 1997). However, the certainty and integrity of the micrographs produced by these methods have never been absolutely clear and sample preparation methods are very tedious, sensitive and often risk introducing artefacts into the system.

2.3.3 Confocal laser scanning microscopy (CLSM)

One of the most powerful developments in microscopy is that of CLSM. This method of microscopy provides better resolution than conventional light microscopy or fluorescence microscopy. So far, CLSM has been used indirectly to study capsules of LAB cells. Capsules are indicated indirectly by clear zones, which separate the cells from the casein micelles (Hassan, Frank, Farmer, Schmidt & Shalabi, 1995a; Hassan, Frank, Farmer, Schmidt & Shalabi, 1995b). Currently, no workers in this field have yet used fluorescent dyes to directly stain EPS in a fermented milk system. The difficulty lies in the fact that unless specific sugar residues can be identified in the EPS structure, it is not possible to select a sugar-specific fluorescent stain. In addition, non-specific polysaccharide stains, though available commercially, are futile as non-EPS materials in the fermented milk system may be stained. The bacterial cell wall polysaccharides may also fluoresce and can be easily mistaken for EPS.

Polysaccharides can be distinguished using lectins conjugated with a fluorescent dye (Brooker, 1995; Yiu, 1993). Lectins are oligomeric proteins with saccharide-binding sites that can bind particular glycoconjugates. The lectin soybean agglutinin (SBA), which is isolated from *Glycine max*, selectively binds terminal α- and β-N-

acetylgalactosamine and galactopyranosyl residues. This lectin exists as a tetramer and has a molecular weight of approximately 1.2 x 10^5 Da (Haugland, 1996).

Lectins conjugated with Alexa Fluor 488 dye are versatile fluorescent stains and have been used to detect cell surface and intracellular glycoconjugates by microscopy and flow cytometry, localization of glycoproteins in gels, precipitation of glycoproteins in solutions and agglutination of specific cell types (Haugland, 1996). Alexa Fluor 488 dye has an absorption and fluorescence emission maxima of ~495nm and ~519 nm, respectively. In addition, Alexa Fluor is insensitive to pH ranging from pH 4 to 10 (Haugland, 1996). The EPS produced by *Lactobacillus delbrueckii* subsp *bulgaricus* RR was reported to be a heteropolymer of D-galactopyranosyl, D-glucopyranosyl and L-rhamnopyranosyl residues (Gruter et al., 1993). The structure is shown in Figure 2.1.

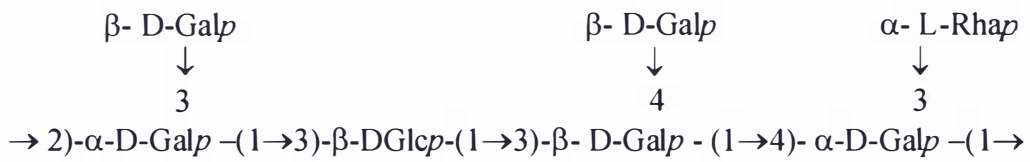

Figure 2.1 Structure of EPS produced by *Lactobacillus delbrueckii* subsp *bulgaricus* RR (Gruter et al., 1993)

The structural analysis of EPS produced by other LAB has been widely studied and most of the EPS produced are branched with repeating units of α- and β- linkages. Though one may differ from the other in overall structure, their monomeric composition was similar with D-galactose, D-glucose and D-rhamnose present in different ratios (Cerning, 1990; De Vuyst & Degeest, 1999a). Based on the best available information, it is appropriate to use lectin soybean agglutinin (SBA) conjugated with Alexa Fluor 488 to probe the location of EPS in the fermented culture. Identifying the location and distribution of EPS in a fermented culture medium will help in understanding the rheological properties of the system and in developing an effective EPS isolation and purification regime.

2.4 Isolation, Purification and Quantification of EPS

Many EPS isolation regimes are based on physical, chemical, enzymatic or a combination of the different methods. These methods usually have three main functions, namely, to disrupt EPS-EPS, EPS-proteins and EPS-cells interactions.

With the physical methods, shear is usually applied to separate EPS from bacterial cell surfaces as well as EPS that are physically entrapped by the medium components (usually proteins). Shaking, stirring or pumping the culture medium has also been used to generate shear. A high shear level may be provided by sonication under defined conditions. However, caution should be taken so that cell lyses do not occur as it may complicate purification procedures. Application of heat, for example, at 80°C to boiling temperature, for approximately 10-60 min, has also been used in several studies, sometimes combined with shear provided by shaking (Nielsen & Jahn, 1999). Centrifugation is usually employed to separate the soluble EPS fraction from cell biomass (Hebbar et al., 1992; Troch, Philip-Hollingworth, Orgambide, Dazzo & Vanderleyden, 1992). Separation of cell biomass is easy in a clear growth medium. However, in a complex medium containing aggregated proteins such as caseins, centrifugation will result in the removal of insoluble protein aggregates as well as cell biomass, and any EPS that are bound to them. Shear created by centrifugation may, only to a limited extent, separate bound EPS (Nielsen & Jahn, 1999). Another problem facing centrifugation is the high viscosity of the culture medium that hinders deposition of the cells (Cerning, 1990). For this, high speed centrifugation has been proposed as an effective method for EPS separation (Brown & Lester, 1980).

Many of the chemical methods rely on the disruption of the electrostatic interactions between EPS molecules, promoting an extraction of water-soluble compounds. Alkaline treatment using sodium hydroxide causes many charged groups, such as carboxylic groups in some polysaccharides, to be ionised because their isoelectric points are generally in the pH range of 4-6. The pH range reported in various studies using alkaline treatment varies from 9 to 13 (Nielsen & Jahn, 1999). This results in a strong repulsion between EPS molecules within the EPS network. Boiling and alkaline treatments have been reported to cause disruption of EPS molecules (Karapanagiotis,

Rudd, Sterritt & Lester, 1989). At pH values above 9, the covalent disulfide bonds in some EPS, for example, glycoproteins, are broken (Zayas, 1997) and the uronic acids are degraded (Haug, Larsen & Smidsrod, 1967). The result is a marked change in the structure of the macromolecules. Another approach to isolating EPS is to replace divalent cations with monovalent ions. The presence of divalent cations, mainly Ca^{2+} and Mg^{2+}, can promote EPS-EPS interactions, with the formation of EPS gel network. By removing these ions, the EPS matrix tends to fall apart. Divalent cations can be removed by using ion-exchange resins e.g. Dowex, or by using a complexing agent such as EDTA. "Dowex" used as a method appears to be a gentle method and does not cause disruption of EPS (Frolund, Palmgren, Keiding & Nielsen, 1996; Karapanagiotis et al., 1989). The use of EDTA, a chelating agent, on the other hand may affect cell wall integrity by removing divalent cations from the cell wall, leading to cell lysis with the release of intracellular components (Johnson & Perry, 1976).

In many protocols for EPS isolation, a step to remove protein from the sample is included. Trichloroacetic acid (TCA) or sulphosalicyclic acid are commonly used to precipitate proteins from the culture medium (Cerning, Bouillanne, Landon & Desmazeaud, 1992; Toba, Uemura & Itoh, 1992; van den Berg et al., 1995; Yang, Huttunen, Staaf, Widmalm & Tenhu, 1999). Besides the acid precipitation method, removal of intact proteins can be achieved by enzymatic hydrolysis using proteases (Abbad-Andaloussi et al., 1995; Cerning et al., 1992). The EPS in the aqueous solution are then isolated by ethanol precipitation (Ariga et al., 1992; Cerning et al., 1992; Urashima et al., 1999; van den Berg et al., 1995; Yang et al., 1999) or by ultrafiltration (Toba et al., 1992) or a combination of both (Abbad-Andaloussi et al., 1995; Tuinier, Zoon, Olieman et al., 1999).

Purification of the isolated EPS can be achieved by ethanol precipitation, diafiltration (Toba et al., 1992; Tuinier, Zoon, Olieman et al., 1999), dialysing against several changes of water (Yang et al., 1999) or by passing through an ion exchange column (Abbad-Andaloussi et al., 1995; Ariga et al., 1992; Cerning, 1990; Urashima et al., 1999). Besides the more conventional methods of recovering EPS, a pure fraction of the EPS can be obtained using a gel filtration column with suitable molecular weight

cut-off (Cerning, 1990; Ricciardi, Parente, Aquino & Clementi, 1998; van den Berg et al., 1995). Usually, the final stage of EPS recovery process is lyophilization, after which the EPS can be quantified or stored for further characterisation (Ariga et al., 1992; Cerning et al., 1992; Tuinier, Zoon, Olieman et al., 1999; van den Berg et al., 1995; Yang et al., 1999). Quantification of EPS subsequent to isolation and purification commonly employs the phenol-sulphuric acid method based on total carbohydrate determination (Dubois, Gilles, Hamilton, Rebers & Smith, 1956).

2.5 Characterisation of Polysaccharides

2.5.1 Viscosity

Most polysaccharides, used as thickeners, exist in solutions as disordered flexible chains (random coils). When the concentration of polysaccharide in a solution increases, the viscosity of the solution also increases. At least two concentration domains exist as the number of macromolecules is increased from the dilute to the concentrated regime. Interpretation of the concentration domains first requires an understanding of the degree of space occupancy by individual macromolecules at infinite dilution.

2.5.2 Intrinsic viscosity

At infinite dilution, chain-chain interactions are negligible. This is because individual macromolecules are far apart from each other and are free to move independently in the solution. The difference in the rheological properties among polysaccharide solutions are due to the difference in the conformations adopted by individual macromolecules in solutions. The conformation adopted by a macromolecule will have an effect on the hydrodynamic volume of the macromolecule. A fundamental parameter used to characterise the hydrodynamic volume occupied by an individual macromolecule in solution is the intrinsic viscosity $[\eta]$. The intrinsic viscosity is an inherent parameter of the polymer molecule in solution and is useful in predicting the thickening ability of various polysaccharides. In addition, it has been used in generalising the flow behaviour of some random coil polysaccharides (Launay, 1996; Launay, Doublier & Cuvelier, 1986; Morris & Ross Murphy, 1981).

2.5.2.1 Relationship between intrinsic viscosity and molecular characteristics

One of the earliest empirical models used to determine the viscosity of a dilute suspension containing impermeable spherical macromolecules is based on the Einstein equation (Einstein, 1906, 1911) given as:

$$\eta = \eta_s(1+2.5\phi) \qquad (1.1)$$

where η is the viscosity of the suspension, η_s is the viscosity of the solvent and ϕ is the volume fraction (volume of spheres divided by total volume) of the spherical macromolecules.

The intrinsic viscosity $[\eta]$ can be obtained by rearranging equation (1.1) to give:

$$[\eta] = \frac{(\eta - \eta_s)}{\eta_s} = 2.5\phi \qquad (1.2)$$

Since $[\eta]$ is a measure of the hydrodynamic volume of individual macromolecules in a solvent, it can be expected that $[\eta]$ is dependent on the molecular weight (although indirectly) (Debye & Bueche, 1948), the conformation of the macromolecules as well as the solvent quality (Launay et al., 1986). The volume fraction ϕ can be expressed in the terms of polymer concentration c given as:

$$\phi = \frac{N_A c V}{M} \qquad (1.3)$$

where N_A is the Avogardro's number, c is the concentration, M is the molecular weight and V is the hydrodynamic volume of the molecule.

Combining equations (1.2) and (1.3) gives:

$$[\eta] = \frac{2.5 N_A V}{M} \qquad (1.4)$$

The above model has been found useful for globular proteins (Launay et al., 1986) but is inadequate to characterise most polysaccharides since the conformation of a polysaccharide is seldom spherical and compact. For flexible chain molecules, as in most polysaccharides, the parameter V is proportional to the volume occupied by the chain based on the assumption that the solvent within the coil is bound to the polymer chain i.e. the spheres are not free-draining. Hence, the volume is proportional to the cube of the radius of the equivalent sphere. Equation (1.4) according to Debye & Bueche (1948) is expressed as:

$$[\eta] = 2.5 \frac{N_A}{M} \frac{4\pi R_H^3}{3} \qquad (1.5)$$

where R_H is the hydrodynamic radius.

Alternatively, equation (1.4) can be written:

$$[\eta] \propto \frac{(r_g^2)^{\frac{3}{2}}}{M} \qquad (1.6)$$

where r_g^2 is the mean-square radius[1].

Polymer chains with stiff backbones have higher r_g values compared to flexible linear chains (of similar molecular weight) which have much lower hydrodynamic dimensions. A branched polymer molecule on the other hand has a smaller $[\eta]$ than a linear chain of similar molecular weight since the former assumes a more compact conformation.

Various empirical formula have been proposed to explain the relationship between $[\eta]$ and molecular dimension and shape. One such example is given by the Mark-Houwink-

[1] A measure of the dimension of a polymer molecule based on averaging the mean-square distance of chain units from the centre of mass for all conformations. For linear polymers, the term, mean-square end-to-end distance is used, whereas mean-square radius is also applicable to branched and ring-shaped molecules.

Sakurada equation which suggests that $[\eta]$ is dependent on molecular weight and is given as:

$$[\eta] = KM_v^{\alpha} \qquad (1.7)$$

where α is the exponent, K is a constant and M_v is the viscosity-average molecular weight.

The exponent α is related to the degree of molecular expansion and hence depends on the stiffness of the polymer backbone and the polymer-solvent interactions. For Gaussian coils (flexible, linear chain polymers), the exponent α is ~0.5 in a theta solvent[2] and approaches 0.8 in a very good solvent[3] (Flory, 1953). The above relation is based on an equivalent sphere and it is assumed that the macromolecules exist as non free-draining coils. The parameter K mainly depends on the geometry of the inter-residue linkages within the polymer chain. High values of K can be expected for highly expanded coil dimensions.

If a free draining coil is assumed, the solvent is considered unperturbed by the polymer since the solvent can move through the polymer chain at the same velocity with the rest of solvent. In this case, α ranges from 1.0 to 1.2 for random coils. For rod-shaped molecules, α approaches 1.8. For highly branched polymers, values of α smaller than 0.5 can be expected (Lapasin & Pricl, 1995; Launay et al., 1986).

The values K and α can be determined using a series of polymer samples with narrow molecular weight distribution (so that $M_n \sim M_v \sim M_w$) by measurements of $[\eta]$ and the average molecular weights. The latter can be obtained from methods such as light scattering. However, the use of this equation to deduce the shape of the

[2] A theta solvent is a sufficiently poor solvent for the polymer so that it exactly compensates for excluded volume effect as polymer molecules have a relatively low affinity for solvent and tend to move closer to neighbouring polymer molecules. A polymer in such a state is said to be in its ideal condition. The molecular dimensions are unperturbed by intramolecular interactions – an ideal neutral random coil.

[3] In a good solvent, solvent-polymer contacts are preferred. Polymer-solvent interaction leads to coil expansion, increasing the values of r_g. The excluded volume effect is prominent due to repulsion between intramolecular segment leading to chain expansion.

macromolecules is now considered inadequate due to the effects of chain branching, high polydispersity of the molecular weight and the complex hydrodynamics of semi-flexible chains (Morris, 1989).

Another model that describes the relationship between intrinsic viscosity and coil dimensions according to the Flory-Fox equation (Flory & Fox, 1951) can be expressed as:

$$[\eta] = \frac{\phi\left(r^2\right)^{\frac{3}{2}}}{M_w} \qquad (1.8)$$

where ϕ, the Flory coefficient ranges from 2.0-2.8 x 10^{23} mol^{-1} depending on the solvent power and the conformation of the molecules assumed; with $\langle r^2 \rangle^{1/2}$ (root-mean-square end-to-end distance) equal to $\left(6r_g^2\right)^{1/2}$ in nm; and [η] in mL/g (Lapasin & Pricl, 1995).

The equation shows the dependence of intrinsic viscosity on molecular weight and relates chain flexibility through r^2. The more flexible the linear chain, the lower is r^2 for a given M_w. Equation (1.8) applies only to random coil polymers but not for polymer molecules with stiff conformation as in the example of xanthan gum (Doublier & Cuvelier, 1996).

From the discussion, it is clear that the intrinsic viscosity depends on the conformation adopted by the individual macromolecules in a solution. Therefore, $[\eta]$ is directly influenced by the molecular weight and the degree of stiffness of the polymer molecules. When a macromolecule is relatively inflexible (e.g. rod shape), it will orientate according to the direction of the flow and the forces exerted by random Brownian motion, giving rise to a large coil dimension. For macromolecules assuming a flexible chain (random coil) conformation, the orientation of the macromolecule is further complicated by a "reversible elastic molecular deformation" (Lapasin & Pricl, 1995, p.269), favouring a less extended coil of lower hydrodynamic volume. Macromolecules which assume a spherical conformation "rotate" in the direction of the

flow but the individual coil volume occupied will be lower than the above. Hence, $[\eta]$ is a shear dependent function and, in order to obtain meaningful data, it should be determined at zero-shear viscosity. This is obtained from the viscosity measured at a sufficiently low shear rate where the flow curve of the solution demonstrates Newtonian behaviour. Elimination of intermolecular interactions is assumed through extrapolation to infinite dilution. The intrinsic viscosity has the dimensions of volume per unit mass, expressed as mL/g and can be written as:

$$[\eta] = \left[\frac{\eta_o - \eta_s}{c\eta_s} \right]_{c \to 0} \qquad (1.9)$$

where η_o is the zero-shear viscosity of the solution and η_s is the viscosity of the solvent.

2.5.2.2 Intrinsic viscosity of polyelectrolytes

The preceding discussion assumes that the macromolecules are neutrally charged. For macromolecules which possess a net charge (also known as polyelectrolytes), intramolecular electrostatic repulsions will affect the size of the molecular structure. When a polyelectrolyte solution is diluted with water, the ionic strength of the solution decreases (the ionic strength is due solely to the charged groups of the polyelectrolytes). This leads to an increase in intramolecular repulsion between equal-sign charges on the macromolecule backbone causing the hydrodynamic volume to increase as the chain expands (Doublier & Cuvelier, 1996). The electrostatic repulsions can be shielded by counter ions, and hence are reduced by the addition of salt. This usually leads to a more compact molecular structure and a decrease in $[\eta]$. Most charged polysaccharides are anionic polyelectrolytes possessing sulphate or carboxyl groups (Launay et al., 1986).

The electrostatic charges therefore have important effects on the conformation of the charged macromolecules and hence, the rheological properties. Consequently, equation 1.9 no longer applies when the ionic strength is altered during dilution (Launay, 1996). Polyelectrolyte effects can be overcome by maintaining a constant ionic strength. Experimentally, this can be achieved by dialysing the most concentrated polymer solution against a salt solution of an appropriate ionic strength and using the dialysate for all subsequent dilutions. This procedure is known as the isoionic dilution (Morris,

1995; Ross-Murphy, 1995). Polyelectrolyte intrinsic viscosity increases almost linearly with $I^{-½}$, as shown in equation (1.10).

$$[\eta] = [\eta]_{\infty} + SI^{-\frac{1}{2}} \qquad (1.10)$$

where $[\eta]^{\infty}$ is the intrinsic viscosity at infinite ionic strength, I is the ionic strength of the solution and S is a constant.

From the plot of the intrinsic viscosity (obtained from a series of known ionic strength solutions) as a function of the reciprocal of the square root of the ionic strength, the intrinsic viscosity at infinite ionic strength, $[\eta]_{\infty}$, for which the electrostatic repulsions are completely screened, can be determined by extrapolating to the intercept at infinite ionic strength (Pals & Hermans, 1952). This can then be related to the intrinsic viscosity of a neutral polymer of similar chain length and molecular geometry (Smidsrod, 1970). However, linear extrapolation to infinite ionic strength is not always valid especially in high ionic strength solution since there is a marked deviation from equation (1.10) (Bohdanecky & Kovar, 1982; Smidsroed, Andresen, Grasdalen, Larsen & Painter, 1980; Tobitani & Ross-Murphy, 1997).

From the linear plot of equation (1.10), the constant S can be used as a quantitative measure of chain stiffness between different polyelectrolytes. However, this is only possible when comparisons of different polymers are made at a constant molecular weight. The constant S is directly proportional to the molecular weight of polymer and depends on the nature of counterions (Lapasin & Pricl, 1995; Smidsrod & Haug, 1971). Smidsrod & Haug (1971) suggested an empirical parameter B which relates to chain flexibility. The parameter B can be determined easily by obtaining the value of S from the isoionic dilution procedures of a polymer and measuring its intrinsic viscosity (molecular weight does not need to be known) at one particular ionic strength (0.1M NaCl). The expression is written as:

$$S = B([\eta]_{0.1})^{\nu} \qquad (1.11)$$

where the exponent ν generally varies only a little between 1.2 and 1.4, and $[\eta]_{0.1}$ is the intrinsic viscosity at 0.1M ionic strength.

Therefore, using the average value of 1.3 for the exponent v, B can be obtained directly by measurement of the $[\eta]$ of a polymer at different ionic strengths. The parameter B has been found to correlate well with theoretical parameters of chain flexibility. Morris & Ross-Murphy (1981) reported the parameter B to be inversely proportional to persistence length for all polyelectrolytes.

2.5.2.3 Determination of intrinsic viscosity from experimental data

Intrinsic viscosity of a polymer can be determined experimentally using a capillary viscometer to measure the relative viscosities over a range of dilute polymer concentrations. The capillary viscometers of the Ostwald, Fenske or Ubbelohde types are effectively used to obtain high precision measurements of low viscosity Newtonian fluids (Launay, 1996). The following equations briefly describe the general principles of the capillary viscometer and how viscosity readings can be obtained. The viscosity η based on the Poiseuille equation is:

$$\eta = \left[\frac{\pi \Delta P r^4 t}{8vl}\right] \qquad (1.12)$$

where η is the viscosity (Pa.s), P is the pressure of the liquid sample (g/cm^2), r is the radius of the capillary (cm), v is the volume (cm^3), l is the length of the capillary and t is the efflux time in seconds. The change in hydrostatic pressure denoted by ΔP is given as:

$$\Delta P = \rho g \Delta h \qquad (1.13)$$

where ρ is the density and Δh is the change in height.

Combining equation (1.12) and (1.13),

$$\eta = \left(\frac{\pi h g r^4}{8vl}\right)\rho t \qquad (1.14)$$

The constant ($\pi hgr^4/8vl$) is written as k, hence equation (1.14) becomes:

$$\eta = k\rho t \qquad (1.15)$$

The constant, k can be obtained by comparison with the known viscosity of a reference liquid, such as water. For relatively short flow times, there is a need to include the kinetic energy correction factor. Equation (1.15) then becomes:

$$\frac{\eta}{\rho} = kt - \frac{k^1}{t^2} \qquad (1.16)$$

The kinetic energy correction factor, k^1, can be determined experimentally from a series of trials on liquids of known viscosities and densities. Equations (1.12) to (1.16) are useful for obtaining the absolute viscosity of Newtonian fluids.

In obtaining the intrinsic viscosity of a polymer solution, k and k^1 can be eliminated by using water as a reference fluid and calculating the relative viscosity η_{rel}. This makes the determination of intrinsic viscosity by capillary viscometer very simple. A series of dilute polymer solutions is required. The time it takes for a volume of the polymer solution (t) to flow through a thin capillary is compared to the time for a solvent (t_s) to flow. The flow time is proportional to the viscosity (η), and inversely proportional to the density (ρ).

$$t_s = \frac{\eta_s}{k\rho_s} \qquad (1.17)$$

$$t = \frac{\eta}{k\rho} \qquad (1.18)$$

where η_s is the viscosity of the solvent, η is the viscosity of the solution, ρ_s is the density of the solvent and ρ is the density of the solution. From equations (1.17) and (1.18), the relative viscosity η_{rel} is given by:

$$\eta_{rel} = \frac{t\rho}{t_s\rho_s} \qquad (1.19)$$

From the relative viscosity, the specific viscosity η_{sp} which is the fractional change in viscosity upon the addition of polysaccharide is given by:

$$\eta_{sp} = \frac{\eta - \eta_s}{\eta_s} \qquad (1.20)$$

Related to these terminologies are the reduced viscosity and the inherent viscosity. Reduced viscosity is defined by:

$$\eta_{red} = \frac{\eta_{sp}}{c} \qquad (1.21)$$

where c is the mass concentration of the polymer expressed in g/mL. The inherent viscosity is defined by:

$$\eta_{inh} = \frac{(\ln \eta_{rel})}{c} \qquad (1.22)$$

Both η_{red} and η_{inh} are determined from viscosity determinations at dilute polysaccharide concentrations. These two parameters are dependent on concentration. When both η_{red} and η_{inh} are plotted as a function of concentration, two curves are obtained. At very dilute concentrations, the higher order terms are negligible and can therefore be ignored. The plot of η_{red} gives the Huggins equation:

$$\frac{\eta_{sp}}{c} = [\eta] + K'[\eta]^2 c \qquad (1.23)$$

and the plot of η_{inh} gives the Kraemer equation:

$$\frac{(\ln \eta_{rel})}{c} = [\eta] + K''[\eta]^2 c \qquad (1.24)$$

where K' is the Huggins coefficient, K'' is the Kraemer coefficient and $[\eta]$ the intrinsic viscosity in mL/g. For a random coil polymer, $K' - K'' = 0.5$ (Morris, 1989).

The Huggins constant K' is a measure of hydrodynamic interactions between macromolecule pairs (Bohdanecky & Kovar, 1982; Morris, 1989) and usually has values between 0.3 and 0.8, with values of 0.3-0.4 for a polymer in good solvents and 0.5-0.8 for polymers in theta solvents. For values above 0.8, aggregation of the macromolecules is likely to occur (Doublier & Cuvelier, 1996).

The value of $[\eta]$ is obtained from both plots by extrapolation to infinite dilution (~zero concentration) to eliminate any effects due to chain-chain interactions in the solution. The two plots must converge on the y-axis at the point corresponding to $[\eta]$.

$$[\eta] = \left[\frac{\eta_{sp}}{c}\right]_{c\to 0} = \left[\frac{\ln \eta_{rel}}{c}\right]_{c\to 0} \qquad (1.25)$$

In order to ensure accuracy, measurements are carried out at constant temperature and the measured time, t, should exceed 100 s (Flory, 1953). It should be emphasized that in determining $[\eta]$, the concentrations of polysaccharide solution must be low enough to eliminate the effect of chain-chain interactions through the solvent and the shear rate applied must be sufficiently low to obtain Newtonian behaviour. It is to be noted that even at very dilute concentration, Newtonian behaviour cannot be assumed (Lapasin & Pricl, 1995) as some polysaccharides at dilute concentration may show pseudoplastic behaviour from moderately low to high shear rates. In such cases, it is necessary to ensure that the operating shear rates correspond to the Newtonian plateau (Mitchell, 1979). Hence, determination of intrinsic viscosity by capillary viscometers has to be made with care especially for flexible coil or more severely, for rigid rods polymers which tend to align with the direction of the shear, causing pronounced shear thinning effects (Ross-Murphy, 1984). Alternative techniques such as the use of rotational viscometers to determine $[\eta]$ from the values that are obtained in the Newtonian region (η_o) may have to be sought. However, the results obtained from rotational viscometers are usually less precise (Launay, 1996).

2.5.2.3.1 Shear rate determination in a capillary viscometer

The viscosity measured by a capillary viscometer is not obtained at a defined shear rate but depends on the rate of flow of fluid through the capillary. The shear rate of the polymer solution in the capillary viscometer can be calculated by:

$$\dot{\gamma} = \frac{8V}{D} \qquad (1.26)$$

where $\dot{\gamma}$ is the shear rate (s^{-1}), V is the velocity and D is the diameter of the capillary. V is obtained by:

$$V = \frac{Q}{A} \qquad (1.27)$$

where Q is the flow rate (volume of the bulb divided by time) and A is the surface area of the capillary $(\pi(D/2)^2)$.

2.5.3 From dilute to concentrated regime

At least two concentration domains can be determined from a polymer solution as the number of macromolecules is increased from the dilute to the concentrated regime. In the dilute regime, individual polymeric coils can be visualised as "islands of coils scattered in the sea of the liquid solvent" (Lapasin & Pricl, 1995, p.253). Only intramolecular hydrodynamic interactions within individual macromolecules may occur. It is also assumed that that the individual macromolecules behave like impenetrable spheres. An increase in the number of macromolecules in solution will cause an increase in viscosity from that of solvent (η_s) to a value, η, at a given temperature. The viscosity increase is the result of the Brownian motion of the polymer coils and the perturbation of flow of the solvent caused by the individual polymer coils. Therefore, under a given flow condition, the differences in rheological behaviour are ascribed to individual macromolecule intrinsic property (Lapasin & Pricl, 1995). Viscosity varies almost linearly with concentration for many polysaccharides with $\eta_{spo} \propto c^{1.1-1.4}$ (Doublier & Cuvelier, 1996; Morris, 1995) where η_{spo} is the specific viscosity at zero-shear rate.

As the concentration of the disordered chains in aqueous solution increases, it will reach a stage when the individual coils begin to touch and collide with each other. A further increase in the polymer concentration in solution is only possible if the coils overlap and interpenetrate each other. The concentrated solution can be visualised as a temporary entanglement network. Entanglements behave as temporary crosslinks, as junction zones formed are continuously disrupted and reformed among the chains (Graessley, 1974). It is this physical entanglement of the polysaccharide that causes a marked

increase in viscosity (Graessley, 1982). Based on the concept of chain entanglements, Bueche (1962) derived the following relation:

$$\eta_{spo} \sim c^{3.5} \qquad (1.28)$$

In another model proposed by De Gennes (1971, 1983) known as the *reptation model*, in the concentrated regime, every chain is surrounded by other chains. All possible conformations adopted by a single chain in its Brownian motion are greatly limited because of the topological constraints imposed by surrounding molecules (Lapasin & Pricl, 1995). Individual chains can only move by wriggling through a hypothetical 'tube' in any direction formed by all the other chains in the three-dimensional space. Based on the reptation concept, De Gennes (1976) predicted the concentration dependence of viscosity as:

$$\eta_{spo} \sim c^{3.75} \qquad (1.29)$$

For polysaccharides to perform efficiently as thickeners, the concentrated regime must be reached. In the concentrated domain, the zero-shear viscosity increases much more steeply with increasing concentration. Studies carried out by Morris, Cutler, Ross-Murphy & Rees (1981) on random coil polysaccharides obtained a value of $\eta_{spo} \sim c^{3.3}$. The transition from a dilute regime to a concentrated regime of the polysaccharide solutions is characterised by the generalised concentration-dependence of zero-shear rate viscosity curve obtained by the log-log plot of the zero-shear specific viscosity (η_{spo}) as a function of $c[\eta]$ (Figure 2.2). The coil overlap parameter $c[\eta]$ measures the extent of space-occupancy of the polymer (Morris, 1989). Plotting η_{spo} against $c[\eta]$ instead of c removes the influence due to chain shape and size. The results obtained from different random coil polysaccharides including dextran, λ-carrageenan, carboxylmethylamylose, etc have been reported to superimpose closely regardless of the primary structure and molecular weights (Morris et al., 1981). Extrapolation of the concentrated region to the dilute region was found to intercept at $c[\eta] \sim 4$ and $\eta_{spo} \sim 10$ mPas for both charged and neutral random coil polysaccharides (Morris et al., 1981).

Exceptions to this generalised curve for random coil polysaccharides have been reported for galactomannans, guar gum and locust bean gum, with higher values of $\eta_{spo} \sim c^{5-5.75}$ and $c[\eta]$ occurring at ~2.5 (Morris et al., 1981). It has been suggested that high exponent values are the result of chain-chain interactions from substituted groups on the polymer backbone forming some sort of less stable 'junction zones'. This is often referred to as 'hyper entanglements' (Morris, 1995; Newlin, Lovell, Saunders & Ferry, 1962; Robinson, Ross-Murphy & Morris, 1982).

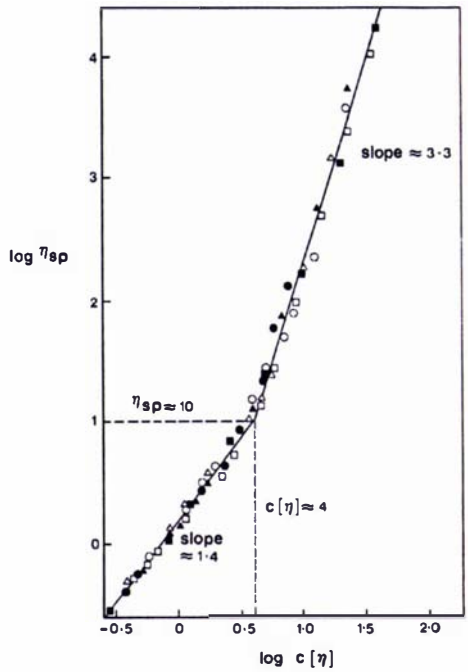

Figure 2.2 Generalised Concentration dependence of viscosity for random coil polysaccharides (Morris et al., 1981).

Launay et al (1986) suggested a third intermediate concentration regime, the semi-dilute regime (Figure 2.3). This intermediate regime is characterised by a continuous curvature from the upper limit of the dilute regime c^* to the lower limit of the concentrated regime, denoted by c^{**}. When the upper limit of the dilute regime c^* is reached, it indicates the beginning of coil touching and overlapping of the polysaccharide molecules. The polysaccharide solution is said to enter into the semi-dilute regime (Lapasin & Pricl, 1995). The gradual change in the slope of the zero-shear specific viscosity is due to the increasing intermolecular chain-chain contact. The cross-over from the dilute to the semi-dilute region has a reported value of $c[\eta]$ ~2.5-4

for many polysaccharides (Lapasin & Pricl, 1995). The factors affecting broadness of this domain ($c^* < c < c^{**}$) are currently unclear. It is suggested that they depend on solvent quality (the better the solvent, the broader the intermediate domain (Doublier & Cuvelier, 1996)), hydrodynamics of individual chains, polydispersity, extrapolation method and polymer-polymer interactions (Ross-Murphy, 1994). At concentrations above c^{**}, the concentrated domain is reached. The three concentration domains can be described by the expression according to Martin (Lapasin & Pricl, 1995; Spurlin, Martin & Tennent, 1946):

$$\eta_{spo} = c[\eta]\exp(K_M c[\eta]) \qquad (1.30)$$

where K_M is a dimensionless parameter which depends on the polymer-solvent pair.

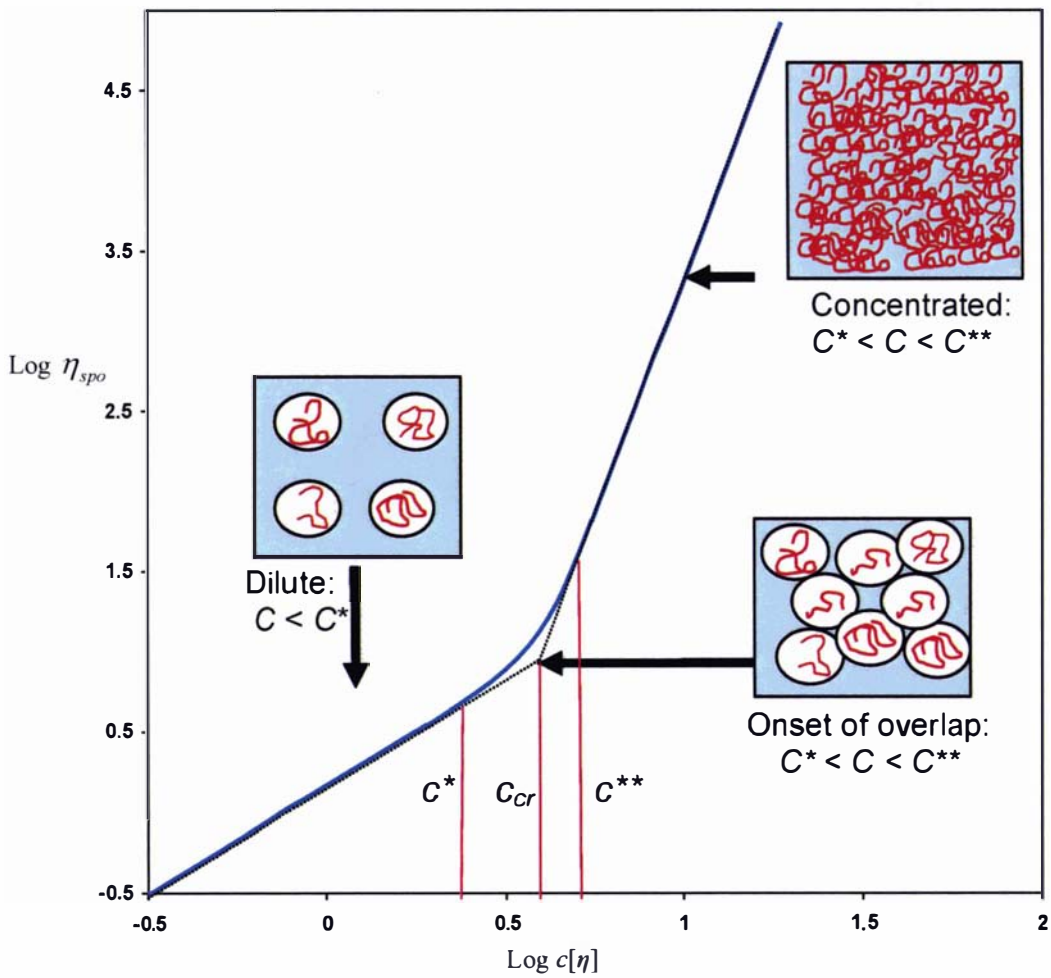

Figure 2.3 The concentration dependence of the zero-shear viscosity showing three concentration domains.

In describing the domains, Tuinier, Zoon, Stuart, Fleer & De Kruif (1999) proposed an alternative equation for fitting the concentration dependence curve of the EPS produced by *Lactobacillus lactis* subsp.*cremoris* B40:

$$\eta_{spo} = [\eta]c + \frac{1}{25}([\eta]c)^{\frac{7}{2}} \qquad (1.31)$$

From the above, it is clear that the rheological properties of a polymer are governed by the degree of space occupancy adopted by the polymer rather than the primary sequence structure. The degree of space occupancy of polymers in turn depends on the penetrability of individual macromolecules. For penetrable and deformable macromolecules, the total space-occupancy can exceed 100% volume fraction due to interpenetration. For rigid impenetrable spheres, the maximum critical packing fraction is much lower than 100% (Morris, 1989). The critical packing fraction for impenetrable spheres has been reported to be ~60% (Ross-Murphy, 1995). For anisotropic particles, packing concentration is even lower. Thus, a higher viscosity can be expected for rigid macromolecules in the concentrated regime with values of log η_{spo}~c^{5-8} (Lapasin & Pricl, 1995).

2.5.4 Shear rate dependence of viscosity

For macromolecules which adopt an almost spherical conformation, such as some globular protein molecules, at concentrations below c^*, the viscosity shows very little dependence on shear rate and very often one can assume Newtonian behaviour. This is not always the case for random coil polysaccharides since the individual molecules are aligned with the direction of the flow and become 'stretched out' as the rate of shear increases. Therefore, even at concentrations well below c^*, polysaccharide coils may exhibit pseudoplastic behaviour as the shear rate increases. Similarly, the shear rate dependence of viscosity for rigid rod like molecules is even more pronounced as the motion includes a progressive orientation of the chains along the direction of the flow.

As the concentration of polysaccharide in a solution increases, the coils begin to overlap and interact with each other. For the solution to flow, sufficient stress must be present to disrupt the intermolecular entanglements. This explains why the viscosity of the solution is highly dependent on the rate of shear. However, at sufficiently low shear rates, polymer solutions generally exhibit Newtonian behaviour (i.e. zero-shear viscosity η_o). This can be explained by the concept of relaxation time, which is generally defined as the time required for the applied stress to relax. Newtonian behaviour is observed at very low shear rates because the relaxation time needed for disruption of entanglements is the time needed for re-entanglement. In other words, there is sufficient time for new entanglements to form between different coils and the overall entanglement remains constant, hence viscosity is independent of shear.

As the shear rate increases above the critical shear rate ($\dot{\gamma}_c$), the behaviour becomes shear thinning. This happens when the relaxation time needed for re-entanglement is longer than the time needed for the disruption of entanglements (there is insufficient time for new entanglements to form between different chains and the overall entanglement decreases leading to a decrease in the apparent viscosity). The relaxation time of such a system increases with increasing concentration. The relaxation time can be calculated from the spring and bead model of Rouse (Ferry, 1980; Rouse, 1953) and is given by:

$$\tau_p = \frac{6(\eta_o - \eta_s)M}{p^2\pi^2 RTc} \qquad (1.32)$$

where τ_p is the relaxation time, T is the absolute temperature, M is the molecular weight of the polymer and R is the Boltzman constant given as 1.380658 x 10^{-23} J/K. The longest relaxation time is when p=1, where p is the constant reflecting the ratio of chain segments to total chain length. Note that in the Rouse model, no consideration is given to polymer-polymer interactions. The only hydrodynamic interaction is between the polymer chains and the solvent molecules.

For solutions of random coil polymers, the onset of non-Newtonian pseudoplastic behaviour occurs at the critical shear ($\dot{\gamma}_c$). The relationship between shear rate and the longest relaxation time is given as:

$$\tau_1 \dot{\gamma}_c \sim 1 \qquad (1.33)$$

where $\dot{\gamma}_c$ is the critical shear rate at the longest relaxation time.

Various theories have been proposed to explain the shear thinning behaviour. These include intramolecular hydrodynamic interactions, a change in the volume of solvent that is regarded as bound with the coil, the 'internal' viscosity of the coil, and the finite extensibility of the polymer chains (Mitchell, 1979). The shear thinning characteristic of the flow curve is commonly fitted using the power law equation:

$$\tau = K\dot{\gamma}^n \qquad (1.34)$$

where τ is the shear stress (Pa), $\dot{\gamma}$ is the shear rate (s^{-1}), K is the consistency index, and n is the flow behaviour index, always less than 1 for shear-thinning behaviour.

For Newtonian behaviour, $n = 1$, and K becomes the viscosity η. For fluids exhibiting non-Newtonian behaviour, η is not a constant but varies with the applied shear rate, and is given as the apparent viscosity, η_{app}. The non-Newtonian behaviour frequently extends over several decades of shear rates. An increase in K indicates an increase in viscosity at any particular shear rate. Although the pseudoplastic behaviour of polysaccharides is fitted by the power law equation and provides a reasonably linear fit on a log-log plot over several decades of shear rates, it is inadequate if a broad range of shear rates is to be explored (Morris, 1989).

At very low shear rates, a first Newtonian plateau, referred to as the zero-shear rate viscosity, denoted by η_o, can be obtained in most polymer solutions. The occurrence of the zero-shear rate viscosity has been explained by the concept of relaxation time. At very high shear rates, a second Newtonian viscosity, denoted by η_∞, is reached. The very high shear causes elongation, stretching and orientation of the polymer chains,

hence minimum constant viscosity is obtained. Experimentally, it is not always possible to obtain η_∞ because the shear rate is so high that shear degradation or flow instability may occur (Mitchell, 1979).

Different polysaccharide solutions differ in their zero-shear viscosities and at the shear rates at which the onset of shear thinning behaviour occurs. Typical characteristics of shear dependency of polysaccharide solutions for a very large shear range are illustrated by the flow curve in Figure 2.4. Such behaviour is known to be typical of macromolecular solutions and has been reported for galactomannans as well as for other non-gelling polysaccharides (Morris et al., 1981).

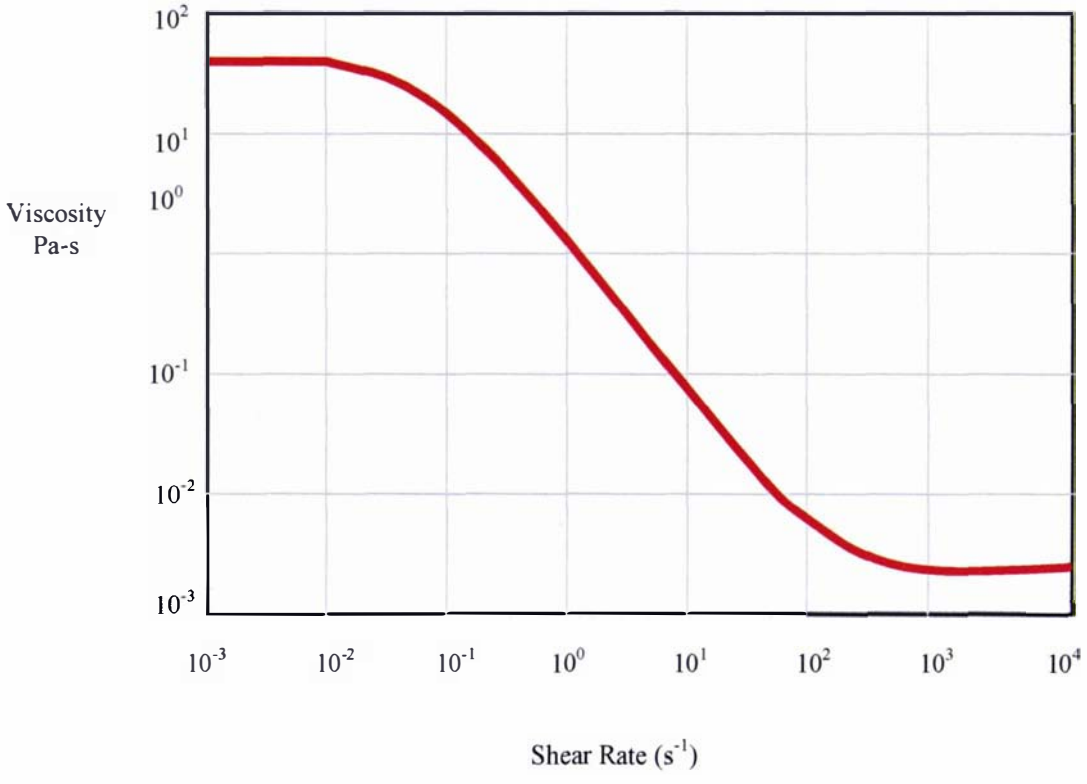

Figure 2.4 Flow curve of a typical polysaccharide solution over a broad range of shear rates. At very low shear rate, a plateau defining the first limiting Newtonian viscosity (η_o) is reached. Beyond a critical shear rate ($\dot{\gamma}_c$), the behaviour became shear thinning. At very high shear rates, the second limiting viscosity (η_∞) is reached.

The flow curve in Figure 2.4 can be described using equations like the Cross (Cross, 1965; Doublier & Launay, 1981; Launay et al., 1986; Morris, 1989) and Carreau (Carreau, 1972) models as described in equations (1.35) and (1.36) respectively:

$$\eta = \eta_\infty + \frac{\eta_0 - \eta_\infty}{1+(\lambda\dot{\gamma})^{1-n}} \qquad (1.35)$$

$$\eta = \eta_\infty + \frac{\eta_o - \eta_\infty}{(1+(\lambda\dot{\gamma})^2)^{(1-n)/2}} \qquad (1.36)$$

where η is the viscosity at a given shear rate $\dot{\gamma}$; λ is the structural relaxation time; n is the exponent of the power-law approximation in the middle shear rate region; η_o is the limiting Newtonian viscosity at very low shear rate, and η_∞ is the limiting Newtonian viscosity at very high shear rate. Equation (1.35) can be simplified by setting η_∞ to zero or the viscosity of the solvent. In practice, fitted values of η_∞ are often negative (Launay & Pasquet, 1982) and are very small compared with η_o. Simplifying equation (1.35) gives:

$$\eta = \frac{\eta_o}{1+(\lambda\dot{\gamma})^{1-n}} \qquad (1.37)$$

Based on equation (1.37), Morris et al. (1981) showed that the generalised shear rate dependence of viscosity η can be obtained from different entangled random coils polysaccharide solutions through a log-log plot of (η/η_o) as a function of log $(\dot{\gamma}/\dot{\gamma}_{0\,1})$ where $\dot{\gamma}_{0\,1}$ is the shear rate required to reduce η to $\eta_o/10$ as shown in Figure 2.5.

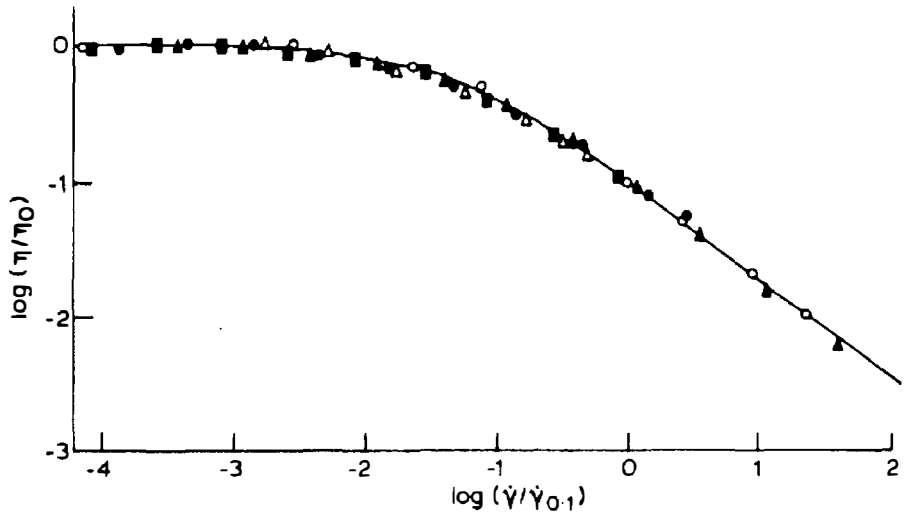

Figure 2.5 Generalised shear rate dependence of viscosity for entangled random coil polysaccharide solutions superimposed closely irrespective of primary structure, molecular weight, temperature and solvent condition for different random coils polysaccharides ((Morris et al., 1981).

The plot is fitted using the popular Cross-type model proposed by Morris et al. (1981):

$$\eta = \frac{\eta_o}{1+\left(\lambda\frac{\dot{\gamma}}{\dot{\gamma}_{0.1}}\right)^{0.76}} \qquad (1.38)$$

The exponent value of 0.76 is generally representative of polysaccharides with random coil conformation (Morris, 1990). Other values of 0.78 (Launay, Cuvelier & Martinez-Reyes, 1997) and 0.75 (Bueche & Harding 1958) have been suggested although higher values have been reported for synthetic polymers with much lower polydispersity indices (Morris, 1995).

2.5.5 Polysaccharide gels

A gel can be generally defined as a colloidal two-phase system which exhibits viscoelastic properties, where the dispersed phase forms a three-dimensional network within the continuous solvent phase. Gel formation can be triggered by many different mechanisms.

In chemical gels, gelation occurs because of covalent crosslinks which are characterised by a permanent stability of the network. The crosslinked networks are effectively homogeneous throughout the system.

In physical gels, as in many gelling polysaccharides, intermolecular associations are the result of weaker, reversible, non-covalent, physical interactions. These include hydrogen bonds, Coulombic, dipole-dipole, van der Waals and hydrophobic interactions (Lapasin & Pricl, 1995). These forces are weak but they act cooperatively to achieve gel stability. At sufficiently high concentration, interactions amongst chains take place forming regions of ordered conformation (junction zones). Each chain may form junction zones with different neighbouring chains eventually forming a three-dimensional network structure. The number and position of physical crosslinks fluctuate with time/temperature since the crosslinks are of finite energy and lifetime (Kavanagh & Ross-Murphy, 1998). Hence, junction zones are not distributed homogeneously throughout the entire network giving isotropic and anisotropic regions. The degree of heterogeneity of these regions depends on the mechanisms of chain association, the extension of the junction zones and their distribution through the system (Lapasin & Pricl, 1995). Although chain-chain interactions are important for gel formation, excessive interactions may render the polysaccharides insoluble instead of gel forming. There must be sufficient chain-chain interactions to establish a network and sufficient chain-solvent interactions to prevent collapse of the network (Morris, 1986). In addition, the proportion of ordered polysaccharide chains and disordered polysaccharide chains between junction zones is important in determining final gel properties (Dea, 1993). The strength of the gel depends on the strength of intermolecular bonding at the junction zones (Whistler, 1993). Association of polysaccharide chains leading to gel formation may be promoted in several ways by:

- reducing chain-solvent interactions such as by reducing water activity e.g. using a high concentration of sugar to promote low-water-activity-mediated gelation of high methoxyl pectin.
- decreasing interchain electrostatic chain repulsion e.g. addition of salt to increase ionic strength e.g. cation-mediated gelation of alginate.
- increasing chain-chain association e.g. during freezing, the effective polymer concentration is increased and gels can form upon thawing such as in the freeze-thaw-mediated gelation of locust bean gum.

Conformational changes in the molecules due to changes in temperature or solvent conditions (pH, ionic strength, counter ions, etc.) may enhance interactions among polymer chains. These may take the form of double helices which may further associate through ion binding. Different mechanisms of crosslinking have been proposed for polysaccharides as shown in Figure 2.6.

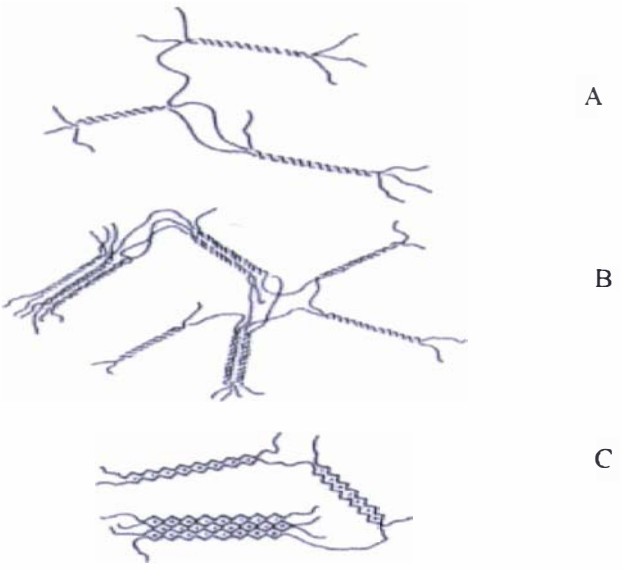

Figure 2.6 Mechanisms of polysaccharide gel formation. (A) formation of double helices crosslinks. (B) Association of double helices induced by ions. (C) Association of chain by ion binding (Clark & Farrer, 1995).

2.5.5.1 Strong and weak gels

On the basis of rheological properties, polysaccharide gels can be classed under two major categories: strong and weak gels. Strong gels possess the general features of true gels. Under small deformation conditions, they exhibit typical behaviour of viscoelastic solids. As deformation increases above a critical value, they rupture rather than flow.

Weak gels on the other hand exhibit rheological properties that lie between viscous solutions and strong gels. The macromolecules of a weak gel may align themselves like rigid rods such that they are closely and weakly associated (non-covalent bonds). These temporary networks are easily formed and disrupted due to external factors such as shear, temperature and ionic strength (Morris, 1986). Under small deformation, weak gels resemble the mechanical spectrum of strong gels, particularly at low frequencies. However, when subjected to a large deformation such as in a steady shear flow, they flow rather than fracture. The three-dimensional network undergoes progressive breakdown into smaller clusters and flows like a dispersed system. The differences between strong gels, weak gels and entangled solutions can be clearly evidenced by means of oscillatory flow measurements.

Of course, polysaccharide chain associations may be limited to the formation of molecular clusters forming micro-aggregates instead of extending throughout the whole system as three-dimensional networks. In the former, connectivity exists only within a short distance scale whereas, in a gel network, it spans the entire system. The rheological behaviour of a micro-gel system depends on the volume fraction of the disperse phase, the rigidity of the micro gel particles and the solvent viscosity. At sufficiently high concentrations, micro gel dispersions display solid-like behaviour at low stresses and their rheological properties are similar to those of weak gels. Interpretation of the rheological properties of such system needs to be carried out with caution.

2.5.5.2 Oscillatory measurements

The majority of food materials including gels and concentrated polysaccharide solutions can be considered to fall under the viscoelastic category. The rheological properties can

be characterised by the viscous and the elastic parameters which can be determined by oscillatory measurements using a stress-controlled rheometer (Roa, 1999). By applying a stress (τ) to incur a small deformation, the resultant strain (γ) of the material is measured. If the material is perfectly elastic, then the resultant stress wave is exactly in phase with the strain wave (Figure 2.7).

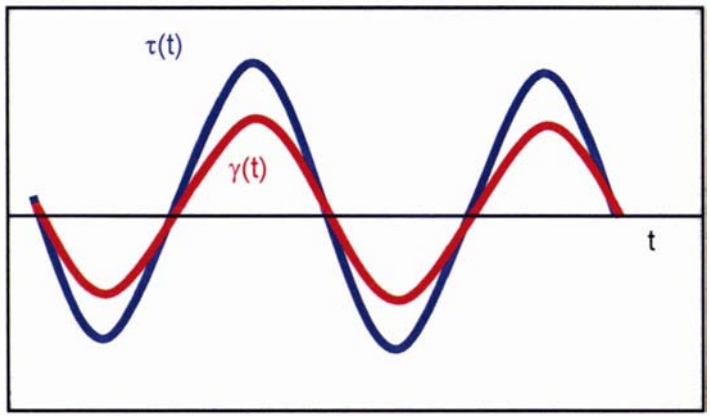

Figure 2.7 Sinusoidal oscillatory shear of a perfectly elastic body with the stress wave exactly in phase with the strain wave (adapted from Roa, 1999).

On the other hand, if the material is a purely viscous fluid, the resultant stress wave will be exactly 90° out-of-phase with the imposed deformation, since the rate of change of the sinusoidal oscillation is at its maximum when the strain is 0 as shown in Figure 2.8. Most foods exhibit viscoelastic properties that lie between the two extremes (Figure 2.9).

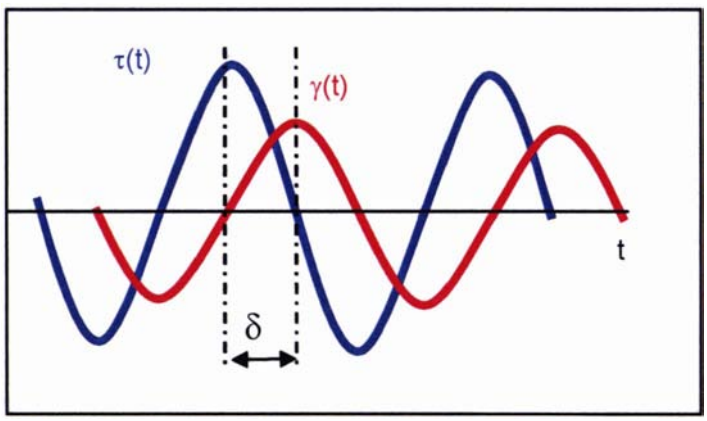

Figure 2.8 Sinusoidal oscillatory shear of a perfectly viscous body with stress and wave 90° out of phase (adapted from Roa, 1999).

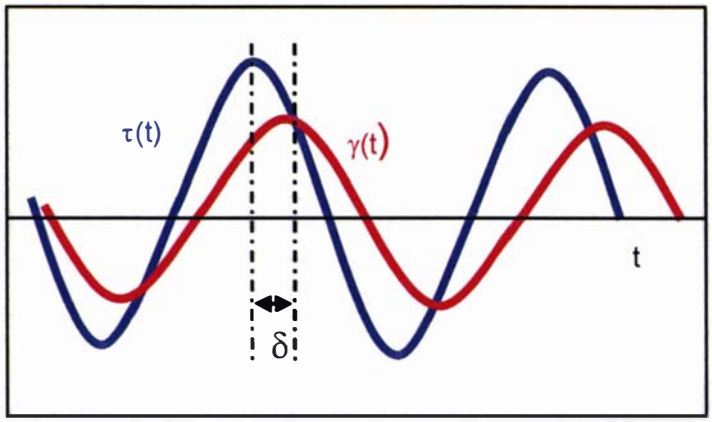

Figure 2.9 Sinusoidal oscillatory shear of a viscoelastic material with stress wave between 0° (in-phase) and 90° (out-of-phase) of the strain wave (adapted from Roa, 1999).

In general, the stress wave will have a phase difference, denoted by δ ($0<\delta<90°$), and is usually expressed as *tan* δ to indicate a measure of the viscous/elastic ratio for the material at a specific angular frequency (ω).

The stress-strain waves can be described by the following equations. The dynamic strain $\gamma(t)$ is given by:

$$\gamma(t) = \gamma_0 \sin(\omega t) \qquad (2.1)$$

where γ_0 is the maximum strain

The dynamic stress measured is expressed as:

$$\begin{aligned} \tau(t) &= \tau_0 \sin(\omega t + \delta) \\ &= \tau_0 \{\sin(\omega t)\cos\delta + \cos(\omega t)\sin\delta\} \end{aligned} \qquad (2.2)$$

where τ_0 is the maximum stress and δ is the phase angle (loss angle) between the stress and strain.

Therefore, for purely elastic behaviour, where $\delta = 0$, equation (2.2) becomes:

$$\tau(t) = \tau_0 \sin(\omega t) = G\gamma_0 \sin(\omega t) \qquad (2.3)$$

where G is the shear modulus

For pure viscous behaviour, where $\delta = 90°$, equation (2.2) becomes:

$$\tau(t) = \tau_o \cos(\omega t) = \eta \dot{\gamma}_o \cos(\omega t) \qquad (2.4)$$

where η is the viscosity and $\dot{\gamma}_0$ is the shear rate during oscillatory motion.

At small strain within the linear region, $\tau_0 \propto \gamma_0$. Equation (2.2) can be re-written as:

$$\tau(t) = \gamma_0 \left[\frac{\tau_0}{\gamma_0} \cos\delta \sin(\omega t) + \frac{\tau_0}{\gamma_0} \sin\delta \cos(\omega t) \right] \qquad (2.5)$$

The elastic (in-phase) and the viscous (out-of-phase) components of the stress wave are separate entities. The in-phase, shear storage (or elastic) modulus which measures the energy stored during each oscillatory cycle is denoted as G':

$$G'(\omega) = \left(\frac{\tau_0}{\gamma_0} \right) \cos\delta \qquad (2.6)$$

The out-of-phase, shear loss modulus (or viscous) modulus which measures the energy dissipated, denoted as G'':

$$G''(\omega) = \left(\frac{\tau_0}{\gamma_0} \right) \sin\delta \qquad (2.7)$$

Equation (2.5) to (2.7) can be written in two equivalent forms:

$$\tau(t) = G' \gamma_0 \sin(\omega t) + G'' \gamma_0 \cos(\omega t) \qquad (2.8)$$

or written with corresponding viscosity functions, η' and η'',

$$\tau(t) = \eta'' \dot{\gamma}_o \sin(\omega t) + \eta' \dot{\gamma}_o \cos(\omega t) \qquad (2.9)$$

The loss tangent, $\tan\delta$ is given by:

$$\tan\delta = G''/G' \qquad (2.10)$$

The complex modulus, G^* is given by:

$$G^* = \frac{\tau(t)}{\gamma(t)} = G' + iG'' \qquad \text{Where } i^2 = -1$$

$$|G^*| = \sqrt{G'^2 + G''^2} \qquad (2.11)$$

The complex viscosity, η^* is defined as:

$$\eta^* = \eta' - i\eta''$$

$$|\eta^*| = \sqrt{\eta'^2 + \eta''^2} \qquad (2.12)$$

Based on complex modulus, η^* is related to G^* by:

$$\eta^* = \frac{G^*}{i\omega} = \frac{G' + iG''}{i\omega} = \frac{G'}{i\omega} + \frac{G''}{\omega}$$

$$= \frac{G''}{\omega} + \left(\frac{iG'}{i \times i\omega}\right) = \frac{G''}{\omega} - \frac{iG'}{\omega} \qquad (2.13)$$

Based on equations (2.12) and (2.13),

$$\eta' = \frac{G''}{\omega} \quad ; \quad \eta'' = \frac{G'}{\omega} \qquad (2.14)$$

It is to be noted that only in the small strain limit will the correct G' and G'' plots be obtained. A strain sweep test is first performed to determine the linear viscoelastic region where G' and G'' is independent of γ at a fixed frequency (e.g. 1 Hz) as shown in Figure 2.10.

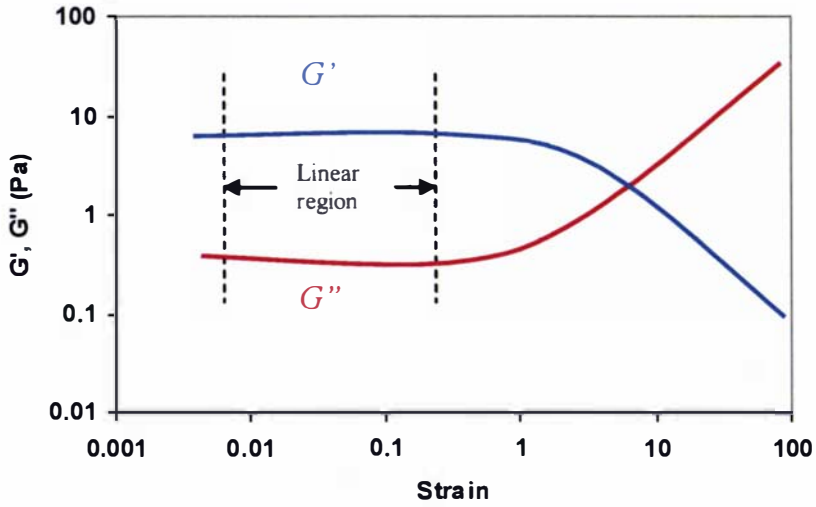

Figure 2.10 Mechanical spectra: G' and G" with region showing linear viscoelasticity as a function of strain at a constant frequency.

This limiting strain depends on the nature of the system. Most physically, non-covalently crosslinked systems are strain independent at very small deformations e.g. 0.2-0.3%. For an entanglement network, the linear viscoelastic region may extend to large strains of the order of units. In a strain sweep, *G'* generally departs from linearity sooner than *G"*. Therefore, the selection of a suitable operating strain for small deformation test is usually based on the elastic component only. Under the small deformation, the mechanical spectra (*G'*, *G"*) from a frequency sweep test can then be determined correctly. The mechanical spectra (*G'* and *G"*) can provide a better understanding of the rheological behaviour of viscoelastic materials.

The entire *G'* and *G"* spectra can be obtained if a wide range of frequencies can be reached (e.g. 10 decades). Unfortunately, no mechanical instrument is capable of covering such a wide frequency range. To get around this limitation, one can operate by increasing the temperature or the concentration of the solution which can be equivalent to lowering the effective frequency of the experiment. The mechanical spectra of *G'* and *G"* plotted logarithmically against frequency is shown in Figure 2.11.

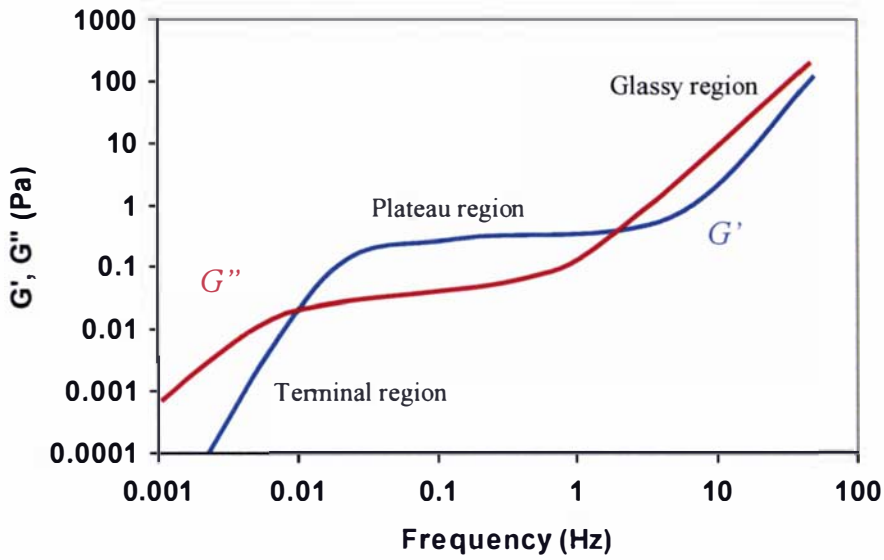

Figure 2.11 Mechanical spectra, G' and G", over an extended range of frequencies (adapted from Lapasin & Pricl, 1995).

At low frequency (long time), the polymer molecules are rearranged in all possible configurations within the period of an oscillatory cycle. The force in phase with displacement is negligible and G' vanishes compared to G'' (Lapasin & Pricl, 1995).

The region at higher frequencies (where $G' > G''$) is known as the plateau region. At even higher frequencies, both G' and G'' increase as the material becomes more "glassy". At high frequency of oscillation, there will be no time for rearrangement of molecules within the period of an oscillatory cycle. Instead the polymer molecules are confined to bending and stretching of the chemical bonds (Lapasin & Pricl, 1995).

2.5.5.3 Oscillatory measurements for polymer solutions and gels

When a dilute flexible random coil polymer solution is subjected to a small strain oscillatory test, at low frequency, G'' dominates over G'. $G' \propto \omega^2$ and $G'' \propto \omega$ as shown in Figure 2.12.

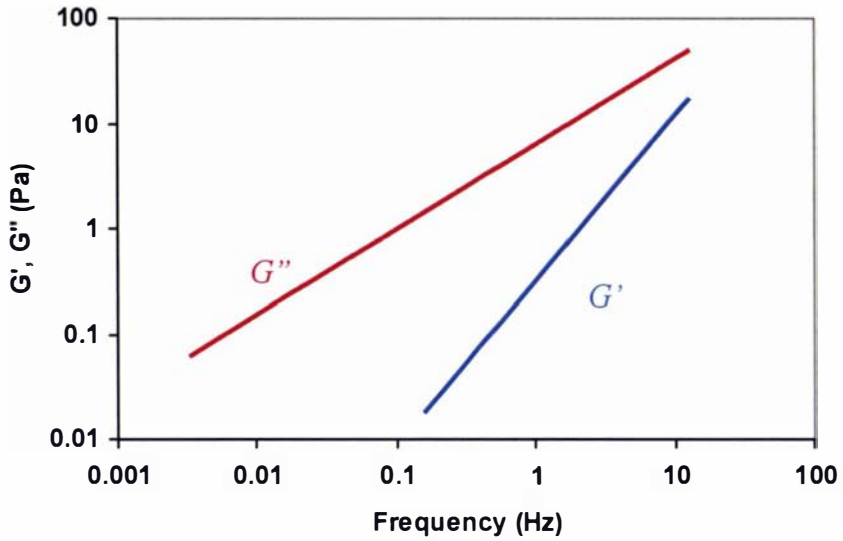

Figure 2.12 Mechanical spectra, G' and G" of a dilute solution of a random coil polymer (adapted from Lapasin & Pricl, 1995).

In semi-dilute to concentrated flexible random coil polymer solutions, *G'* begins to dominate over *G"* so that a cross over is observed as the frequency increases (see Figure 2.13). At higher frequencies, *G'* and *G"* are less frequency dependent as typical of an 'entanglement' network (Ferry, 1980). An entanglement network behaves as a liquid (*G"*>*G'*) at frequencies below the relaxation time. However, the entanglement network behaves as a gel (*G'*>*G"*) at frequencies above the relaxation time (rate of entanglements). At frequencies above the relaxation time, the physical entanglements of the polymer chains have insufficient time to disentangle and flow. Hence, the network behaves like a crosslinked gel. As the coil overlap concentration of the polymer increases, the relaxation time progressively increases.

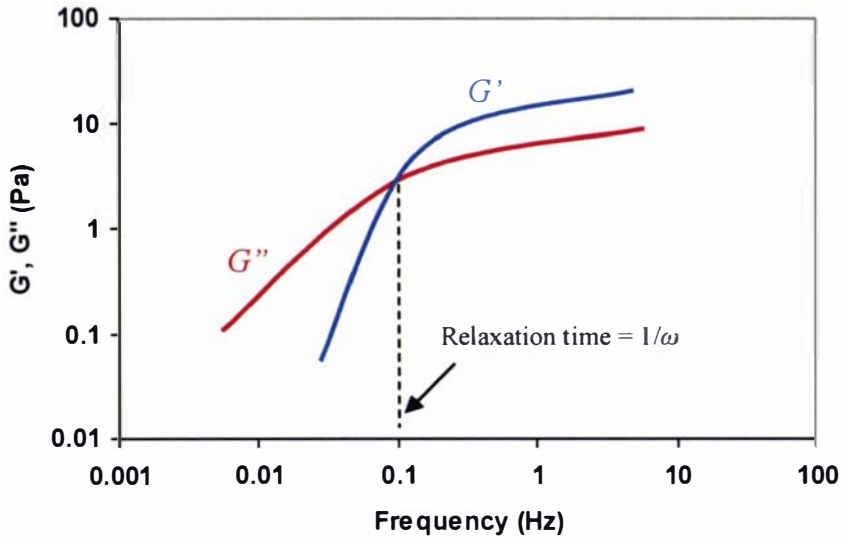

Figure 2.13 Mechanical spectra of a a semi-dilute to concentrated solution of a random coil polymer (adapted from Lapasin & Pricl, 1995).

For a perfectly elastic Hookean solid, G' is several decades higher than G'' and is independent over a wide range of frequencies, including very low frequencies (i.e. infinitely long times). For a relatively strong gel, G' is typically 1-2 decades greater than G'' over the frequency range from 10^{-2} to 10^{2} Hz (rad/s) as shown in Figure 2.14.

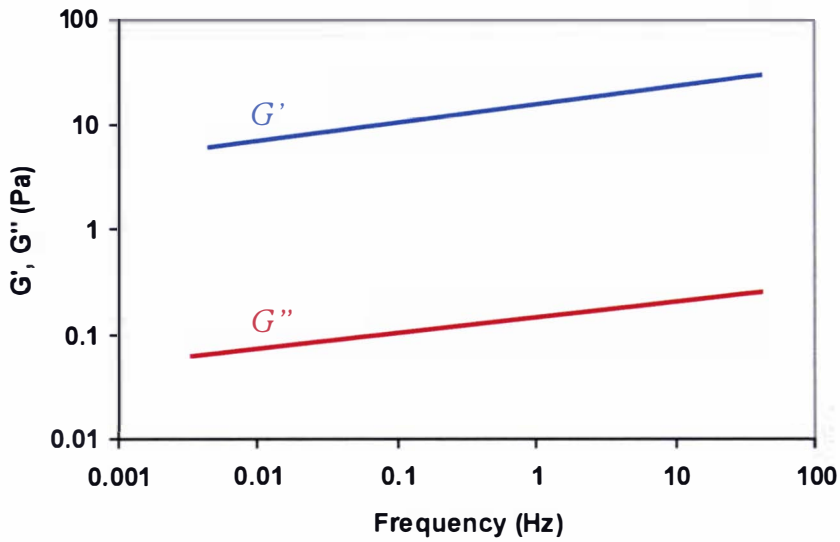

Figure 2.14 Mechanical spectra: G' and G" of a relatively strong biopolymer gel (adapted from Lapasin & Pricl, 1995).

The greater the difference between G' and G'', the stronger is the gel. However, the behaviour of a strong gel does not necessarily associate with high values of G'. The mechanical spectra consist of two neatly parallel lines (G' and G'') and may be horizontal or may increase slightly with increasing frequency. The latter may be attributed to 'network defects' such as dangling chain ends, trapped entanglements, loops, etc (Ross-Murphy, 1992). Weak gels exhibit similar mechanical spectra of strong gels except that G' is less than one decade greater than G''. Based on the mechanical spectra of a frequency sweep tests, strong gels, weak gels and entangled solutions can be differentiated.

2.5.6 Relationships between steady-shear and oscillatory measurements

A popular empirical relationship known as the Cox-Merz rule states that the dynamic viscosity (η^*) versus frequency (ω) curve corresponds with the steady shear flow viscosity (η) versus shear rate ($\dot{\gamma}$) curve as shown in Figure 2.15 Theoretically, however, these functions are quite independent, and there is no general explanation for such a correspondence to exist (Renardy, 1997). Although this relationship has been used to estimate steady flow viscosity data from the dynamic rheological data (which is easier to perform), it is not always valid for all polymer solutions.

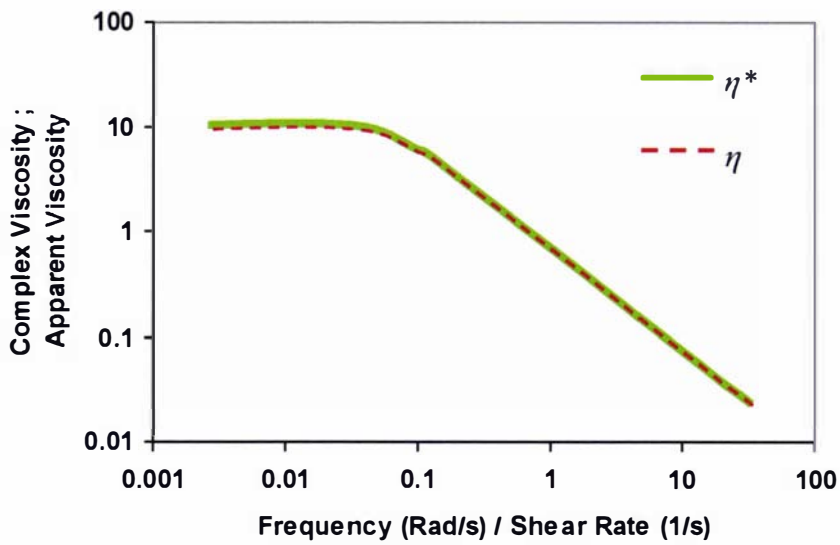

Figure 2.15 The superposition of the apparent viscosity versus shear rate curve and dynamic viscosity versus frequency curve based on the Cox-Merz rule.

In an entangled network, the frequency (ω) dependence of η^* superimposes closely on the shear rate ($\dot{\gamma}$) dependence of the steady-shear viscosity (η) at equivalent $\dot{\gamma}$ and ω according to the Cox-Merz rule (Cox & Merz 1958). This generalised rule shows that the viscosity is dependent on the time scale of molecular rearrangements under small deformation (oscillatory) as it is dependent on the rate of shear under large deformation (Morris, 1995). Superposition of $\eta\dot{\gamma}$ and $\eta^*(\omega)$ has been reported for many polysaccharide solutions including guar gum (Richardson & Ross-Murphy, 1987). However, this superposition is not always valid for a number of weak polysaccharide gels including rhamsan and welan (Robinson, Manning & Morris, 1991). Such a behaviour is usually associated with the tendency to form aggregated structures or dispersions, which are then broken down under the applied strain (Ross-Murphy, 1992). Unlike a true solution, there are no such structures to destroy.

2.5.7 Static light scattering

The following sections provide an overview of the theory and common terminologies in static light scattering technique for the determination of molecular weight, size and conformation of macromolecules in solution.

2.5.7.1 Theory of light scattering

When a beam of light is passed through a solution containing particles, a small proportion of the light is scattered from the incident beam. Light scattering occurs when polarizable particles in a sample interact with the oscillating electric field of a beam of light. The varying field induces oscillating dipoles in the particles and these scatter light in all directions. The amount of scattered signal is proportional to concentration and molecular weight. Therefore, for small molecular weight species up to approximately 10^3 Da, a relatively high concentration is required to produce sufficient light scattering signal (Wyatt, 1993). On the other hand, for larger molecular species, such as macromolecules with molecular weight from ~10^6 Da, the molecular parameters of individual molecules can be studied in highly dilute solutions. In the dilute regime, the macromolecules are separated by long distances, and intermolecular interactions only weakly interfere with the measured scattered light (Burchard, 1994b). However, in a semi-dilute regime, interactions between macromolecules will strongly

affect the measured quantities. Under such instances, interpretation of light scattering results has to be treated with caution.

Light scattering is based on two fundamental principles. Firstly, the amount of light scattered is directly proportional to the molecular weight and the solute concentration, with the assumption that there is no absorbance of the light nor fluorescence from the macromolecules (Wyatt, 1993). Secondly, the angular variation of scattered light is directly related to the size of the molecule. These principles are explained by the Rayleigh-Debye-Gans light scattering model for dilute macromolecule solutions (Zimm, 1948):

$$\frac{R_{(\theta)}}{Kc} = M_w P_{(\theta)} - 2A_2 c M_w^2 P_{(\theta)}^2 \qquad (3.1)$$

where:

$R_{(\theta)}$ is the Rayleigh excess scattering, the excess intensity of light scattered at angle θ (i.e., the intensity due to the solute),

K is an optical constant,

c is concentration of solutes (g/mL),

M_w is the weight-average molecular weight, $P_{(\theta)}$ is the scattering function,

A_2 is the second virial coefficient.

The optical constant K is derived from equation (3.2).

$$K = 4\pi^2 n_o^2 \left(\frac{dn}{dc}\right)^2 \lambda^{-4} N_a^{-1} \qquad (3.2)$$

where:

dn/dc is the differential refractive index increment of the solvent-solute solution with respect to a change in solute concentration,

n_o is the solvent refractive index at λ,

λ is the incident wavelength in vacuum,

N_a is the Avogadro's number (6.022×10^{23}).

K should be large for sufficiently high scattering intensity (Burchard, 1994a).

The Rayleigh excess scattering is represented by:

$$R_{(\Theta)} = \frac{I_\theta r^2}{I_o V} \tag{3.3}$$

where:

I_θ is the scatter intensity,

I_o is the incident beam intensity,

V is the volume of scattering medium

r is the distance between the center of scattering volume and the detector.

The scattering function $P_{(\theta)}$ to the first order is represented by:

$$P_{(\theta)} = 1 - \left(\frac{16\pi^2 n_o^2 r_g^2 \sin^2 \theta/2}{3\lambda^2} \right) \tag{3.4}$$

where:

n_o is the solvent refractive index

r_g^2 is the mean-square radius

The Zimm treatment (Zimm, 1948) is an accurate graphical method for the derivation of the light scattering parameters when angular dependence comes into play (Evans, 1972). Besides Zimm's equation, the angular dependence of scattered light intensity can also be described by two other equations known as the Debye and Berry fit methods (Berry, 1966; Debye, 1947). The following section discusses each of these methods.

2.5.7.2 Zimm, Debye and Berry plots

To construct a Zimm plot, Kc/R_θ is plotted against $\sin^2(\theta/2) + xc$. Data at each concentration are fitted by polynomials in $\sin^2(\theta/2)$ to the angular variation, and at

each angle by polynomials in c to the concentration variation. The parameter x is an arbitrary constant factor chosen so that the data points are sufficiently spread out. The Zimm formalization is given in equation (3.5):

$$\frac{Kc}{R_\theta} = \frac{1}{M_w P_\theta} + 2A_2 c \qquad (3.5)$$

Note that when $\theta \to 0$, $P_\theta = 1$ (Maezawa & Takagi, 1983; Wen, Arakawa & Philo, 1996), the zero angle limit is:

$$\lim_{\theta \to 0} \frac{Kc}{R_\theta} = \frac{1}{M_w} + 2A_2 c \qquad (3.6)$$

The limiting slope (m_c) of the zero angle projection at low concentration with respect to Kc yields the second virial coefficient, A_2 is:

$$m_c = \frac{2A_2}{k} \qquad (3.7)$$

On the other hand, as ($c \to 0$), the second virial coefficient term is negligible and the zero concentration limit gives:

$$\lim_{c \to 0} \frac{Kc}{R_{(\theta)}} = \frac{1}{M_w P_\theta} \qquad (3.8)$$

The limiting slope (m_θ) of the zero concentration projection with respect to $\sin^2\left(\frac{\theta}{2}\right)$ at low angle yields the mean-square radius (r_g^2) is:

$$m_\theta = \frac{16\pi^2 r_g^2}{3\lambda^2 M_w} \qquad (3.9)$$

The mutual intercept ($y_{c\theta}$) of the zero concentration and zero angle lines gives the reciprocal of the weight-average molecular weight.

$$y_{c\theta} = \frac{1}{M_w} \qquad (3.10)$$

The Debye Plot is similar to the Zimm plot except that the y-axis is the reciprocal of that used for the Zimm plot, i.e. $\frac{R_{(\theta)}}{Kc}$ versus $\sin^2\left(\frac{\theta}{2}\right)$. When $\theta \to 0$, $P_\theta = 1$ and the zero angle limit is:

$$\lim_{\theta \to 0} \frac{R_{(\theta)}}{Kc} = M_w - 2A_2 c M_w^2 \qquad (3.11)$$

The limiting slope (m_c) of the zero angle projection at low concentration with respect to Kc yields the second virial coefficient, A_2 is:

$$m_c = -\frac{2A_2 M_w^2}{k} \qquad (3.12)$$

On the other hand, the zero concentration limit gives:

$$\lim_{c \to 0} \frac{R_{(\theta)}}{Kc} = M_w P_\theta \qquad (3.13)$$

The limiting slope (m_θ) of the zero concentration projection with respect to $\sin^2\left(\frac{\theta}{2}\right)$ at low angle yields the mean-square radius (r_g^2) is:

$$m_\theta = -\frac{M_w 16\pi^2 r_g^2}{3\lambda^2} \qquad (3.14)$$

The mutual intercept ($y_{c\theta}$) of the zero concentration and zero angle lines gives the weight-average molecular weight.

$$y_{c\theta} = M_w \qquad (3.15)$$

The Berry method of data fitting is carried out by plotting Square root of $\sqrt{Kc/R_\theta}$ versus $\sin^2\left(\frac{\theta}{2}\right)$ as

$$\sqrt{\frac{Kc}{R_\theta}} = \frac{1}{\sqrt{M_w P_\theta}} + A_2 c \sqrt{M_w P_\theta} \qquad (3.16)$$

Usually, all methods provide similar results especially for small molecular weight species. The Zimm method is linear over a broad range of molecular weights. However, the method becomes less accurate for molecular weights over about one million Da (Stepan Podzimek 2001, personal communication, 24th Feb). The application of linear regression in the Zimm method sometimes requires discarding of outlying data at higher angles and concentrations. The deviation from linearity is related to molecular conformation (as conformation deviates from a random coil) (Wyatt, 1993). Higher order terms in $P_{(\theta)}$ may be employed to allow for non-linear behaviour of data points at higher angles and concentrations. Often, linear extrapolation is still possible near zero concentration and zero angles where the molecular parameters of interest (M_w, r_g^2, A_2) are obtained. The Zimm method is generally suitable for small to mid-size molecules ($(r_g^2)^{1/2}$ = 20-50nm) so that $P_{(\theta)}$ is close to unity. A higher polynomial to the angular variation (> 1) in the Zimm plot is usually necessary for molecules whose molecular weight is above 3.0 x 10^5Da.

If linear regression fails for most angles, the non-linear Debye plot is preferred especially for polymers of high molecular weights and larger root-mean-square (RMS) radius, denoted by $\left(r_g^2\right)^{1/2}$ (Wyatt, 1993). The Debye fit method is useful over a wide range of molecular weights. However, with increasing molecular weight, the Debye fit method usually requires higher order polynomials. In such a case, the Berry fit which requires lower order polynomials than the Debye method is preferred. Berry method is usually suitable for large molecules ($\left(r_g^2\right)^{1/2}$ ~ 100nm) with molecular weights ranging from 1 to 10 x 10^6Da (Hanselmann, Burchard, Lemmes & Schwengers, 1995; Yoo & Jane, 2002).

2.5.7.3 Multi-Angle Laser Light Scattering (MALLS)

The multi-angle laser light scattering (MALLS) photometer from Wyatt Technology (DAWN DSP, Santa Barbara, USA) employs the light scattering theory to calculate the molecular weight of macromolecules. A schematic diagram of the DAWN DSP photometer is shown in Figure 2.16. A laser (632.8nm) is used as a light source to

provide a monochromatic and a well-collimated beam. The laser beam passes into the solution, and the intensity of scattered light measured at different angles (typically 15-160°) by photodiodes spaced around the flow cell. At any one angle, solvent scattering is subtracted from solution scattering to ensure that the scattering used for the molecular weight calculation is due to the solute alone. However, accurate determination of the solute concentration is usually difficult for dilute solutions. As such, the specific refractive index increment (*dn/dc*) which appears in the light scattering equations must be separately and accurately measured at higher concentrations prior to determining the molecular parameters of macromolecules by light scattering. For a sample containing heterogeneous molecular species, *dn/dc* must be measured at each elution, and for polyelectrolytes, isoionic dilution procedures must be carried during sample dilution (Wyatt, 1993).

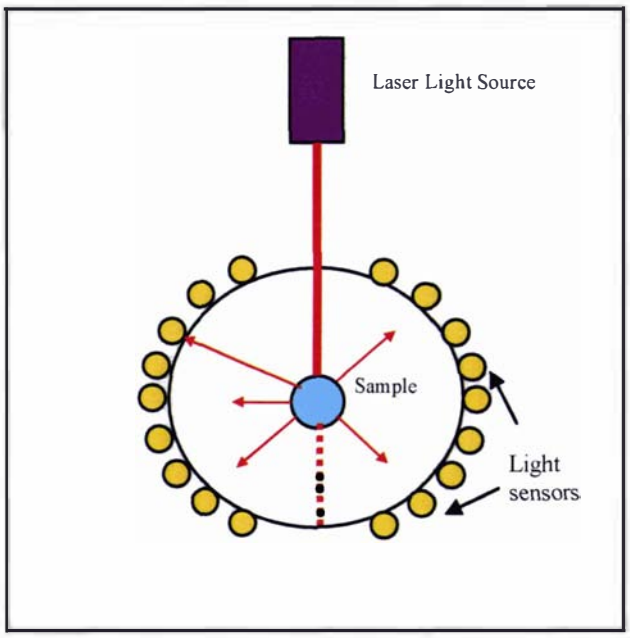

Figure 2.16 Schematic of the DAWN DSP photometer.

The following section discusses the two different modes, namely, the batch and chromatography modes, in which the MALLS can be operated.

2.5.7.3.1 Batch mode

In the batch mode, a series of dilute polymer concentrations is required and the intensities of light scattered at each concentration are measured by photodiodes at

several angles. Determination of weight-average molecular weight (M_w), the z-average mean-square radius $\left(r_g^2\right)_z$, and the second virial coefficient (A_2) can be determined by means of the Zimm, Debye or Berry plot.

2.5.7.3.2 Chromatography mode

In the chromatography mode, different molecular species are first separated using a gel filtration chromatography (GFC) column according to their hydrodynamic size. The largest molecules pass through the column and elute first while the smaller species are retained in the interstices of the column packing material and elute last. It is important to note that the column separation assumes that each volume contains a monodispersed fraction and thus possess a unique molecular weight. However, the molecular weight at each volume is only as good as the separation of the column (Shortt, 1993). If the molecular species are poorly separated, then each elution slice will contain a broad range of molecular weights and the results obtained are an average of a broad range of molecular weights. This is true for highly branched molecules where size varies only over a narrow range as opposed to linear molecules where the size varies over a broad range of molecular weights.

The Astra software (version 4.5) from Wyatt Technology displays light scattering chromatograms representing different molecular species eluting from the column. Scattered light at 90° is commonly used to obtain the highest scattering signal (Takagi, 1990; Wen et al., 1996). The data obtained from each slice of the chromatogram can be fitted using models such as the Debye, Zimm or Berry equation. The Astra software provides the options for selecting the best model that fits the light scattering data.

Additional information such as the polydispersity index and the concentration of the material eluting in small, individual slices of the GFC chromatogram can also be determined (Wyatt, 1993). In the chromatography mode, the second virial coefficient (A_2) is often ignored since the concentration of the molecules is very low by the time

they reach the light scattering detector (Wyatt, 1993). The following section defines some of the terminologies commonly used in light scattering theory.

2.5.7.4 Molecular weight distribution

Since it is typical of macromolecules to consist of a mixture of many molecular species, molecular weights are often expressed as average values. The molecular weight averages can be expressed as number-average, weight-average or z-average. The number-average molecular weight (M_n) is obtained by:

$$M_n = \frac{\sum c_i}{\sum (c_i / M_i)} \qquad (3.17)$$

The weight-average molecular weight (M_w) is expressed as:

$$M_w = \frac{\sum (c_i M_i)}{\sum c_i} \qquad (3.18)$$

The z-average molecular weight is obtained by:

$$M_z = \frac{\sum c_i M_i^2}{\sum c_i M_i} \qquad (3.19)$$

where c_i, and M_i is the concentration and molecular weight of the i^{th} slice.

2.5.7.5 Mean-square radius

The mean-square radius of a macromolecule can be determined from the angular dependence of the intensities of scattered light. The mean-square radius is generally defined as "the distance from the center of mass of a body at which the whole mass could be concentrated without changing its moment of rotational inertia about an axis through the center of mass" (Rudin, 1982a, p.92). It is given by the sum over all distances of the scattering elements from the center of mass or the sum of all intramolecular distances in the macromolecule (Burchard, 1994a) and depends on the internal mass distribution of the molecules. However, it does not measure the molecule's external geometry (Wyatt, 1993) and there are no assumptions made about the shape of the macromolecule, whether it is a sphere, random coil, rod, etc. The

mean-square radius can be expressed as number-average $\left(r_g^2\right)_n$, weight-average $\left(r_g^2\right)_w$ or z-average $\left(r_g^2\right)_z$ and are described by the following equation:

$$< r_g^2 >_n = \frac{\sum (c_i / M_i) r_i^2}{\sum (c_i / M_i)} \qquad (3.20)$$

$$< r_g^2 >_w = \frac{\sum c_i r_i^2}{\sum c_i} \qquad (3.21)$$

$$< r_g^2 >_z = \frac{\sum c_i r_i^2 M_i}{c_i M_i} \qquad (3.22)$$

where r_i^2 is the mean-square radius and M_i is the molecular weight at i^{th} slice.

The above equations used in the Astra software are based on the corresponding average molecular weights (i.e. M_n, M_w, M_z) with an assumption of a random coil conformation where mean-square radius of each molecular species is proportional to its molecular weight and is not based on true moments of a statistical distribution (Wyatt, 1993).

In Dawn DSP MALLS, the mean-square radius is presented in Astra as the RMS radius $\left(r_g^2\right)^{1/2}$, also known as the radius of gyration. The MALLS can estimate RMS radius of molecular species greater than 1/20th of the incident light (laser beam of 632.8nm). As such, a value of less than 15-20nm cannot be reliably estimated (Dollinger, Cunico, Krunitani, Johnson & Jones, 1992). At low angle, the RMS radius becomes negligible as described in equation (3.6). If additional information, such as the shape of the macromolecule is available, the dimension of the macromolecule can be estimated. For a random coil, where N is the number of units of length L,

$$\left(r_g^2\right)^{1/2} = \sqrt{\frac{N}{6L}} \qquad (3.23)$$

For a sphere where r is the radius of sphere,

$$\left(r_g^2\right)^{1/2} = \sqrt{\frac{3}{5r}} \qquad (3.24)$$

For a rod where L is the length of rod,

$$\left(r_g^2\right)^{1/2} = \sqrt{\frac{1}{12L}} \qquad (3.25)$$

2.5.7.6 Polydispersity index

In biopolymers such as polysaccharides, the molecular species contain more than a single molecular weight. While the weight-average molecular weight defines the central tendency of the molecular weight distribution, the spread is defined by the polydispersity index. The spread of a distribution reflects the distribution of the molecular weights of the sample about their mean. The difference between M_w and M_n provides a measure of the degree of heterogeneity in the molecular weight distribution (Flory, 1953). Therefore, the ratio of M_w/M_n is often used as a measure of the polydispersity index of the sample. Larger values of M_w/M_z indicate a very wide spread while a truly monodispersed macromolecule has M_w/M_n equal to unity. It is always true that $M_z > M_w > M_n$, with the equality occurring only if all the species in the sample have the same molecular weight (i.e. monodispersed). However, such polymeric materials have not been possible to synthesise at present. The smallest polydispersity ratio that has been obtained is that of polystyrenes from very careful anionic polymerisation that have M_w/M_n ratio as low as 1.04 (Rudin, 1982b).

2.5.7.7 Second Virial Coefficient (A_2)

In light scattering, the second virial coefficient $\left(A_2\right)$ is used to determine the macromolecules-solvent interaction. It can be obtained by Zimm, Debye or Berry plot method using a series of macromolecule concentrations with the MALLS operating in the batch mode (Rudin, 1982b).

There are several factors influencing the A_2 values. These include the nature of macromolecule and solvent, the molecular weight distribution and concentration of the macromolecule, the temperature of solution, and the presence or absence of branching of the macromolecule chain. The value of A_2 decreases with increasing molecular weight of the solute and increasing branching of the molecular structure. Both factors tend to result in more compact structures, which are less swollen by the solvent. Better solvents on the other hand, result in more highly swollen structures and hence, higher A_2 values.

As the temperature of the solvent increases, most macromolecules become more soluble. Hence, A_2 increases with temperature. As the temperature is reduced to a sufficiently low temperature, A_2 may actually be zero. This is known as the Flory-theta temperature, which is defined as the temperature at which the particular macromolecule becomes unperturbed even at high dilution in a particular solvent. A solvent at which the theta temperature is experimentally attainable is known as a theta solvent for the particular macromolecule. Under theta conditions, the diameter of the macromolecule chain in solution is similar to the diameter of the bulk macromolecule in amorphous form at the same temperature. The macromolecule segment does not attract the solvent molecules to penetrate its chain structure (Sun, 1994). The segment-segment repulsive forces and the segment-solvent attractive forces are exactly compensated by the segment-segment attractive forces. The solvent neither swells nor shrinks the macromolecule and it is said to be in its "unperturbed" state. The macromolecules which are unperturbed by the solvent are separated far enough from each other so that they are not entangled. The attraction of macromolecule segments to each other achieves the exclusion of the solvent molecules. Consequently, the excluded volume becomes smaller and the overall macromolecule become compact and the RMS radius will also decrease. Theta solutions are not normally used for molecular weight measurements, because they are on the verge of precipitation (Rudin, 1982b). If A_2 is less than zero, the solvent is considered a poor solvent. The macromolecule may precipitate from the solution when A_2 is a large negative number.

When a macromolecule is in a good solvent, polymer-solvent interactions are strong. The macromolecule allows the solvent to interact with and penetrate its chain structure filling its holes and cavities. No two segments in the same chain can come close together due to a repulsive force between macromolecule segments.

2.5.7.8 Specific refractive index increment (dn /dc)

The specific refractive index increment, denoted by *dn/dc*, describes how much refractive index of a macromolecule solution changes with respect to the concentration of the solute, expressed as mL/g (Wyatt, 1993). A key requirement for the determination of molecular weight from light scattering is the value of *dn/dc*. The *dn/dc* value is dependent on the wavelength of the light source. For some compounds, the *dn/dc* values can be obtained from the lists compiled by (Huglin, 1972; Theisen et al, 2000). The *dn/dc* must be obtained for an unknown molecular species before determining the M_w and $\left(r_g^2\right)^{1/2}$.

2.5.7.9 Molecular conformation

The RMS radius of a macromolecule in solution depends on the molecular weight, its structure (extent of branching) and the degree to which it is swollen by the solvent. In many cases, RMS radius can be described by the power-law behaviour:

$$\left(r_g^2\right)^{1/2} = KM_w^{\nu} \qquad (3.26)$$

where K is a constant and ν is the exponent. For a random coil in a good solvent, ν ~0.6, for a rigid rod, ν ~1, and for spherical shape molecules, ν ~0.33 (Burchard, 1994b; Wyatt, 1993). The geometrical dimension of linear molecules can be predicted from a log-log plot of $\left(r_g^2\right)^{1/2}$ as a function of M_w (based on relatively narrow mass distribution), and the exponent (ν) can then be determined from the gradient. However, a good separation of the molecular species must be present, otherwise the procedure yields erroneous results (Wyatt, 1993).

2.5.7.10 Characterisation of polysaccharides by static light scattering

The technique of static light scattering has been widely used to characterise the molecular weight, size and conformation of polymers (including polysaccharides) in dilute solutions. In solution, polysaccharides can adopt the conformation of random coils, rod-like chains, helices, or form aggregates depending on solvent conditions (Ding, Jiang, Zhang & Wu, 1998). Characterisation of food polysaccharides is not a simple task because of their complex structure (compared to synthetic polymers), high polydispersity, presence of charged groups (as in the case of polyelectrolytes) and their ability to form aggregates (Fishman, Rodriguez & Chau, 1996; Harding, 1995). Moreover, low molecular weight impurities such as proteins present can complicate analysis of experimental data (Capron, Grisel & Muller, 1995). The aggregation of polysaccharide molecules is a major problem hampering the effectiveness of the light scattering technique. Some examples of polysaccharides that have the ability to aggregate include carrageenans, pectins, hyaluronic acid, alginates gellan and xanthan (Anthonsen, Varum, Hermansson, Smidsrod & Brant, 1994). Light scattering studies of aggregated polysaccharide may result in distorted Zimm plots or yield negative second virial coefficients (Anthonsen et al., 1994; Chapman, Morris, Selvendran & O'Neill, 1987). Different procedures have been employed to obtain solutions without contamination from aggregates. Some of these procedures include heating, enzyme treatment, chemical treatment (e.g. dimethyl sulfoxide) filtration, ion exchange, ultracentrifugation, ultrafiltration, sonication, etc (Capron et al., 1995; Chanliaud, Roger, Saulnier & Thibault, 1996). Therefore, a proper procedure to prepare polysaccharide solutions for light scattering studies is essential to obtain meaningful results.

Chapter 3

Observation of Exopolysaccharides in Culture Media by Confocal Laser-Scanning and Scanning Electron Microscopic Techniques

3.1 INTRODUCTION

Many bacterial strains secrete extracellular polymeric substances that are viscoelastic in nature. The majority of these extracellular polymers are polysaccharides. In some strains of bacteria, these polysaccharides can occur on the surface of cells. This layer is referred to as 'glycocalyx', 'capsule' or 'slime layer', depending on the degree of adhesion to the surface of the cell wall. In most cases, the polysaccharides are secreted into the environment in the form of slime (De Vuyst et al., 2001). When this occurs, the polysaccharides are then known as exopolysaccharides (EPSs).

Various microscopy techniques, including light microscopy, electron microscopy, confocal laser scanning microscopy (CLSM) and atomic force microscopy (AFM), have been used to probe the structural, topological and geometrical characteristics of biological materials. Each technique is based on different operational principles and provides different insights into the physical characteristics of biological systems. Atomic force microscopy has been employed to study the structure of purified polysaccharides (Brant, 1999; Kirby, Gunning & Morris, 1995; Kirby, Gunning, Morris & Ridout, 1995; Morris et al., 1997). However, the use of AFM was considered unsuitable for imaging EPS in a culture medium due to interference from components such as proteins and other insoluble materials, which are not easily differentiated from EPS in AFM images.

In this chapter, a novel and non-invasive procedure using CLSM was developed to probe the location and distribution of EPS in culture media. The images obtained using CLSM were evaluated together with those obtained through scanning electron microscopy (SEM). The effects of pH on the structural characteristics of the culture media were also investigated using both SEM and CLSM.

3.2 MATERIALS AND METHODS

3.2.1 Culture media preparation

The bacterial strain used for this investigation, *Lactobacillus delbrueckii* subsp. *bulgaricus* NCFB 2483 (NCIMB 702483), was obtained from the National Collection of Industrial and Marine Bacteria (Aberdeen, Scotland) and denoted as 2483. The seed culture of 2483 was grown in 10% (w/v) reconstituted skim milk (RSM) at 37°C for 24 h. The seed culture was inoculated (1% v/v) into different growth media and incubated at 37°C for 24 h. The culture media and treatments applied were as follows:

- Milk permeate (Fonterra Co-operative Group Ltd, New Zealand) + 0.5% (w/v) yeast extract (Gibco-BBL). Note that the milk permeate was a by-product of the ultrafiltration of skim milk.
- Milk permeate + 0.5% (w/v) yeast extract + 5% (w/v) skim milk powder (SMP) (Fonterra Co-operative Group Ltd, New Zealand)
- Milk permeate + 0.5% (w/v) yeast extract + 5% (w/v) SMP with Flavourzyme [1] (Novozymes Ltd, Bagsvaerd, Denmark) treatment
- Milk permeate + 0.5% (w/v) yeast extract + 5% (w/v) SMP with Flavourzyme treatment and pH adjusted to 8, 9 or 10 using 1M NaOH (Sigma-Aldrich)

Flavourzyme treatment was carried out by adding 100μL of 10% (w/v) Flavourzyme solution (prepared in Milli-Q water) to a 10g sample and incubating in a water bath shaker at 50°C for 4 h. Control samples which included a milk permeate medium containing 5% (w/v) SMP plus 0.5% (w/v) yeast extract (without 2483), a 5% (w/v) lactose (Sigma-Aldrich) solution and a 3% (w/v) galactose (Sigma-Aldrich) solution were prepared. In addition, two non-'ropy' strains of LAB, namely *Streptococcus thermophilus* (ST1) and *Lactobacillus helveticus* (LH30) (Fonterra Co-operative Group Ltd, New Zealand) were grown in a milk permeate medium containing yeast extract (0.5% w/v) and SMP (5% w/v) at 37°C for 24 h.

[1] Flavourzyme is a fungal protease/peptidase complex developed for protein hydrolysis under neutral or slightly acidic conditions.

3.2.2 Sample preparation for confocal laser-scanning microscopy

Each sample (50 μL) was mixed with 50 μL of 0.1% (w/v) fluorescent lectin (Lectin SBA from *Glycine max* – soybean, Alexa Fluor 488 conjugate L-11271, Molecular Probes, Eugene, Oregon, USA) solution on a glass slide. A cover slip was then placed on the sample. The preparation was left for ~30 min in the dark at room temperature. Subsequently, the samples were viewed using a CLSM (Leica TCS 4D MMRBE, Leica Lasertechnik, Heidelberg, Germany) equipped with an argon/krypton laser source and a 100X oil immersion objective lens to give a 1000X magnification.

3.2.3 Sample preparation for scanning electron microscopy

The preparation of samples for SEM was adapted from the procedures described by Schellhaass and Morris (1985). A template of cylindrical studs (diameter: 4mm and length: 10mm) was made and used (see Figure 3.1) to create cavities in the agar for sample encapsulation.

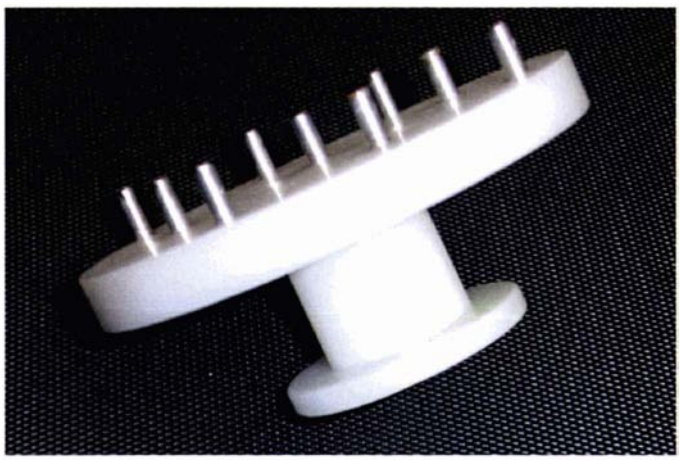

Figure 3.1 A template of cylindrical studs used as a mould to create cavities for encapsulating samples in agar.

A 3% (w/v) agar solution was poured almost to the brim of the petri dish and the cylindrical studs were immersed in the agar solution. The template was removed when the agar had solidified, leaving behind cylindrical cavities. Approximately 20μL of sample was dispensed into each of the cylindrical cavities. This was subsequently overlaid with the agar and allowed to solidify at room temperature. After solidification, small cubes encapsulating the sample were cut from the agar.

The agar cubes were fixed overnight in 3% glutaraldehyde (Sigma-Aldrich) prepared in 0.1M cacodylate buffer (pH 7.2) (Sigma-Aldrich). They were rinsed three times with diluted cacodylate buffer (1x 0.1M cacodylate: 1x water) at 5 min intervals. Secondary fixation was carried out using 1% osmium tetroxide (OsO_4) (ProSciTech, Queensland, Australia) in 0.1M cacodylate buffer for 1 h and followed by three rinses of the diluted cacodylate buffer. The fixed samples were subjected to dehydration using a series of increasing concentrations of acetone (25%, 40%, 60%, 70%, 90% and two changes of 100% for 20 min each). The final dehydration step involved a Polaron E300 Critical Point Dryer (Bio-Rad/EBS, Agawam, MA, USA) with liquid CO_2. Each sample was mounted on double-sided tape glued to an aluminum supporter and sputter coated with gold in a sputter coater (Bal-Tec SCD 050, Liechtenstein, Switzerland). The specimen was then viewed using the 250 MK III Scanning Electron Microscope (Stereoscan, Cambridge, UK).

3.3 RESULTS AND DISCUSSION

3.3.1 Probing EPS by CLSM

In this study, the selection of a suitable fluorescent label was based on its affinity for β-galactopyranosyl residues reported to be present in many EPSs structures of LAB (Gruter et al., 1993). Among the many fluorescent stains available commercially, Lectin SBA Alexa Fluor was selected since it binds the terminal α-, β-N-acetylgalactosamine and galactopyranosyl residues. Other fluorescent dyes such as Cellufluor (Easson, Sinskey & Peoples, 1987) and Calcofluor White M2R (Weaver & Zibilske, 1975) were also evaluated using a fluorescence (UV) microscope. However, both the bacterial cells and the EPS were stained by both Cellufluor and Calcofluor White M2R dyes. These two fluorescent stains were too general for targeting the EPS alone because of their affinity for β(1→3) and β(1→4) glycosyl linkages. Note that the application of fluorescent lectin conjugates to stain EPSs was a new concept and had not been reported when the work was carried out. However, recently a similar method of staining EPS using wheat germ agglutinin Alexa Fluor 488 has been reported (Hassan, Frank & Qvist, 2002).

The use of CLSM technique in conjunction with Lectin SBA Alexa Fluor conjugate was found to be effective for imaging the location and distribution of 2483 EPS in a culture medium. In the CLSM micrographs shown in Figures 3.2a to 3.2f, only the EPS was stained. Note that all micrographs shown are representative of the sample. The control samples (without bacterial culture), namely milk permeate containing 5% (w/v) SMP and 0.5% (w/v) yeast extract; 5% (w/v) lactose; and 3% (w/v) galactose solutions, showed no image. From the micrographs, the EPS was found to be distributed as aggregates in the fermented system. Many more EPS aggregates could be seen in the medium containing SMP. This was consistent with the different levels of EPS determined through analysis (~150mg/L as opposed to ~400mg/L). The different levels of brightness were probably due to the partial obscuration of the fluorescence by the coagulated protein matrix. When the protein matrix was removed by enzymic hydrolysis, the EPS aggregated into larger clusters.

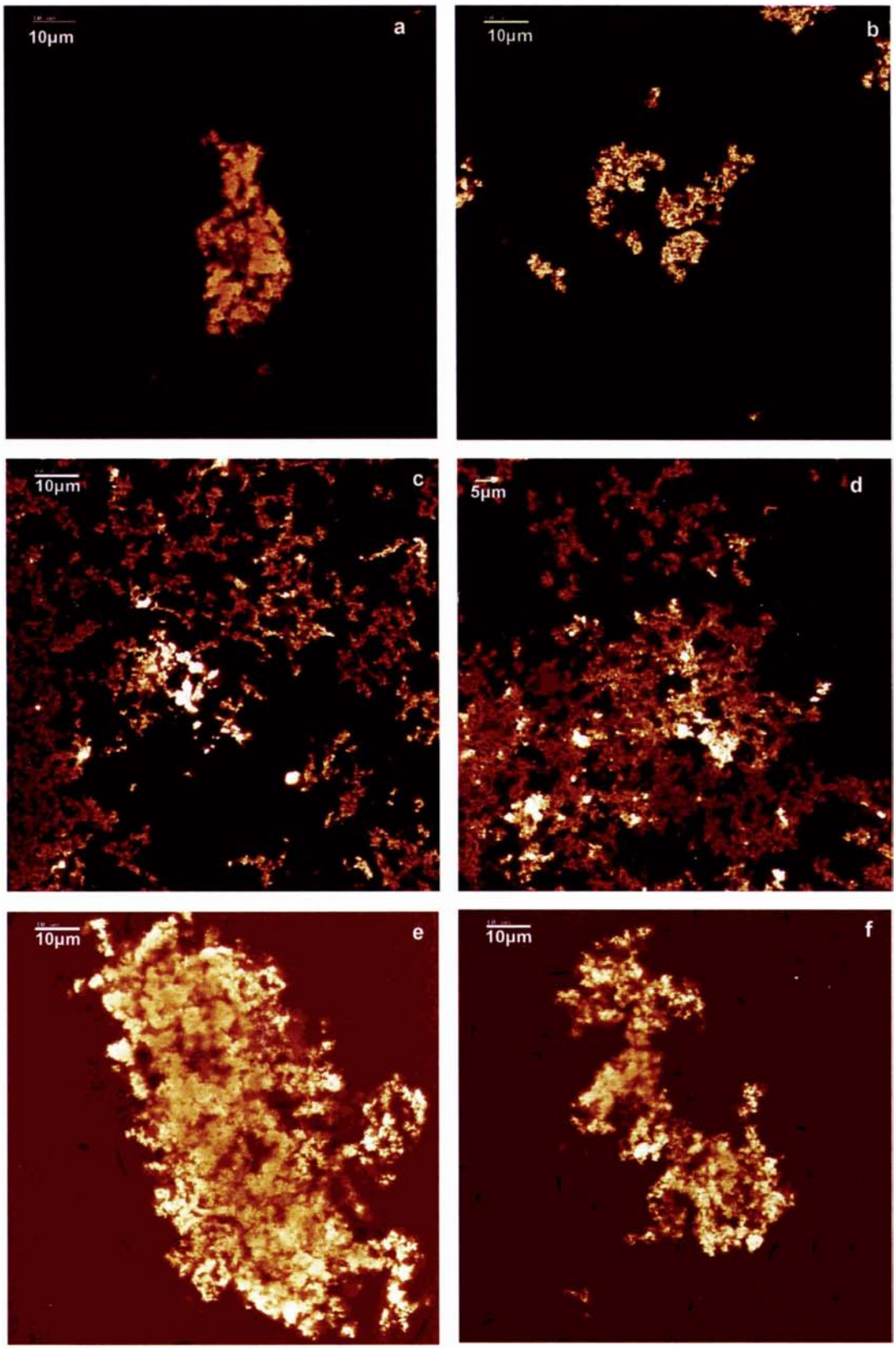

Figure 3.2 Micrographs obtained from CLSM showing 2483 EPS stained with Lectin SBA Alexa Fluor conjugate; (a & b) EPS in a milk permeate containing 0.5% (w/v) yeast extract, (c & d) EPS in a milk permeate containing 0.5% (w/v) yeast extract and 5% (w/v) SMP, (e & f) EPS in a milk permeate containing 0.5% (w/v) yeast extract and 5% (w/v) SMP with Flavourzyme treatment at pH 7.

It was also noted that the bacterial cells were not visible under the laser beam, indicating that the EPS was not accumulated on the bacterial cell surface as a slime layer. This was confirmed by the Maneval staining method (Corstvet, Gentry, Newman, Confer & Rummage, 1982; Maneval, 1941) performed using a light microscope which showed that no capsular polysaccharide was present for 2483 (see Appendix A).

3.3.1.1 Lectin conjugates and EPS of 'non-ropy' strains

A separate experiment was conducted using 'non-ropy' strains of *Streptococcus thermophilus* (ST1) and *Lactobacillus helveticus* (LH 30) grown in 10% (w/v) skim milk media. Micrographs obtained (not shown) indicated that EPSs were also produced by the 'non-ropy' cultures. The absence of 'ropy' characteristics in the ferment of a LAB culture therefore does not indicate the absence of EPS. The EPS produced by the 'non-ropy' strains merely had different rheological properties due to the differences in size and conformation of the EPS molecules. It was also found that the levels of EPS produced by the 'non-ropy' strains were lower (~60-90mg/L) compared with the levels of 2483 EPS (~150mg/L) in milk permeate culture medium. The results indicated that the SBA lectin conjugates can be used effectively to detect EPS regardless of its rheological properties, as long as there are terminal α- and β-N-acetylgalactosamine and/or galactopyranosyl residues present in the polymer structure.

3.3.1.2 Future applications of lectin conjugates in EPS studies

Commercially, many lectins with affinity for different sugar residues are available from various sources. Some examples of lectins include Concanavaline A with specificity for terminal α-D-mannosyl and α-D-glucosyl residues, *Anguilla anguilla* with specificity for α-L-fucosyl residues, and *Bandeiraea simplicifolia* with specificity for terminal α-D-galactosyl and N-acetyl-α-D-galactosaminyl residues. In some polysaccharides such as gellan, pectin, gum arabic (Baird & Smith, 1989), and EPSs produced by different strains of LAB (Ricciardi et al., 2002; Urashima et al., 1999; van Casteren, Dijkema, Schols, Beldman & Voragen, 1998; van den Berg et al., 1995), rhamnose is a common sugar found among the repeat units of the polymer molecules. Since rhamnose is not a common sugar used in growth media, its presence can be used as an effective detection site for many EPSs. The use of rhamnose as a detection site is effective because it is

easier to determine the composition of polysaccharides (e.g. by high performance liquid chromatography) than to unravel the terminal ends of the sugar residues (e.g. by methylation analysis) of different EPS molecular structures. The use of a lectin specific only to rhamnose may improve the accuracy for targeting EPS. Although lectins specific to rhamnose have been isolated from the eggs of catfish (Hosono et al., 1999), they are not commercially available.

An area that is worth further investigation is the use of fluorescent lectin conjugates, based on the principles of enzyme-linked-immunosorbent assay (ELISA), to quantify the intensity of fluorescence and to relate that intensity to EPS level. In addition, apart from fluorochrome, lectin conjugated with other compounds such as electron-dense gold and enzyme-linked peroxidase can be used as labels for electron microscopy and colourimetric methods for detecting EPS respectively. These types of lectin conjugates are already available commercially but have not yet been explored for this purpose. If however, in the event that no lectins or stains are specific for an EPS, the fluorescent-antibody technique (Corstvet et al., 1982) for making highly specific labels could be considered.

3.3.2 Probing EPS by SEM

The micrographs of the 2483 culture obtained using SEM (Figures 3.3 and 3.4) were comparable to typical 'ropy' cultures (Bottazzi & Bianchi, 1986; Schellhaass & Morris, 1985; Skriver et al., 1995; Toba et al., 1990). In the milk permeate medium, bacterial cells could be seen entrapped in a web matrix (Figure 3.3). The web matrix was much thicker in the culture medium containing SMP and obscured the bacterial cells (Figure 3.4). Among the web matrix were aggregates which appeared to be present in larger quantities in the medium containing SMP. When the medium containing SMP was treated with Flavourzyme to hydrolyse the milk proteins, the aggregates were largely reduced but the web structure still remained (Figure 3.5a). The aggregates were most likely to be proteins whereas the web matrix was likely to be the EPS. A lactose crystal could also be seen (Figure 3.5b), and the bacterial cells had fallen out of the web (Figure 3.5c).

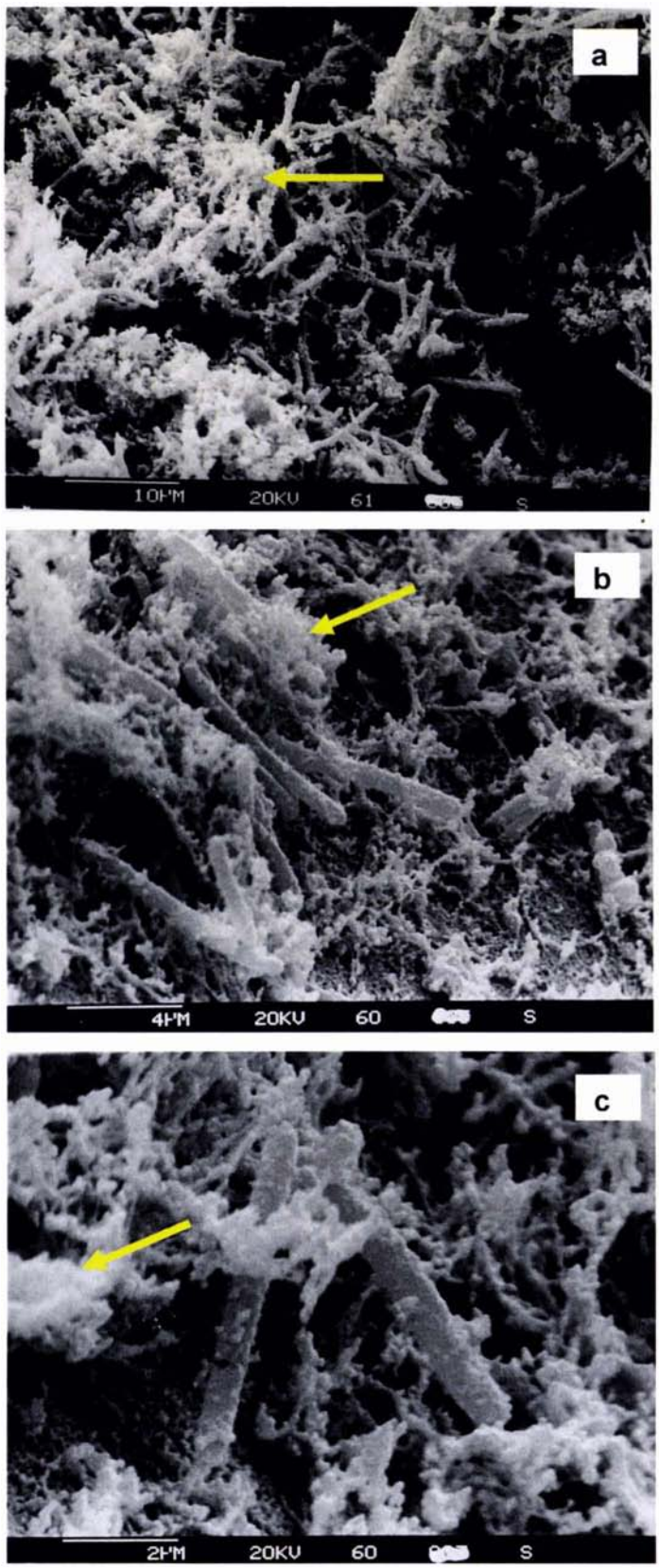

Figure 3.3 Micrographs of 2483 culture grown in a milk permeate medium containing 0.5% (w/v) yeast extract obtained using SEM. Arrows indicate protein aggregates. (a) 2000X magnification; (b) 5000X magnification and (c) 10,000X magnification.

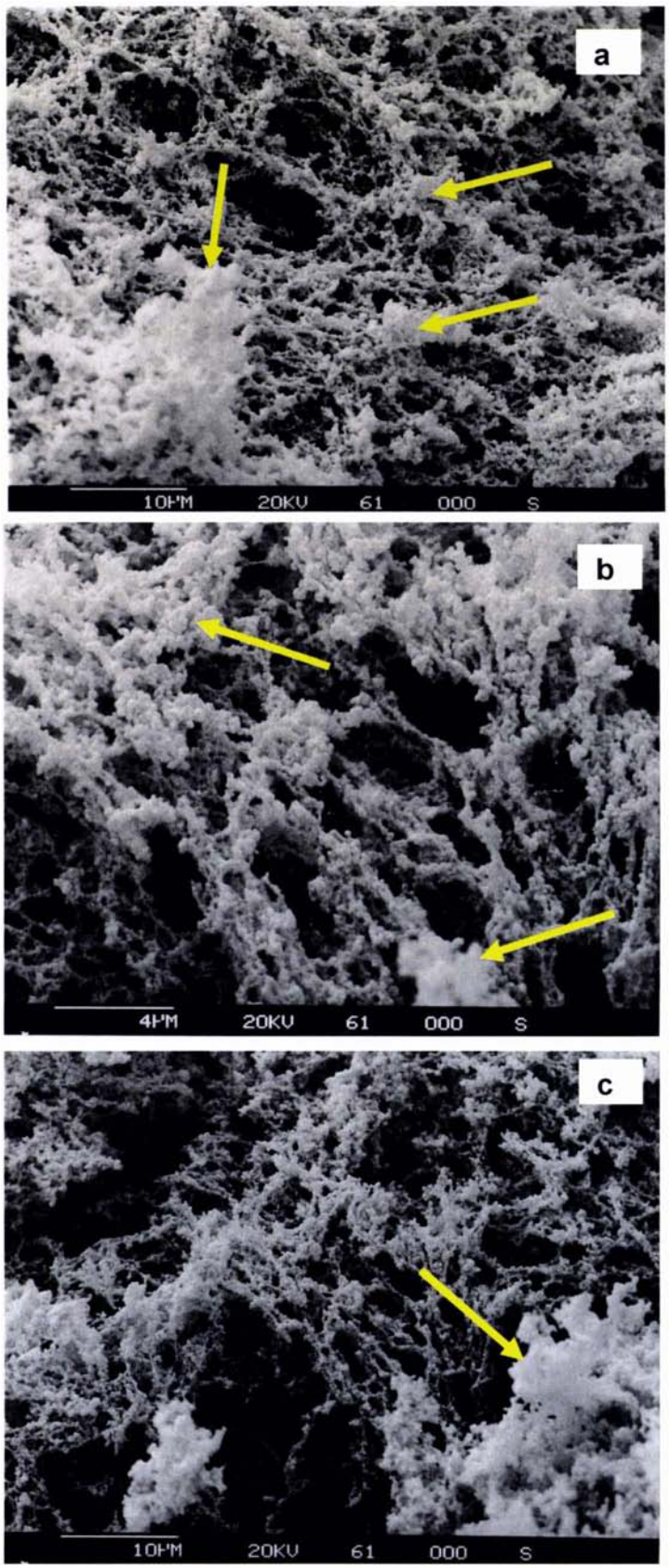

Figure 3.4 Micrographs of 2483 culture grown in a milk permeate medium containing 0.5% w/v yeast extract and 5% (w/v) SMP obtained using SEM. Arrows indicate protein aggregates. (a & c) 2000X magnification and (b) 5000X magnification.

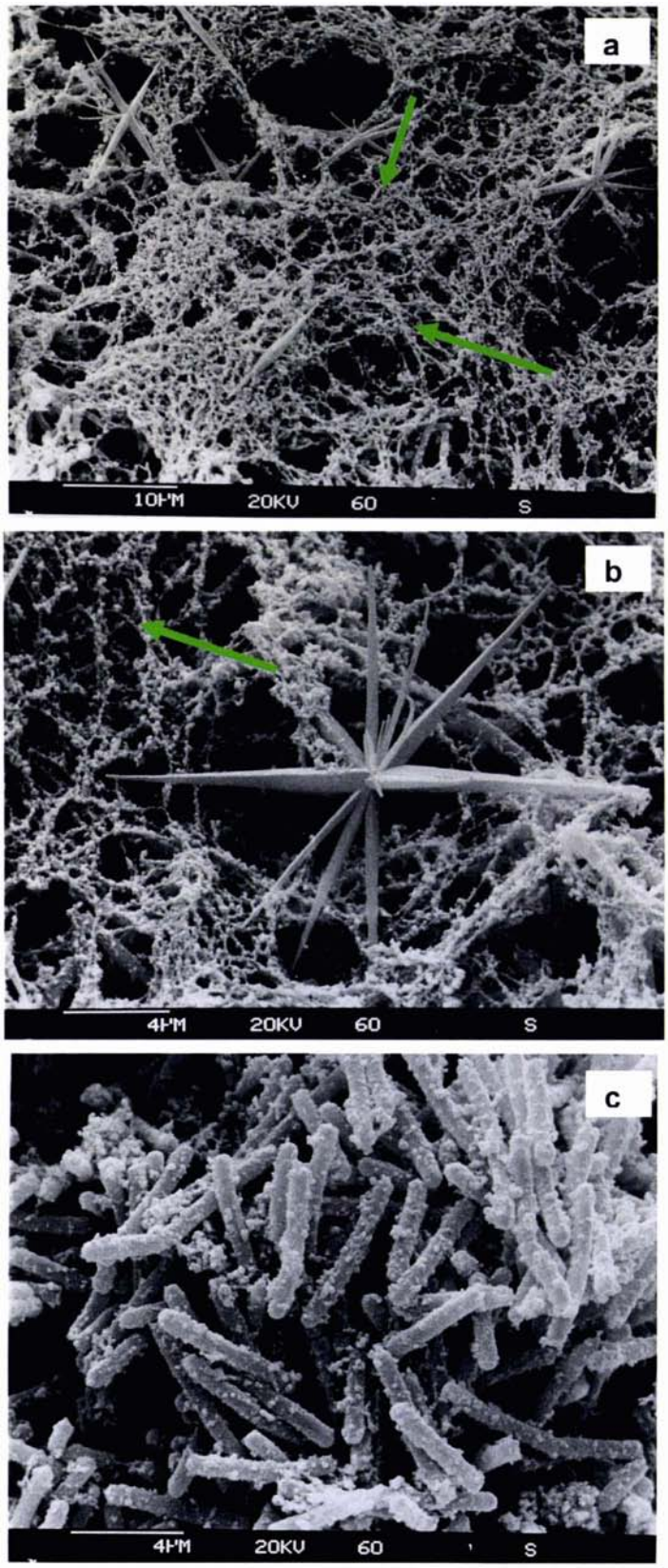

Figure 3.5 Micrographs of 2483 culture grown in a milk permeate containing 0.5% (w/v) yeast extract and 5% (w/v) SMP with Flavourzyme treatment (50°C, 4h) obtained using SEM; (a & b) Arrows show distinct web EPS matrix after Flavourzyme treatment, (c) most of the bacterial cells trapped in the protein aggregates were released upon Flavourzyme treatment.

3.3.2.1 EPS web structure formation in SEM micrographs

The changes seen in the CLSM and SEM micrographs can be explained by the illustration given in Figure 3.6. When the pH is decreased to 3.9 after 24h fermentation at 37°C, casein micelles are destabilised and form a gel with a series of channels and pores through which the EPS in the continuous phase can flow. In the culture medium, the bacterial cells are entrapped within and around the protein matrix. The bacterial cells are believed to be partially responsible for the void spaces in the protein matrix (Kalab et al., 1983; Toba et al., 1990). The EPS produced by the bacteria filled the interstices and channels of the protein matrix and reinforced the protein matrix structure possibly through EPS-protein interactions. This explains why yoghurt made with a 'ropy' culture usually reduces syneresis (Cerning, 1995; Sikkema & Oba, 1998). Figure 3.6b shows the distribution of EPS within the protein matrix. The bacterial cells have been deliberately excluded to simplify the illustration. During the critical point drying stage of SEM processing, the removal of moisture in the system leads to shrinkage and concentration of the EPS, resulting in the observed web structure. The proteins appear as deposits and aggregates among the web structures. This is illustrated in Figure 3.6c. In the protein hydrolysed samples, the SEM micrographs reveal a more distinct EPS web structure, which remains intact subsequent to Flavourzyme treatment. The web structure shows how the EPS was distributed in the protein matrix (Figure 3.6d).

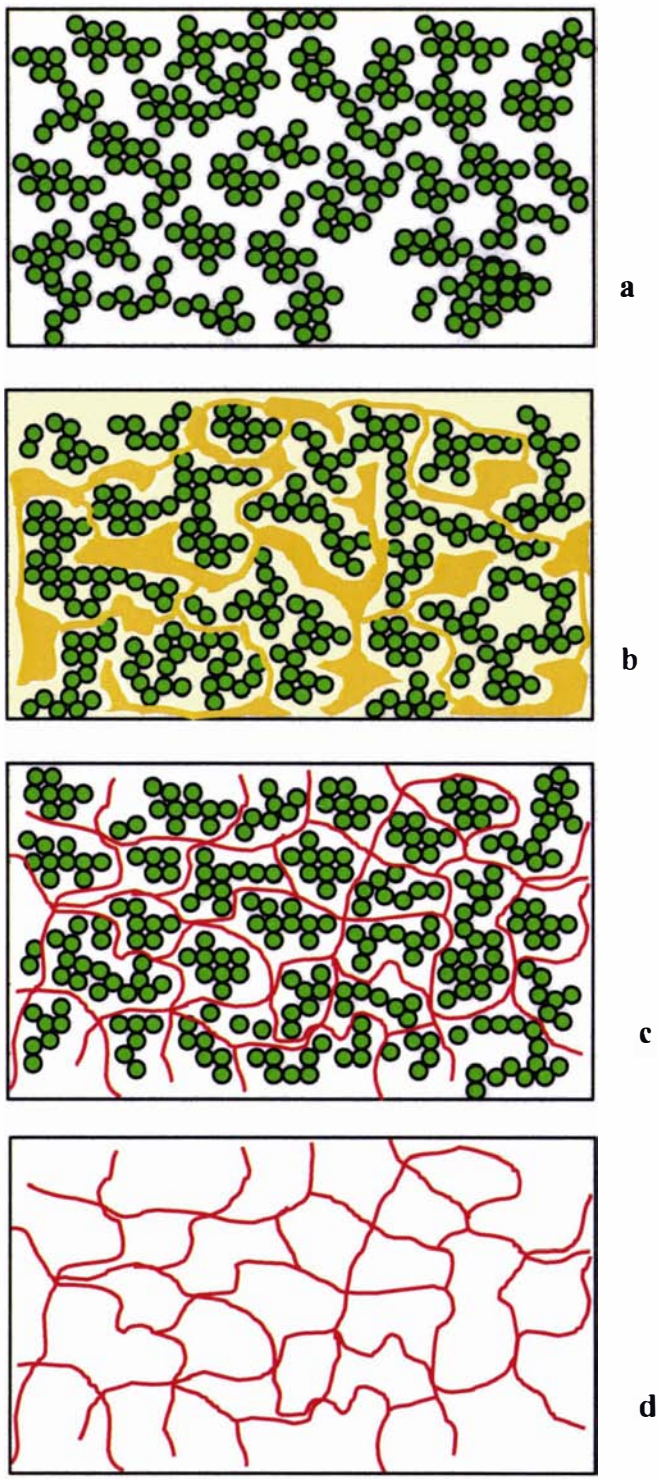

Figure 3.6 (a) Protein aggregates forming a matrix at low pH in the fermented culture medium; (b) EPS filled the interstices of the protein matrix; (c) Web structure of EPS formed within the protein matrix observed after SEM critical point drying; (d) Distinct web EPS remained after Flavourzyme treatment observed after SEM critical point drying.

3.3.3 Effect of pH on EPS

The effects of increasing pH on the EPS in a 2483 culture medium were investigated using the CLSM and SEM. The culture medium used was a milk permeate-based medium containing 0.5% (w/v) yeast extract and 5% (w/v) SMP. Increasing the pH of culture medium from 3.9 to 10 with 1M NaOH led to a progressive reduction of EPS aggregates observed by CLSM. At pH 10, no EPS could be seen (Figure 3.7).

Under the condition of increasing pH, it was noted that the viscosity and 'ropy' characteristics were reduced markedly. The reduction in viscosity was not only due to the probable modification of the EPS structure but also to the dissociation of the casein aggregates. At pH 10, the extent of protein aggregation was markedly reduced as seen in the micrographs obtained using SEM (see Figure 3.8). The original 'ropy' characteristic of the culture medium could hardly be detected. The EPS web structure was also largely destroyed as seen in the Flavourzyme treated sample at pH 10 (Figure 3.9). This suggests that the native EPS chemical structure is modified and disrupted under the alkaline pH. However, at this pH, the bacterial cells remain intact. The effect of high pH on EPS functionality has not been previously reported and would require further studies.

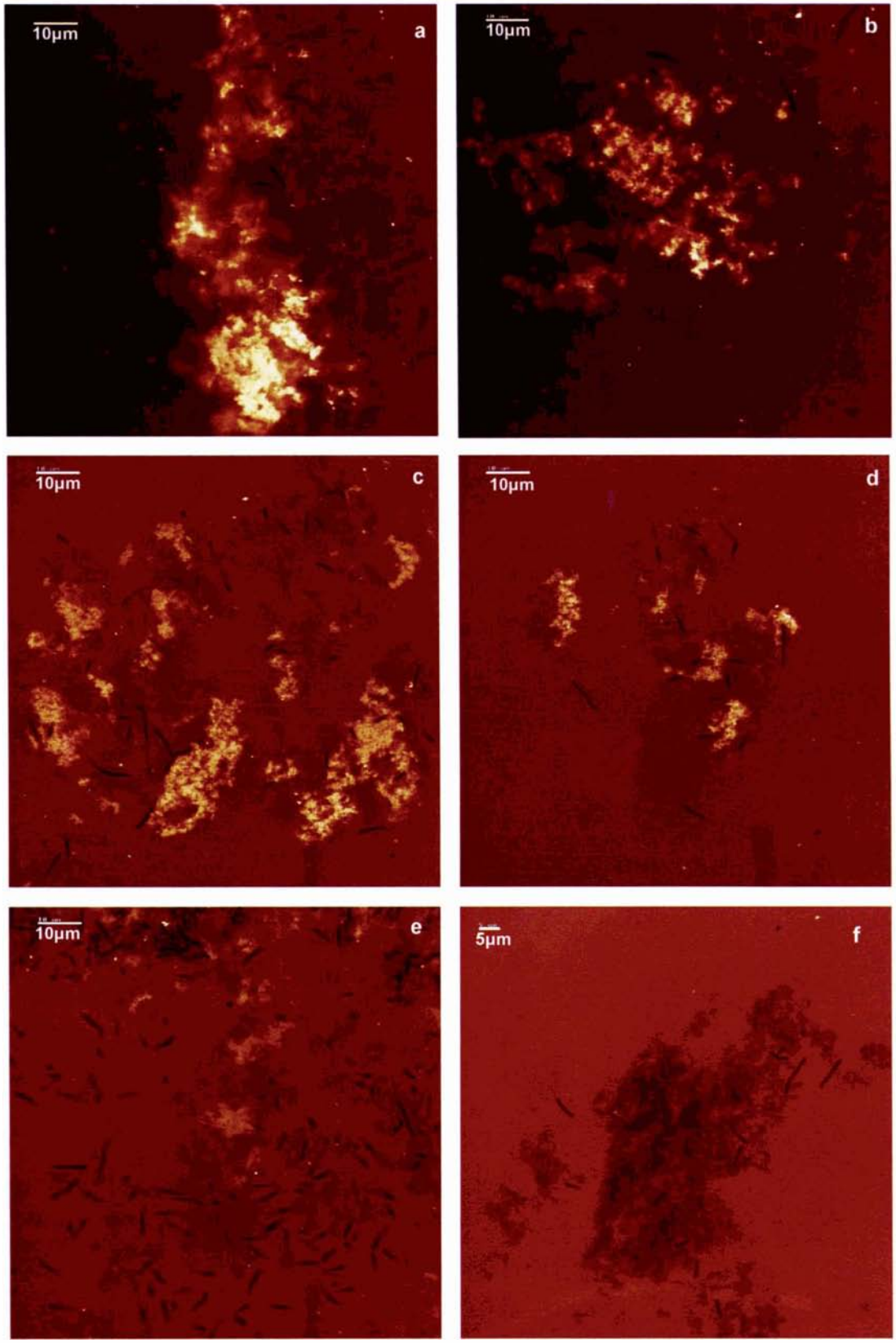

Figure 3.7 2483 culture grown in a milk permeate containing 0.5%w/v yeast extract and 5% w/v SMP. The culture medium was treated with Flavourzyme (50°C, 4h) and adjusted to respective pH using 1M NaOH. (a & b) pH 8; (c & d) pH 9 and (e & f) pH 10. The EPS stained with Lectin SBA Alexa Fluor.

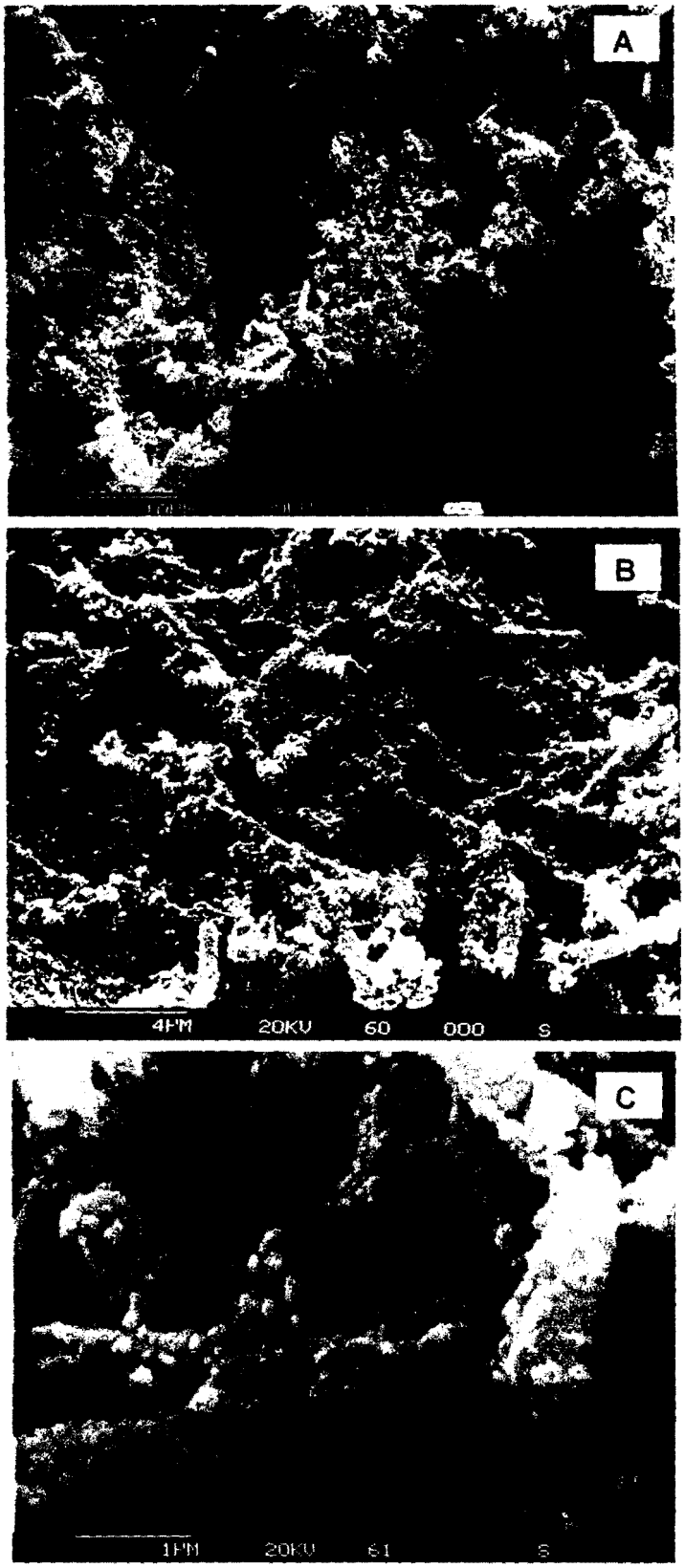

Figure 3.8 2483 culture grown in a milk permeate containing 0.5%w/v yeast extract and 5% w/v SMP. The culture medium was adjusted to pH 10 using 1M NaOH. (a) 2000X magnification; (b) 5000X magnification and (c) 50,000X magnification.

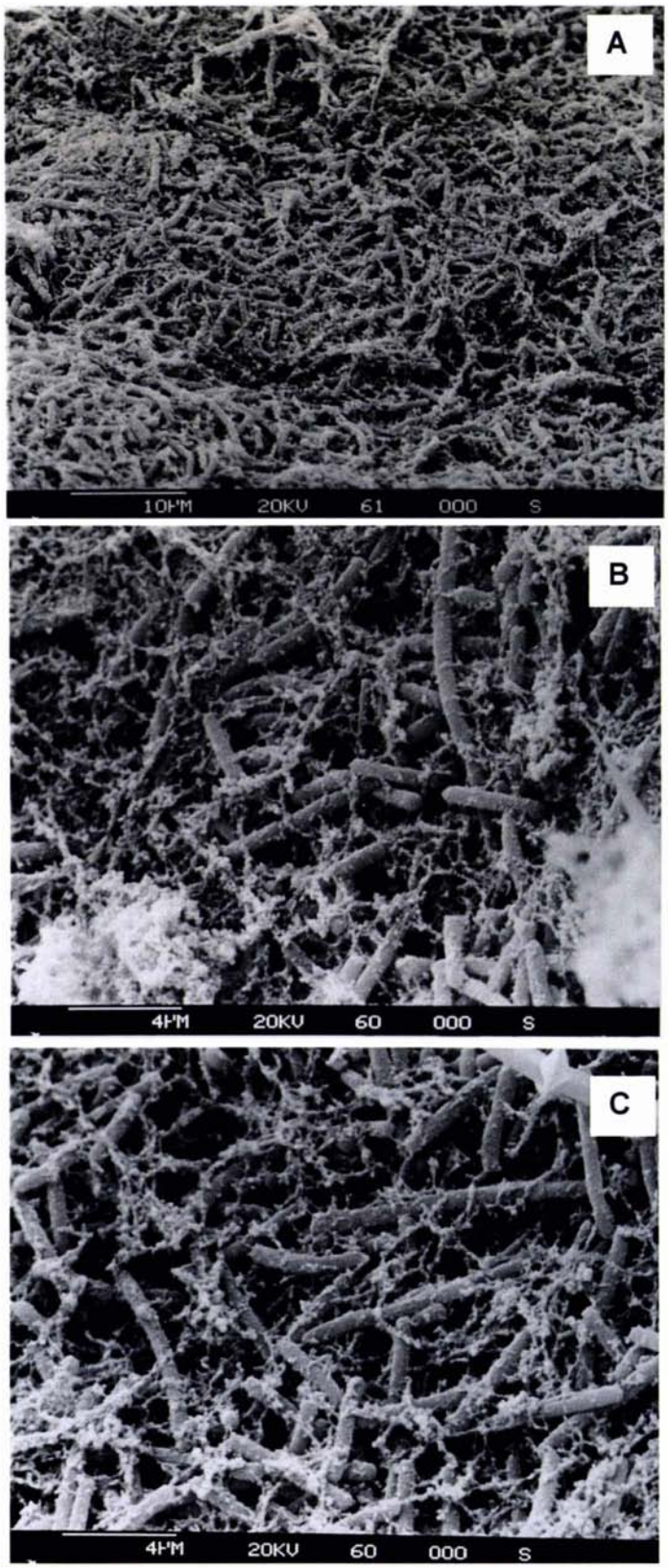

Figure 3.9 2483 culture grown in a milk permeate containing 0.5%w/v yeast extract and 5% w/v SMP. The culture medium was treated with Flavourzyme (50°C, 4h) and adjusted to pH 10 using 1M NaOH. (a) 2000X magnification; (b & c) 5000X magnification.

3.4 CONCLUSIONS

The use of CLSM, together with fluorescent lectin conjugates, has proven effective for imaging EPS in milk permeate-based media. The CLSM micrographs reveal that EPS occur as aggregates in the culture medium. Unlike SEM, the sample preparation procedures for CLSM did not require rigorous chemical processing steps that could introduce artefacts and complicate image interpretation. The success of CLSM relied primarily on the selection of an appropriate fluorescent stain, SBA lectin Alexa Fluor conjugate. This stain had no effect on proteins, lactose or bacterial cells present in the media. Instead, the fluorescent lectin conjugates had strong affinity for the EPS due to the presence of galactopyranosyl residues in the EPS chemical structure (see Chapter 5). Experiments carried out on the 'non-ropy' strains of LAB grown in milk media showed that EPS was also produced but with different rheological characteristics. The SEM micrograph showed EPS as a web distributed through the interstices of the protein matrix. The formation of the intricate web structures could be attributed to the dehydration of the EPS during critical point drying process of the SEM specimens.

From this study, it was also found that at neutral and low pH (~pH 3.9), the EPS aggregates remained intact. However, as the pH was increased, (pH 8-10), the EPS aggregates appeared to be disrupted. Furthermore, the observed 'ropy' characteristics of the culture medium were much reduced. The effect of high pH on EPS structure would require further studies since polysaccharides are generally known to be stable under mild alkaline conditions.

Chapter 4

Development of an Improved Assay for Quantification of Exopolysaccharides in Milk-based Media

4.1 INTRODUCTION

Different exopolysaccharide (EPS) assays have been developed by many researchers over the last two decades (Abbad-Andaloussi et al., 1995; Bouzar, Cerning & Desmazeaud, 1996; Cerning et al., 1992; De Vuyst & Degeest, 1999b; Doco, Carcano, Ramos, Loones & Fournet, 1991; Dupont, Roy & Lapointe, 2000; Gamar-Nourani, Blondeau & Simonet, 1997; Gamar-Nourani, Blondeau & Simonet, 1998; Gancel & Novel, 1994; Garcia-Garibay & Marshall, 1991; Gorret, Maubois, Ghoul & Engasser, 2001; Grobben et al., 1995; Gruter et al., 1993; Kimmel & Roberts, 1998; Kimmel, Roberts & Ziegler, 1998; Looijesteijn, van Casteren, Tuinier, Doeswijk-Voragen & Hugenholtz, 2000; Mozzi, Graciela de Giori , Oliver & Graciela de Valdez 1996; Nakajima et al., 1990; Petry, Furlan, Crepeau, Cerning & Desmazeaud, 2000; Racine et al., 1991; Ricciardi et al., 1998; Smith & Pace, 1982; Toba et al., 1992; Torino, Taranto & De Valdez, 2001; Urashima et al., 1999; van den Berg et al., 1995; Yang et al., 1999). All these methods involve a combination of techniques to separate, precipitate, purify and quantify the EPS in a culture medium. Some of the techniques used to isolate and/or purify EPS include size–exclusion chromatography, anion exchange chromatography, ultra-filtration, dia-filtration, centrifugation, dialysis, ultrasonication and lyophilization. Common techniques used for precipitating EPS include ethanol, acetone, propanol, isopropanol, cetyltrimethylammonium bromide (CTAB) and 3,5,6-triphenyl-2,3,5,6-tetraaza bicycle-1-hexene (commercially known as nitron) (Azeredo & Oliveira, 1996). In culture media containing proteins, trichloroacetic acid (TCA) and enzyme treatments have been commonly employed to precipitate and hydrolyse the proteins respectively. The quantification of EPS subsequent to isolation and purification commonly employs the phenol-sulphuric acid method (Dubois et al., 1956).

Many of the assays are reliable for determining the levels of EPS for cultures grown in chemically defined and/or semi-defined media. However, for complex media, such as those containing milk, the EPS values are inaccurate due to the non-EPS components, present in the media, often interfering with the assay. Consequently, improvements to existing EPS assays are essential in order to determine more accurately the amount of EPS produced in both semi-defined and complex media.

Quantifying the amount of EPS in a complex system (e.g. fermented milk) is a difficult task. During fermentation, the lactic acid produced causes aggregation of casein particles leading to the formation of a weak gel. The gel in which the bacterial cells, lactose and other minor components are entrapped, is a highly complex network structure of proteins and EPS (see Chapter 3). Careful separation of the EPS from non-EPS components, particularly proteins, lactose and bacterial cells, is necessary (Cerning, 1990), as the inclusion of such components could influence the results of the chemical methods employed for total carbohydrate determination. Cerning et al. (1992) reported that a culture medium containing yeast extract could also interfere with EPS assay due to the presence of mannans. The aim of the work reported in this chapter was to develop a more reliable assay for quantification of EPS in complex media, such as milk.

4.2 MATERIALS AND METHODS

4.2.1 Fermentation of 2483 culture

The seed culture of 2483 was grown in a 10% (w/v) reconstituted skim milk (RSM) and fermented at 37°C for 24 h. The seed culture was inoculated (1% v/v) into the following growth media and incubated for 24 h at 37°C:

- Milk permeate (Fonterra Co-operative Group Ltd, New Zealand).
- Milk permeate with the addition of 10% (w/v) lactose (analytical grade, BDH) and 1.02% (w/v) milk protein concentrate (ALAPRO 4560, Fonterra Co-operative Group Ltd, New Zealand).
- Reconstituted skim milk prepared by dissolving 10% (w/v) skim milk powder (SMP) (Fonterra Co-operative Group Ltd, New Zealand) in water.

All culture media were free-steamed at 100°C for 10 min and cooled to room temperature prior to inoculation with the 2483 seed culture. Fermentation of the 2483 culture was carried out at 37°C for 24 h in a 1L Duran bottle.

4.2.2 Enzymes used for protein hydrolysis

The enzymes used are listed as follows:

- Flavourzyme (Novozymes Ltd, Bagsværd, Denmark)
- Mixture of Neutrase (Novozymes Ltd) and Protease A "Amano" 2 (Amano Enzyme, Nayoga, Japan) (denoted as *Enzyme A*).
- Promod 215P (Biocatalysts, Wales, UK) (denoted as *Enzyme B*).
- Promod 215P and Flavopro 192P (Biocatalysts) (denoted as *Enzyme C*).
- Flavorpro 192P (denoted as *Enzyme D*).

Each enzyme was either dissolved or diluted in Milli-Q water and then filtered through a 0.2μm filter (Millipore) to make a 10% (w/v) enzyme preparation.

4.2.3 Quantification of total carbohydrates

Chemical analysis for the determination of total carbohydrate was adapted from the phenol-sulphuric acid method (Dubois et al., 1956). Phenol solution (5% w/v) was first prepared by dissolving 10g phenol (BDH) in Milli-Q water (water purified by treatment with a Milli-Q apparatus, Millipore Corp. Bedford, MA, USA) in a 500mL volumetric flask. (Note that phenol is a toxic chemical and careful handling is necessary!) Sample (1mL) was mixed with 1mL phenol solution (5% w/v) followed by the addition of 5mL concentrated sulphuric acid. The sample was left at room temperature for 30 min prior to measuring the absorbance at 485nm using a spectrophotometer (Ultrospec 2000, Amersham Pharmacia Biotech, Piscataway, NJ, USA). The total amount of carbohydrate was determined based on a standard calibration curve prepared using glucose or dextran (Sigma-Aldrich, average molecular weight: $2x10^6$ Da).

4.2.4 Standard curves for glucose and dextran

Solutions of analytical grade glucose (Sigma-Aldrich) were prepared in distilled water at various concentrations (20, 40, 60, 80, 100, 120 and 140 μg/mL). The absorbance for each standard solution was determined by the phenol-sulphuric acid method. The glucose standard curve was obtained by plotting absorbance at 485nm as a function of glucose concentration. A standard curve for dextran (Sigma-Aldrich, average molecular weight: $2x10^6$ Da) was also obtained by the same procedure.

4.3 METHODOLOGY DEVELOPMENT: STAGE 1

4.3.1 Evaluation of existing methods for EPS determination

Two EPS assays were evaluated using the culture medium of 2483 grown in milk permeate supplemented with 10% (w/v) lactose and 1% (w/v) milk protein concentrate (ALAPRO 4560, Fonterra Co-operative Group Ltd, New Zealand). The first method, referred to here as the *Acid Addition Method* was carried out according to the procedure described by Kimmel et al. (1998) which was originally developed by Gancel & Novel (1994). The second method used was adapted from the procedures utilised by Cerning et al. (1994) and is referred to as the *Ethanol Precipitation Method.* Each of the methods used to determine the 2483 EPS content in the culture medium is described in Appendix B. The amounts of EPS from the culture medium determined by the *Acid Addition* and E*thanol Precipitation Methods* are shown in Table 4.1.

Table 4.1 The average 2483 EPS (μg/mL) recovered using the *Acid Addition* and the *Ethanol Precipitation Methods*. Fermentation of the 2483 culture was performed at 37°C for 24 h. The control samples did not contain the 2483 culture.

Samples	Acid Addition Method		Ethanol Precipitation Method	
	Duplicate 1	Duplicate 2	Duplicate 1	Duplicate 2
Control	285	209	60	63
2483	294	444	106	71

The EPS levels obtained showed large variations between the two methods. The EPS levels obtained by the *Acid Addition Method* were much higher than those obtained by the *Ethanol Precipitation Method.* The discrepancy between the results in this study appeared to be reflected in the EPS levels reported by Kimmel et al. (1998) and Cerning et al. (1994), with values ranging from 200-500μg/mL and 15-130μg/mL respectively. As both groups of researchers used different species of *Lactobacilli (Lactobacillus delbrueckii* subsp. *bulgaricus* RR and *Lactobacillus casei* CG11 respectively) and the cultures were grown in different media, some differences in the EPS levels would be expected. However, the intrinsic nature of the isolation and purification procedures between the two methods also appeared to have a strong influence on the disparity of the levels of EPS determined.

The growth medium used by Kimmel et al. (1998) was a semi-defined medium containing only low molecular weight components. The culture media used by Cerning et al. (1994) included a chemically-defined medium and a milk ultrafiltrate supplemented with casamino acids (an acid hydrolysed casein). In such growth media, the EPS produced could be quantified with greater ease and reliability. However, the culture medium used for 2483 fermentation contained milk protein as well as lactose. The presence of such components has likely contributed to the high total carbohydrate levels as seen in the control samples, particularly in the *Acid Addition Method*. Furthermore, the result of the fermentation was the formation of a complex network with highly viscous and 'ropy' characteristics. A diagrammatic representation of the culture medium before and after fermentation is illustrated in Figure 4.1.

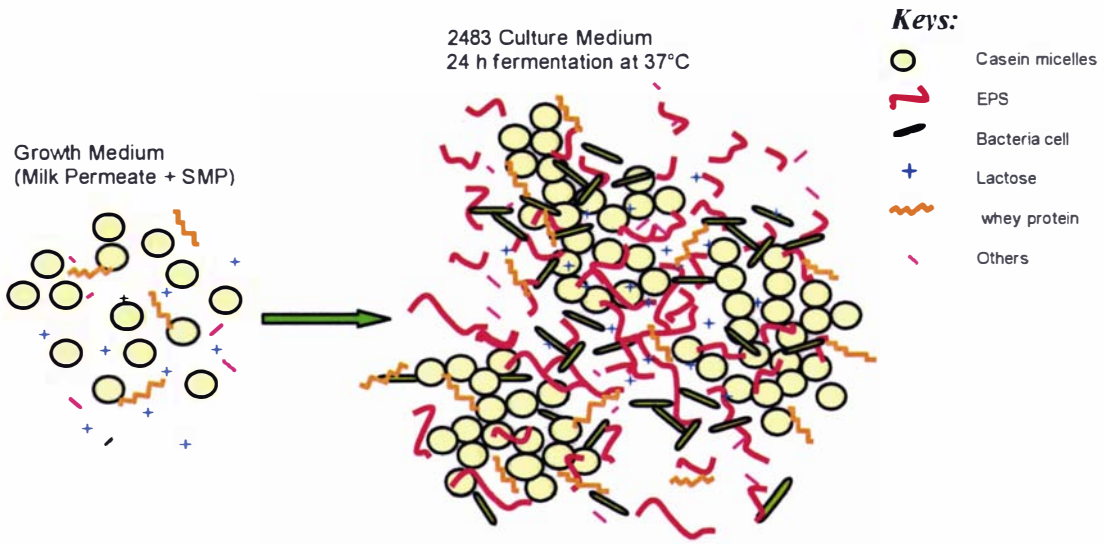

Figure 4.1 A diagrammatic representation of the culture medium before and after fermentation. Note that the illustration is not drawn in proportion.

The difficulty involved in isolating the EPS from such a viscous and complex system is widely recognised (Cerning & Marshall, 1999; De Vuyst & Degeest, 1999b). In order to identify the causes of variations in EPS levels, each processing step employed in the methods was carefully evaluated. The likely causes of variation are as follows:

- *Incomplete protein hydrolysis and EPS entrapment/binding*

  Boiling the culture medium in the initial step was intended to stop further bacterial growth and inactivate EPS degrading enzymes. However, this caused coagulation and aggregation of proteins, especially in a low pH environment (pH of ~3.5). Subsequent Pronase treatment did not appear to fully hydrolyse the proteins in the coagulum. The medium remained cloudy due to a large amount of suspended matter which entrapped or interacted with some of the EPS in the continuous phase. The removal of the suspended matter via centrifugation also resulted in the removal of an unaccounted amount of EPS.

- *Incomplete protein precipitation*

  In the *Acid Addition Method*, the final concentration of the TCA in the medium was too low (2% v/v) to precipitate any proteins left in the medium. The presence of proteins appeared to influence the results obtained by the phenol-sulphuric analysis, resulting in higher total carbohydrate levels. In order to precipitate proteins present in the medium, the concentration of TCA should be at least 10% (v/v) (Gancel & Novel, 1994). However, in the case of the 2483 culture medium, the use of TCA may be unsuitable due to possible EPS-protein interactions. Removal of proteins could cause the removal of the EPS at the same time.

- *Insolubility of lactose*

  In the *Ethanol Precipitation Method*, lactose crystals were formed because of poor solubility of lactose in ethanol (~75% v/v). These lactose crystals which were precipitated from the media (control and test samples) adhered strongly to the wall of the test tube. The lactose crystals also appeared to attract the precipitated EPS (as seen by an increased amount of white precipitates appearing on the test tube wall of the test sample compared to the control sample). When the EPS precipitates were recovered from the ethanol solution for dialysis, the EPS which interacted with the lactose crystals and adhered strongly to the wall of the test tube was not accounted for. At the same time, some of the lactose crystals that were dislodged from the wall of the test tube were included with the EPS precipitates and some of the lactose crystals remained insoluble throughout the dialysis process. Moreover, the partially

hydrolysed proteins (due to incomplete enzymatic hydrolysis) that remained in the supernatant after centrifugation were also precipitated by the ethanol. All these non-EPS components created major problems in determining the actual EPS levels employing the phenol-sulphuric acid method.

In both methods, dialysing the samples at low temperature (4°C) and over a two day period was probably insufficient to allow all the low molecular weight sugars (mono and di-saccharides) present to diffuse out of the dialysis membrane. This was particularly true for lactose crystals (from EPS-lactose precipitates), some still remaining insoluble after the 48 h dialysis. Determination of the amount of EPS which included the residual lactose resulted in a higher total carbohydrate level. This was often mistaken as the concentration of EPS. Prolonging the dialysing process e.g. up to 5 days (Gorret et al., 2001; van Calsteren et al., 2002) or raising the temperature of dialysis could however, cause bacterial build-up in the dialysis tubing, unless an antimicrobial agent such as sodium azide was used. Any bacterial growth could lead to an unaccounted degradation of EPS, thereby causing erroneous EPS results.

While the two protocols gave unreliable data based on the 2483 culture medium, they could be reliable when used in a less complex medium. It is essential to thoroughly understand the characteristics of the main components in the culture medium and the key processing parameters when applying any EPS assay. Hence, refining the procedures for EPS assay in a complex culture medium is necessary. An effective assay depends on effective isolation and purification procedures of EPS that completely remove non-EPS components present in the medium.

4.4 METHODOLOGY DEVELOPMENT: STAGE 2

Various means to exclude interfering components such as proteins and lactose, and at the same time, ensuring minimal EPS loss during the various treatment steps were considered in the subsequent stages of development.

4.4.1 Evaluation of EPS recovery based on added dextran

Since the amount of EPS produced by 2483 culture was unknown, it was impossible to determine which method would reliably quantify 2483 EPS in complex culture media. In order to assess the reliability of an EPS assay, a system was devised based on the addition of a known amount of dextran to different growth media (without bacterial culture). An ideal EPS assay would account for all the dextran added.

Dextran (0.1g) was dissolved in 100mL of growth medium (without culture). The amount of dextran recovered from the medium was used as a basis to evaluate the effectiveness of the different steps influencing EPS recovery. The different media (including controls) were:

- Milk permeate
- Milk permeate + dextran
- Milk permeate + 2% (w/v) lactose
- Milk permeate + 2% (w/v) lactose + dextran
- Milk permeate + 2% (w/v) lactose + 1% (w/v) milk protein concentrate ALAPRO 4560
- Milk permeate + 2% (w/v) lactose + 1% (w/v) milk protein concentrate ALAPRO 4560 + dextran
- Water + dextran

All samples were acidified to pH 4 (with 1M lactic acid) to simulate the pH condition of typical lactic acid culture fermentation. The samples were centrifuged at 1,900*g* for 10

min (Hermle Z320 centrifuge, Wehingen, Germany). The supernatant (0.1mL) of each sample was mixed with distilled water (0.9mL), followed by the addition of 9mL of chilled absolute ethanol. The sample was left overnight at 4°C and then centrifuged at 12,000*g* for 10 min at 4°C (Sorvall Centrifuge RC5C, SS-34 rotor, Dupont Company, Wilmington, DE). The supernatant was discarded and the pellet was re-suspended in 1mL distilled water. Another 9mL of absolute ethanol was added in the second ethanol precipitation step and was left overnight at 4°C. The sample was centrifuged again at 12,000*g* for 10 min at 4°C and the pellet re-suspended in 1mL water. Total carbohydrates were determined in duplicate using the phenol-sulphuric acid method. The amount of dextran recovered was read against the dextran calibration curve. The percent dextran recovered from each medium is shown in Table 4.2.

Table 4.2 Amount of dextran (μg/mL) recovered from different growth media without bacterial culture by the *Ethanol Precipitation Method*.

Media	Total Carbohydrate (μg/mL)	Dextran Recovered w/v (%)
Milk permeate	19±1.1	-
Milk permeate + dextran	297±3.5	28±0.5
Milk permeate + lactose	69±2.1	-
Milk permeate + lactose + dextran	339±4.8	27±0.6
Milk permeate + lactose + ALAPRO 4560	120±3.5	-
Milk permeate + lactose + ALAPRO 4560 + dextran	420±6.5	30±0.9
Water + dextran	769±4.2	77±1.2

Note: Amount of dextran added =1000μg/mL. The levels of dextran recovered were obtained by subtracting the respective control. Values represent mean ± standard deviation (n=3)

The highest percentage of dextran recovered (77%) was obtained from the sample with water as the solvent. In all the milk permeate-based media, the percentages of dextran recovered decreased drastically to ~27%–30% (w/v). This suggested that the media components had interfered with dextran under acidic pH condition which resulted in the loss of dextran during the processing steps. A noteworthy observation was that all the control samples (i.e. without added dextran) showed different levels of total carbohydrates. The total carbohydrate level in the control milk permeate medium was very low but the level increased by approximately three times in the control milk

permeate medium with added lactose (2% w/v). The highest level of total carbohydrate among the control samples was found in the control milk permeate medium with added lactose and ALAPRO 4560 (1% w/v).

From the above, two intertwined problems were deduced. This include the loss of dextran during the processing steps which led to an incomplete recovery of dextran. Furthermore, the high total carbohydrate levels in the absence of added dextran was likely due to the presence of lactose (some of which became insoluble in ethanol) and proteins in the control media. Several key areas in the processing steps that are likely to affect dextran recovery were considered. These included determining a suitable centrifugation regime for the separation of precipitated polysaccharides; improving lactose solubility in order to reduce the total carbohydrate baseline of control samples; optimising ethanol concentration for maximum polysaccharide precipitation and exploring suitable enzymes to hydrolyse milk proteins in the culture media.

4.4.1.1 Determination of a suitable centrifugation regime to improve dextran recovery

Determination of a suitable centrifugation regime for separation of the precipitated polysaccharides was carried out by visual assessment. Blue dextran 2000 (weight-average molecular weight ~2.0 x 10^6 Da, Amersham, Phamacia Biotech) was used because any losses during the processing step would be visible. The dextran was dissolved in water, mixed with absolute ethanol as described previously; and centrifuged at 12,000*g* for 10 min, 12,000*g* for 30 min, 18,000*g* for 30 min or 27,000*g* for 40 min at 4°C (Sorvall Centrifuge RC5C, SS-34 rotor, Dupont Company, Wilmington, DE).

When decanting the supernatant, a part of the pellet was found to be easily dislodged from the centrifuge tube into the supernatant. This was observed after the ethanol precipitation step for all centrifugation regimes, with the exception of 27,000*g* for 40 min. The centrifugation regimes in many previously reported EPS assays employed lower gravitational force and/or shorter centrifugation time (Bouzar et al., 1996; Cerning et al., 1992; Cerning et al., 1994). Only a few researchers employed

centrifugation regimes such as 27,000*g* for 30 min (Grobben et al., 1998) and 28,100*g* for 30 min (van Casteren et al., 1998), that were close to the one found to be the most effective in the present study (i.e. 27,000*g* for 40 min).

4.4.1.2 Optimising ethanol concentration for maximum dextran recovery

Dextran solution (0.1% w/v) at 0.1mL was mixed with 9.9mL 30%, 40%, 50%, 60% or 70% v/v ethanol. All samples were left overnight at 4°C and centrifuged at 27,000*g* for 40 min at 4°C. The pellet was dissolved in 1mL Milli-Q water and the EPS level determined using the phenol-sulphuric acid method.

Table 4.3 Recovery of dextran (dissolved in water) at different ethanol concentrations. All samples were subjected to ethanol precipitation once unless indicated otherwise.

Concentration of Ethanol (%v/v)	Average Dextran recovered (µg/mL)
30	0
40	689
50	713
60	924
70	982
70 (ethanol precipitated twice)	979

Note: Amount of dextran added to water = 1000 (µg mL)

The recovery rates of dextran at different ethanol concentrations are shown in Table 4.3. It is clear from the above data that 70% (v/v) ethanol was sufficient to precipitate all dextran present. An additional ethanol precipitation using 70% (v/v) ethanol did not affect dextran recovery.

4.4.1.3 Determination of lactose solubility in ethanol

Chilled ethanol (9mL) was added to 1mL lactose solution (2% w/v) such that the final concentration of the ethanol was 90%, 80%, 70% or 60% (v/v). The samples were left overnight at 4°C and then visually assessed for the formation of lactose crystals.

Lactose crystals were observed in samples containing 90% (v/v) or 80% (v/v) ethanol but no lactose crystals were formed at ethanol levels ≤ 70% (v/v). From the observation, it was evident that lactose, being less soluble in ethanol than in water, formed crystals when the concentration of ethanol exceeded the solubility threshold of the lactose. In all EPS assays known so far, this crucial step generally escapes attention. Consequently, the lactose crystals are analysed along with the EPS, giving higher EPS levels. This also explains why a higher level of total carbohydrates was obtained in the milk permeate supplemented with lactose, compared to the milk permeate medium without the added lactose (Table 4.2). To decrease the extent of lactose crystal formation, the ratio of water in ethanol could be increased. However, the concentration of ethanol should be sufficiently high to allow complete precipitation[1] of the EPS.

4.4.1.4 Selection of a suitable enzyme based on dextran recovery

The use of proteinase to hydrolyse proteins in culture media has been commonly employed in many EPS methods (Bouzar et al., 1996; Cerning et al., 1992; Kimmel et al., 1998). However, some of these enzymes may possess residual glucanase activity. Consequently, it was necessary that the selected enzyme used for protein hydrolysis would not cause polysaccharide hydrolysis. Each enzyme was diluted in Milli-Q water and then filtered through a 0.2μm filter (Millipore) to make a 10% (w/v) enzyme preparation.

An enzyme preparation (100μL) was added to 0.1% (w/v) dextran solution (10mL) and incubated in a water bath shaker at 50°C for 4 h. The dextran sample was subjected to ethanol precipitation twice, each left overnight at 4°C in a 70% (v/v) ethanol followed by a centrifugation regime of 27,000*g* for 40 min, at 4°C. The pellet obtained was dispersed in 1mL of Milli-Q water. The total dextran was analysed based on the phenol-sulphuric acid method as described earlier.

[1] Polysaccharides such as dextran exist as expanded random coils in water. The addition of ethanol decreases the polysaccharide-solvent affinity. At higher ethanol concentrations, the intermolecular forces between the polysaccharide macromolecules dominate, leading to precipitation of polysaccharides (Smith and Pace, 1982).

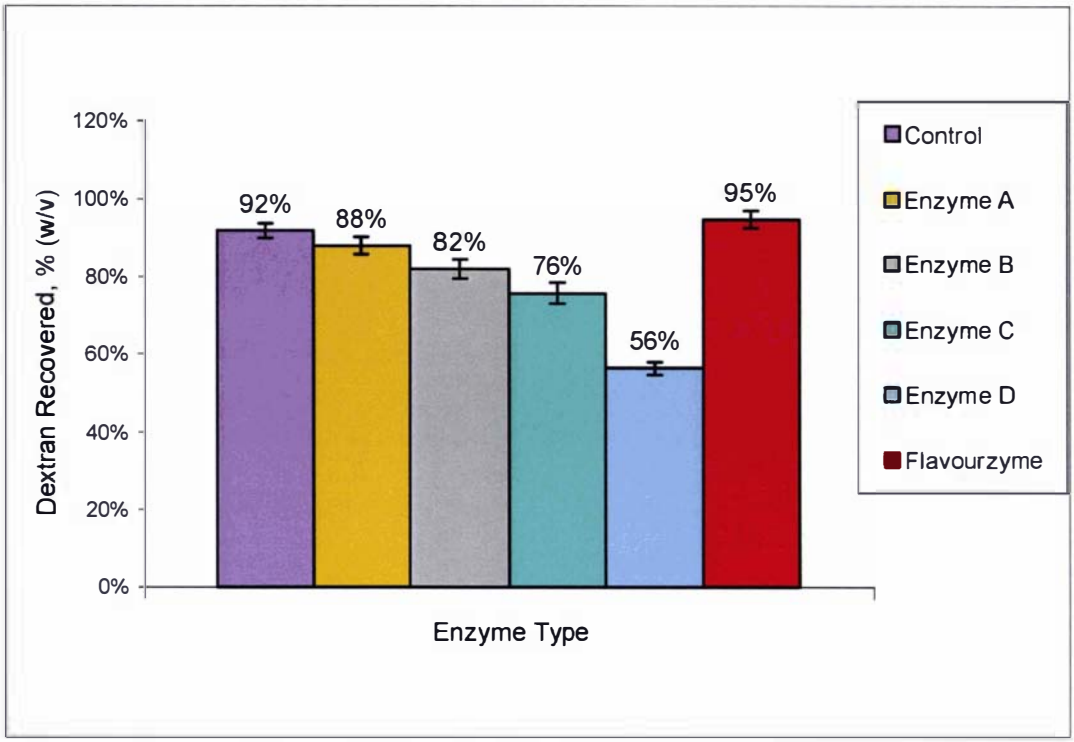

Figure 4.2 Percentage of dextran recovered after 4 h treatment with various proteolytic enzymes at 50°C. The error bars indicate the standard deviations based on three replicates.

The levels of dextran after the samples were treated with various enzymes are shown in Figure 4.2. The results indicated that the highest amount of dextran (95%) was recovered from the sample treated with Flavourzyme followed by *Enzyme A*. Neither of these two enzymes appeared to hydrolyse the polysaccharides. However, *Enzymes B, C* and *D* showed a decrease in the percentage of dextran recovered, possibly due to some glucanase activity.

4.4.2 Evaluation of different enzymes for EPS recovery

The above enzyme solutions were evaluated in 2483 culture medium. The growth medium for 2483 was made up of 40% (v/v) RSM and 60% (v/v) milk permeate medium, and the mixture was then free-steamed at 100°C for 10 min. Note that the milk permeate medium used was supplemented with 2% (w/v) lactose and the RSM solution consisted of 10% (w/v) SMP. The seed culture of 2483 was inoculated (1% inoculum) aseptically in 100mL of the growth medium. The samples taken at 0h incubation were regarded as the control samples and the fermented 2483 culture medium (24 h, 37°C) were the test samples. The pH values of the control and test samples were adjusted to

pH 7 using 1M NaOH solution before the addition of the enzyme preparations. A control sample (without enzyme treatment) was also included in the experimental design. All samples were incubated at 50°C in a water bath shaker at an agitation speed of 150 rpm for 4 h. Following this, each sample was divided into two portions. One portion (0.1mL) of the sample (*Whole*) was subjected to 70% (v/v) ethanol precipitation twice at 4°C and treated as described earlier. The other portion of the sample was centrifuged at 9,000*g* for 10 min in order to obtain the *Supernatant*. The *Supernatant* (0.1mL) was subjected to ethanol precipitation and centrifugations as described above.

Table 4.4 Effects of different enzymes on 2483 EPS recovery in a medium containing 40% (v/v) RSM and 60% (v/v) milk permeate. The values are expressed as mean ± SD obtained from three replicate measurements.

Enzyme Type	0h incubation (Control) µg/mL		24h incubation (Test) µg/mL		EPS Level (Test minus Control) µg/mL	
	Whole[a] *w*	*Supernatant*[b] *x*	*Whole*[a] *y*	*Supernatant*[b] *z*	*Whole (y-w)*	*Supernatant (z-x)*
Nil	180±2.1	18±1.5	464±3.8	135±2.2	284	117
A	34±0.3	57±1.2	236±2.5	163±2.1	202	106
B	58±0.9	53±1.8	365±5.6	122±2.3	307	69
C	74±1.1	43±2.1	303±2.1	126±1.9	229	83
D	49±1.1	63±1.6	395±2.1	112±2.0	346	49
Flavourzyme	35±0.8	31±0.7	331±2.3	235±1.7	296	204

[a]*Whole : samples underwent direct EPS processing.*
[b]*Supernatant : samples centrifuged to remove cells suspended solids from the continuous phase prior to EPS processing.*

All control samples (both *Whole* and *Supernatant*) showed the presence of some carbohydrate (Table 4.4). The control sample without enzyme treatment showed higher level of total carbohydrate (180µg/mL) as compared to the samples with enzyme treatment. Among all the control samples, both *Enzyme A* and Flavourzyme gave the lowest carbohydrate values for the control (*Whole*) samples (~34µg/mL). To account for the total carbohydrate (non-EPS) contributed by the control samples, the total carbohydrate values of test samples were subtracted from the respective control samples (i.e. test – control) as shown in Table 4.4.

In the case of test samples, treatment with Flavourzyme showed the highest recovery (~69%) of EPS in the *Supernatant*. However, all the other enzymes appeared to cause EPS degradation to a certain extent.

4.4.3 Evaluation of Flavourzyme on bacterial cell integrity

The effect of Flavourzyme on bacterial cell integrity was examined using transmission electon microscopy (TEM). This was to ensure that the levels of EPS found in the *Supernatant* did not include intracellular materials. A fermented culture medium (milk permeate containing 10% (w/v) SMP) was hydrolysed with Flavourzyme (100µL of 10% w/v enzyme to 10g sample) for 4 h at 50°C. The control sample was without Flavourzyme treatment. The TEM sample preparation procedures are given in Appendix C. The micrographs obtained by TEM (see Figure 4.3) showed that Flavourzyme did not damage 2483 cell wall or cell membrane. Hence, no bacterial intracellular materials were leached out into the continuous phase to interfere with the EPS quantification.

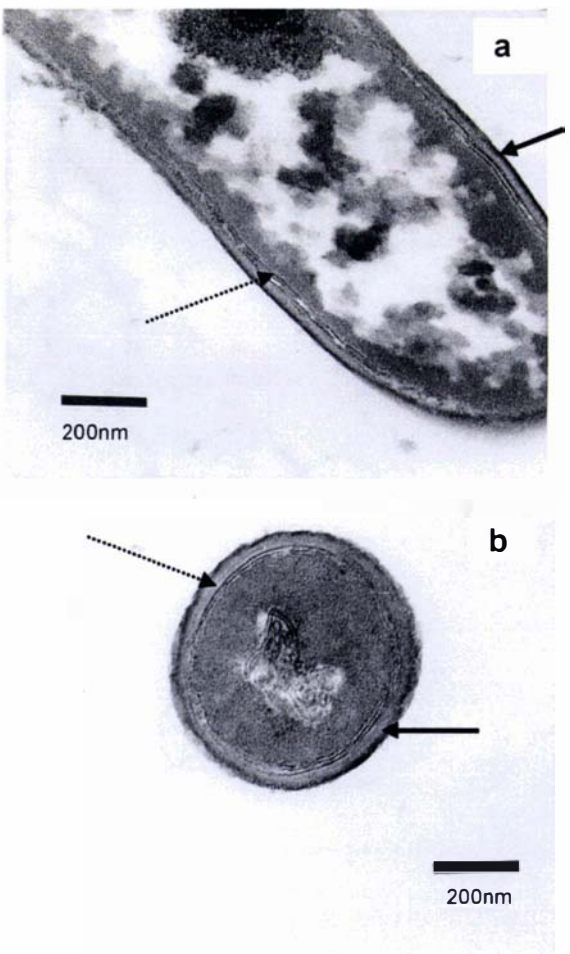

Figure 4.3 Micrographs of 2483 culture obtained using TEM. (a) 2483 in milk permeate containing yeast extract and SMP before Flavourzyme treatment (b) sample after Flavourzyme treatment (50°C, 4 h). Filled arrows indicate cell wall; dotted arrows indicate cell membrane.

4.5 METHODOLOGY DEVELOPMENT: STAGE 3

4.5.1 Recovery of EPS from media containing different percentages of RSM

It appears that the inadequacy of many EPS assays lay mainly with the interference from proteins (especially casein) in the growth media. The protein aggregates not only have the potential to entrap or interact with EPS, but also interfere with the phenol-sulphuric acid method. The effects of the addition of different levels of RSM to the growth media were evaluated to test the robustness of the improved methodology.

The growth media for 2483 were prepared by adding different amounts (0%, 5%, 10%, 20%, 40%, 70% or 100% v/v) of RSM to each of the milk permeate media, which was supplemented with 2% (w/v) lactose. The samples were processed as described previously (Section 4.4.2) and the results are shown in Table 4.5.

Table 4.5 EPS recovered from Flavourzyme treated culture media containing different proportions of RSM added to milk permeate The values are expressed as mean ± SD obtained from three replicate measurements.

RSM in milk permeate (% v/v)	0h incubation (control) µg/mL		24h incubation (test) µg/mL		*EPS Value* (test minus control) µg/mL		EPS recovery in *Supernatant* (%)
	Whole[a] *w*	*Supernatant*[b] *x*	*Whole* *y*	*Supernatant* *z*	*Whole* *(y-w)*	*Supernatant* ***(z-x)***	$\frac{(z-x)}{(y-w)}$
0	8±0.5	8±1.2	87±2.5	80±2.1	79	72	91
5	17±1.6	14±1.2	125±3.1	101±2.7	108	87	81
10	17±1.8	13±1.2	188±3.5	132±3.2	171	119	70
20	16±1.7	20±1.5	242±5.4	168±3.8	226	148	66
40	44±1.91	45±1.8	273±5.5	197±3.5	229	152	66
70	152±2.9	92±2.1	406±6.8	254±4.2	254	162	64
100	198±2.8	96±2.5	448±7.1	256±4.0	250	160	64

[a] *Whole: samples underwent direct EPS processing.*
[b] *Supernatant: samples centrifuged to remove cells/suspended solids from the continuous phase prior to EPS processing.*

In the case of the control samples, the results from both *Whole* and *Supernatant* showed that increasing the proportion of RSM resulted in increasing levels of total

carbohydrates, especially ≥ 40% (v/v) RSM. The amounts of insoluble material left after Flavourzyme treatment also increased with increasing RSM addition, as seen from the size of pellets obtained by centrifugation. Comparing the *Whole* and *Supernatant* of the control samples, the total carbohydrate levels were very similar when the amount of RSM ranged from 0% to 40% (v/v). However, with the addition of ≥ 70% (v/v) RSM, the difference between the *Supernatant* and *Whole* became evident.

In the test samples, the EPS levels of the *Supernatant* were generally lower than the *Whole*. The results indicated that interactions between EPS and the insoluble components in the culture media had occurred in such a way that the separation of the insoluble components (including bacterial cells) also resulted in the separation of some of the EPS. It was also noted that the EPS levels of the *Supernatant* were similar to the *Whole* when the media did not contain any RSM. However, the percentage of EPS recovery in the *Supernatant* decreased from approximately 90% to 70% when the levels of RSM increased from 0% to 20% (v/v). Moreover, the percentage of EPS in the *Supernatant* seemed to plateau at ~65% in samples with RSM levels ≥ 40% (v/v).

It was considered that the EPS results obtained from either the *Whole* or *Supernatant* could not be regarded as absolute EPS values. However, the *Whole* was considered to give the best estimated EPS values. The EPS values obtained from the *Supernatant* samples were generally underestimated, as some of the EPS which was bound to the bacterial cells and insoluble components was removed during the centrifugation step. When reporting the amount of EPS in milk permeate medium containing RSM, the best estimated EPS values could be obtained by subtracting the EPS values of the test samples from the control samples using the *Whole* samples. In doing so, a slight underestimation of the final EPS values is to be expected since the total carbohydrate baseline (i.e. non-EPS components in the growth medium) after the fermentation process would be slightly lower than that (total carbohydrate baseline) before the fermentation as a result of nutrient utilisation. However, the underestimated EPS values could probably be compensated when bacterial cells were included in the *Whole* sample for EPS analysis. The bacterial cells would cause a slight increment in the EPS values because of their sugar-containing intracellular components. Therefore, these two factors

were assumed to nullify each other bringing the best estimated EPS values very close to the absolute values.

4.5.2 Validation of the revised EPS assay

This validation of EPS assay focused on the processing steps from the first ethanol precipitation through to the phenol-sulphuric acid method. The medium used for this work was based on 40% (v/v) RSM in milk permeate. Thirty-four samples obtained from the same batch of 2483 culture medium were processed and analysed for EPS according to the revised protocol. Coefficient of variation, the standard deviation of the mean (expressed as a percentage) was used to measure the precision of the method. The results of the EPS assay on the 34 samples are shown in Table 4.6.

Table 4.6 Levels of EPS determined 34 times based on *Whole* 2483 culture medium.

Sample	EPS (ug/ml)	Sample	EPS (µg/mL)
1	210	18	215
2	192	19	216
3	193	20	216
4	195	21	218
5	200	22	220
6	202	23	220
7	203	24	222
8	204	25	222
9	207	26	223
10	208	27	224
11	209	28	227
12	210	29	227
13	212	30	228
14	213	31	229
15	214	32	233
16	214	33	233
17	214	34	236

Mean = 214.9, Standard Deviation = 11.5

$$Coefficient\ of\ Variation = \frac{SD}{Mean} x100\% = 5.3\%$$

With the revised EPS assay, a coefficient of variation of ~5% was obtained. A major part of this variation was however contributed by the phenol-sulphuric method (Dubois et al., 1956). An increase in the levels of RSM could cause an increase in the variability of the EPS results. On the other hand, a decrease in the EPS variation could be expected when the medium contained lower levels of RSM. The improved procedures to quantify EPS are summarised in Figure 4.4. This method could reliably be used to quantify EPS in chemically-defined, semi-defined and complex media which contains up to 10% (w/v) SMP.

Revised Protocol for EPS Assay

1. *Swirl to mix culture medium in bottle to ensure homogeneity.*
2. *Adjust the pH of the sample to pH 7 with NaOH.*
3. *Add 100µL of filter-sterilised Flavourzyme (10% w/w) to 10mL of sample.*
4. *Incubate the sample at 50°C in a shaker for 4 h.*
5. *Vortex the sample for ≈ 15s.*
6. *Pipette 2.9ml of distilled water and 7ml of chilled absolute ethanol into the polypropylene Nalgene centrifuge tube.*
7. *Pipette 100µL of culture medium into the centrifuge tube.*
8. *Leave the sample overnight at 4°C.*
9. *Centrifuge samples (maximum of 8 tubes at a time) at 27,000g, 4°C for 40 min using SS 34 rotor. Ensure tubes are balanced within ±0.1g before centrifuging.*
10. *After centrifugation, **carefully** decant supernatant (pour away from pellet).*
11. *Invert the tubes on a piece of paper towel for ~ 10 min.*
12. *Pipette 3ml of distilled water to re-disperse the pellet in the centrifuge tube.*
13. *Pipette 7ml of chilled absolute EtOH into the centrifuge tube.*
14. *Repeat step 8-10.*
15. *Re-suspend pellet in 1ml of distilled water.*
16. *Transfer the sample to a fume hood.*
17. *Prepare a blank sample using distilled water (1mL).*
18. *Add 1ml of 5% (w/v) phenol solution to the sample and mix using a vortex (15s).*
19. *Add 5mL of concentrated sulphuric acid directly to sample.*
20. *Mix the sample thoroughly using a vortex.*
21. *Leave the sample to stand for 30 min.*
22. *Read absorbance at 485nm. Use the blank as the reference sample.*
23. *Obtain the amount of EPS from the glucose standard curve.*
24. *Amount of EPS is multiplied by 10 to account for the dilution factor.*
25. *Amount of EPS = EPS of the Test sample - EPS of Control sample.*

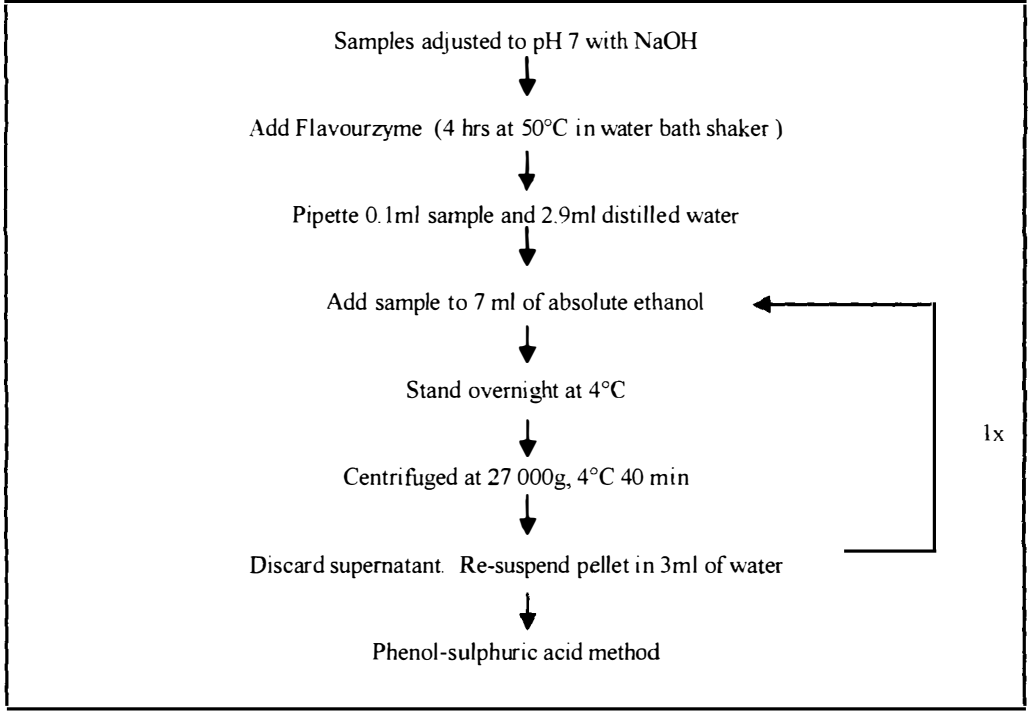

Figure 4.4 Step-by-step method for EPS assay

4.6 CONCLUSIONS

Although many procedures have been developed for quantification of EPS during the last decade, many procedures are not capable of providing good estimates of the levels of EPS produced in a complex growth medium. A common problem which results in poor estimation of EPS levels is the presence of low molecular weight carbohydrates (e.g. lactose) which become insoluble in ethanol, and are consequently included in the EPS analysis. Besides, little consideration is given to the type of proteolytic enzyme used to hydrolyse proteins as some of these enzymes appeared to possess glucanase activity. In addition, some methods did not take into account the total carbohydrates contributed by the control (blank) samples. Although each of these factors might seem trivial on its own, the error could accumulate to a significant value when all these factors are considered. The revised methodology is capable of obtaining reproducible results (~5% coefficient of variation). This revised method could be extended to assay EPS produced by other strains, including non-LAB. The improved assay could also be considered in complex growth media including those containing as high as 10% (w/v) skim milk solids.

Chapter 5

Isolation of Exopolysaccharides produced by *Lactobacillus delbrueckii* subsp. *bulgaricus* grown in Milk Permeate-based Medium

5.1 INTRODUCTION

Isolating and purifying EPSs produced by LAB grown in a milk medium is a difficult task (Cerning, 1990). This is because of EPS-protein, EPS-EPS and protein-protein interactions in the fermented system. Furthermore, bacterial cells are distributed throughout and entrapped in the complex protein and EPS network. In the 2483 culture, the EPS not only occupies the interstices of the protein aggregates but also possibly interacts with the proteins, resulting in a viscous and 'ropy' ferment. Forces involved in the interactions within an EPS producing culture broth include van der Waals, electrostatic interactions, hydrogen bonds and hydrophobic interactions (Christensen & Characklis, 1990). Therefore, the strategy to isolate EPS is dependent on the type of interactions that bind the EPS molecules together with the other medium components present, especially proteins and ions. In some EPSs, such as glycoproteins, covalent bonds are present (Emerson & Ghiorse, 1993). Unfortunately, the dominating forces may be different from one type of EPS-protein aggregate to another (Nielsen & Jahn, 1999) and various methods must be tested. An ideal separation protocol will not alter the EPS structure (i.e. preserve their native form) nor induce bacterial cell lysis. At the same time, it must be able to isolate most, if not all, of the EPS from the non-EPS components in the medium. Once the EPS is isolated, the rheological properties can be expected to differ from the fermented broth due to the reasons outlined above.

The aim of this investigation was to isolate and purify 2483 EPS in its native state for rheological and molar mass characterisation. The criteria for developing a suitable EPS isolation regime are as follows:

- Achieve optimal recovery of EPS in the continuous phase with no or minimal inclusion of non-EPS components.

- Employ simple methods without harsh chemical/physical processing steps to avoid modification of EPS structure.
- Methods employed can potentially be adapted for industrial scale-up in view that the isolated EPS may be isolated for other applications, for example, as a food stabiliser.

Two types of growth media (milk permeate-based medium and hydrolysed milk permeate-based medium) were used for 2483 EPS production. In the milk permeate-based medium, a combination of conventional methods was used to free the EPS from the protein aggregates so that the EPS could be isolated from the continuous phase of the culture medium. The effects of shear, sonication, enzyme, heat and pH on the 'release' of EPS in the aqueous phase were investigated. Once in the aqueous phase, the soluble EPS was separated by centrifugation from the insoluble components, such as cells and protein aggregates. On the other hand, isolation of EPS from the hydrolysed milk permeate-based medium was carried out by separating cell biomass using high speed centrifugation. The EPS in the aqueous phase was then isolated by ethanol precipitations. The two different approaches (using different culture media) to obtain native 2483 EPS were evaluated in this study. In addition, the carbohydrate composition of the isolated and purified 2483 EPS was determined.

5.2 Materials and Methods

5.2.1 *Fermentation of 2483 culture in milk permeate-based medium*

The 2483 seed culture was grown in 200mL of 10% (w/v) reconstituted skim milk powder (SMP) medium and incubated at 37 °C for 18 h. This was used to inoculate the milk permeate-based medium which consisted of 5.0% (w/v) SMP and 0.5% (w/v) yeast extract added to milk permeate. The growth medium (250mL) was free-steamed to 100°C for 10 min and was allowed to cool to room temperature before inoculating with 1% (v/v) 2483 seed culture. The fermentation was carried out at 37°C for 24 h.

5.2.2 *The hydrolysed milk permeate-based medium*

Another growth medium which consisted of 10.0% (w/v) SMP (Fonterra Co-operative Group Ltd, New Zealand) and 0.5% (w/v) yeast extract (Gibco-BBL) in milk permeate (Fonterra Co-operative Group Ltd, New Zealand) was prepared by adding 0.1% v/v Alcalase (Novozymes Ltd, Bagsvaerd, Denmark) solution to the growth medium and stirring for 30 min at 50°C. This was followed by the addition of 0.1% (w/v) Flavourzyme (Novozymes Ltd, Bagsvaerd, Denmark) solution and incubating for 2 h at 50°C with continuous agitation. The purpose of adding Alcalase (a proteinase) before Flavourzyme (a peptidase) was to maximise the hydrolysis of the milk proteins within the 2 h period. The medium was then neutralised to pH 7 using 2M NaOH and put through a pilot-scale ultra-filtration unit (220KPa inlet, 160KPa outlet, 50°C). The spiral-wound design ultra-filter (HFK 131, Koch Membrane Systems, Wilmington, MA, USA) has a molecular weight cutoff of 25 KDa. The UF permeate obtained (denoted as *hydrolysed milk permeate-based medium*) was used as the growth medium for 2483 EPS production. The fermentation of the 2483 culture in the hydrolysed milk permeate-based medium would not be successful unless a specially prepared seed culture was used. A detailed description of preparing the seed culture and the observations made are outlined in Appendix D. The hydrolysed milk permeate-based medium was flushed with nitrogen gas for 15 min and heated by free-steaming in an autoclave for 10 min at 100°C. Upon cooling to room temperature, the seed culture (1% v/v) was used as the inoculum. Fermentation was carried out at 37°C for 24 h.

5.2.3 Determination of EPS composition

The purified 2483 EPS (5mL) was hydrolysed with 2M aqueous trifluoroacetic acid (TFA) by heating in a sealed tube at 120°C for ~2 h. The hydrolysate was diluted with water after cooling and evaporated to dryness using a rotary evaporator at 70°C under vacuum. The sample was then reconstituted in Milli-Q water. The composition of the sample was determined by pulsed amperometry using a Dionex ED 40 electrochemical detector (Dionex, Sunnyvale, CA, USA) at Fonterra Co-operative Group Ltd (New Zealand) after separation on a Dionex PA1 column (250 x 4.6) with a PA1 guard column (Dionex, Sunnyvale, CA, USA). The filtered sample (0.2µm) was injected into the column and delivered to the detector at a flow rate of 1mL/min by a Dionex GP50 HPLC pump. For each run, the column was washed with 10mL of 200mM NaOH followed by a 10mL equilibration with 18mM NaOH before injection. A Dionex AS3500 autosampler was used to inject the samples and standards. The monosaccharides were then separated isocratically with 18mM NaOH. Both pump and detector were controlled by Dionex Peaknet 5.2 software. The column was maintained at 30°C with a column heater. Standard solutions of glucose, galactose, rhamnose and mannose in Milli-Q water were prepared (0.01, 0.02, 0.03, 0.04 and 0.05g/L) and filtered (0.2µm) prior to sample injection.

5.3 RESULTS AND DISCUSSION

The EPS isolation methods employed are discussed according to the type of growth media, i.e. the milk permeate-based medium followed by the hydrolysed milk permeate-based medium.

5.3.1 Isolation of EPS from milk permeate-based culture medium

In the milk permeate-based medium, various treatments were used to maximise EPS isolation. The factors investigated included the effects of pH, shear, sonication, heat and enzyme (Flavourzyme) on EPS recovery.

5.3.1.1 Effect of pH

The milk permeate-based 2483 culture medium was dispensed into seven portions. One was without pH adjustment (pH 3.9) and the others were adjusted to pH 5, 6, 7, 8, 9 and 10, respectively, using 2M NaOH. All control samples (at 0 h incubation) were first adjusted to pH 3.9 with lactic acid and then adjusted to the respective pH as with the test samples. EPS assay was carried out in duplicate for both the *Supernatant* and the *Whole* samples (i.e. the entire sample prior to centrifugation). The *Supernatant* was obtained by centrifuging the samples at 4,000*g* for 15 min using a bench-top micro centrifuge (Biofuge 13, Heraeus Sepatech GmbH, Osterode, Germany). Control samples (i.e. samples of culture media at 0 h incubation) were also subjected to the above treatments. The results of the effects of pH on the levels of isolated EPS are shown in Figure 5.2.

During fermentation, the casein micelles aggregated under the acidic environment as a result of reduced electrostatic repulsions between casein micelles (Tuiner and de Kruif, 1999; Lucey *et al.*, 1996). The resulting complex protein matrix formed had been shown, using microscopy, to entrap and possibly interact with the EPS (see Chapter 3). In the sample without any pH adjustment (i.e. at pH 3.9), only 34% of EPS was obtained in the *Supernatant* since most of the EPS had been entrapped in the casein micelle aggregates. Centrifuging the samples therefore resulted in a substantial removal of EPS together with the protein aggregates and bacterial cells.

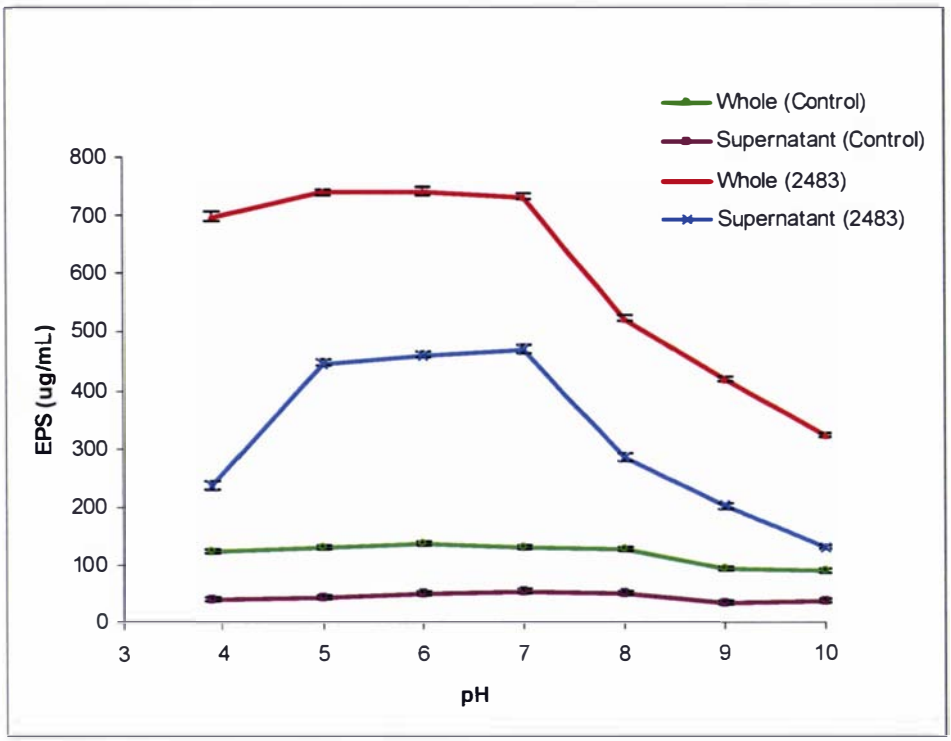

Figure 5.2 Effects of pH on EPS levels in the whole and supernatant samples. Determination of EPS was carried out in triplicate. Error bar indicates mean ± SD.

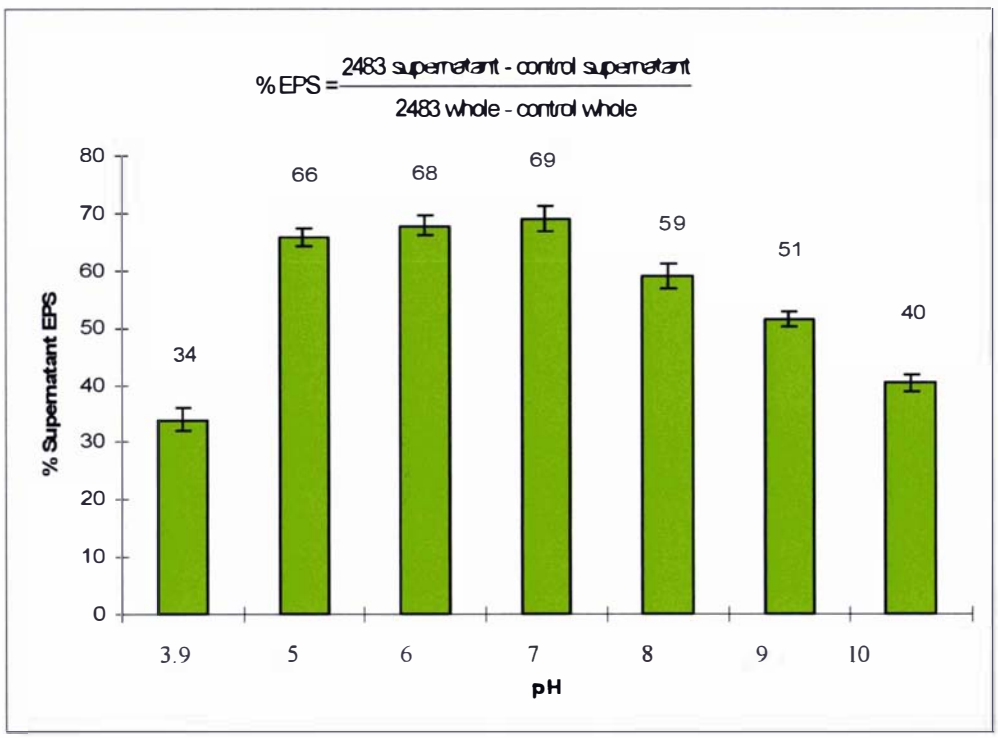

Figure 5.3 Percentage of EPS obtained in the supernatant at different pH values. Determination of EPS was carried out in triplicate. Error bar indicates mean ± SD.

The pH of the culture medium was increased to disperse the casein micelle aggregates and free the entrapped EPS. By doing so, the EPS in the *Supernatant* was found to increase markedly with increase in pH 3.9 to 5.0. Interestingly, there were only slight increases in EPS levels from pH 5.0 to pH 7.0. However, with further increases in pH (pH 8.0 and above), the levels of EPS were found to decrease. The concentrations of EPS in the *Whole* sample remained constant between pH 3.9 and 7.0, but decreased at higher pH values. The general trend indicated that increasing the pH value above the neutral pH resulted in decreasing EPS levels (see Figure 5.2). In terms of the properties of the culture medium, the observed 'ropy' characteristics were unaffected in the pH range from 5.0 to pH 7.0. However, from pH 8.0 to pH 10.0, the 'ropy' characteristics of the culture broth decreased drastically. This is consistent with the microscopy results reported in Chapter 3. The percentages of EPS in the *Supernatant* over a wide pH range are shown in Figure 5.3. The maximum 'release' of EPS in the *Supernatant* was found to occur between pH 5.0 and pH 7.0.

5.3.1.2 Effects of shear, heat and Flavourzyme

In this experiment, various treatments were applied to the milk permeate-based culture medium at pH 7. The effectiveness of each method was evaluated based on the levels of EPS in the *Supernatant*. The treatments given to the 2483 culture media were:

- Untreated culture medium at pH 3.9.
- Culture medium adjusted to pH 7 using 2M NaOH.
- Culture medium (pH 7) followed by heating at 85°C for 30 min.
- Culture medium (pH 7) followed by homogenisation using a shear mixer (Heidolph DIAX 600, Typ 10G) for 1 min at 25°C.
- Culture medium (pH 7) followed by ultrasonication at full amplitude for 20 s using a MSE Ultrasonicator (MSE Scientific Instruments, Crawley, United Kingdom).
- Culture medium (pH 7) followed by the addition of 0.01% (w/v) Flavourzyme. The enzymatic hydrolysis was carried out at 50°C for 2 h in a water bath with continuous agitation.
- Flavourzyme-treated sample heated at 85°C for 30 min.

The results of the various treatments on the levels of isolated EPS are shown in Figure 5.4. The percentages of EPS in the *Supernatant* are shown in Figure 5.5. Increase in EPS levels in the *Supernatant* was obtained when samples were adjusted to pH 7.0 (compared to the control sample). Homogenisation or sonication applied to the culture medium at pH 7 did not further improve EPS recovery. Instead, a slight reduction in EPS levels was observed. This was probably caused by an increase in non-EPS components suspended in the *Supernatant*. Heat treatment resulted in a complete loss of 'ropy' characteristics and a decrease in EPS levels as seen in both the *Whole* and *Supernatant* samples. The EPS probably underwent some changes in its molecular structure with heat treatment.

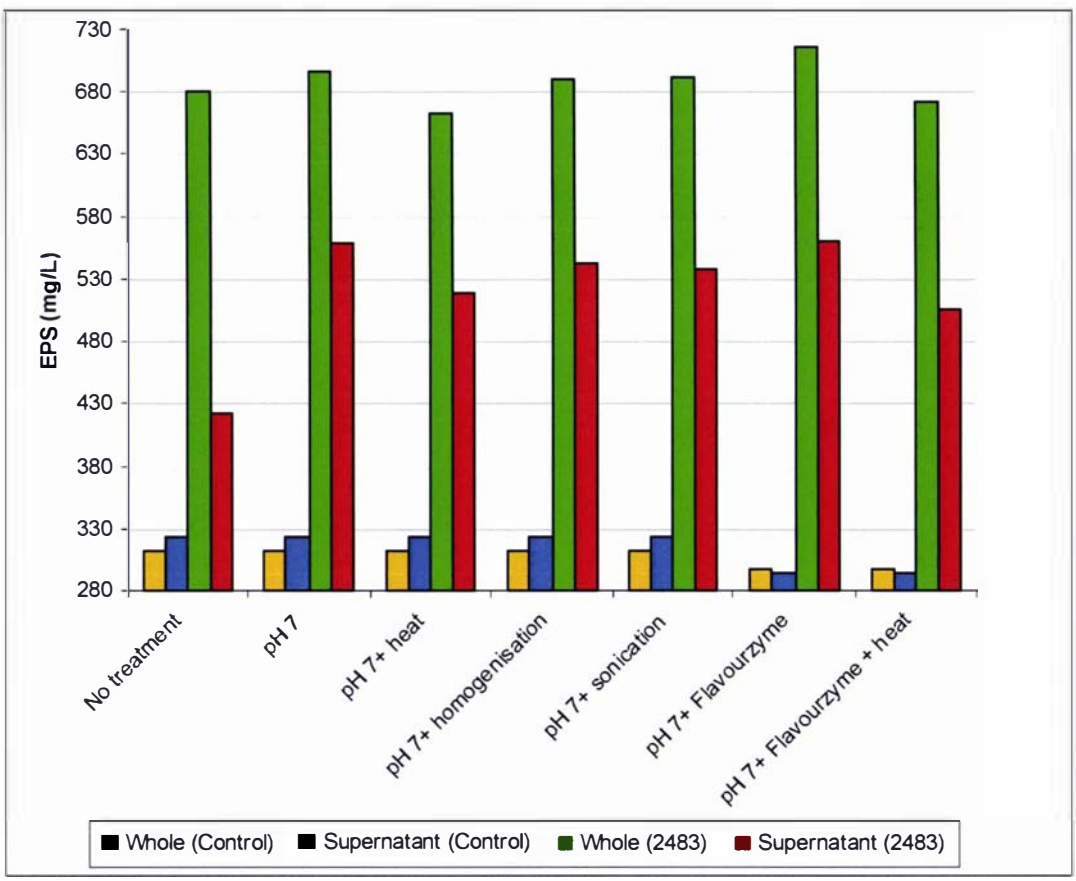

Figure 5.4 Effects of heat, shear, sonication and Flavourzyme on EPS levels in the *Whole* and *Supernatant* samples.

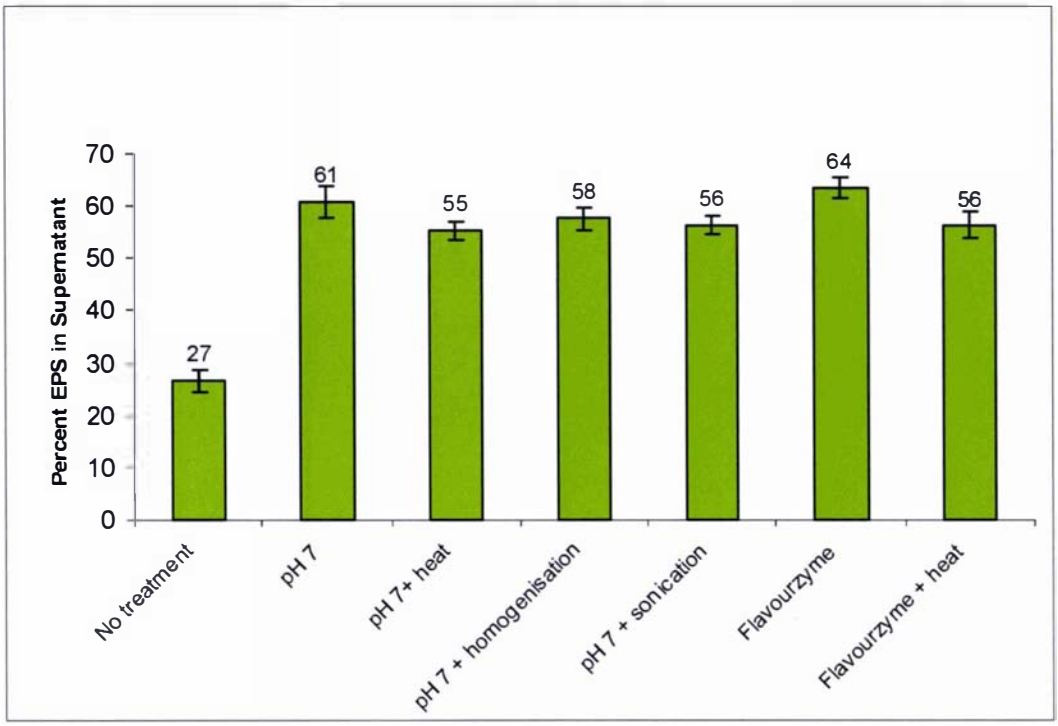

Figure 5.5 Percentage of EPS in the *Supernatant* resulting from different treatments. Determination of EPS was carried out in triplicate. Error bar indicates mean ± SD.

Treatment with Flavourzyme slightly increased the level of EPS recovered in the *Supernatant*. The samples adjusted to pH 7.0 and those treated with Flavourzyme appeared to be less viscous due to the 'disaggregation' of the casein micelle aggregates and hydrolysis of the protein aggregates. However, the 'ropy' characteristics of the media were still present in both samples, indicating that the EPS functional properties (hence, the EPS structure) probably remained unaltered under these conditions. The most important difference between the two samples was that the *Supernatant* of the Flavourzyme treated sample appeared clear after centrifugation, whereas the *Supernatant* of the sample at pH 7 remained opaque. Based on this, Flavourzyme treatment was a preferred option since most of the EPS could be recovered from the *Supernatant* without interference from the casein particles.

5.3.2 The hydrolysed milk permeate-based culture medium

In the previous section, Flavourzyme treatment was employed after fermentation which markedly improved EPS recovery. However, it was also recognised that some

intermediate molecular weight peptides may have formed as a result of incomplete enzymatic hydrolysis. These peptides could not be removed by centrifugation and could therefore interfere with subsequent purification of the EPS. In this study, a new procedure was developed that used the hydrolysed milk permeate-based medium (See *Section 5.2.2*) as the growth medium for EPS production. This approach ensured that only small molecular species (not more than 2.5 x 10^4 Da) were present in the growth medium before fermentation. Since the weight-average molecular weights of EPS produced by many LAB range between 10^4 to 10^6 Da (Cerning & Marshall, 1999; Grobben et al., 1997), the 2483 EPS (assumed to be within the molecular weight range) was isolated by precipitation with ethanol, while the small molecular weight species remained in the continuous phase. The removal of any interfering intermediate molecular species would improve EPS purity. This step was crucial so that accurate characterisation could be carried out on the purified EPS without interference from non-EPS components. Photographs of the hydrolysed milk permeate-based medium before and after fermentation with the 2483 culture are shown in Figures 5.6a and 5.6b respectively.

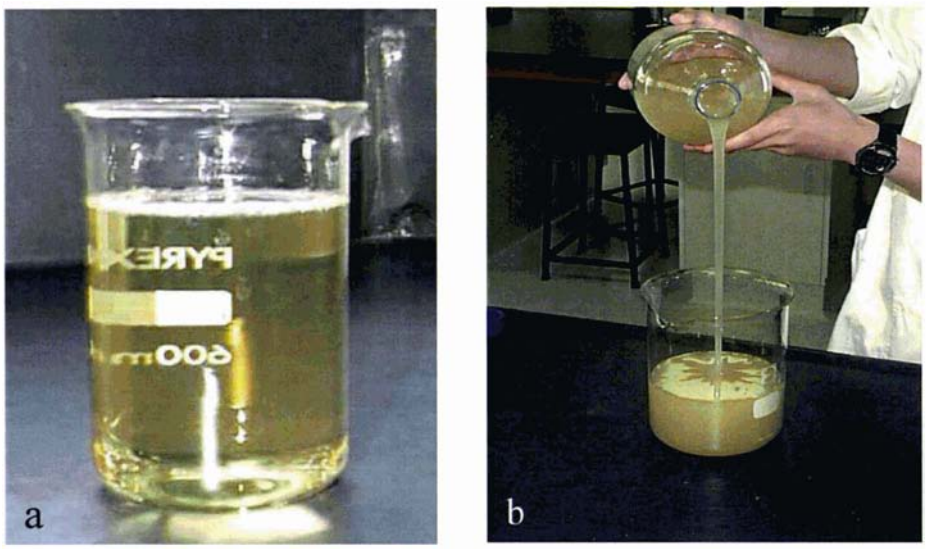

Figure 5.6 The hydrolysed milk permeate-based medium (a) before inoculation of 2483 and (b) after 24 h fermentation by 2483 at 37 °C. The latter shows viscoelastic properties of the 'ropy' broth.

The hydrolysed milk permeate-based medium was found to be effective as 2483 grew well in this medium and produced EPS at reasonably high levels (~400 µg/mL) comparable to many other strains of LAB (see Table 5.3). In addition, the EPS could be easily isolated using these simple procedures.

5.3.2.1 Separation of bacterial cells

In the preliminary trials, separation of EPS after incubation was attempted by employing a combination of microfiltration (MF) and the UF processes. The MF process was used to separate the bacteria and other large particles from the medium containing dissolved EPS. The MF membrane was a spiral-wound design (Model MFK 603, Koch Membrane Systems, Wilmington, MA, USA) and a pore size of 0.1 to 0.25μm. The permeate of the MF process obtained was then concentrated by the UF membrane (HFK 131). However, this procedure did not work as EPS was lost during the MF process. Analysis of the MF permeate and retentate for EPS concluded that a large amount of EPS was bound to the MF membrane.

An alternative method using high speed centrifugation (31,000*g* for 30 min at 20°C IEC B-22M Programmable Centrifuge, International Equipment Company, MA, USA) to separate the bacterial cells. A clear 'ropy' *Supernatant* and a firm pellet were obtained. The *Supernatant* was then filtered through a 0.44μm membrane filter followed by 0.2μm membrane filter to obtain a *Supernatant* free of particles larger than 0.2μm. A picture of the filtered culture medium is shown in Figure 5.7.

Figure 5.7 Filtered culture medium without bacterial cells. The culture medium showed 'ropy' characteristics.

5.3.2.2 Isolation of EPS

To precipitate the EPS from the medium, one part of the culture medium was added to 3 parts of cold absolute ethanol. The precipitated EPS was immediately recovered by winding around a glass rod. Figures 5.8a and 5.8b show EPS precipitate formed in ethanol and the recovery of EPS by means of a glass rod. The remaining cloudy ethanol mixture was left overnight at 4°C forming a brownish precipitate which settled at the bottom of the beaker. For ease of description, the EPS precipitate recovered by the glass rod is termed as 'Precipitate A' and the precipitate recovered in the solvent mixture after being held overnight at 4°C as 'Precipitate B'. The different characteristics of Precipitate A and Precipitate B suggest that they were probably two distinct EPS fractions. Comparisons between the two precipitates are given in Table 5.1.

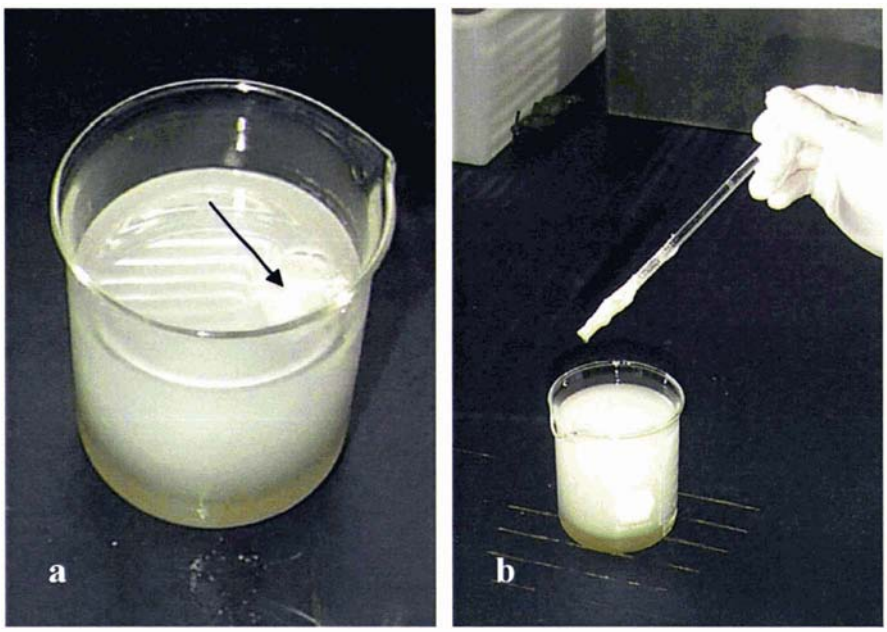

Figure 5.8 EPS precipitate formed in ethanol. (a) Arrow shows "cotton-ball" like precipitate (Precipitate A) which was recovered by winding around a glass rod as shown in (b).

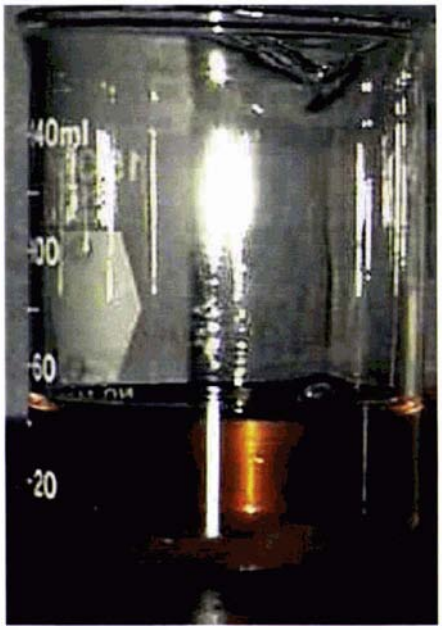

Figure 5.9 Precipitate B was only partially soluble in water after stirring for 8h at 4°C. A clear supernatant and an insoluble sediment layer were obtained upon standing.

Table 5.1 Comparisons between Precipitate A and Precipitate B obtained from 2483 EPS.

Precipitate A	Precipitate B
Formed "cotton-like" threads instantaneously during the addition of sample to ethanol (3:1).	Formed tiny precipitates in the ethanol-sample mixture over a period of time. Precipitate B was obtained after holding for ~16 h at 4°C. Amount of precipitates increased time.
Accounted for ~71% (w/w) of total EPS fraction.	Accounted for the remaining 30% (w/w) of total EPS fraction.
Could be recovered by winding around a glass rod since the EPS precipitate adhered to it.	Recovery was achieved by centrifugation.
Dissolved readily in water with only a small amount of insoluble material (~1-5% w/w), resulting in a slightly cloudy mixture.	Poor solubility in water resulting in a cloudy suspension. The mixture settled as two distinct layers after 8 h of stirring at 4°C (see Figure 5.9), i.e. a clear brownish *Supernatant* and a bottom layer of insoluble precipitate. The total carbohydrate level of the sediment was ~3x higher than the *Supernatant*.
Soluble EPS exhibited viscous and 'ropy' characteristics in solution.	Soluble EPS did not exhibit viscous or 'ropy' characteristics.

From the above, it appears that 2483 EPS consisted broadly of two fractions, a soluble and an insoluble fraction. The 2483 EPS fractions appeared to be consistent with the two EPS fractions of another strain of *Lactobacillus delbrueckii* subsp. *Bulgaricus* NCFB, reported by Grobben et al. (1997). They found the two EPS fractions with molecular masses of approximately 1.7×10^6 Da and 4×10^4 Da, both in almost equal amounts. In their case, the solubility of the two fractions was not described. Insoluble EPS fractions have only been reported for EPS produced by *Streptococcus thermophilus* (Cerning, Bouillanne, Desmazeaud & Landon, 1988).

5.3.2.3 Purification of EPS

Purification of the EPS fraction was carried out by first dissolving Precipitate A in distilled water and then centrifuging at 2000*g* for 20 min (Centrifuge; Hermle Z320, Wehingen, Germany). The *Supernatant* was then precipitated in cold ethanol (1:3) and the precipitate was again recovered using a glass rod. This procedure was repeated several times as a method to purify the EPS fraction. With each ethanol precipitation, the ethanol-sample mixture became increasingly clear after the EPS precipitate was removed. By approximately the 7^{th} or 8^{th} ethanol precipitation, a clear ethanol-sample mixture was left after the precipitate was removed. The clarity of the ethanol-sample mixture provided a visual indication of the purity of the EPS sample. The purified precipitate was white in colour and was readily and completely soluble in water giving a clear EPS solution with 'ropy' characteristics. Figures 5.10a and 5.10b show the EPS after the 3^{rd} ethanol precipitation step. The precipitate was formed almost instantaneously when added to the cold ethanol. After removal of the precipitate, the ethanol-sample mixture was still slightly cloudy at this stage. Figures 5.11a and 5.11b show EPS precipitation at the 6^{th} ethanol precipitation step. The ethanol-sample mixture appeared relatively clear after EPS precipitate was removed.

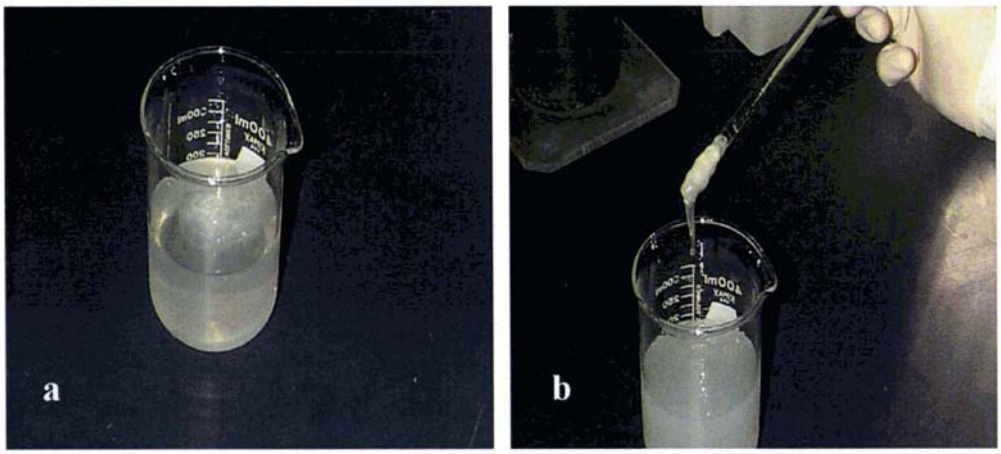

Figure 5.10 EPS precipitate formed after the 3rd ethanol precipitation; (a) white cotton thread-like EPS precipitate (b) the 'cloudy' ethanol mixture after removal of the precipitate.

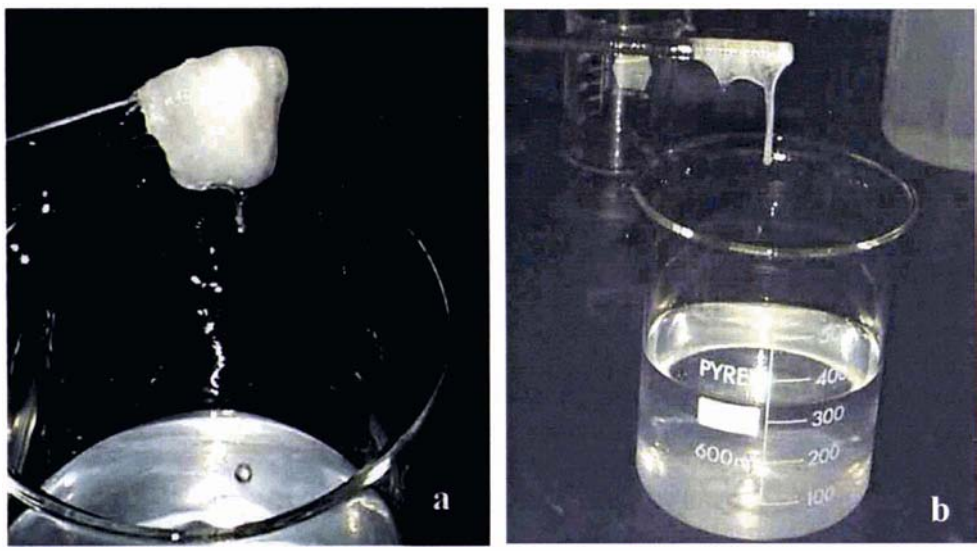

Figure 5.11 EPS precipitate formed after the 6th ethanol precipitation; (a) the EPS precipitate recovered by a glass rod and (b) the clear ethanol-sample mixture.

5.3.3 Purity of EPS

When EPS (Precipitate A) obtained from the first ethanol precipitation was dissolved in water, it was slightly yellowish in colour. The colour was considered to be due to compounds formed from the Maillard reaction which occurred during heat treatment of the hydrolysed milk permeate-based medium. With each ethanol precipitation, the yellowish colour of the precipitate gradually faded and a white precipitate was obtained after the 3rd ethanol precipitation.

Figure 5.12 shows that the purity of the EPS improved with the increasing number of ethanol precipitation steps. After the 7th ethanol precipitation step, the percentage purity (~98%) remained relatively constant. The data shown in Figure 5.12 are based on the dry weight of EPS and the phenol-sulphuric acid method for total sugar determination (Dubois, Gilles, Hamilton, Rebers & Smith, 1956). The elemental analysis of the freeze-dried EPS fraction (see Table 5.2) carried out using the Carlo Erba Elemental Analyser EA 1108 (Carlo Erba Instruments, Milan, Italy) by an independent certified laboratory (for methods, see Appendix E) showed the presence of nitrogen (~3% w/w) which could be due to the interaction of some peptides (from the growth medium) with the EPS. The ratio of carbon, hydrogen and oxygen is consistent with the empirical formula, $(CH_2O)_n$, for a typical polysaccharide consisting mainly of hexoses The main steps from incubation of the 2483 culture to the purification of EPS are summarised in Figure 5.13.

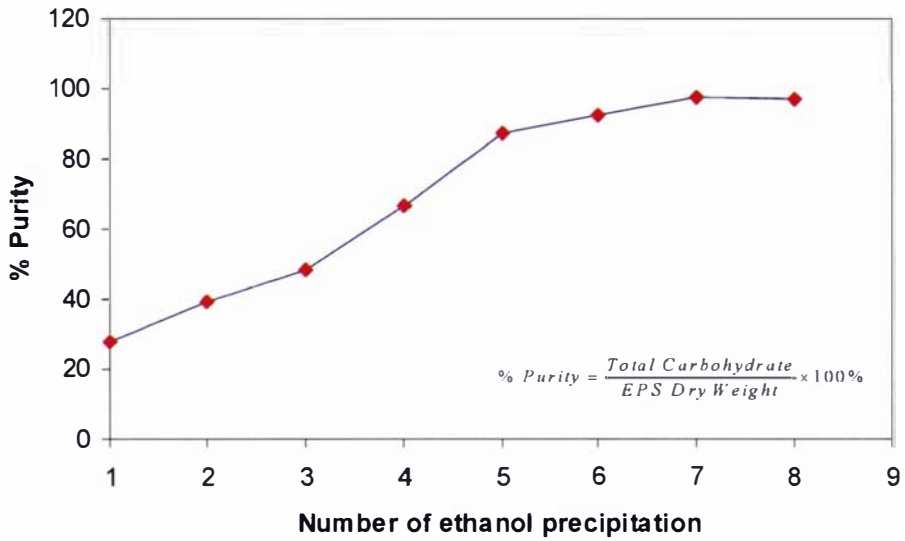

Figure 5.12 Effect of number of ethanol precipitation steps on EPS purity calculated on a dry weight basis (EPS was dried in an vacuum oven at 70°C for 24 h). The total carbohydrate was determined using the phenol-sulphuric acid method.

Table 5.2 Elemental analysis of freeze-dried purified 2483 EPS

	Carbon	Hydrogen	Oxygen	*Nitrogen*
% (w/w)	39.13	6.21	50.31	*2.81*
Moles	*3.26*	*6.21*	*3.14*	*0.2*

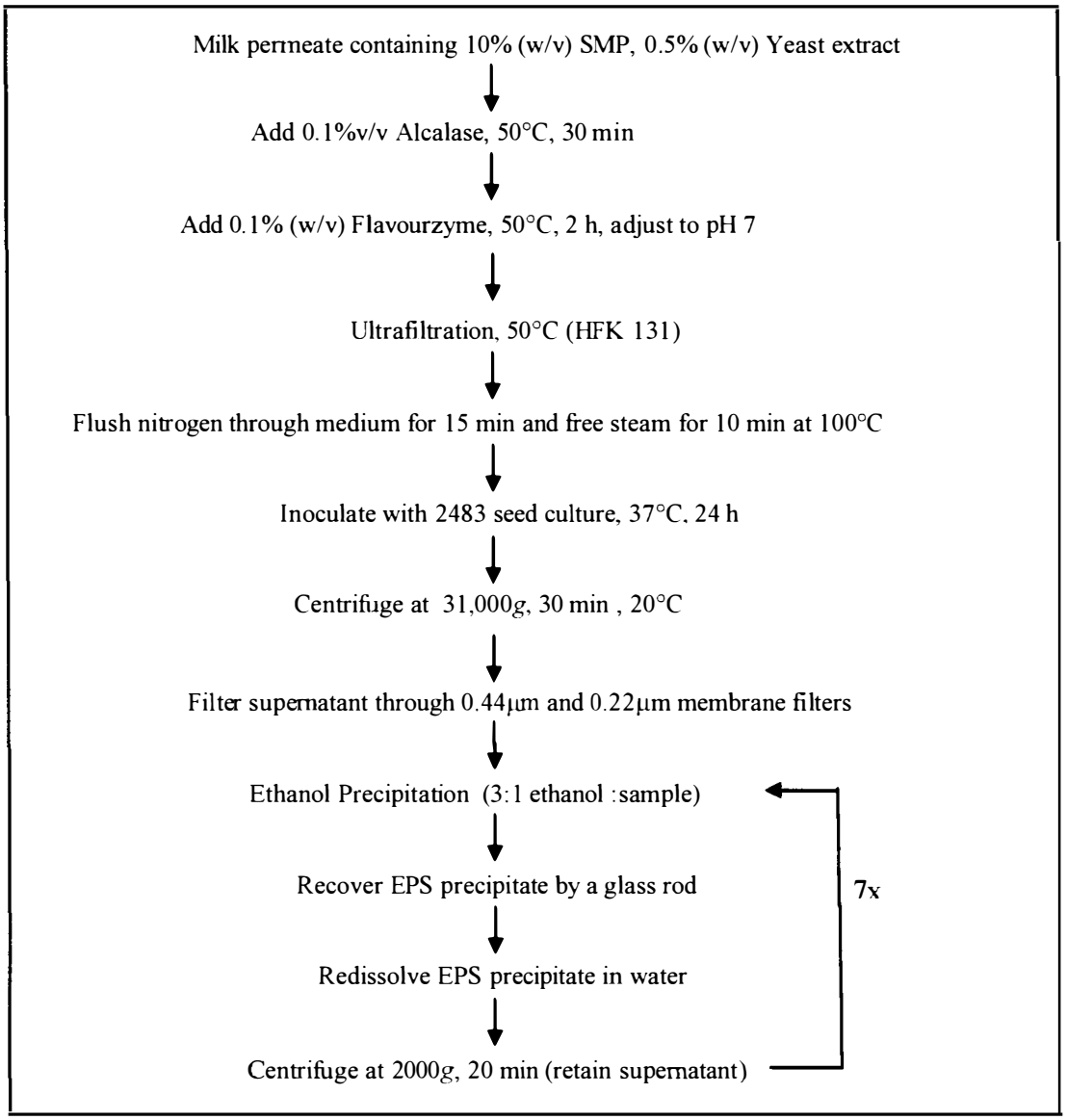

Figure 5.13 Steps involved in EPS isolation and purification.

5.3.4 Composition of 2483 EPS

Preliminary experiments on hydrolysis of the purified 2483 EPS, using 1M H_2SO_4 and heat treatment at 100°C for 5 h, did not achieve complete sugar hydrolysis. The use of trifluoroacetic acid (TFA) and heat treatment at 120°C for 2 h (performed in a sealed tube) on the other hand, achieved complete hydrolysis of the EPS. The use of TFA was advantageous in that it was easily removed by evaporation. The 2483 EPS was found to be a heteropolysaccharide made up of monosaccharide units of galactose, glucose, rhamnose and mannose in the ratio of approximately 5:1:0.6:0.5. There was also a trace amount of glucosamine (Figure 5.14).

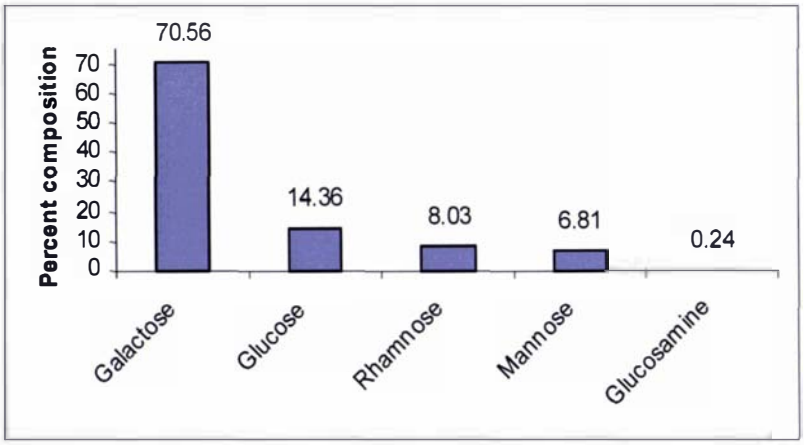

Figure 5.14 Composition of EPS determined by pulsed amperometry using a Dionex ED 40 electrochemical detector.

The compositions and levels of EPS produced by 2483 in the hydrolysed milk permeate-based medium and some other strains of LAB are given in Table 5.3. Galactose or glucose generally appeared to be the most frequently occurring monosaccharide in many LAB (Cerning, 1990). Other sugars have also been reported, which include rhamnose (Cerning, Bouillanne, Desmazeaud & Landon, 1986; Grobben et al., 1997; Gruter, Leeflang, Kuiper, Kamerling & Vliegenthart, 1993; Nakajima et al., 1990), N-acetylgalactosamine (Doco, Wieruszeski & Fournet, 1990), N-acetylglucosamine (Yamamoto, Murosaki, Yamauchi, Kato & Sone, 1994), fructose (Manca de Nadra, Strasser de Saad, Pesce de Ruiz Holgado & Oliver, 1985), xylose, mannose and arabinose (Cerning, 1990; Cerning et al., 1988). Other substituents such as phosphate, acetyl and glucoronic acid may occasionally be present in EPS molecules (Ruas-Madiedo, Hugenholtz & Zoon, 2002).

Table 5.3 Sugar compositions and levels of EPS produced from LAB.

Organism	Sugar Composition	Molar Ratio	EPS mg/L	References
Lactobacillus delbrueckii subsp. *bulgaricus* NCFB 2483	Galactose:Glucose:Rhamnose: Mannose	5:1:0.6:0.5	400-600	
Lactobacillus delbrueckii subsp. *bulgaricus* CNRZ 416	Galactose:Glucose:Rhamnose	4:1:1	285	(Cerning et al., 1986)
Lactobacillus delbrueckii subsp. *bulgaricus* CNRZ 737	Galactose:Glucose:Rhamnose	4:1:1	424	(Cerning et al., 1986)
Lactobacillus delbrueckii subsp *bulgaricus* CNRZ 1187	Galactose:Glucose: Mannose	14:9.4:1	110	(Bouzar, Cerning & Desmazeaud, 1996)
Lactobacillus delbrueckii subsp. *bulgaricus* NCFB 2772	Galactose:Glucose:Rhamnose	6.8:1:0.7	130	(Garcia-Garibay & Marshall, 1991; Grobben et al., 1997)
Lactobacillus delbrueckii subsp *bulgaricus* RR	Galactose:Glucose:Rhamnose	5:1:1	220	(Gruter et al., 1993; Kimmel, Roberts & Ziegler, 1998)
Lactobacillus delbrueckii subsp. *bulgaricus* CRL 420	Glucose:Fructose	1:2		(Manca de Nadra et al., 1985)
Lactobacillus casei CRL 87	Galactose:Rhamnose	1:1.1	488	(Mozzi, Graciela de Giori , Oliver & Graciela de Valdez 1996)
Lactobacillus lactis subsp. *cremoris*	Galactose:Glucose:Rhamnose	1.8:1.5:1		(Nakajima et al., 1990)
Lactobacillus rhamnosus ATCC 9595M	Rhamnose:Glucose:Galactose	3.7:2:1	1280	(Dupont, Roy & Lapointe, 2000; van Calsteren, Pau-Roblot, Begin & Roy, 2002)
Lactobacillus rhamnosus C83	Glucose:Galactose	2:3		(Vanhaverbeke et al., 1998)
Lactobacillus rhamnosus C83	Glucose: Galactose	1:1	131	(Gamar-Nourani, Blondeau & Simonet, 1997; Gamar-Nourani, Blondeau & Simonet, 1998)
Lactobacillus sakei 0-1	Glucose:Rhamnose	3:2	1400	(Degeest, Janssens & De Vuyst, 2001; Robijn, Imberty et al., 1996; van den Berg et al., 1995)
Streptococcus thermophilus Sts	Galactose: Rhamnose	5:2	127	(Faber, Zoon, Kamerling & Vliegenthart, 1998)
Streptococcus thermophilus OR901	Galactose:Rhamnose	5:2		(Bubb, Urashima, Fujiwara, Shinnai & Ariga, 1997)
Streptococcus thermophilus	Galactose:Glucose:N-acetylgalactoseactosamine	2: 1: 0.7		(Doco et al., 1990)
Streptococcus thermophilus LY03	Galactose:Glucose	4:1	546	(De Vuyst, Vanderveken, Van de Ven & Degeest, 1998; Degeest & De Vuyst, 1999)
Streptococcus thermophilus SY	Glucose:Galactose:Rhamnose	2:4.5:1	152	(Ricciardi et al., 2002)
Streptococcus thermophilus SFi20			143	(Navarini et al., 2001)
Streptococcus thermophilus SFi39	Glucose:Galactose	1:1		(Lemoine et al., 1997)
Streptococcus thermophilus SFi12	Galactose:Rhamnose:Glucose	3:2:1		(Lemoine et al., 1997)
Streptococcus thermophilus MR-1C	Galactose:Rhamnose:fucose	5:2:1		(Low et al., 1998)
Lactococcus lactis subsp. *cremoris* NIZO B40	Galactose:Glucose:Rhamnose	1.3:2.2:1	520	(Looijesteijn & Hugenholtz, 1999; Tuinier, Zoon, Olieman et al., 1999)
Lactococcus lactis subsp. *cremoris* SBT 0495	Galactose:Glucose:Rhamnose	1.75:1.45:1	150	Toba et al.,1990
Lactococcus lactis subsp. *cremoris* ARH53	Galactose:Glucose:Rhamnose	1:1.7:0.6	263	(Yang, Huttunen, Staaf, Widmalm & Tenhu, 1999)

The sugar composition of 2483 EPS was different from other strains of *Lactobacillus delbrueckii* subsp. *bulgaricus* (Table 5.3). However, there is a general similarity in that galactose is always the predominant monosaccharide, except for the EPS from *Lactobacillus delbrueckii* subsp. *bulgaricus* CRL 420, which are composed of only glucose and fructose (Manca de Nadra et al., 1985). Differences in EPS composition are likely to occur in different bacterial strains as shown by many workers. Changes in media components have also been shown to influence EPS composition (Looijesteijn & Hugenholtz, 1999) as reported for EPS produced by *Lactobacillus delbrueckii* subsp. *bulgaricus* NCFB 2772 (Grobben, Smith, Sikkema & De Bont, 1996) and *Lactobacillus casei* (Kojic et al., 1992). Sometimes, differences in EPS composition could be due to the poor separation of monosaccharides by different chromatographic techniques and the conditions under which the separation procedures were carried out. Moreover, some of the extraction and purification methods employed for the EPS may include contaminants from cellular materials. The composition of monomers determines the primary structure which ultimately influences the polysaccharide hydrodynamic conformation and, hence, its rheological properties.

5.4 CONCLUSIONS

The separation of the 2483 EPS from culture medium containing milk proteins (casein aggregates in particular) has proven to be a complex task. For such a culture medium, an effective method to separate the native EPS was to use Flavourzyme to hydrolyse the aggregated proteins. The EPS could then be recovered by ethanol precipitation. This procedure allowed only 64% of the EPS to be isolated and the EPS included protein contaminants from the medium. In addition, the native EPS was exposed to Flavourzyme which may alter its structure, hence, functionality. The treatment of culture medium by heat or under alkaline conditions (pH >7) was found to be detrimental to EPS (both levels and functionality).

A better approach to obtaining native EPS was to hydrolyse the milk proteins followed by ultrafiltration to obtain a clear permeate consisting of only small molecular weight species (<25 kDa). The hydrolysed milk permeate-based medium was found to be suitable for the growth of 2483, producing EPS of ~400mg/L. The EPS produced was easily isolated first by centrifugation to remove the bacterial cells followed by ethanol precipitation of the EPS. This method allowed maximum recovery of EPS from the growth medium.

In the isolation of 2483 EPS, two EPS fractions were obtained. Only the soluble fraction was of interest since it showed 'ropy' characteristics. Purification of the EPS fraction was achieved by subjecting the EPS to seven ethanol precipitation steps. Approximately 98% pure EPS was obtained using this procedure. None of the steps involved in the downstream processing employed harsh chemical or physical methods so that the integrity of the EPS structure was retained as indicated by the observed 'ropy' and viscous characteristics of the EPS solution when the precipitate was dissolved in water. The sugar composition of the soluble EPS fraction included galactose, glucose, rhamnose and mannose in the ratio of approximately 5:1:0.6:0.5 with traces of glucosamine. The methods used to produce, isolate and purify EPS were simple, relatively rapid and could be adapted for industrial scale operation.

Chapter 6

Light Scattering and Viscometric Studies of purified 2483 Exopolysaccharides

6.1 INTRODUCTION

Polysaccharides, categorised as gums or hydrocolloids, are commonly used as food ingredients because of two important functional properties – their ability to thicken aqueous solutions and/or form gels under specific conditions. Polysaccharides are usually added in small amounts to effectively change the flow behaviour of the aqueous phase, bringing about a change in the rheological properties of food systems.

The viscosity of a system is influenced by the ability of the polymer to perturb the solvent flow. At the molecular level, the geometrical conformation of a polysaccharide molecule in solution (which is influenced by length, shape, flexibility/stiffness and the presence of substituted groups) plays a significant role in the physico-chemical properties of food systems. Therefore, large and stiff molecules have a greater ability to increase solution viscosity than small and flexible molecules at the same concentration. The chemical composition of the molecule has little effect compared to the space occupied by the macromolecules in solution as their positions fluctuate in the flowing liquid due to Brownian motion. Other factors influencing the conformation adopted by polysaccharide molecules in a solution include temperature, charge density, counter ions, solvent quality, rate of shear and polymer concentration.

Knowledge of the molecular conformation and the rheological properties of a polysaccharide solution is essential if the functional properties of polysaccharides in food systems are to be well understood (Cesaro, 1994). In the present study, the physical properties of the purified EPS, produced by *Lactobacillus delbrueckii* subsp. *bulgaricus* NCFB 2483, were studied. The molecular parameters of the EPS (which include molar mass, radius of gyration, conformation in solution, etc) were determined using the multi-angle laser light scattering (MALLS) technique carried out in both

chromatography and batch modes. In addition, the flow characteristics and the intrinsic viscosity of 2483 EPS solutions were determined. The rheological characteristics of the 2483 EPS were compared with commercial dextran and λ-carrageenan.

6.2 MATERIALS AND METHODS

6.2.1 Sample preparation for static light scattering experiments

The mobile phase or solvent used in light scattering experiments was Milli-Q water with the addition of 0.02% w/v sodium azide. The solution was filtered through a 0.2μm filter (Millipore) followed by a 0.025 μm filter (Millipore) and degassed for ~1 h at room temperature. All glass apparatus that was in contact with the mobile phase and samples was first acid washed (5% v/v nitric acid), followed by thorough rinsing with water to minimise contamination by dust particles.

The freeze-dried 2483 EPS sample was dissolved in pre-filtered Milli-Q water containing 0.02% w/v sodium azide and filtered through a 0.2μm filter during sample loading into the flow cell. The concentration of 2483 EPS solutions used in the batch mode ranged from 2.11x 10^{-6} to 1.05 x 10^{-5} g/mL, and was 4.56 x 10^{-6} g/mL in the chromatography mode.

6.2.1.1 Determination of the specific refractive index increment (dn/dc)

To determine the *specific refractive index increment* (*dn/dc*) of 2483 EPS, the following procedure was carried out. Solutions of NaCl, at various concentrations, were measured using a differential refractometer (R401, Waters, Milford, MA) to obtain a plot of differential refractive index (DRI) voltage (*V*) versus NaCl concentration. The DRI response factor (*dV/dn* ~3.6 x 10^{-4}) was obtained by dividing the gradient of the plot by the *dn/dc* value of NaCl (1.74mL/g at 633nm, 25°C). Similar plots were obtained using dextran (Sigma, M_w ~2.0 x 10^6 Da) and 2483 EPS solutions. The slope (*dV/dc*) was divided by the DRI response factor (dV/dn) to obtain the *dn/dc* values. Determination of the *dn/dc* value was carried out in duplicate.

6.2.1.2 Multi-Angle Laser Light Scattering (MALLS) in batch mode

The setup for the batch mode experiments involved the use of a multi-angle laser light scattering (MALLS) photometer (DAWN DSP, Wyatt Technology, Santa Barbara, CA, USA) and a differential refractometer (R401, Waters, Milford, MA), connected in

series. The DAWN DSP is fitted with 16 photo-detectors placed at discrete angles around the sample cell (K-5 flow cell) to detect the scattered intensity of laser light. The light source is a helium neon laser with an operating wavelength of 632.8nm. Normalisation to the detector at 90° was carried out using 1% w/v dextran solution (Sigma) of a weight-average molar mass (M_w) of 9.5 x 10^3 Da prior to the test run. The dextran solution was loaded into the MALLS by a syringe at a rate of 30mL per minute using a syringe with a 0.2μm filter attached so that the samples were filtered just before entering the flow cell. A baseline was established using only the solvent before and after sample loading. Normalisation was performed at the beginning of each batch mode experiment using the same solvent used to prepare the EPS solutions. The EPS samples were loaded into the system from the lowest to the highest concentrations. Data for each sample were collected for approximately 2-3 min after the light scattering signal was stable. The Astra software was used to analyse light scattering data using the Berry plot to obtain the weight-average molar mass (M_w), the z-average RMS radius ($(\langle r_g^2 \rangle_z)^{1/2}$) and the second virial coefficient (A_2).

6.2.1.3 Gel-filtration Chromatography combined with Multi-Angle Laser Light Scattering in chromatography mode

When operating under the chromatography mode, the gel-filtration chromatography (GFC) column (SB-806 HQ, Shodex, Japan) was coupled to a high-performance liquid chromatography (HPLC) system (GBC Scientific Equipment Ltd, Victoria, Australia), the DAWN DSP MALLS photometer and the differential refractometer. The HPLC system consists of a HPLC pump (model LC 1150), an ultra-violet (UV) absorbance detector (model LC 1200) and a system organizer (model LC 1440, GBC Scientific Equipment Ltd, Victoria, Australia). The GFC column (8.0 x 300mm) was packed with polyhydroxymethacrylate gel which is suitable for analysis of water-soluble polymers. The particle size of the gel was 13μm with pore size of 1x10^3 Angstrom. The column had a maximum pressure and flow rate of 30kgf/cm^2 and 1.2mL/min respectively. The GFC column was suitable for a wide molecular weight range of 1 x 10^3 to 2 x 10^7 Da based on pullulan in water.

The mobile phase, which was continuously gassed with helium, was pumped through the GFC column at a flowrate of 0.5mL/min under low pressure (~20 psi). The eluant from the GFC column then flowed through the UV detector operating at 280nm, through the flow cell of the MALLS photometer, and eventually the differential refractometer before exiting the system. A simplified illustration of the GFC-MALLS setup is shown in Figure 6.1.

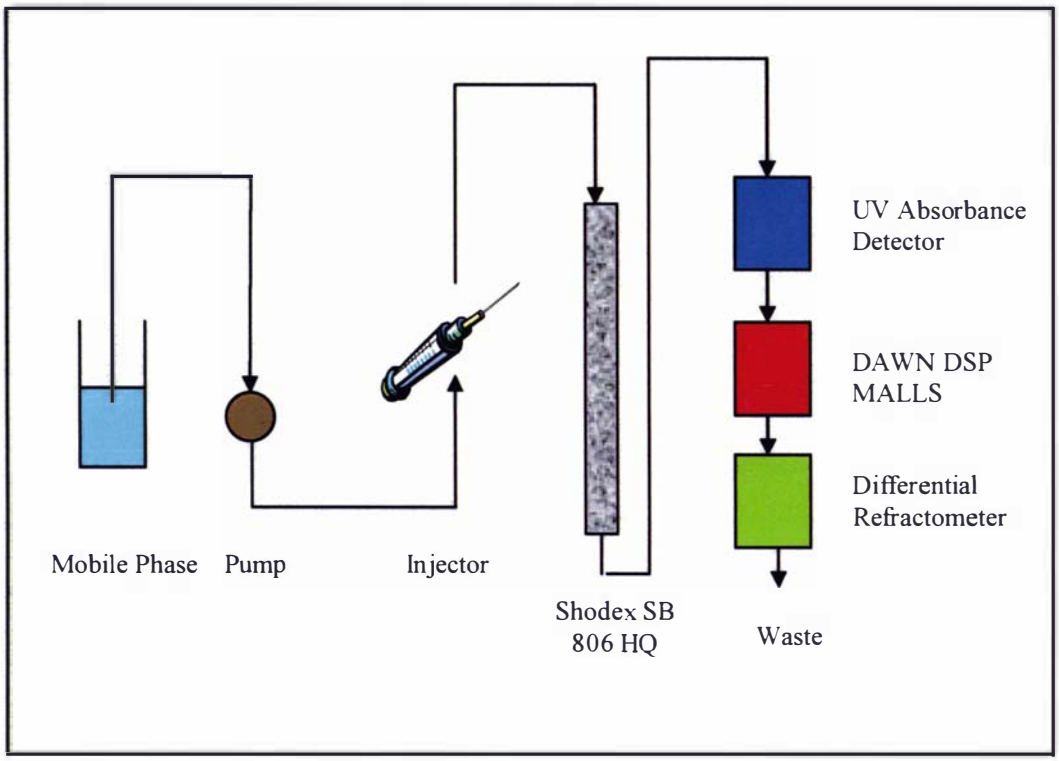

Figure 6.1 Flow diagram of GFC-MALLS setup.

The Astra software (version 4.5, Wyatt Technology Corp., Santa Barbara, USA) provided on-line monitoring of UV, light scattering and DRI signals. Before introducing any sample into the column, a stable baseline was established using only the mobile phase. The responses to light scattering intensity of the photodiodes arrayed around the scattering cell were normalised to the detector at 90° with 1% w/v dextran solution (Sigma) with M_w ~9.5 x 10^3 Da and $(r_g^2)_z^{1/2}$ of ~5nm. Normalisation was carried out at the same flow rate as the test samples. Note that the molecular dimensions of the sample used to measure normalisation coefficients for the instrument

were less than 1/20th of the wavelength of incident light so that the light scattering was isotropic (i.e. equal in all directions). Generally, M_w less than 5.0 x 10^4 Da and polydispersity of less than 1.1 are recommended (Wyatt Technical Notes, 1997).

The 2483 EPS sample (20 μL) was loaded into the column through an injection port and the molecular species were separated in the column at 25°C over an elution time of ~40 min. The separation of the molecular species was shown as UV, light scattering and DRI chromatograms in the Astra software. Upon completion of each run, the chromatograms were aligned to correct for the time delay of the sample reaching the detectors (i.e. UV, MALLS, and DRI detectors). The data were analysed by selecting the appropriate slice on the light scattering chromatogram and fitted using the Berry equation to generate molecular parameters (M_w and $(r_g^2)_z^{1/2}$) of the EPS sample. The molecular parameters of 2483 EPS were calculated based on light scattering and DRI data. The MALLS detectors determined the intensity of light that was scattered by the 2483 EPS molecules, while the DRI detector determined the polymer concentration. The UV signal provided an indication of the presence of proteins and peptides.

6.2.2 Viscometric studies of 2483 EPS

6.2.2.1 Flow curves of 2483 EPS solution

Two commercial polysaccharides, namely, dextran (Sigma, M_w ~2 x10^6 Da) and λ-carrageenan (FMC, Viscarin GP 209, M_w ~1 x10^6 Da), were used as reference samples for comparative purposes. Both λ-carrageenan and dextran are non-gelling polysaccharides. Water was used as the solvent for preparing 2483 EPS and dextran solutions. However, the λ-carrageenan solution was prepared (1%w/v) in 0.075M KCl and then dialysing (molar mass cutoff: 6000-8000 Da) overnight against 0.075M KCl at 4°C. The dialysate was used in subsequent dilution of the sample (according to isoionic dilution procedure) to prepare solutions of various concentrations (Lapasin & Pricl, 1995).

The flow curves from different concentrations of 2483 EPS (0.11-0.34% w/v), dextran (1-15% w/v) and λ-carrageenan (0.04-1% w/v) solutions were determined over a range

of shear rates using the Paar Physica rotational viscometer MC1 (Anton-Paar, Graz, Austria) with double-gap attachment (MS Z1 DIN). All samples were centrifuged at 6000*g* for 10 min to remove air bubbles prior to carrying out the steady shear at 20°C. The shear stress and shear rate data were obtained from the RheoSOLVE version 2.1 software.

Before carrying out the above, 2483 EPS at 0.24% w/v was assessed by performing a 'thixotropic' loop under steady shear from 0 to 1000 s^{-1} and then back to 0 s^{-1} over a duration of 2 minutes. In addition, 2483 EPS solution was tested in the presence of salt to determine whether its viscosity was affected, as it would be, in the case of a polyelectrolyte polymer. The EPS solutions (0.1%, 0.05% and 0.05% w/v) were prepared in Milli-Q water, 0.01M NaCl and 0.1M NaCl. The relative viscosity of each sample was determined using a capillary viscometer Cannon-Fenske capillary viscometer (Viscometer no. 100, 821K, Cannon Instrument Co., USA) at 20°C.

6.2.2.2 Intrinsic viscosity determination

Dilute solutions of 2483 EPS (0.001-0.09% w/v), dextran (0.2-1.0 % w/v) and λ-carrageenan (0.01-0.1% w/v) were prepared. Both the 2483 EPS and dextran were diluted with Milli-Q water, whereas the diluted λ-carrageenan samples were prepared using the 0.075M KCL dialysate based on the isoionic dilution procedure. The samples were dissolved in the respective solvents at room temperature and centrifuged at 6,000*g* for 10 min. Centrifugation of the samples was carried out to remove any undissolved matter.

Viscosity measurements of the samples were performed using two viscometry techniques: a Cannon-Fenske capillary viscometer (Viscometer no. 100, 821K) and the Paar Physica rotational viscometer. With the capillary viscometer, the relative viscosity (η_{rel}) of the sample was measured at 20°C using water as a reference sample. Each sample (5mL) was loaded into the capillary viscometer and allowed to equilibrate for ~5 min before measuring the efflux time. The viscometer had a capillary diameter of 0.63mm ± 2% and a bulb volume of 3.1mL ± 5%. The instructions for cleaning and

operating the capillary viscometer are found in ASTM D 445, D446 and ISO 3105. Relative viscosity was obtained according to equation (1.19). The density of EPS solution at 20°C was obtained using a pycnometer. The data obtained were fitted using the Huggins and Kraemer functions. Intrinsic viscosity, $[\eta]$, was determined by extrapolating the two linear functions to zero concentration in order to obtain the average values at the intercept.

With the Paar Physica viscometer, a 25mL sample was required for each measurement. The steady shear flow curve for each sample was carried out in duplicate. Intrinsic viscosity was also determined by fitting the zero-shear specific viscosities, obtained from the flow curves, in the Huggins and Kraemer functions.

6.3 RESULTS AND DISCUSSION

6.3.1 Light scattering studies on 2483 EPS

6.3.1.1 Specific refractive index increment (dn/dc) of polysaccharide

The *dn/dc* value obtained for dextran was ~0.14mL/g which agrees with reported values compiled by Theisen et al. (2000). The *dn/dc* obtained for 2483 EPS was ~0.41mL/g. The value was considered high compared to many polysaccharide samples which usually have *dn/dc* values ranging from 0.13-0.18 mL/g (Fishman et al., 1997; Theisen, Johann, Deacon & Harding, 2000). The *dn/dc* value obtained was based on the assumption that all the molecular species within the sample have the same refractive index.

6.3.1.2 Multi-Angle Laser Light Scattering (MALLS)

The light scattering data of 2483 EPS obtained through batch mode experiments were plotted using the Berry equation and fitted to a second order polynomial (Figure 6.2). The Berry method has been shown to determine M_w of large molecules with greater accuracy (Hanselmann et al., 1995; Yoo & Jane, 2002). Some angles, usually the very low and high showed noisy signals, and hence, were excluded.

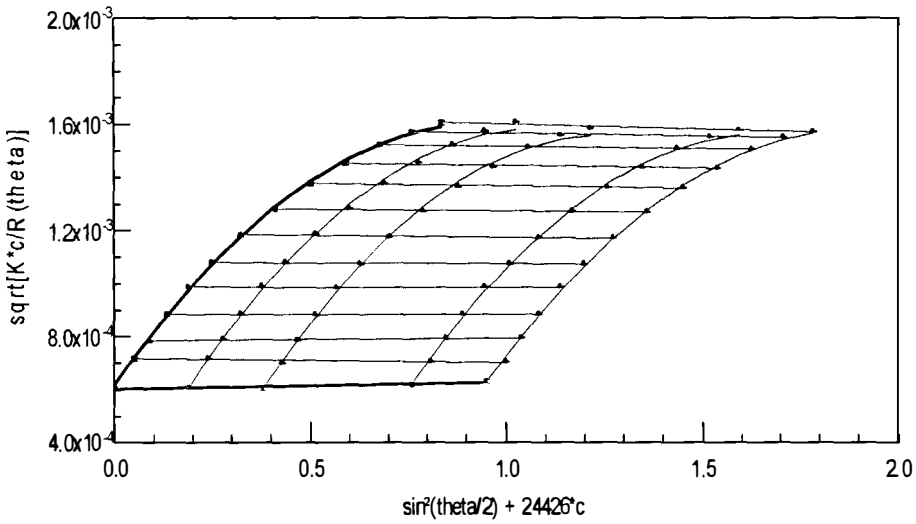

Figure 6.2 Berry plot for 2483 EPS in aqueous solution at 25°C at 2nd order detector fit angle. Concentrations of the EPS solution were 2.11, 4.22, 8.44 x 10^{-6} and 1.05 x 10^{-5} g/mL. The M_w, $(r_g^2)_z^{1/2}$ and A_2 are 2.67 ± 0.04 x 10^6 Da, 169.8 ■ 2.1 nm and 1.38±0.66 x 10^{-3} (mol mL/g^2) respectively.

The M_w obtained by the batch mode for 2483 EPS was ~2.7 x 10^6 Da, which lies within the range of molar masses of EPS obtained from different strains of LAB reported by various researchers (Table 6.1). The $(r_g^2)_z^{1/2}$ value was relatively large (~170nm), suggesting that the 2483 EPS molecules were rather long chains (i.e. more linear than branched). The positive A_2 value for 2483 EPS samples suggests that water was a good solvent for the EPS molecules.

Table 6.1 Molecular weight of EPSs produced by different Lactic acid bacteria

Lactic Acid Bacteria	Molecular Weight (10^6 Da)	References
Lactobacillus delbrueckii subsp. *bulgaricus* CNRZ 416	0.5	(Cerning et al., 1986)
Lactobacillus delbrueckii subsp. *bulgaricus* CNRZ 737	0.5	(Cerning et al., 1986)
Lactobacillus lactis subsp. *cremoris*	1.7	(Nakajima et al., 1990)
Lactobacillus delbrueckii subsp. *bulgaricus* NCFB 2772	1.7	(Grobben et al., 1997)
Lactobacillus sakei 0-1	6.0	(Degeest et al., 2001, Robijn, Gutierrez et al., 1996; van den Berg et al., 1995)
Streptococcus thermophilus	1.0	(Doco et al., 1990)
Streptococcus thermophilus SFi39	2.0	(Lemoine et al., 1997)
Streptococcus thermophilus SFi12	2.0	(Lemoine et al., 1997)
Streptococcus thermophilus Sts	3.7	(Faber et al., 1998)
Streptococcus thermophilus LY03	1.8	(De Vuyst et al., 1998; Degeest & De Vuyst, 1999)
Streptococcus thermophilus SY	5.0	(Ricciardi et al., 2002)
Lactococcus lactis subsp. *cremoris* SBT 0495	1.8	(Toba et al., 1990)
Lactococcus lactis subsp. *cremoris* LC330	1.0	(Marshall, Cowie & Moreton, 1995)
Lactococcus lactis subsp. *cremoris* NIZO B40	1.6	(Looijesteijn & Hugenholtz, 1999; Tuinier, Zoon, Olieman et al., 1999)
Lactococcus lactis subsp. *cremoris* SBT 0495	2.6	(Higashimura, Mulder-Bosman, Reich, Iwasaki & Robijn, 2000)
Bifidobacterium longum BB-79	2.0	(Roberts, 1995)
Bifidobacterium longum ATCC 15707	*1.2*	(Abbad-Andaloussi et al., 1995)

6.3.1.3 Gel-filtration Chromatography combined with Multi-Angle Laser Light Scattering (GFC-MALLS)

The superimposed signals (UV, DRI and light scattering at 90°) of the 2483 EPS are shown in Figure 6.3. The first DRI peak of the chromatogram (from the left) and the high light scattering signal indicated the large molecular weight fraction of interest. The fractions that were eluted subsequent to the first peak contained relatively smaller molecular species (approximately $<10^3$ Da), and hence, no light scattering signal (due to poor light scattering to noise ratio) was observed. Different fractions of the molecular species separated by the column were detected by the DRI and/or UV detectors, producing signals proportional to the concentrations of the molecular species. Generally, the separation of the 2483 EPS molecules was successfully achieved using the Shodex SB 806 HQ column.

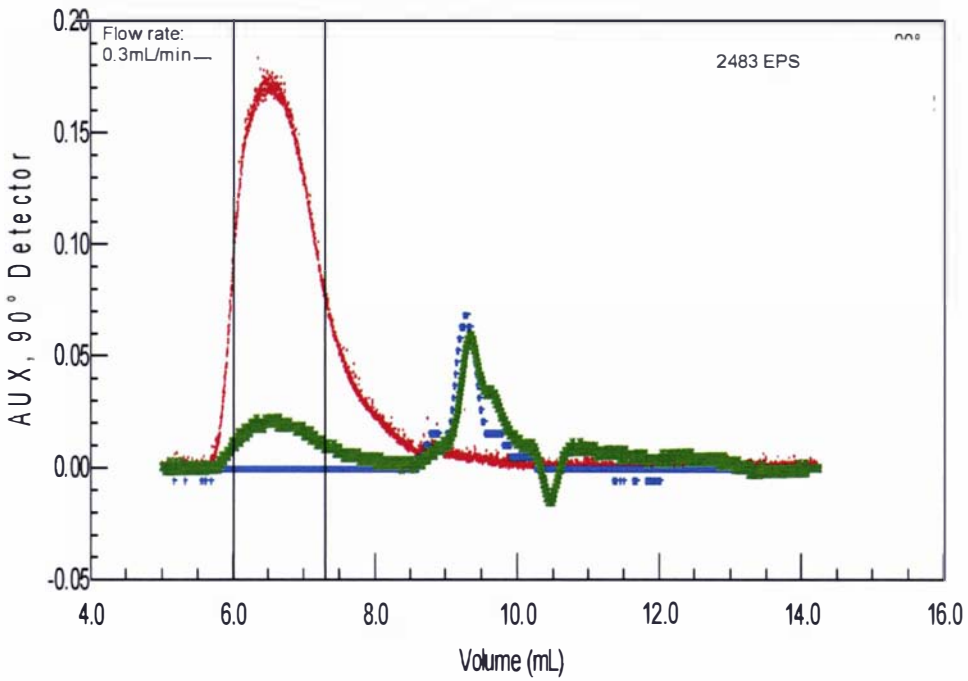

Figure 6.3 Light scattering (red), DRI (green) and UV(blue) signals from 2483 EPS sample separated using Shodex SB-806 HQ column. The light scattering signal was traced for the detector at a 90° angle. Scaling factor for DRI and UV signals is 0.9. The two vertical lines indicate the boundaries of peak and represent the area of the chromatograms selected for molecular weight determination by the ASTRA software.

Selection of an appropriate model (e.g. Zimm, Debye or Berry equation) to fit light scattering data is crucial in determining the molecular weight and RMS radius of the samples (Yoo & Jane, 2002). Of equal importance is the consideration of an appropriate order of polynomial, especially for scattering intensities at low angles, as it can affect the values of M_w and $(r_g^2)_z^{1/2}$ (Capron et al., 1995). From the results of this study, the Berry equation and second order polynomial provided the best fit to the data within the selected fraction (Figure 6.3). The molecular parameters for 2483 EPS derived from the Berry plot are shown in Table 6.2. The values of M_w and $(r_g^2)_z^{1/2}$ are generally in agreement with those obtained in the batch mode. A slight variation is, however, expected for M_w obtained by GFC-MALLS. This is because the M_w obtained by the GFC-MALLS technique was based on a specific eluted EPS fraction, separated by the GFC column. Whereas in the batch mode, the M_w was obtained by averaging all molecular species present in the EPS sample, including the small molecular species and impurities.

Table 6.2 Molecular parameters of 2483 EPS obtained by GFC-MALLS.

Molecular Weight (Da)	
M_n	1.88 ± 0.32 x 10^6
M_w	2.16± 0.37 x 10^6
M_z	2.62 ● 1.04 x 10^6
Root Mean Square Radius (nm)	
$(r_g^2)_n^{1/2}$	141.0 ± 11.3
$(r_g^2)_w^{1/2}$	151.0 ± 10.8
$(r_g^2)_z^{1/2}$	164.6 ± 10.4
Polydispersity	
M_w/M_n	1.15 ± 0.27
M_z/M_n	1.40± 0.64
Fit method	
Model	Berry
Order of polynomial	2

6.3.1.3.1 Molecular weight distribution and polydispersity

The molecular weight distribution and the scattered intensity of the first eluted 2483 EPS fraction from the column are shown in Figure 6.4. The linear decrease in the molecular weight with elution volume indicates a good separation of the molecular species from the gel filtration column. The molecular weight of the EPS fraction ranges from ~$1.0x10^6$ to $3.5x10^6$ Da. High polydispersity indices have been reported for natural polysaccharides, as in the case of dextran, which has a value (M_w/M_n) of around 4.0 (Fishman et al., 1996). The polydispersity index (M_w/M_n) for 2483 EPS was surprisingly low (~1.15). A low M_w/M_n value of ~1.13 has previously been reported by (Tuinier, Zoon, Olieman et al., 1999) for EPS from *Lactococcus lactic* subsp. *cremoris* NIZO B40.

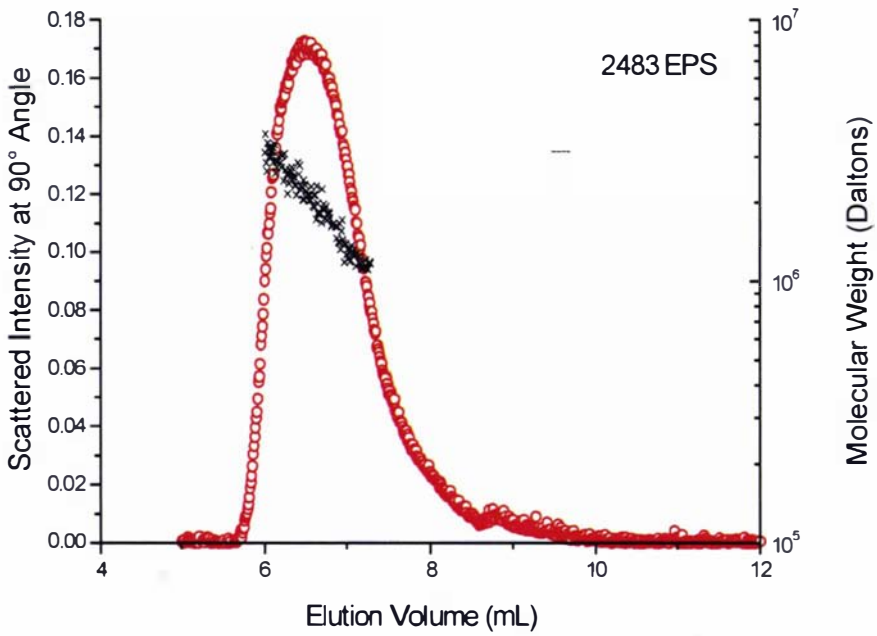

Figure 6.4 Light scattering signal at 90° (o) and molecular weight distribution (x) as a function of elution volume for 2483 EPS.

6.3.1.3.2 Molecular conformation

The conformation of the 2483 EPS molecules may be predicted from a log-log plot of the $(r_g^2)_z^{1/2}$ versus M_w as shown in Figure 6.5.

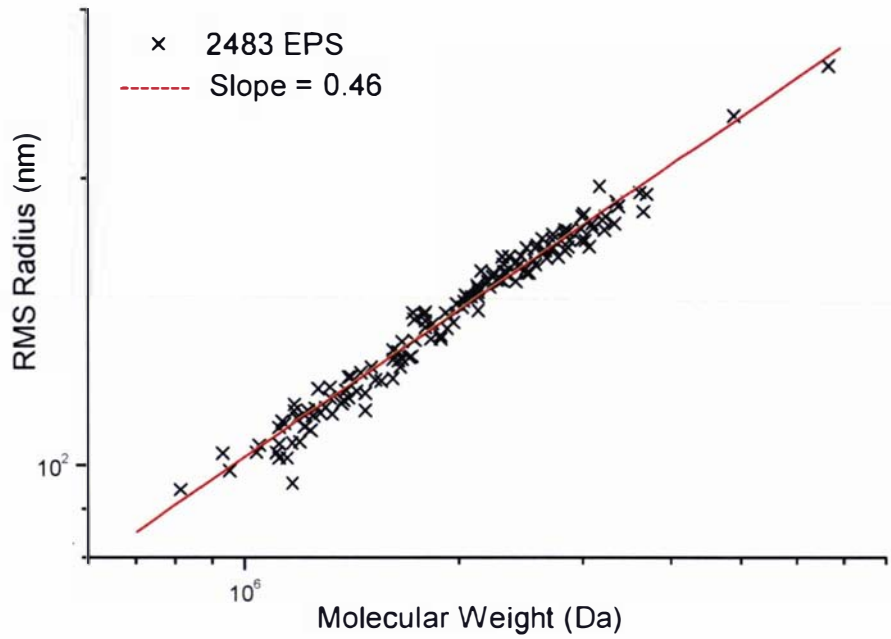

Figure 6.5 Weight-average molar mass as a function of z-average (RMS) radius for 2483 EPS.

The slope obtained from linear regression provides an approximation of the shape of a polysaccharide molecule in solution. Generally, gradient of 0.3, 0.5 or 0.6, implies a sphere, random coil or stiff rod conformation, respectively (Podzimek, 1994). The gradient obtained for 2483 EPS was 0.46, suggesting that the bacterial polysaccharide molecule adopts a flexible random coil conformation in aqueous solution.

6.3.2 Viscometric studies on 2483 EPS

6.3.2.1 Time-dependent behaviour of 2483 EPS solution

Preliminary assessment of 2483 EPS showed that the polysaccharide solution at concentration ≥ 0.24% (w/v) exhibited shear-thinning behaviour. Since no hysteresis loop was observed (Figure 6.6), it implies that the viscosity of 2483 EPS solution is

time-independent. In addition, there was no evidence of the 2483 EPS forming a gel. So far, no reported LAB strain produces EPS with gelling properties.

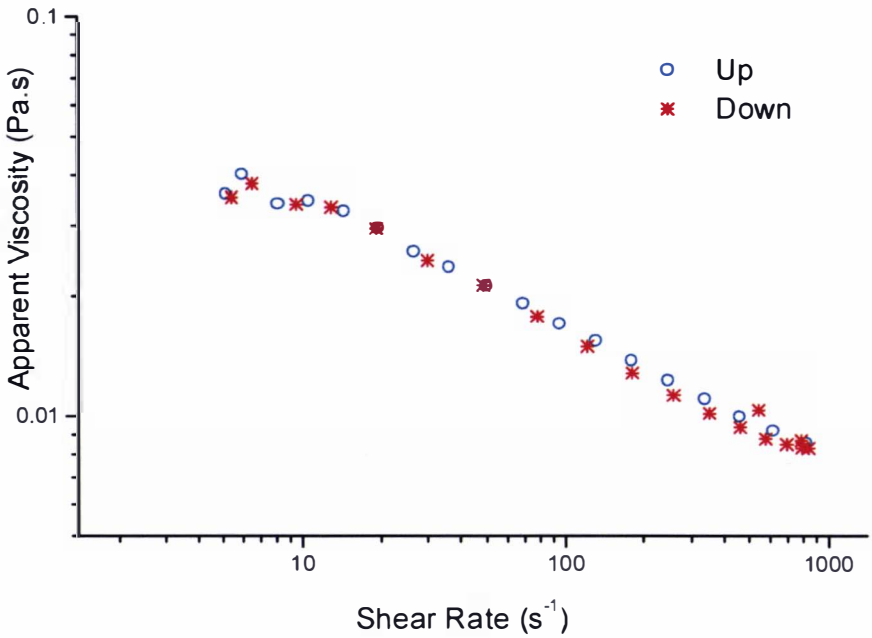

Figure 6.6 Steady flow curve of EPS (0.28% w/v) subjected to increasing (up) shear rate followed by a decreasing (down) shear rate. The two curves superimposed, indicating that 2483 EPS does not exhibit thixotropic behaviour.

6.3.2.2 Effects of ionic strength on the viscosity of 2483 EPS

The EPS produced by many strains of lactobacilli are generally neutral heteropolysaccharides (Bouzar et al., 1996; Cerning et al., 1992; Gruter et al., 1993; Kojic et al., 1992; Uemura, Itoh, Kaneko & Noda, 1998; Yamamoto et al., 1994). However, other LAB strains which produce negatively charged heteropolysaccharides (polyelectrolytes), have been reported. These include *Lactococcus lactis* subsp. *cremoris* Sbt 0495 (Higashimura et al., 2000); *Lactobacillus sake* 0-1 (Robijn, Imberty et al., 1996; van den Berg et al., 1995) and *Lactobacillus acidophilus* LMG9433 (Robijn, Gutierrez et al., 1996). For all concentrations of EPS assessed in this study, the relative viscosities remained unchanged whether the EPS was dissolved in 0.01M, 0.1M NaCl or Milli-Q water. This suggests that 2483 EPS is a neutral polysaccharide (non-polyelectrolyte) since the solution viscosities were not affected by changes in the ionic

strength of the solvent. Therefore, in all rheological measurements, the 2483 EPS solutions were prepared using water as the solvent.

6.3.2.3 Shear rate dependence of zero-shear viscosity

6.3.2.3.1 Flow curves of 2483 EPS, λ-carrageenan and dextran

The flow curves of 2483 EPS, λ-carrageenan and dextran, obtained using the Paar Physica viscometer over a wide range of concentrations, are shown in Figures 6.7, 6.8 and 6.9 respectively.

For 2483 EPS, at sufficiently low shear rates, due to the limitation of the Paar Physica viscometer, the limiting zero shear-rate viscosity (η_o) was not fully measured, particularly for low concentration solutions and even with the use of the most sensitive test cell (MS Z1 DIN double gap). As the rate of shear increased, shear-thinning behaviour was observed. The decrease in the apparent viscosity as the shear rate increases is well-known among many non-gelling polysaccharides, including λ-carrageenan (Lapasin & Pricl, 1995). The critical shear rate ($\dot{\gamma}_R$) at which the flow curves departed from Newtonian behaviour was also seen to decrease as the polysaccharide concentrations increased. This was due to the increasing restriction of the individual polymer chains as the concentration of the polymer increased. Hence, a longer time was necessary to form new entanglements to replace those disrupted by shear, causing the Newtonian region to move to lower shear rates (Graessley, 1974; Morris et al., 1981).

The experimental data of both 2483 EPS and λ-carrageenan were fitted by the Carreau and Cross models in equations (1.36) and (1.35) using the Origin software (version 5). The flow behaviour index (n) for each flow curve was determined using the power law equation. The flow behaviour index was then used in both the Carreau and Cross equations to fit the experimental data of each corresponding polymer solution. The agreement between fit and experimental values was evaluated using the mean relative deviation (MRD). Both the Carreau and Cross models provided a fairly good fit over a wide shear rate range as indicated by the low values of MRD (Table 6.3). However, at

the low shear rates, where the Newtonian plateau occurs, the Carreau model appeared to provide a better fit than the Cross model (Figures 6.7 and 6.8). Furthermore, the Cross model can give an anomalous value of λ as in the case of the EPS solution with the lowest concentration (Table 6.3). Note that for all the flow curves, the upper limit shear rates were not reached, hence, the second Newtonian plateau was not observed.

Table 6.3 The mean relative deviation (MRD) calculated based on the Cross and Carreau models.

	Cross Model $\eta = \frac{\eta_o}{1+(\lambda\dot{\gamma})^{1-n}}$				**Carreau Model** $\eta = \frac{\eta_o - \eta_\infty}{\left(1+(\lambda\dot{\gamma})^2\right)^{(1-n)/2}}$			
Samples (%w/v)	η_o **(Pa.s)**	**λ (s)**	**1-n**	**MRD[a]**	η_o **(Pa.s)**	**λ (s)**	**1-n**	**MRD[a]**
2483 EPS								
0.34	0.38	3.00	0.46	0.38	0.11	0.29	0.46	0.14
0.25	0.11	0.65	0.38	0.51	0.04	0.10	0.38	0.29
0.17	0.08	43.11	0.24	0.13	0.01	0.05	0.24	0.08
0.11	0.03	1404.94	0.13	0.20	0.01	0.02	0.13	0.15
λ-carrageenan								
1	2.22	5.82	0..38	0.55	0.76	0.59	0.38	0.33
0.5	0.09	0.07	0.31	0.29	0.05	0.06	0.31	0.27
0.4	0.05	0.06	0.31	1.70	0.02	0.01	0.31	0.80
0.3	0.04	0.12	0.28	0.41	0.02	0.01	0.28	0.10
0.2	0.02	0.09	0.25	0.51	0.01	0.004	0.25	0.27
0.1	0.01	0.03	0.10	0.21	0.003	0.003	0.10	0.14

[a] The quality of the fit was based on calculated and experimental values using mean relative deviation, given as : $\left(\sqrt{\sum\left(\left(\eta_{cal}-\eta_{expt}\right)/\eta_{cal}\right)^2}/N\right)\times 100\%$ where η_{cal} is the calculated value based on the fitting model, η_{expt} is the experimental value and N, the total number of data points.

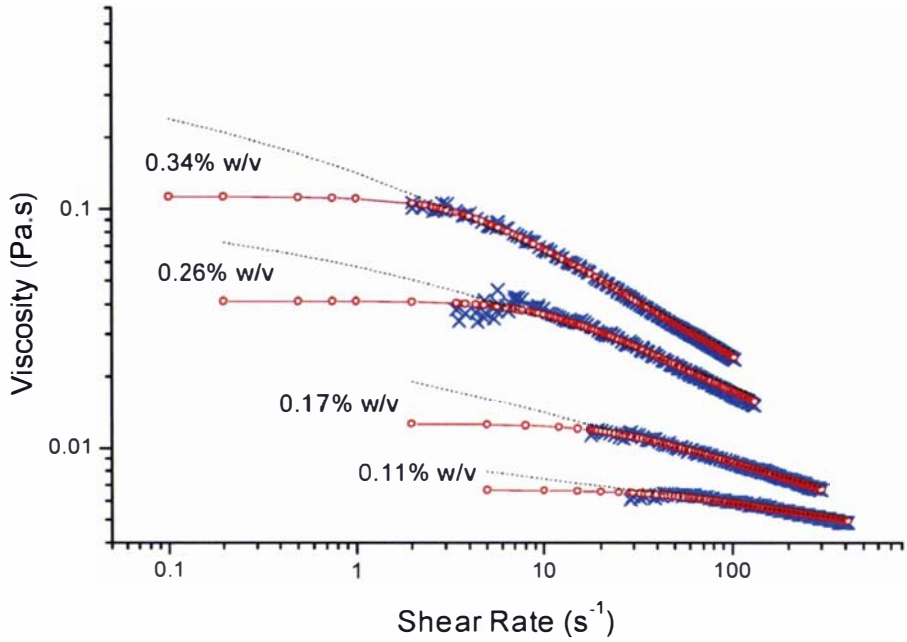

Figure 6.7 Viscosity as a function of shear rate for 2483 EPS in water at 20°C. The crosses (x) are the experimental data and the open circles (o) connected by solid line are calculated values obtained from the Carreau model. Dotted lines are obtained by the Cross model.

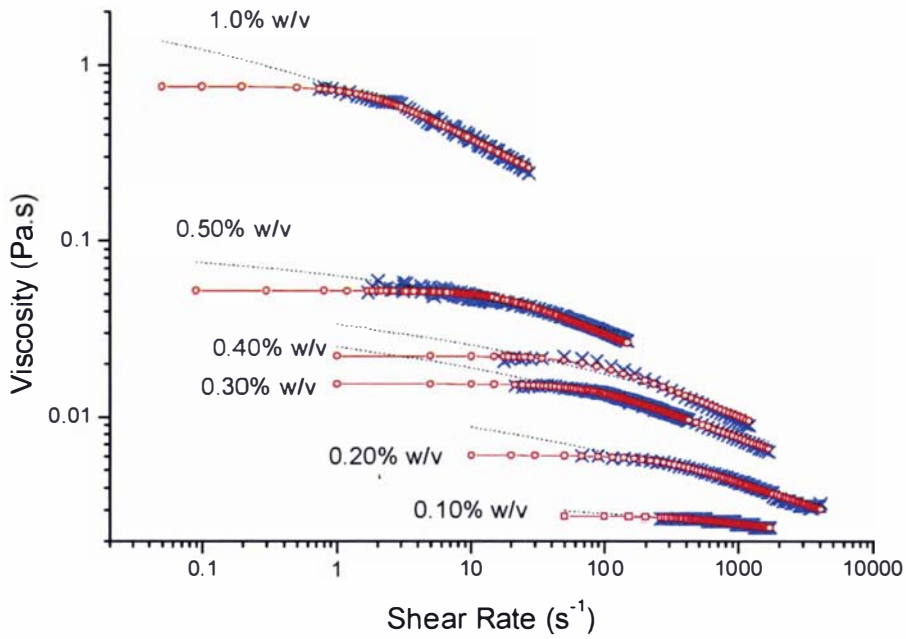

Figure 6.8 Viscosity as a function of shear rate for λ-carrageenan in 0.075M KCL at 20°C. The crosses (x) are the experimental data and the open circles (o) connected by solid line are calculated values obtained from the Carreau model. Dotted lines are obtained by the Cross model.

The flow curves of the dextran (Figure 6.9), on the other hand, exhibited Newtonian behaviour (shear rate independent), even though the dextran used was a high molar mass polysaccharide (M_w~2 x 10^6 Da). Dextran of high molar mass is known to have a highly-branched structure (Nomura, Koda & Hattori, 1990; Sidebotham, 1974). The highly-branched dextran coil likely adopts a compact conformation (resembling a hairy spherical shape molecule) in water, which somewhat resists deformation during the application of shear. Consequently, the shear rate dependence of compact molecules exhibited Newtonian behaviour even at concentrations above c^*. The Newtonian flow behaviour of dextran has also been reported by other researchers (Nomura et al., 1990).

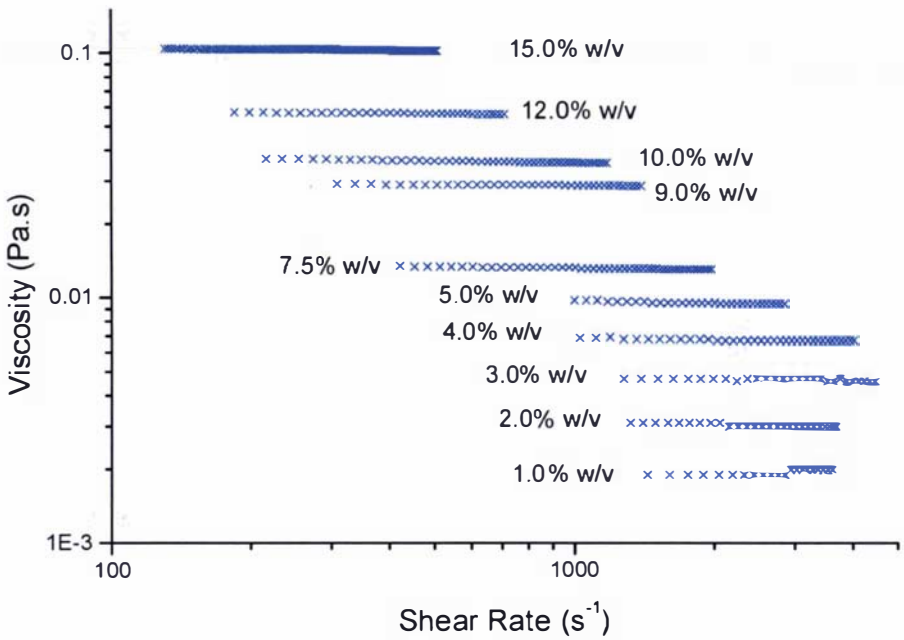

Figure 6.9 Viscosity as a function of shear rate curves for dextran in water at 20°C. The crosses (x) are the experimental data obtained at different dextran concentrations.

From the individual flow curves of both 2483 EPS and λ-carrageenan, it was observed that the critical shear rate ($\dot{\gamma}_R$) decreased as the concentration of the polysaccharide increased. Note that the critical shear rate is the shear rate at which the zero-shear viscosity starts to decrease and is inversely related to the structural relaxation time (τ). As concentration increases, the degree of coil overlap also increases. The increase in the structural relaxation time (τ) and the corresponding decrease in $\dot{\gamma}_R$ as concentration increases can be explained by the concept of coil entanglements (see chapter 2). Under

shear, the time required for disruption of entanglements will obviously increase with concentration. The $\dot{\gamma}_R$ values were estimated from the flow curves at ~97% of zero-shear viscosity (η_o) for 2483 EPS and λ-carrageenan (see Figure 6.10).

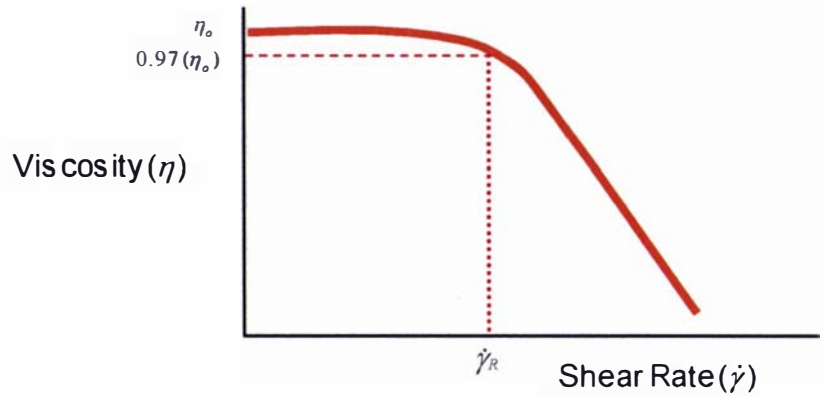

Figure 6.10 Illustration of the approximation of critical shear rate $\dot{\gamma}_R$ at 97% of the zero-shear viscosity (η_o) from a typical flow behaviour of a polysaccharide solution.

The plot of $\dot{\gamma}_R$ as a function of polymer concentrations for 2483 EPS and λ-carrageenan is shown in Figure 6.11. The values of the slopes were -2.80 and -2.77 for 2483 EPS and λ-carrageenan respectively. These values agree substantially with theoretical prediction of -2.75[1] based on De Gennes' reptation model (see equation 1.29; De Gennes, 1976) using the so-called scaling concept (De Gennes, 1979), and combining with Rouse relaxation time (see equation 1.32; Rouse, 1953). The experimental values were also close to the experimental value (-2.6) of EPS from *Lactococcus lactis* subsp. *cremoris* (Tuinier, Zoon, Stuart et al., 1999). Slight deviations from theoretical values are expected due to factors such as polydispersity of biopolymers and the possible effects of intramolecular and intermolecular interferences of the segments of polymer chains (Rouse, 1953).

$\eta_o \sim c^{3.75}$

[1] $\tau_p = \frac{6(\eta_o - \eta_s)M}{p^2\pi^2 RTc} = \frac{6\eta_o M}{p^2\pi^2 RTc} - \frac{6\eta_s M}{p^2\pi^2 RTc} \sim \frac{c^{3.75}}{c} \sim c^{2.75}$

$\dot{\gamma} = \frac{1}{\tau_p} - \frac{1}{c^{2.75}} \sim c^{3.75}$

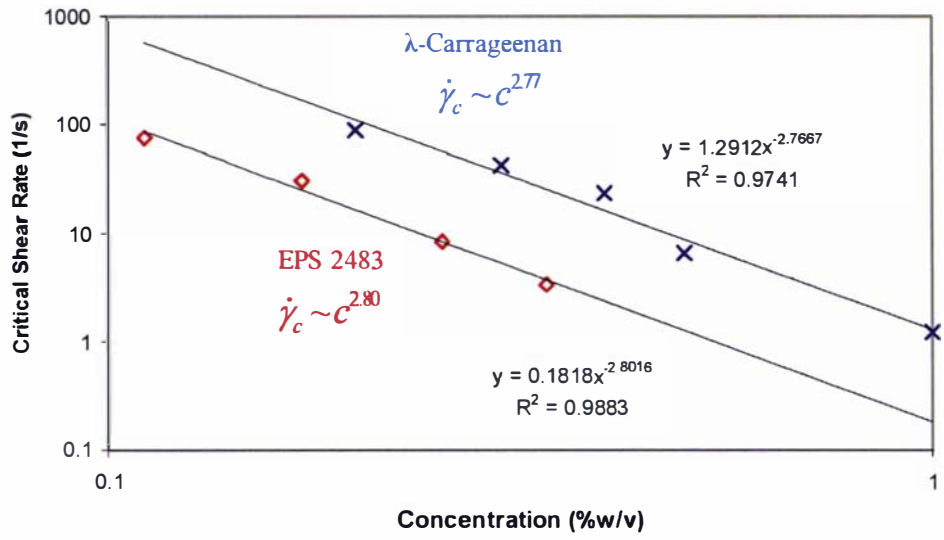

Figure 6.11 Critical shear rate ($\dot{\gamma}_R$) as a function of concentration for 2483 EPS and λ-carrageenan.

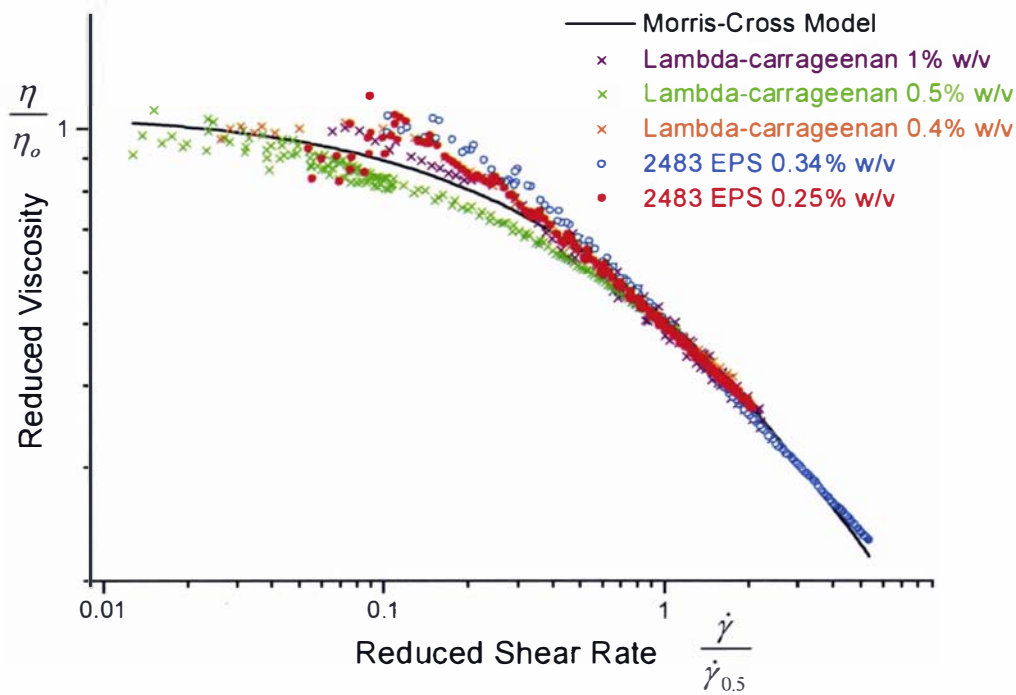

Figure 6.12 Generalised shear rate dependence of viscosity for 2483 EPS and λ-carrageenan. The exponent value (1-*n*) used for the Cross-type model was fixed at 0.76 and the arbitrary values for η_o is 1.0231. Note that $\dot{\gamma}_{0.5}$ is the shear rate which corresponds to the viscosity value of $\eta_o/2$.

By plotting logarithm of reduced viscosity (η/η_o) as a function of reduced shear rate ($\dot{\gamma}/\dot{\gamma}_{0.5}$), a master curve could be obtained from the viscosity-shear rate data of λ-carrageenan and 2483 EPS. All the flow curves superimposed relatively well. However, at lower shear rates, the data appeared more scattered, probably due to a lack of precision of the Paar Physica viscometer when operating at very low shear rates. The data in Figure 6.12 was fitted using the Cross model despite the poor fit at the limiting shear0rate viscosity. Interestingly, an exponent value (1-*n*) of ~0.76 obtained was characteristic of a typical random flexible coil polysaccharide (Morris et al., 1981). The master curve in Figure 6.12 when fitted with the Carreau model gave an exponent value (*n*) of 0.55.

6.3.2.4 Intrinsic viscosity

The Kraemer and Huggins plots obtained by capillary viscometry and rotational viscometry for 2483 EPS, λ-carrageenan and dextran are shown in Figures 6.13, 6.14 and 6.15 respectively. Viscosity measurements obtained from the Paar Physica were normalised with the results obtained for water at 20°C.

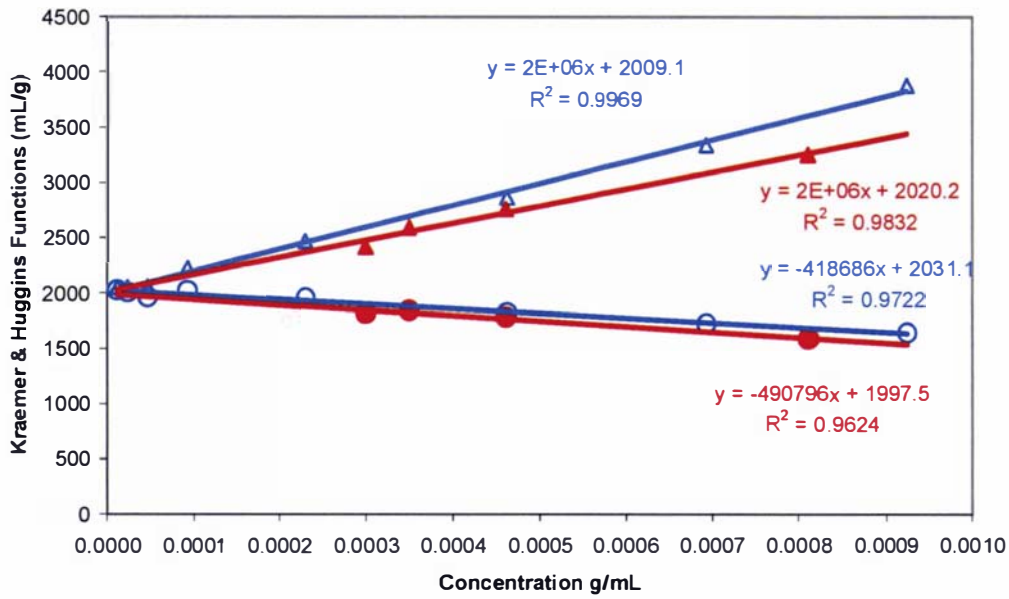

Figure 6.13 Kraemer, $\ln(\eta_r)/c$, (symbol: circles) and Huggins, η_{sp}/c, (symbol: triangles) plots for 2483 EPS. Data in blue were obtained from Cannon-Fenske capillary viscometer and data in red from Paar Physica rotational viscometer.

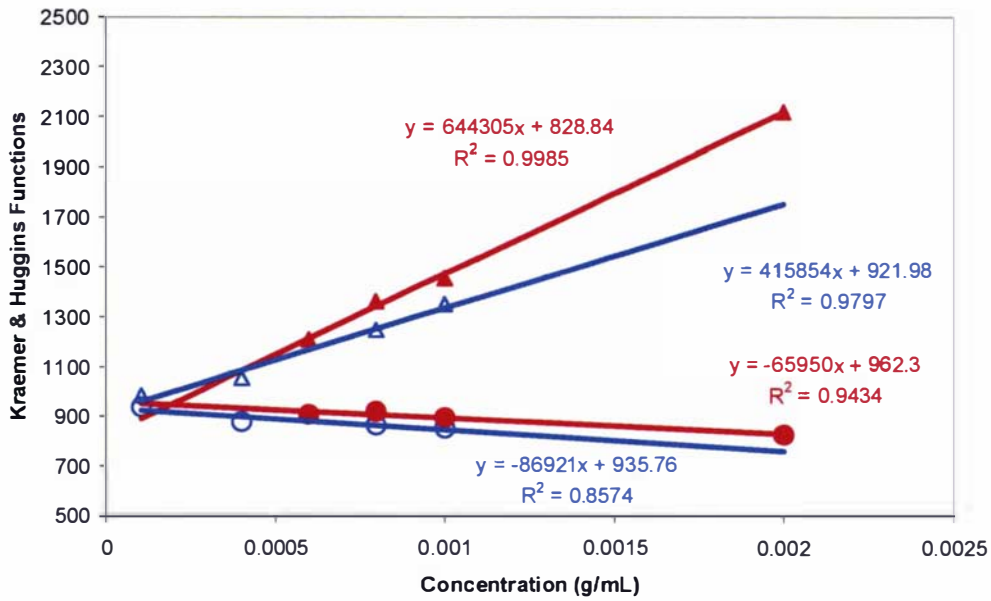

Figure 6.14 Kraemer, $\ln(\eta_r)/c$, (symbol: circles) and Huggins, η_{spo}/c, (symbol: triangles) plots for λ-carrageenan in 0.075M KCl. Data in blue were obtained from Cannon-Fenske capillary viscometer and data in red from Paar Physica rotational viscometer.

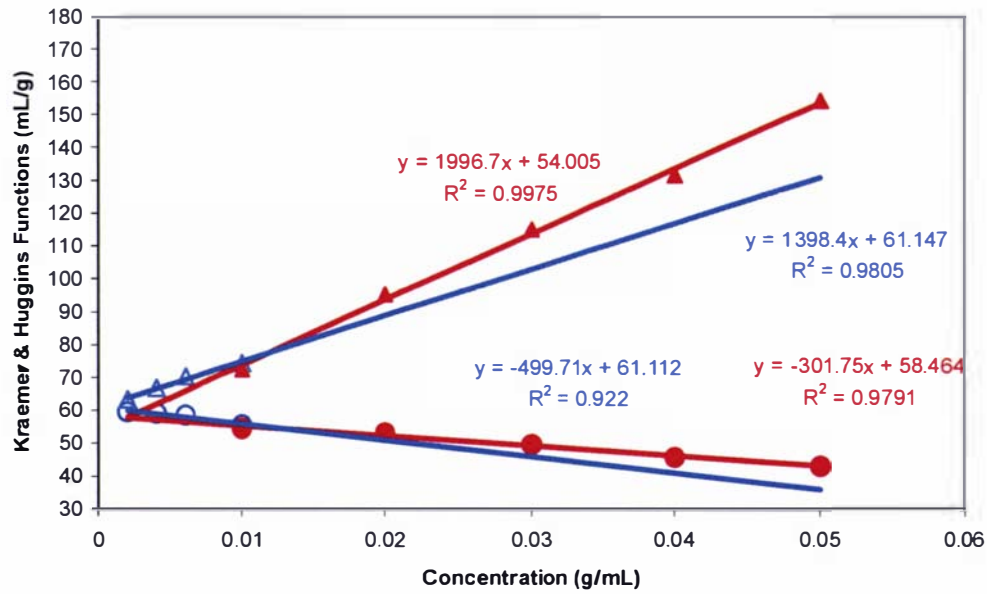

Figure 6.15 Kraemer, $\ln(\eta_r)/c$, (symbol: circles) and Huggins, η_{spo}/c, (symbol: triangles) plots for dextran (2M *Da*) in water. Data in blue were obtained from Cannon-Fenske capillary viscometer and data in red from Paar Physica rotational viscometer.

The intrinsic viscosities and the Huggins and Kraemer constants for the three polysaccharides are shown in Table 6.4. The Huggins constant provides an indication of the hydrodynamic interactions of the polymer with the solvent. The value of K'=0.4 suggests that dextran is in a good solvent. The Huggins constants for 2483 EPS and λ-carrageenan also indicate that both polymers were in a fairly good solvent. The results suggest that dextran was more readily soluble in water as compared with EPS 2483 in water and λ-carrageenan in 0.075M KCl.

The intrinsic viscosities obtained by both viscometric techniques were in good agreement, although some variations in the Huggins and Kraemer constants were evident for dextran and λ-carrageenan. No explanation could be given for the anomalous behaviour other than the possible reason that the Paar Physica viscometer was a less sensitive instrument for accurate viscosity measurements. In addition, the flow curves at dilute concentrations were obtainable over a very limited range of shear rates (less than a decade). The results from the capillary viscometer were of better precision and accuracy as indicated by the values of K'-K'', which were closer to the theoretical value of 0.5.

Table 6.4 Intrinsic viscosities of 2483 EPS, dextran and λ-carrageenan

Samples	Capillary viscometer				Rotational viscometer			
	$[\eta]$ mL/g	Huggins constant K'	Kraemer constant K''	K'-K''	$[\eta]$ mL/g	Huggins constant K'	Kraemer constant K''	K'-K''
EPS	2013	0.4938	-0.1006	0.59	2009	0.4956	-0.1216	0.62
Dextran	61.13	0.3742	-0.1337	0.50	56.23	0.6314	-0.0954	0.73
λ-Carrageenan	928.9	0.482	-0.1007	0.58	895.57	0.8033	-0.0822	0.89

With the capillary viscometer, the rate at which the samples passed through the capillary induced relatively high shear rates ranging from 10^2 to 10^3 s^{-1} based on equations (1.26) and (1.27). Tuinier, Zoon, Stuart et al. (1999) pointed out that polysaccharides exhibit shear-thinning behaviour at this shear rate range even at very low concentrations. However, the viscosity values obtained using capillary viscometer in this study were comparable to the zero-shear viscosity values obtained using the Paar Physica viscometer. From the results, it was evident that at very high dilution of polymer

solutions, the effect of shear thinning could be considered negligible and hence, zero-shear viscosity assumed. Therefore, the intrinsic viscosity measurements using capillary viscometer are considered more accurate and precise.

The intrinsic viscosity of 2483 EPS (2013mL/g) is at least twice that of λ-carrageenan (929 mL/g) and approximately thirty times higher than that of dextran (61mL/g). Intrinsic viscosity values of EPS produced by other *Lactobacillus* species higher than that of 2483 EPS have not been reported to date. Typically, values reported were 450 mL/g (Grobben et al., 1997) and 470mL/g (Cerning, 1990), obtained from different strains of *Lactobacillus delbrueckii* subsp. *bulgaricus*. However, the upper range of intrinsic viscosities of EPS produced by other LAB were comparable to that of 2483 EPS, with *Lactococcus lactis* subsp. *cremoris* ARH53 ($[\eta]$ ~1962mL/g; (Yang et al., 1999)); *Propionibacterium acidi-propionici* ($[\eta]$ ~2200mL/g; (Gorret, Renard, Famelart, Maubois & Doublier, 2003)) and *Streptococcus thermophilus* ($[\eta]$ ~1540mL/g; (Doco et al., 1990)). Tuinier, Zoon, Stuart et al. (1999) reported a higher value ($[\eta]$ ~3200mL/g) for EPS from *Lactococcus lactis* subsp. *Cremoris B40* in spite of a similar molar mass to 2483 EPS, suggesting a relatively stiffer polymer.

The intrinsic viscosity obtained for λ-carrageenan (930 mL/g) was close to the reported value (992.5 mL/g) under the same ionic strength solution (Morris et al., 1981). This value is also quite close to another commercial polysaccharide, guar galactomannan solution ($[\eta]$=1250mL/g), with a molar mass of ~1.65 x 10^6 Da (Robinson et al., 1982). The intrinsic viscosity of dextran was comparable to that of dextran T2000 ($[\eta]$=73mL/g, Pharmacia, Sweden) of a similar average molar mass (2 x 10^6 Da) (Tirtaatmadja, Dunstan & Roger, 2001). In addition, Ioan, Aberle & Burchard (2001) reported a similar value ($[\eta]$=68mL/g) for another dextran sample (2.66 x 10^6 Da).

In spite of its relatively high molar mass, the intrinsic viscosity of dextran was lowest among the three polysaccharides studied. The low hydrodynamic volume occupied by dextran macromolecule is largely attributed to its compact conformation in solution due

to a very flexible and a highly branched molecular structure (Chronakis, Doublier & Piculell, 2000). The conformation of such a macromolecule is like a sphere rather than a chain. The low intrinsic viscosity suggests that dextran has poor thickening ability and would require very high concentrations if high viscosity is desired. Granath (1958) established the Mark-Houwink-Sakurada relationship for dextran according to equation (1.7) where $[\eta]$=1.3 x 10^{-2} $M^{0.28}$ for molar masss greater than 10^5 Da. The exponent value of 0.28 assumes a compact conformation as opposed to 0.5 for flexible chains (Robinson et al., 1982). Using these values and equation (1.7), the calculated intrinsic viscosity for dextran was ~76 mL/g which was close to experimental value in this study (61 mL/g). The slight deviation could be attributed to polydispersity of dextran as reported by McCurdy, Goff, Stanley & Stone (1994). In addition, accurate assessment of the Mark-Houwink parameters (K and α) requires a narrow range of molar mass distribution (McCurdy et al., 1994).

On the other hand, the higher intrinsic viscosities observed for both λ-carrageenan and 2483 EPS suggested that the macromolecules are more linear and probably less branched. If the assumption that both λ-carrageenan and 2483 EPS macromolecules occur as linear flexible chains is valid, the results would suggest that 2483 EPS has a longer chain length, hence, higher radius of gyration, higher molar mass, and hence, higher thickening ability than λ-carrageenan. Of course, such comparison has to be treated with caution since the latter is a polyelectrolyte and its viscosity was determined in an ionic solution (0.075M KCl).

6.3.2.5 Concentration dependence of zero-shear viscosity

Figure 6.16 shows the plot of zero-shear specific viscosity as a function of concentration. As expected, there was an increase in viscosity with increasing concentration of 2483 EPS, λ-carrageenan and dextran. The transition from dilute to concentrated solution is indicated by a marked change in the concentration dependence of viscosity. The experimental data were fitted very well by a continuous function (1.30) according to Martin (Spurlin et al., 1946) for describing polysaccharide solutions from the dilute to the concentrated regime. Note that equation (1.30) does not allow any speculation about the transition between dilute and concentrated regime. The Martin

constant (K_M) provides an indication of polymer-polymer and polymer-solvent interactions (Kasaai, Charlet & Arul, 2000). The results suggest that polymer-solvent interactions were highest for dextran followed by 2483 EPS and λ-carrageenan.

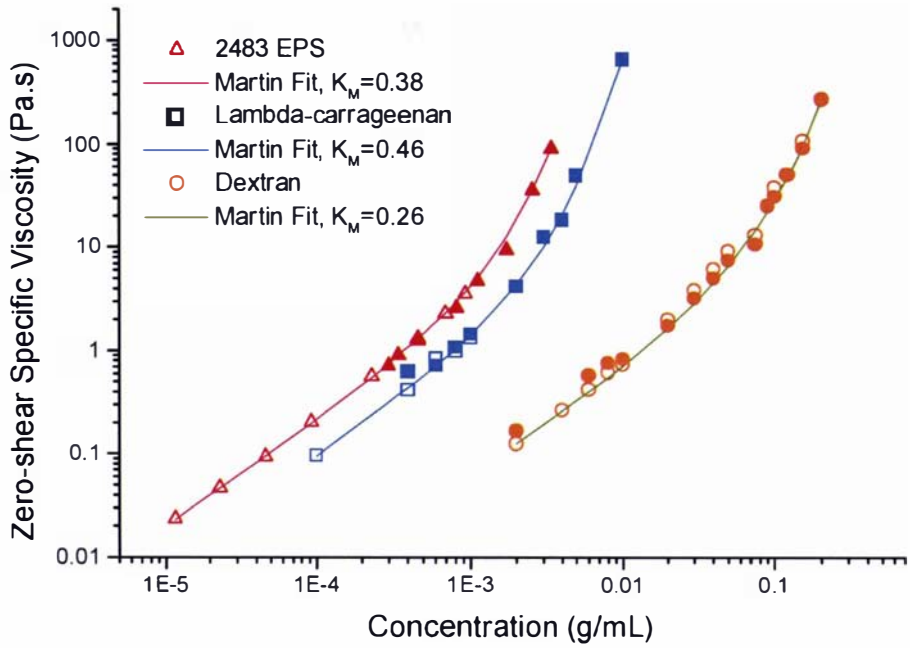

Figure 6.16 Concentration dependence of viscosity with zero-shear specific viscosity as a function of concentration of (•) dextran, (■) λ-carrageenan and (Δ) 2483 EPS. The continuous line represents theoretical fit according to Martin equation. Open symbols are data obtained from capillary viscometer and filled symbols are zero-shear viscosity from the Paar Physica viscometer.

To differentiate between the dilute and concentrated regimes, the experimented data were fitted using the power law as shown in Figure 6.17. In the dilute regime, below the coil overlap concentration, the exponent value was ~1.1-1.2 ($\eta_{spo} \propto c^{1.1-1.2}$). However, in the semi-dilute to concentrated regime, the exponent value increased to ~3.1-3.3 ($\eta_{spo} \propto c^{3.1-3.3}$). The exponent values obtained from the two domains are in good agreement with the experimental data obtained by various researchers for a number of random coil polysaccharides, such as carboxyl methyl amylose, λ-carrageenan, dextran, guar and locust bean gum (Morris et al., 1981). The first concentration domain has been reported to be give gradients between 1.25 to 1.4, and

the second domain between 2.4 to 3.9 (Doublier & Launay, 1981; Morris et al., 1981; Ross-Murphy, 1984; Sabatie et al., 1988).

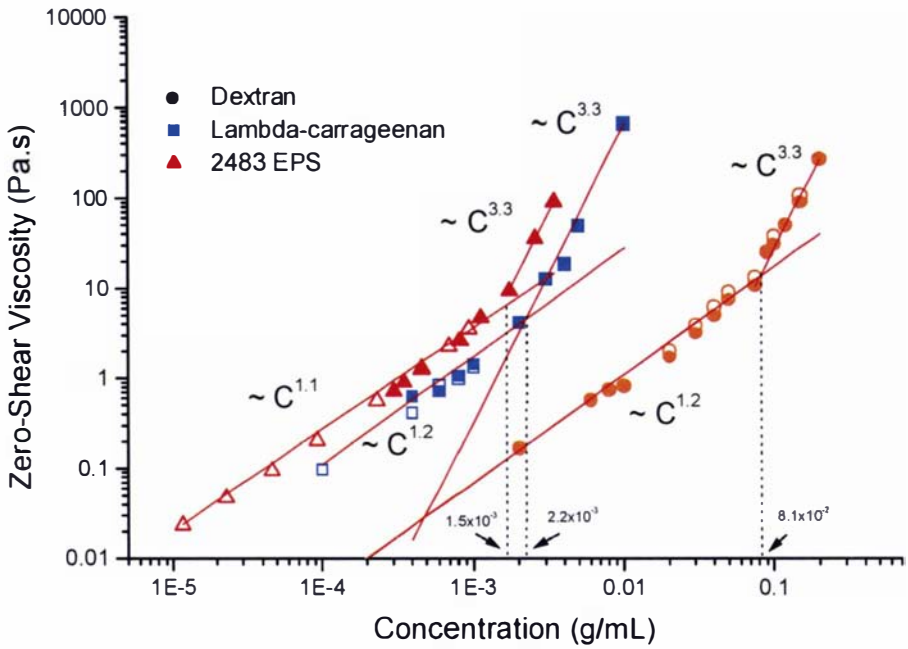

Figure 6.17 Concentration dependence of viscosity with zero-shear specific viscosity as a function of concentration for (•) dextran, (■) λ-carrageenan and (Δ) 2483 EPS. The continuous line represents theoretical fit by power-law approximation. Open symbols are data obtained from capillary viscometer and filled symbols are zero-shear viscosity from the Paar Physica viscometer. The intersections for dextran, λ-carrageenan and 2483 EPS occur at 8.1 x 10^{-2}g/mL, 2.2 x10^{-3} g/mL and 1.5 x 10^{-3}g/mL respectively.

The above plots show that the coil overlap concentration of 2483 EPS occurred at the lowest concentration followed by λ-carrageenan and dextran. Since the coil overlap concentration varies with chain length and the nature of the polymer/solvent system (Morris & Ross Murphy, 1981), it is suggested that 2483 EPS could have a longer chain length due to a higher molar mass than λ-carrageenan (presuming that the degree of branching and polymer/solvent interactions were somewhat similar in both cases). The 2483 EPS would therefore require a lower concentration than λ-carrageenan and dextran to achieve the same viscosity. The results are consistent with the intrinsic viscosities obtained for the three polysaccharides. As for dextran, because of its low $[\eta]$, a much

higher concentration was needed to reach the concentrated regime. The highly branched structure of the dextran forms a barrier to entanglements, preventing easy overlapping of molecules (McCurdy et al., 1994). In the semi-dilute to concentrated regime, entanglements could only occur by the interpenetration of the branched segments.

The concentration dependence of the zero-shear viscosity plot can be reduced to a generalised master curve by plotting η_{spo} as a function of $c[\eta]$ as suggested by Morris et al. (1981). The generalised plot is shown in Figure 6.18. This master curve makes it possible to determine the concentration required for the transition from dilute to concentrated domain for any random coil polysaccharides, as long as $[\eta]$ is a known parameter. The experimental data obtained from the three polysaccharides superimposed well and the master curve resembles that of Morris et al. (1981). It is interesting to note that the master curve may also be applied to a branched system, as in the case of dextran. Similar superposition of the curves has been reported for other highly branched polymers such as amylopectin (Durrani & Donald, 2000).

The master curve was fitted using the continuous Martin model and the exponent value, K_M ~3.3, was obtained. The exponent value is in good agreement with the experimental value obtained by Morris et al. (1981) who reported a value of 3.3 ± 0.3. The exponent value obtained was also in agreement with the exponent values given by the theoretical models of Bueche (1962) and De Gennes (1976) as shown in equations (1.28) and (1.29), respectively. By combining the power law equations for both dilute and concentrated regimes with Martin's model, the crossover from dilute to semi-dilute to concentrated domains can be characterised by $c^*[\eta]$, $c_{cr}[\eta]$ and $c^{**}[\eta]$.

From the plot, the dimensionless coil overlap parameters, $c^*[\eta]$, $c_{cr}[\eta]$ and $c^{**}[\eta]$ were approximately 0.6, 2.9 and 5.7 respectively. The exact factors affecting the broadness of the concentration domains are currently not clear, although they must depend upon the hydrodynamics of the isolated chains, the polydispersity, the fitting method, chain-chain and chain-solvent interactions.

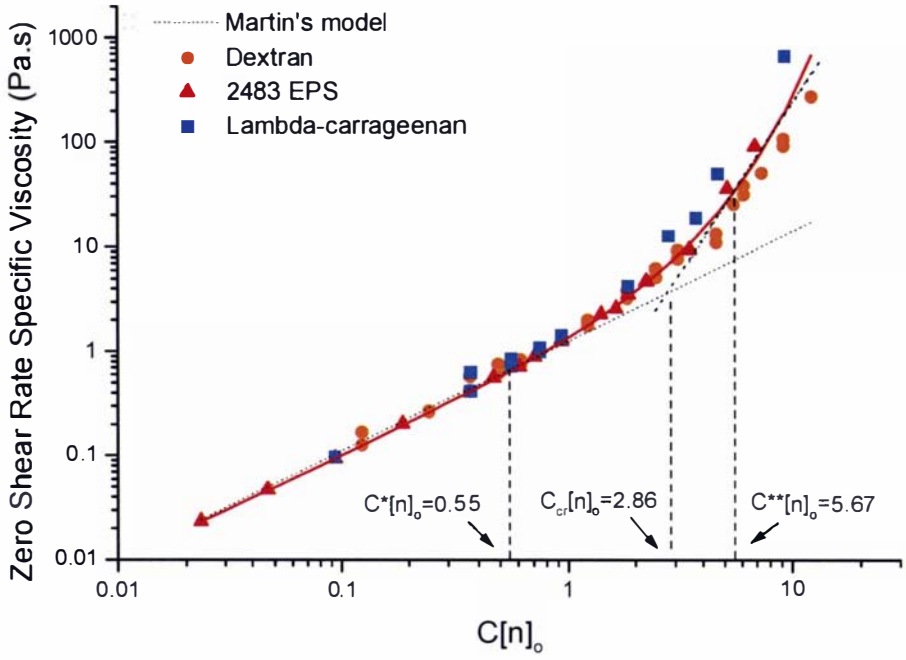

Figure 6.18 Concentration dependence of viscosity master curve for (•) dextran, (■) λ-carrageenan and (▲) 2483 EPS. The approximate crossover concentrations for the three domains: $c^*[\eta]$, $c_{cr}[\eta]$ and $c^{**}[\eta]$ are shown by the arrows. The power law equations for the dilute and concentrated regimes are $y=1.25x^{1.07}$ and $y=0.12x^{3.3}$ respectively.

With known values of $[\eta]$ for any random coil polysaccharide, values of c^*, c_{cr} and c^{**} values can be estimated based on the master curve. From this, c_{cr} for 2483 EPS, λ-carrageenan and dextran were 1.5 x 10^{-3}, 3.3 x 10^{-3} and 5.1 x 10^{-2} g/mL respectively. For effective use of 2483 EPS as a thickener, the working concentration should not be less than c_{cr}.

6.4 CONCLUSIONS

The EPS produced by *Lactobacillus delbreuckii* subsp *bulgaricus* NCFB 2483 was studied using static light scattering techniques and rheological measurements. The EPS is a neutral, non-gelling polysaccharide with a 'ropy' characteristic. The rheological properties of aqueous solutions of EPS demonstrated shear-thinning behaviour. The $[\eta]$ of 2483 EPS, determined using capillary viscometer, was found to be 2013 mL/g, suggesting that the 2483 EPS molecules occupy a relatively large hydrodynamic volume in water compared to the EPSs produced by other strains of lactic acid bacteria. The $[\eta]$ of 2483 EPS was approximately twice that of λ-carrageenan. The high $[\eta]$ and the low coil overlap concentration of 2483 EPS generally suggest better thickening properties compared to λ-carrageenan at similar polymer concentration. From static light scattering data, the M_w and $(r_g^2)_z^{1/2}$ of 2483 EPS were approximately 2 x 10^6 Da and 165nm respectively. Besides, 2483 EPS has an unusually low polydispersity index $(M_w/M_n \sim 1.15)$.

The superimposed flow curves plotted from the reduced viscosity as a function of reduced shear rate fitted using the Cross equation yielded an exponent (1-*n*) of 0.76. In addition, the concentration dependence of the viscosity plot gave a slope of ~1 and ~3.3 in the dilute and concentrated regimes respectively. Furthermore, from the light scattering data, a slope of ~0.5 was obtained from the plot of $(r_g^2)_z^{1/2}$ versus M_w. All these results strongly suggest that 2483 EPS is a flexible, random coil polymer.

Chapter 7

Isolation and characterisation of an Exopolysaccharide produced by *Sphingomonas elodea* ATCC 31461

7.1 INTRODUCTION

The EPS produced by *Sphingomonas elodea* ATCC 31461, known as 'Gellan Gum' has been a subject of interest since its discovery in the 1980s (Kang et al., 1983). Commercially, it is sold as 'Kelcogel' by CPKelco (USA) in both acylated and non-acylated forms. Different gel characteristics can be obtained by varying the degree of acylation (by alkali treatment), as well as the type and concentration of cations. In the native acylated form, its chemical structure consists of a linear anionic heteropolysaccharide based on a tetrasaccharide repeat unit (2 glucose residues, 1 glucoronic acid residue and 1 rhamnose residue) esterified at the (1→3)-linked D-glucose residue with L-glycerate at C2 and acetate approximately at C6 (Morris, 1995). The chemical structure of high acyl gellan is shown in Appendix F. The L-glycerate ester groups prevent close packing of the double-helix structure of gellan molecules, and hence, acylated gellan forms soft but elastic gels. On the other hand, deacylated gellan forms firm but brittle gels due to increases in intermolecular interactions between partnering chains (Lopes, Milas & Rinaudo, 1994).

Physico-chemical studies suggest that gellan molecules become disordered single chains during heating, but upon cooling, form ordered double-helices followed by sol-gel transition (Yuguchi, Urakawa & Kajiwara, 1997). The addition of a small amount of salt readily promotes conformational transition into an ordered double-helix chain (Crescenzi, 1995). Miyoshi, Takaya & Nishinari (1995) suggested that the double-helix formation and sol-gel transition occur almost simultaneously in concentrated gellan solution.

In the presence of divalent cations, strong carboxylate-cation^{++}-carboxylate interactions occur between neighbouring helices, giving structures similar to the 'egg-box' model for calcium-induced alginate and pectin gels (Morris, Gothard, Hember, Manning & Robinson, 1996). In the presence of monovalent cations, the cations bind carboxyl

groups on the helices, promoting close packing by screening of electrostatic repulsion (Morris et al., 1996). This may then be followed by the formation of weak water 'bridges' of carboxylate-cation^{+}-water-cation^{+}-carboxylate interactions (Chandrasekaran, Radha & Giacometti, 1995). Therefore, divalent cations generally give rise to stronger gels with higher elastic moduli at equivalent ionic strength than monovalent cations (Miyoshi et al., 1995).

Many studies have been carried out to explore the effects of adding salt on the mechanical properties of gellan gels (Miyoshi, Takaya & Nishinari, 1994; Nakamura, Harada & Tanaka, 1993; Shimazaki & Ogino, 1993). However, little research has been done to study the conformational changes of gellan molecules in dilute and concentrated solutions at ambient temperature, at low concentrations of monovalent cations.

The aim of this work was to isolate and characterise the EPS (gellan gum) produced by *Sphingomonas elodea* ATCC 31461 grown in a milk permeate-based medium. In this study, two gellan samples, a commercial high acyl gellan (Kelcogel LT100) and a laboratory-purified gellan (31461 gellan) were used. Techniques used included static light scattering and rheological methods. Both gellan samples were converted to their sodium forms (Na-gellan) so that comparison based on their molecular parameters and rheological data could be made. The 31461 and LT100 gellan in their sodium forms are denoted as Na-31461 and Na-LT100, respectively. In addition, xanthan gum (Keltrol), generally known for its stiff molecular conformation due to its double-stranded structure (Navarini, Cesaro & Ross-Murphy, 1992; Shatwell, Sutherland & Ross-Murphy, 1990), and its 'weak gel' characteristics (Cuvelier & Launay, 1986; Ross-Murphy, Morris & Morris, 1983), was used for comparison with the rheological data obtained from Na-gellan samples.

7.2 MATERIALS AND METHODS

7.2.1 Experimental samples

A laboratory-purified gellan produced by S*phingomonas elodea* ATCC 31461, a commercial high acyl gellan gum, Kelcogel LT100 (CPKelco, USA; Lot# 9L0058A CAS No:7101-52-1) and a commercial xanthan, Keltrol (CPKelco, USA; CAS No:11138-66-2) were used in this study. The process of obtaining the laboratory-purified gellan (31461) is described in the following section.

7.2.2 Fermentation, isolation and purification of 31461 gellan

A primary culture of S*phingomonas elodea* ATCC 31461 was grown in a Trypticase Soy Broth (Difco Laboratories) at 30°C for 24 h with continuous agitation (200 rpm). Milk permeate (25mL), pH 6.8, containing 0.1% w/v yeast extract was prepared by free-steaming at 100°C for 10 min in a 250mL shake flask. The growth medium was inoculated with the primary culture and fermented at 30°C for at least 72 h under continuous agitation.

To recover the polysaccharides produced, one part fermented broth was added to three parts chilled absolute ethanol and left overnight. The jelly-like precipitates, which also entrapped a high number of dead bacterial cells, remained insoluble in water at room temperature (~20°C). The precipitates were subjected to further purification as described in the following section.

7.2.3 Preparation of soluble gellan samples

Both the LT100 gellan and ethanol-precipitated 31461 gellan were insoluble in water at room temperature. The former is commercially available as a dried powder and was easily dispersed in water forming minute swollen gel aggregates. The gel aggregates were examined under bright field light microscopy using crystal violet stain.

To study the solution properties of gellan, it was necessary to prevent gel formation. This was achieved by heating the gellan suspension (0.2% w/v) to 90°C. Cation exchange resin (Amberlite IR-120, Na^+ form) was added to the solution (at approximately 1:1 volume) and maintained at the same temperature for ~10 min with gentle and continuous stirring. The solution was decanted from the resin and centrifuged at 31,000*g* at 20°C for 30 min to remove impurities and dead cells. The clear supernatant (1 part) was precipitated in chilled absolute ethanol (3 parts) and left overnight at 4°C. The clear precipitate formed was separated from the solvent by a sieve (1mm) and allowed to drain for ~10 min. The precipitate was redissolved in Milli-Q water (water purified by treatment with a Milli-Q apparatus, Millipore Corp. Bedford, MA, USA) and was subjected to a second and a third ethanol precipitation. The precipitates were then dissolved in water. The purified Na-gellan solution was freeze-dried. Using this procedure, both LT100 gellan and 31461 gellan were converted to their soluble sodium forms (i.e. Na-LT100 gellan and Na-31461 respectively) with purity levels of ~96%. The percent purity was calculated by taking the total sugar of Na-gellan determined by the phenol sulphuric acid method (Dubois et al., 1956) and divided by the dry weight of the sample.

7.2.4 Sample dilution and variation in ionic strength

Freeze-dried Na-LT100 and Na-31461 gellan samples were each dissolved in water (1% w/v) and filtered through a 0.2µm filter. The samples were dialysed overnight at 4°C against either water or NaCl solutions of different concentrations (0.002M, 0.005M, 0.05M and 0.1M). The respective dialysates were used for sample dilution when required. The percent ash content of each sample was determined after dialysis. The Na-gellan sample dialysed against the Milli-Q water was used for intrinsic viscosity determination, steady flow curves measurements and static light scattering studies. All Na-gellan samples (including those dialysed against NaCl solutions) were used for small-deformation oscillatory measurements.

A 1% w/v commercial xanthan was also prepared in water and in NaCl solutions of different concentrations (0.005M, 0.02M, 0.05M, 0.1M, 0.5M and 1M). The samples were dialysed against the salt solutions, so that the respective dialysates were used as

diluents, according to the isoionic dilution procedure (Lapasin & Pricl, 1995). Xanthan solutions were used for all rheological measurements.

7.2.5 Intrinsic viscosity determination

Very dilute solutions of Na-31461 (1.23×10^{-2} to 6.15×10^{-3} % w/v) and Na-LT100 (6.3×10^{-2} to 6.0×10^{-3} % w/v) were prepared from samples initially dialysed against Milli-Q water. In addition, dilute xanthan solutions (1×10^{-2} to 6×10^{-2} % w/v) in different ionic strength salt solutions were prepared. Sample dilution was carried out according to the isoionic dilution method. Intrinsic viscosity was determined using a Cannon-Fenske capillary viscometer as described in Chapter 6.

7.2.6 Steady shear and oscillatory measurements

Steady shear tests were carried out on 1% (w/w) Na-LT100 and Na-31461 gellan samples dialysed against water, and all xanthan samples dialysed against water or NaCl solutions, using the Rheometrics SR-5000 (Rheometrics Instruments, Piscataway, New Jersey, USA). Viscosity measurements were made using a cup and bob geometry. The diameters of the cup and bob measure 28.0mm and 26.0mm respectively. The bob length was 36.0mm and the gap was set at 2.5mm. All measurements were performed in a controlled shear stress sweep mode at a temperature of 20 ± 0.1°C. To remove air bubbles and impurities, all the samples were centrifuged at 6000*g* for 10 min before measurements. The operating shear rate ranged from 10^{-2} to 10^{4} s^{-1}. Flow curves were obtained using the Rheometric Scientific software RSI Orchestrator version 6.4.3.

Dynamic rheological measurements were performed on 1% w/v Na-LT100, Na-31461 and xanthan samples, dialysed against water or NaCl solutions. The rheometer was equipped with a cone and plate geometry. Cone diameter was 40mm and cone angle was 4°. The gap between the cone and the plate was set at 0.05mm. All samples were initially heated to 80°C in a water bath before transferring onto the plate maintained at 60°C by means of a Peltier unit. The temperature was then lowered to and maintained at 20±0.1°C. The samples were allowed to rest for 10 min prior to measurements. For each sample, a dynamic stress sweep test was first performed at a frequency of 0.1 Hz to

determine the limit of the linear viscoelastic region (where G' and G'' is independent of strain amplitude). Using the strain value obtained within the linear viscoelastic region (~ 2-3%), a dynamic frequency sweep test was performed. In addition to the above samples, dynamic frequency sweep tests were performed on 0.42% w/v xanthan, Na-LT100 and Na-31461 gellan dispersed in Milli-Q water.

7.2.7 Multi-angle Laser Light Scattering (MALLS) -batch and chromatography modes

Determination of the *dn/dc* values of both Na-gellan samples and the operation of the light scattering equipment in the batch and chromatography modes were according to the procedures described earlier (see Chapter 6). The mobile phase (Milli-Q water) was filtered through a 0.025µm filter and degassed before use.

In the batch mode, the concentrations of Na-LT100 and Na-31461 gellan ranged from 3.4×10^{-4} to 7.54×10^{-5} g/mL and 2.22×10^{-4} to 6.63×10^{-5} g/mL respectively. The samples were filtered using a 0.2µm filter during sample loading. Another set of samples was prepared for the batch mode by filtering through a 0.2µm filter and holding for ~30 min before loading the sample. The concentrations of these Na-LT100 and Na-31461 samples ranged from to 1.25×10^{-4} to 6.75×10^{-5} g/mL and 2.22×10^{-4} to 6.63×10^{-5} g/mL, respectively. In the chromatography mode, the gellan samples were filtered using a 0.2µm filter during sample loading. The concentrations of Na-LT100 and Na-31461 gellan in the chromatography mode were 7.11×10^{-3} g/mL and 3.32×10^{-3} g/mL, respectively. The concentrations of all samples were determined using the phenol sulphuric assay (Dubois et al., 1956) after the filtration step and the absorbance read against the glucose calibration curve.

7.3 RESULTS AND DISCUSSION

7.3.1 Commercial gellan gum (Kelcogel LT100) and 31461 gellan

Commercial high acyl gellan gum, Kelcogel LT100, formed swollen aggregates when dispersed in water (Figure 7.1). A large number of dead cells (~10^{11} cells/g) appeared to be entrapped within these aggregates as observed by using a light microscopy.

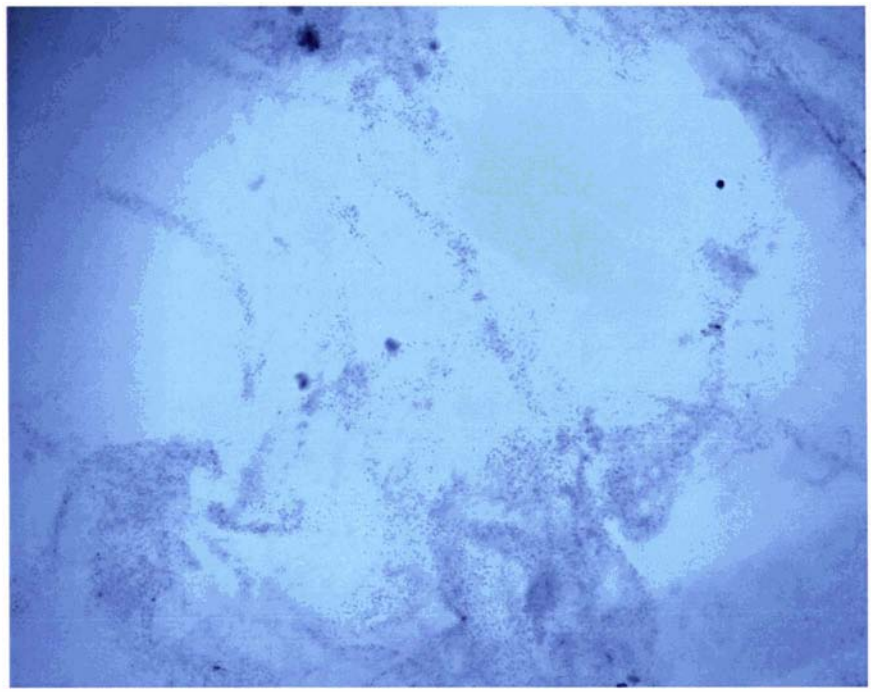

Figure 7.1 Light microscopy (magnification: 1000x) on 0.02% w/v LT100 dispersed in water. The swollen aggregates are stained by crystal violet dye. Entrapped within the aggregates are dead bacteria cells.

When LT100 gellan was heated in water to ~80°C, the dispersed aggregates dissolved in water. However, upon cooling, it formed a gel. Similarly, for 31461 gellan, heating the culture broth followed by cooling also resulted in the formation of a gel. Gelation of gellan samples was mainly cation-mediated, due to their high ash contents (both at approximately 5.8% ash, w/w, on dry weight basis).

In order to study the conformational changes and solution properties of gellan molecules, the gellan samples were converted to their sodium forms using a cation exchange resin, and replacing divalent cations with monovalent cations (Na^+). The

freeze-dried Na-gellan samples were readily soluble in water with no obvious aggregates observed under the light microscope. The percentages of ash in both Na-LT100 and Na-31461 were found to be 3.9% and 4.7%, w/w, (based on dry weight), respectively. The Na^+ concentration was derived from the percentage ash on the assumption that the cation exchange was successfully carried out.

7.3.2 Flow curves of Na-LT100, Na-31461 and xanthan solutions

The flow curves of Na-LT100 gellan and Na-31461 gellan dispersed in water at different polymer concentrations are shown in Figures 7.2 and 7.3, respectively. Typical flow curves obtained for xanthan, dispersed in 0.005M NaCl, are shown in Figure 7.4. For all three polysaccharides, the zero-shear viscosities were reached at relatively low shear rates (10^{-3} – 10^{-1} s^{-1}). As the shear rate increased, pseudoplastic behaviour was observed. The onset of shear-thinning behaviour typically shifted towards lower shear rates as polymer concentration was increased. The curves were fitted by both the Cross and the Carreau models.

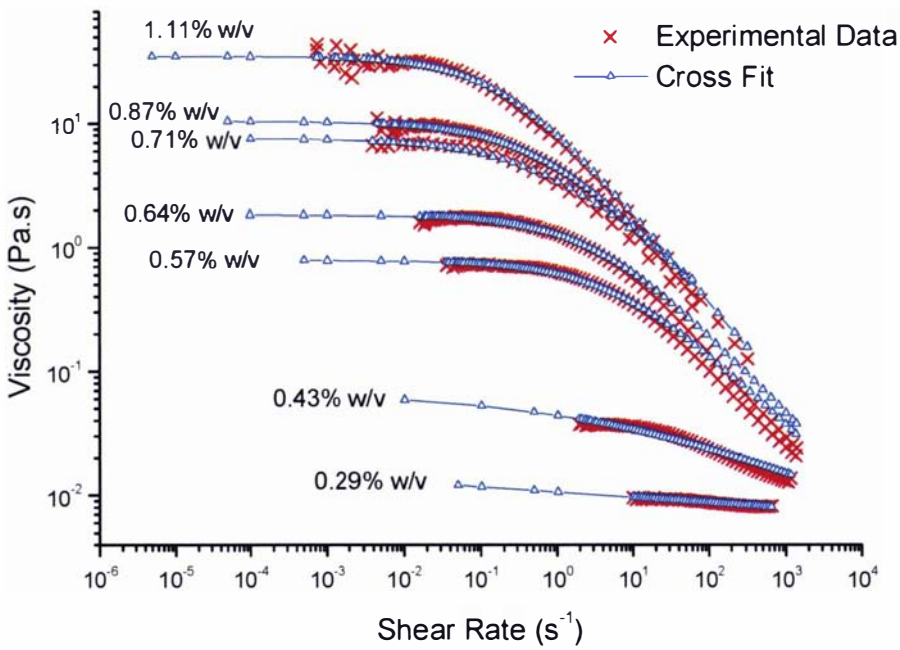

Figure 7.2 Flow curves of Na-LT100 dispersed in Milli-Q water at 20°C. The red crosses (x) are the experimental values and the blue open triangles (△) connected by solid line are calculated values obtained from the Cross model.

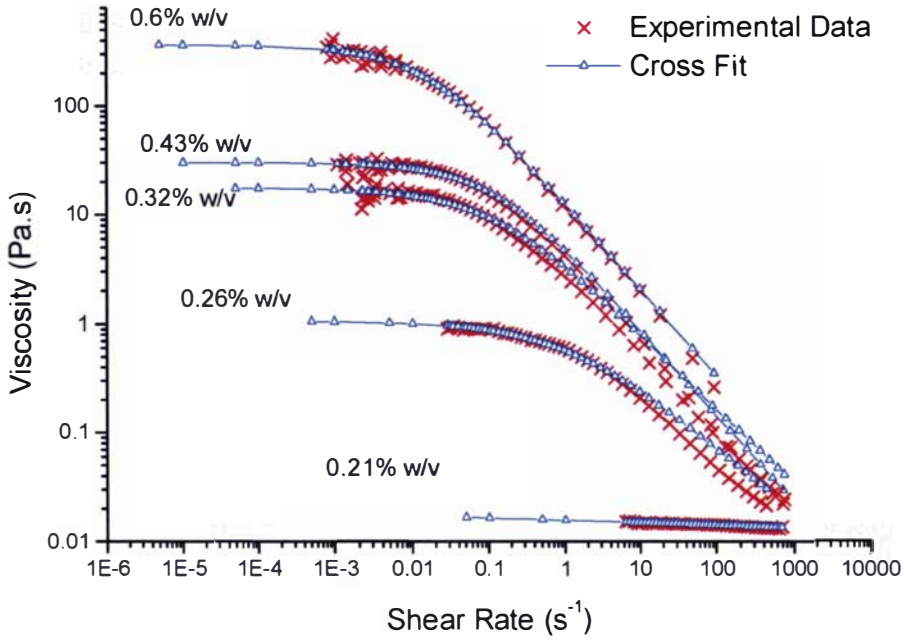

Figure 7.3 Flow curves of Na-31461 dispersed in Milli-Q water at 20°C. The red crosses (x) are the experimental values and the blue open triangles (△) connected by solid line are calculated values obtained using the Cross model.

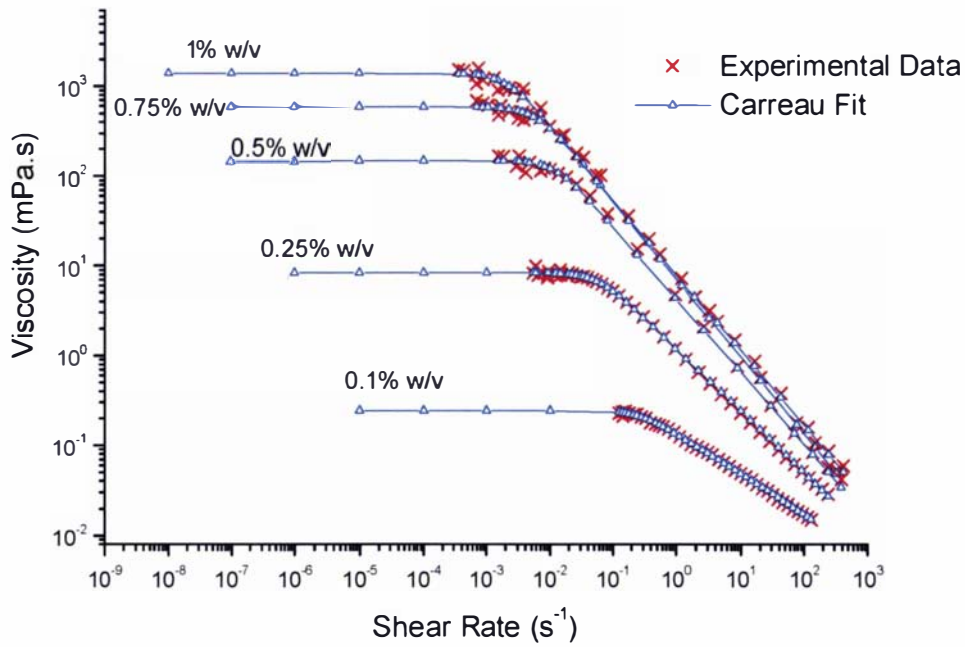

Figure 7.4 Flow curves of xanthan dispersed in 0.005M NaCl at 20°C. The red crosses (x) are the experimental values and the blue open triangles (△) connected by solid line are calculated values obtained using the Carreau model.

Both Na-LT100 and Na-31461 were better fitted using the Cross model as indicated by the lower MRD values (Table 7.1). Poor fits were however observed at low concentrations. On the other hand, xanthan flow curves were better fitted using the Carreau equation. The suitability of Cross model in gellan samples and Carreau model in xanthan samples could be attributed to the differences in the conformational behaviour of macromolecules and differences in the mechanism involved in the intermolecular interactions in concentrated regions.

Table 7.1 The mean relative deviation calculated based on the Cross and Carreau Models.

%/w/v	Cross				Carreau			
	η_o (Pa.s)	τ (s)	1-n	MRD[a]	η_o (Pa.s)	τ (s)	1-n	MRD[a]
Na-LT100								
1.11	35.36	5.49	0.73	1.27	32.43	12.88	0.73	4.58
0.87	10.22	1.72	0.64	0.75	9.30	4.24	0.64	3.27
0.71	7.66	1.42	0.57	2.26	6.74	4.01	0.57	2.72
0.64	1.85	0.29	0.65	1.63	1.63	0.54	0.65	0.97
0.57	0.80	0.14	0.61	1.58	0.71	0.38	0.61	1.81
0.43	0.07	0.12	0.27	1.02	0.04	0.06	0.27	0.24
0.29	0.06	0.0001	0.05	0.19	0.01	0.05	0.05	0.15
NA-31461								
0.60	368.35	68.03	0.79	1.29	309.43	108.95	0.79	4.62
0.43	30.53	8.53	0.79	1.73	28.04	18.64	0.79	3.93
0.32	17.84	8.50	0.69	2.88	15.77	19.19	0.69	2.25
0.26	1.08	0.81	0.60	2.09	0.89	1.64	0.60	1.98
0.21	0.03	8.93	0.04	0.21	0.02	0.03	0.04	0.21
Xanthan in 0.005M NaCl								
1	1773.35	343..35	0.84	4.36	1427.70	484.14	0.84	2.73
0.75	717.00	111.21	0.86	3.99	599.92	167.74	0.86	2.43
0.5	184.95	55.03	0.81	4.69	151.01	81.46	0.81	2.51
0.25	10.38	10.20	0.69	4.12	8.46	17.47	0.69	0.73
0.1	0.62	19.26	0.45	1.54	0.25	3.84	0.45	0.39

[a] The quality of the fit was based on calculated and experimental values using mean relative deviation, given as : $\left(\sqrt{\sum\left(\left(\eta_{cal}-\eta_{expt}\right)/\eta_{cal}\right)^2}\Big/N\right)\times 100\%$ where η_{cal} is the calculated value based on the fitting model, η_{expt} is the experimental value and N, the total number of data points.

In order to study the characteristics of the flow curves of Na-LT100, Na-31461 and xanthan, the Morris-Cross model was used to obtain shear rate dependence of viscosity master curves for each of the polysaccharide samples as shown in Figure 7.5-7.7.

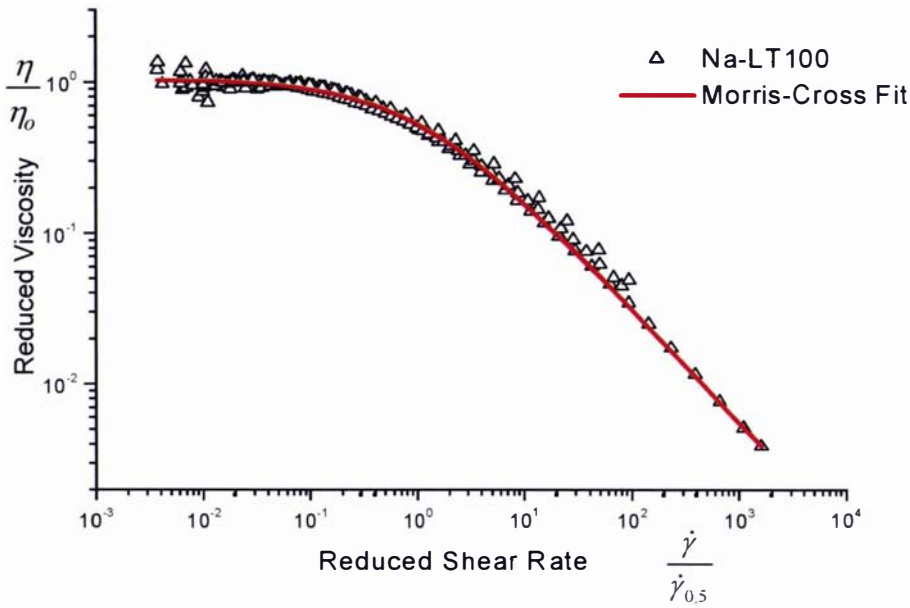

Figure 7.5 Master Curve for shear rate dependence of viscosity of Na-LT100 samples dispersed in Milli-Q water. The data were obtained from samples with polymer concentrations of 1.11%, 0.87% and 0.71% w/v. The exponent value (1-*n*) = 0.76, η_o =1.05 and λ=0.99.

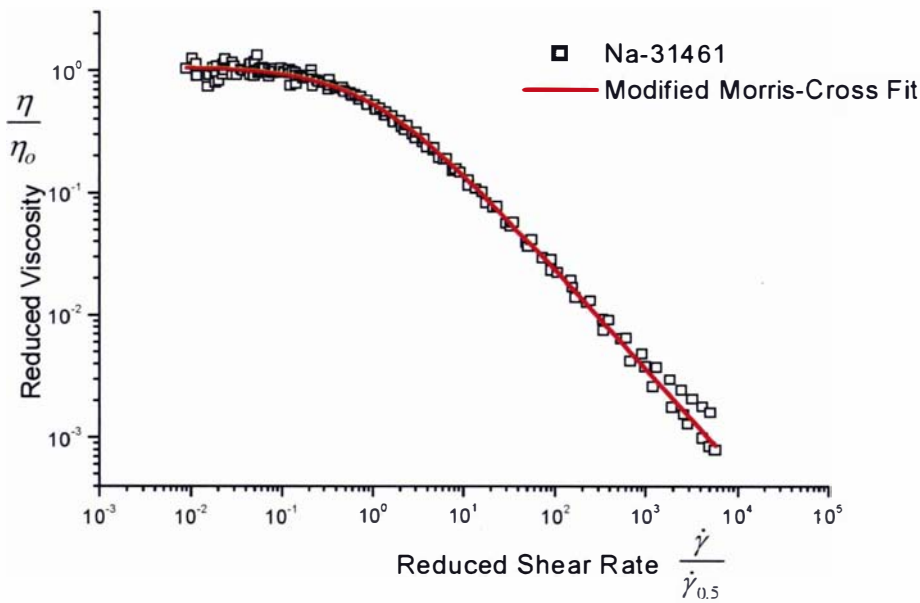

Figure 7.6 Master Curve for shear rate dependence of viscosity on Na-31461 samples dispersed in Milli-Q water. The data were obtained from samples with polymer concentrations of 0.60%, 0.43% and 0.32% w/v. The exponent value (1-*n*) = 0.82, η_o =1.09 and λ=1.05.

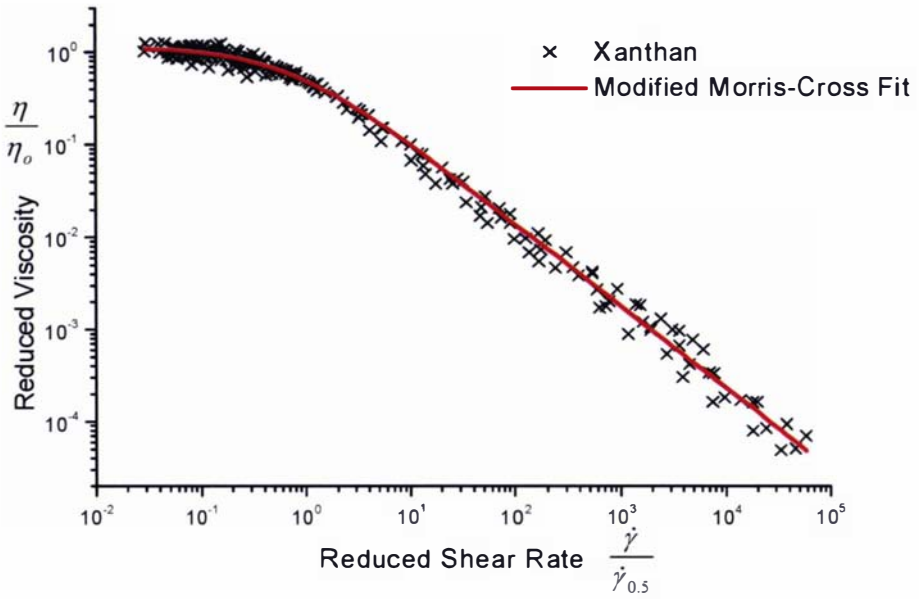

Figure 7.7 Master Curve for shear rate dependence of viscosity for xanthan solution. The data were obtained from 1%, 0.75% and 0.5% w/v xanthan concentration in 0.05M, 0.1M and 0.5M NaCl solutions. The exponent value =0.89, η_o =1.17 and λ=1.42.

It is interesting to note that the exponent of the Cross model (1-*n*) for Na-LT100 master curve was 0.76, which is typical of a flexible random coil polymer, where interaction of the chains is by topological entanglements (Morris et al., 1981). The exponent value obtained from the master curve of Na-31461 was 0.82. The steeper slope of Na-31461 could be attributed to a higher degree of chain stiffness, meaning that the Na-31461 molecule was less flexible than Na-LT100. The semi-flexiblity of gellan molecule has been attributed to its double-stranded conformation (Jampen, Britt & Tung, 2000). In addition, a similar exponent value has been reported for welan polysaccharide, which is also known to adopt semi-flexible conformation (Hember & Morris, 1995; Rouse, 1953). From the above results, the difference in chain stiffness could probably be attributed to the Na-LT100 and Na-31461 molecules adopting a single-stranded and double-stranded conformation, respectively. The change in conformation was likely caused by the higher Na^+ concentration present in Na-31461. This will be discussed in the latter section of this chapter.

For xanthan samples, the exponent value was found to be 0.89. The high exponent value, which implies a larger decrease in viscosity as shear rate increases, could be explained by the higher rate of alignment of the stiff chains as compared to random flexible or semi-flexible coils. For flexible chains, the molecules would first have to be stretched and then aligned in the direction of the flow as the rate of shear increases.

Further comparisons of the polysaccharide samples were made based on Rouse theory of longest relaxation time (Rouse, 1953) and the reptation model of De Gennes (1976) as described in Chapter 6. The experimental data were plotted using critical shear rate ($\dot{\gamma}_c$) as a function of polymer concentration as shown in Figure 7.8. The gradients of the linear plots are given in Table 7.2. The slope for random coils was theoretically predicted to fall between -2.5 to -2.75.

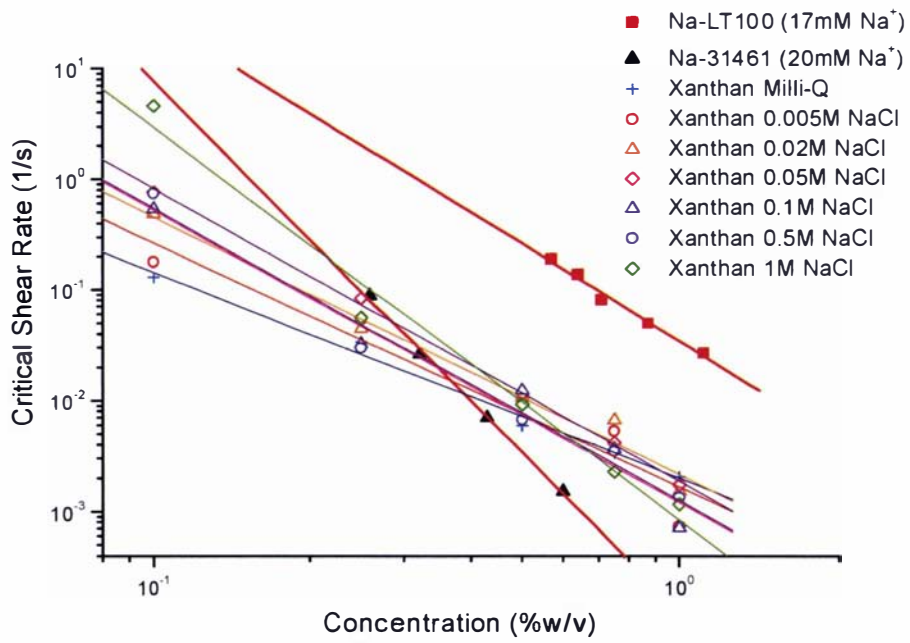

Figure 7.8 Critical shear rate versus concentration of Na-LT100 and Na-31461 gellan dispersed in Milli-Q water, and xanthan dispersed in different concentrations of NaCl. The critical shear rate was obtained at ~95-97% of the zero-shear rate viscosity.

Table 7.2 Gradients and R-values of the linear plot of critical shear rate ($\dot{\gamma}_c$) as a function of concentration for Na-gellan and xanthan samples.

Samples	Gradient	R-value
Na-LT100 in water	-2.94	0.99
Na- 31461 in water	-4.80	0.99
Xanthan in Water	-1.86	0.99
Xanthan in 0.005M NaCl	-2.20	0.96
Xanthan in 0.02M NaCl	-2.33	0.99
Xanthan in 0.05M NaCl	-2.65	0.99
Xanthan in 0.1M NaCl	-2.65	0.98
Xanthan in 0.5M NaCl	-2.64	0.99
Xanthan in 1.0M NaCl	-3.55	0.99

The gradient of the linear plot for Na-LT100 was close to the predicted value of -2.75 indicating that the Na-LT100 molecules closely resembled random coil molecules. The steeper gradient for Na-31461 on the other hand, was a clear indication of its deviation from a random coil polymer. The result probably suggests that the Na-31461 solution was more sensitive to shear, due to its semi-flexible molecules. The exponent values for xanthan samples showed an increasing trend with increasing NaCl concentrations. This was probably due to the screening of electrostatic repulsions with increasing ionic strength. At sufficiently high ionic strength (e.g. 1M NaCl), the screening of the electrostatic charges may lead to weak associations among chains. Hence, with the application of shear, the weak interactions were easily disrupted, showing a greater sensitivity to shear-thinning. It should be noted that the reptation model is meant for describing random coil polymers only. Stiff or semi-flexible polymer chains do not agree with the reptation model theories (Ohshima, Kudo, Sato & Teramoto, 1995). Hence, interpretation of the conformation of molecules (other than random coil polymers) based on the gradient values was empirical and should only be considered in conjunction with other rheological data.

Further evaluation of the xanthan flow curves at different polymer concentrations were carried out by plotting the zero-shear viscosity as a function of salt concentration (Figure 7.9). At low xanthan concentrations ($\leq 0.50\%$ w/v), a decrease in the ionic

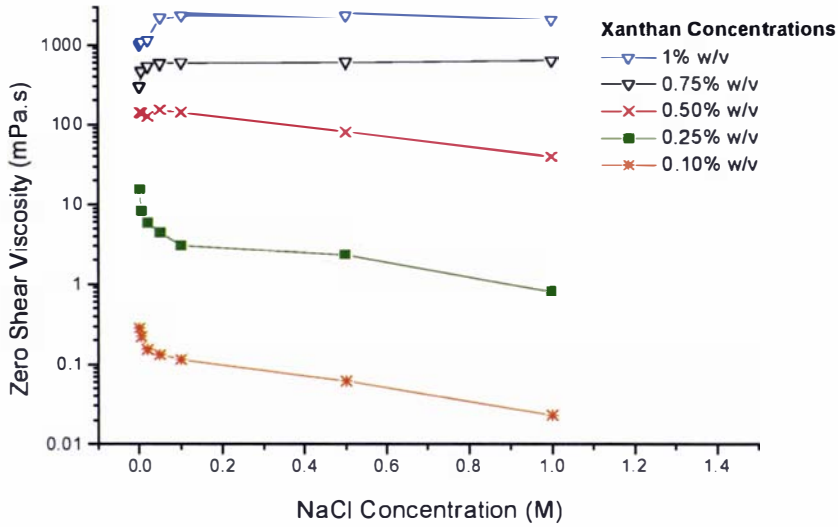

Figure 7.9 Zero-shear viscosity of xanthan solutions as a function of salt concentration.

strength resulted in a non-linear increase in the zero-shear viscosity. This could be attributed to the increase in electrostatic repulsions among the xanthan molecules, with each molecule occupying a larger hydrodynamic volume. In contrast, at higher xanthan concentrations (≥ 0.75% w/v), the zero-shear viscosities increased rather steeply with increasing salt concentration (up to 0.05M NaCl) and then remained almost constant from 0.05M to 1.0M NaCl. The higher zero-shear viscosities could be explained by the close proximity of xanthan molecules so that electrostatic screening by increasing salt concentrations could result in increasing intermolecular interactions between the xanthan molecules (Cuvelier & Launay, 1986; Ross-Murphy et al., 1983). The above results agree with data obtained by other researchers (Arendt & Kulicke, 1998; Pelletier, Viebke, Meadows, & Williams, 2001; Zatz & Knapp, 1984).

7.3.3 Intrinsic viscosity

The Kraemer and Huggins plots for Na-LT100, Na-31461 and xanthan (Figure 7.10-7.12) were obtained using very dilute polysaccharide solutions. Steady shear tests, using the rheometer with a cone and plate attachment, were carried out on the samples to verify that shear-thinning did not occur at the operating shear rates of the capillary viscometer (~10^3 s^{-1}). The intrinsic viscosities which reflect the hydrodynamic volume of individual molecules in solution of the samples are shown in Table 7.3.

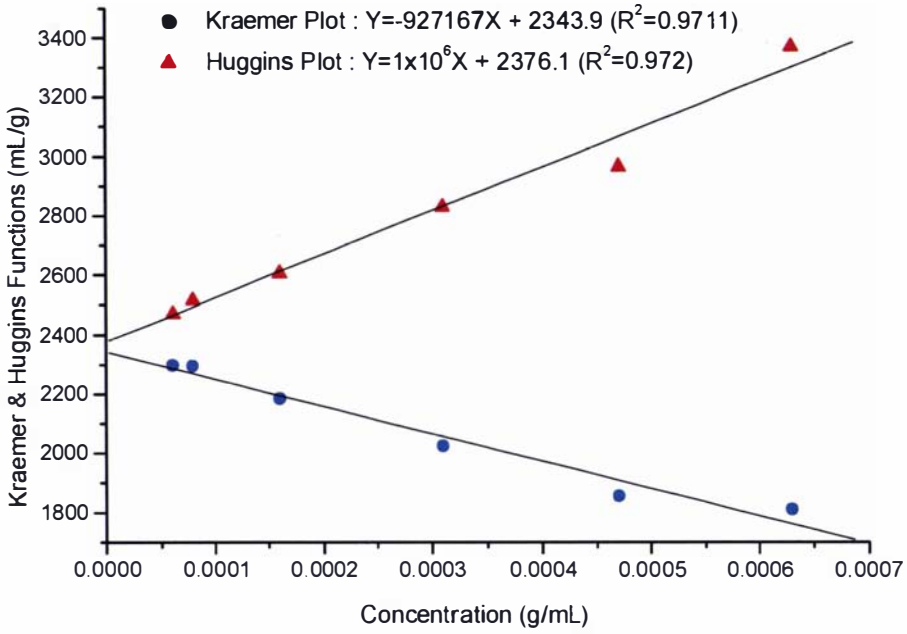

Figure 7.10 Huggins (▲) and Kraemer (●) plots for Na-LT100 solutions.

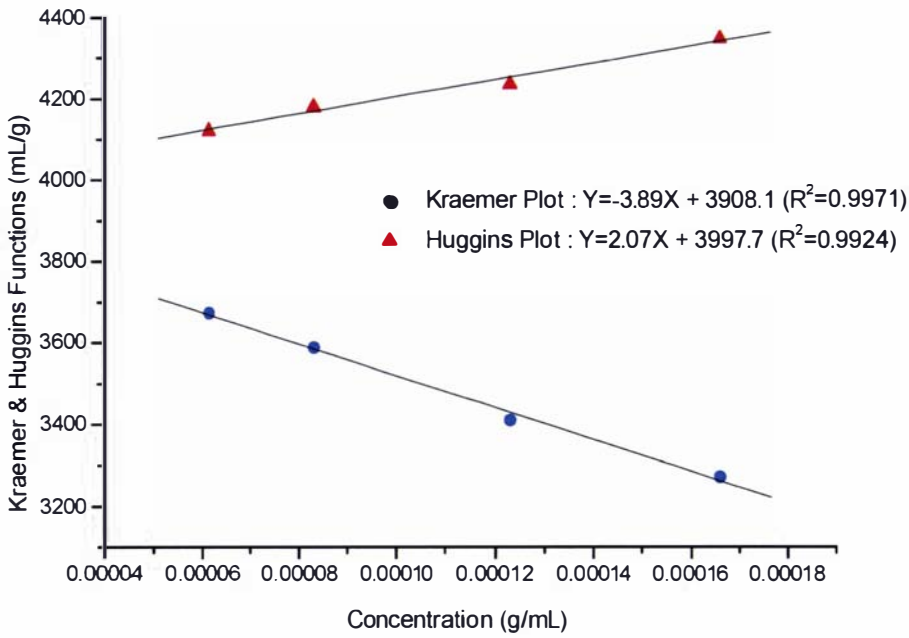

Figure 7.11 Huggins (▲) and Kraemer (●) plots for Na-31461 solution.

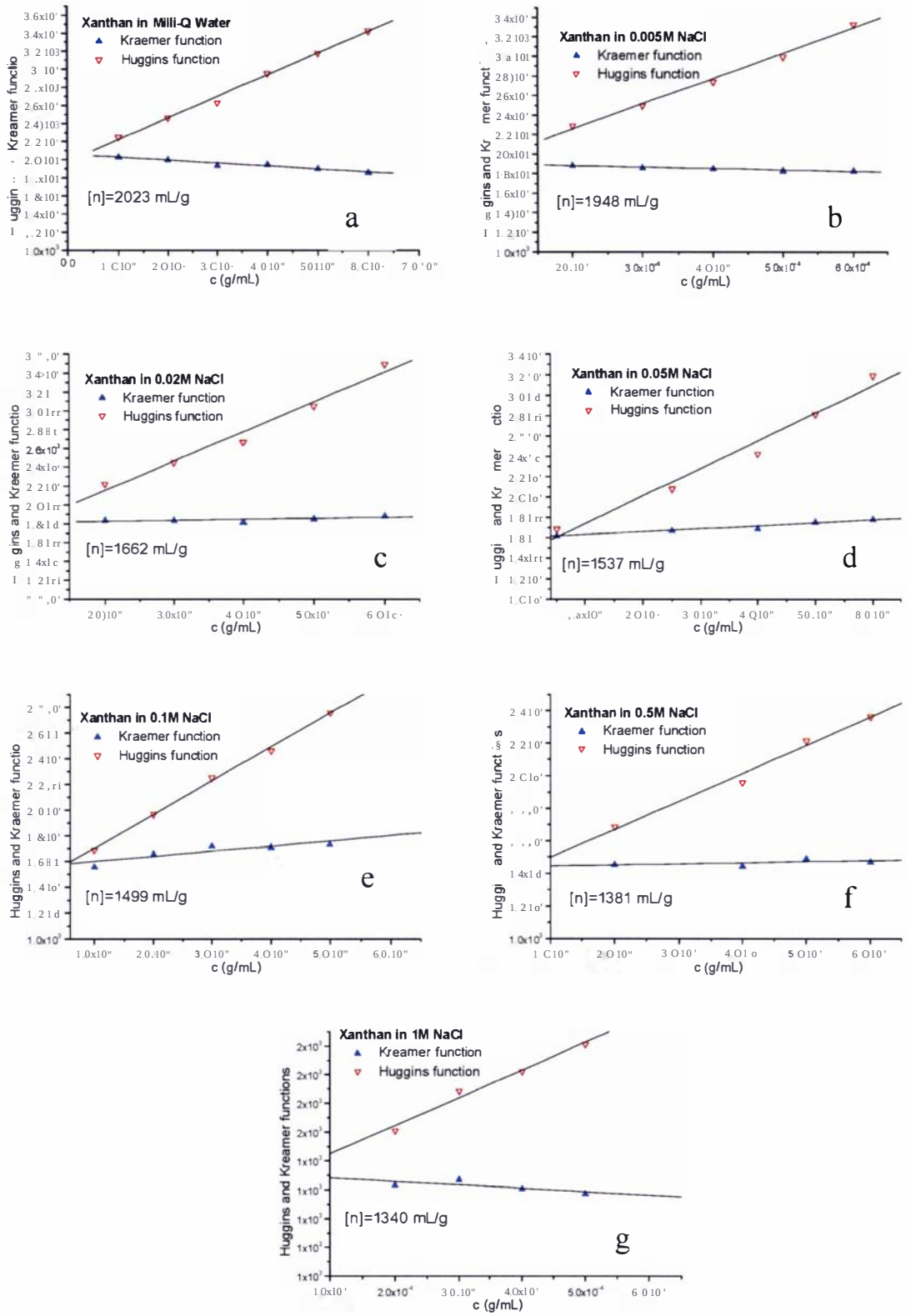

Figure 7.12 Huggins (▽) and Kraemer (▲) plots of xanthan gum solution in (a) water, and in different NaCl concentrations: (b) 0.005M, (c) 0.02M, (d) 0.05M, (e) 0.1M, (f) 0.5M and (g) 1M.

Table 7.3 Intrinsic viscosity of Na-LT100, Na-31461 and xanthan solutions.

Samples	Intrinsic Viscosity [η] mL/g
Na-LT100 in water	2360
Na-31461 in water	3953
Xanthan in water	2023
Xanthan in 0.005M NaCl	1948
Xanthan in 0.02M NaCl	1662
Xanthan in 0.05M NaCl	1537
Xanthan in 0.1M NaCl	1499
Xanthan in 0.5M NaCl	1381
Xanthan in 1.0M NaCl	1340

[1] Note that the intrinsic value was obtained from the average of the two intercepts.

The intrinsic viscosity for Na-31461 was approximately twice that of Na-LT100. This is consistent with the M_w of Na-31461 and Na-LT100 obtained by light scattering measurements (which will be discussed in the later section). The intrinsic viscosity of xanthan solution was found to decrease with increasing salt concentration (Table 7.3). This was due to the presence of salt causing a decrease in intramolecular electrostatic repulsion, which in return resulted in a more compact xanthan molecule.

Since the xanthan molecule has been reported to be double-stranded (Holzwarth & Prestridge, 1977), adopts a stiff conformation (Rinaudo & Mils, 1978) and has a relatively large M_w~2x10^6 Da (Rinaudo & Mils, 1978), it is expected to have a higher intrinsic viscosity than both Na-gellan samples. However, when a comparison was made between Na-gellan and xanthan, the intrinsic viscosity values of both Na-gellan samples were found to be higher than xanthan. This suggests that there were intermolecular associations in both Na-gellan samples. The existence of intermolecular associations of Na-gellan molecules was also supported by the results obtained in the light scattering experiments (which will be discussed in the later section).

7.3.3.1 Determination of chain stiffness of xanthan

The plot in Figure 7.13 shows that the intrinsic viscosity of xanthan increased linearly with $I^{0.5}$. The intrinsic viscosity at infinite salt concentration, $[\eta]^{\infty}$ obtained by extrapolation, was found to be 1327mL/g.

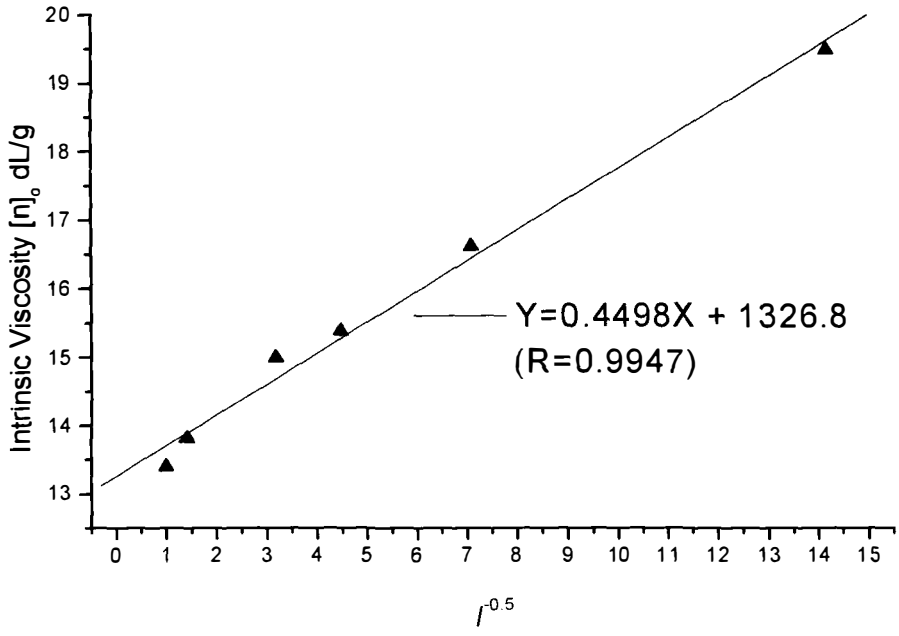

Figure 7.13 Intrinsic viscosity at infinite ionic strength determined by extrapolation of the linear plot. The slope S = 0.4498.

From the plot, the slope S was determined. The empirical Smidsrod stiffness parameter B gives an indication of chain stiffness according to Smidsrod & Haug (1971). Using the equation below, the Smidsrod stiffness parameter, B, could be determined:

$$B = S/([\eta]_{0.1})^{\nu}$$

A low value of B is associated with stiff polymer backbones (Lapasin & Pricl, 1995). In this study, the B value for xanthan molecules was ~0.013, based on an average value of ν~1.3. The parameter $[\eta]_{0.1}$ is the intrinsic viscosity at 0.1M ionic concentration, expressed as dL/g. The *B* value indicates that the xanthan polymer was a relatively stiff polymer, although Tinland & Rinaudo (1989) obtained an even lower *B* value (~0.005). The *B* values for low acyl gellan have been reported to range from 0.015 to 0.05 at very low salt concentration (<0.1M) (Jampen et al., 2000) suggesting that the gellan molecule may adopt a conformation of a semi-flexible chain. In this present study, direct comparison of xanthan with Na-gellan samples could not be made as the gellan polysaccharide formed a gel in 0.1M NaCl solution.

7.3.4 Concentration dependence of zero-shear viscosity

Figure 7.14 shows the concentration dependence of zero-shear viscosity for Na-LT100 and Na-31461. By applying linear regressions to the data points, two concentration domains were obtained for both the Na-gellan samples.

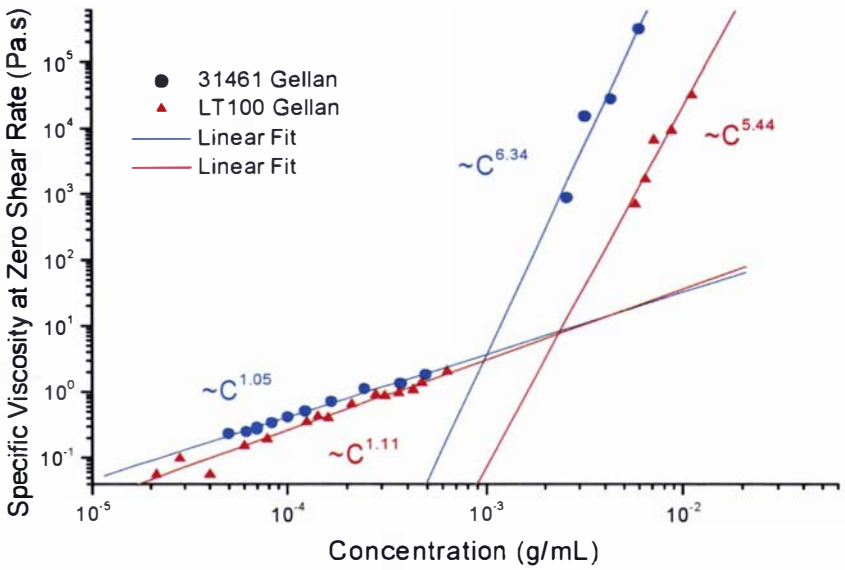

Figure 7.14 Concentration dependence of zero-shear viscosity of Na-LT100 and Na-31461 dispersed in Milli-Q water. The intersections of Na-31461 and Na-LT100 curves occur at 1.0 x10^{-3} g/mL and 2.3 x 10^{-3} g/mL respectively.

The coil overlap concentrations for Na-LT100 and Na-31461 were 0.23% and 0.1% respectively. In the dilute domain below the coil overlap concentration, both Na-gellan solutions behaved very similarly to flexible random coil polymers. However, in the concentrated domain, a very strong concentration dependence of zero-shear viscosity was observed for Na-LT100 ($\eta_{spo} \propto c^{5.4}$) and Na-31461 ($\eta_{spo} \propto c^{6.3}$). The exponent value of Na-LT100 in the concentrated domain was higher than typical random coil polymers. This may not be solely due to the physical entanglements of the polymer chains, but also to intermolecular interactions among Na-LT100 molecules. In Na-31461, the higher exponent value was caused by the entanglements of stiffer gellan molecules (as double-helix structures), as well as the probable intermolecular interactions among helices. The concentration dependence of viscosity for xanthan solutions of different ionic strength is shown in Figure 7.15. The exponent values are shown in Table 7.4.

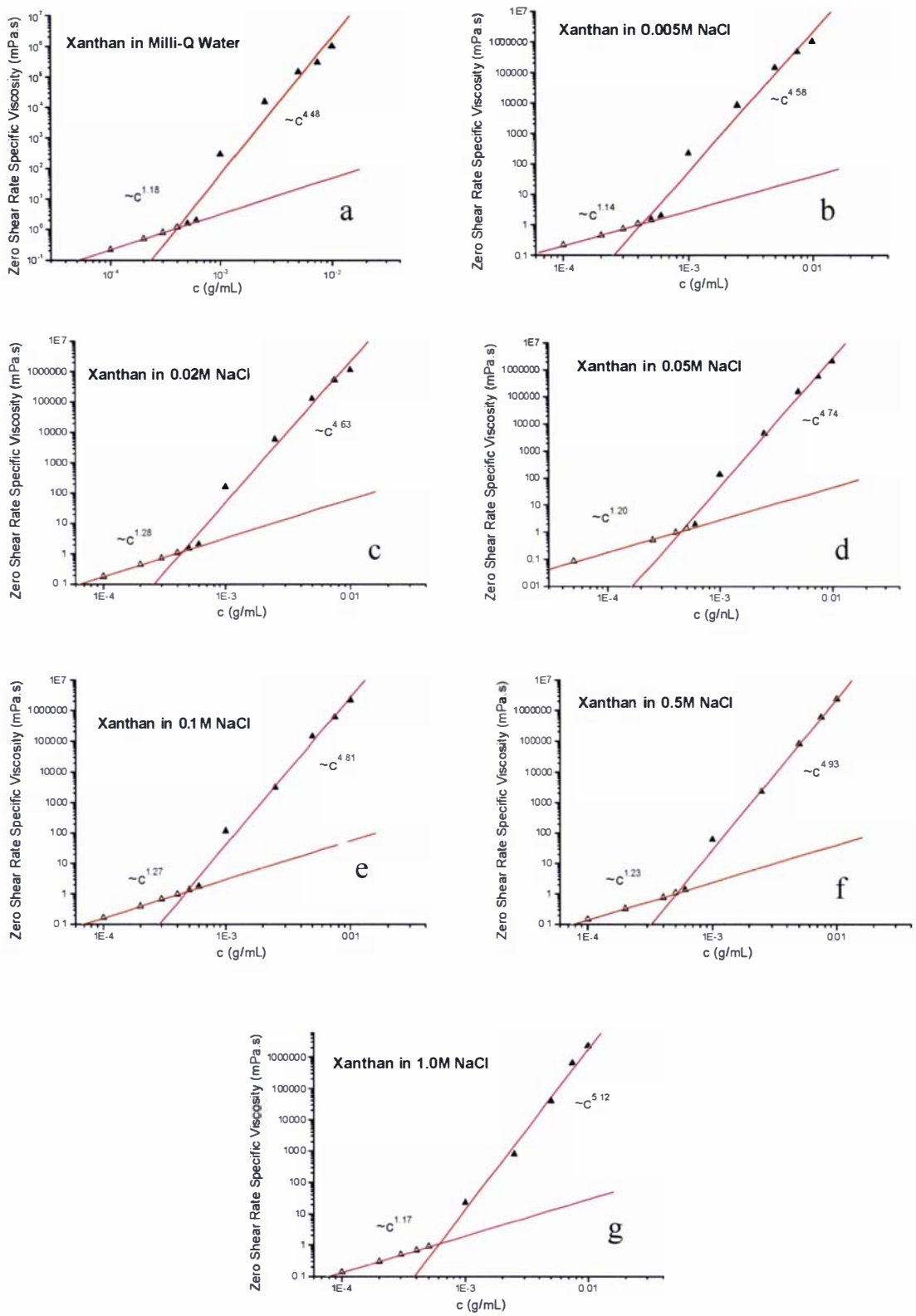

Figure 7.15 Concentration dependence of zero-shear viscosity of xanthan gum solution at different ionic strengths (water, 0.005M, 0.02M, 0.05M, 0.1M and 1M NaCl) with coil overlap concentrations of (a) ~4.02 x 10^{-4}, (b) ~4.23 x 10^{-4}, (c) ~4.43 x 10^{-4}, (d) ~4.46 x 10^{-4}, (e) ~4.78 x 10^{-4}, (f) ~5.12 x 10^{-4}, (g) ~6.07 x 10^{-4} g/mL respectively.

Table 7.4 Concentration dependence of viscosity exponents in dilute and concentrated domains for xanthan solution of different ionic strengths.

Samples	Exponents of Dilute domain	Exponents of Concentrated domain
Xanthan in Water	1.18	4.48
Xanthan in 0.005M NaCl	1.14	4.58
Xanthan in 0.02M NaCl	1.28	4.63
Xanthan in 0.05M NaCl	1.20	4.74
Xanthan in 0.1M NaCl	1.27	4.81
Xanthan in 0.5M NaCl	1.23	4.93
Xanthan in 1.0M NaCl	1.17	5.12

For xanthan samples in the dilute domain, the solutions (regardless of ionic strengths) behaved like a flexible random coil polymer. The solution viscosity was contributed by the Brownian motion of the polymer molecules and the perturbation of flow of solvent caused by individual polymer molecules. Only intramolecular repulsion of the polymer molecules occur in this dilute domain (Rochefort & Middleman, 1987). However, in the concentrated domain, the exponents ranged between 4.5-5.1. The exponent values were fairly close to that reported by Cuvelier & Launay (1986), with $\eta_{spo} \propto c^{4.2}$. The high exponent values obtained for xanthan were attributed to chain stiffness as well as intermolecular associations at high polymer concentrations (Rochefort & Middleman, 1987). The relationship between the exponent value in the concentrated domain and ionic strength appeared linear as shown in the semi-log plot (Figure 7.16). The increase in exponent value with ionic concentration could be explained by increasing chain-chain interactions due to increasing electrostatic screening. When the concentrations of xanthan solutions were below the coil overlap concentrations, increasing salt concentration did not show any clear trend in terms of its exponent values.

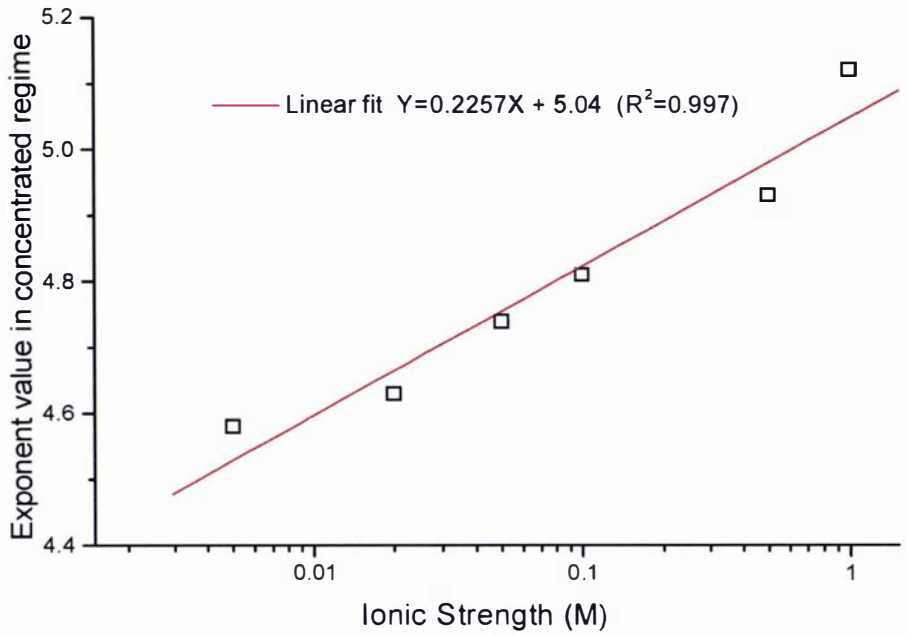

Figure 7.16. Semi-log plot of the exponent value in concentrated domain as a function of ionic strength.

7.3.5 Analysis of sodium gellan molecules by static light scattering

7.3.5.1 Multi-angle Laser Light Scattering (MALLS)

The *dn/dc* values for Na-LT100 and Na-31461 were found to be 0.13mL/g and 0.15mL/g respectively. Both Na-gellan samples were similar to deacylated gellan, which has a *dn/dc* value of 0.136 mL/g at 633nm (Gunning & Morris, 1990).

The light scattering data were fitted to either a Zimm or Berry plot (Figure 7.17 – 7.20). Some angles, usually the very low and high, showed noisy signals and hence they were excluded. From the plot, the various molecular parameters (M_w, $(r_g^2)_z^{1/2}$ and A_2) were obtained (Table 7.5).

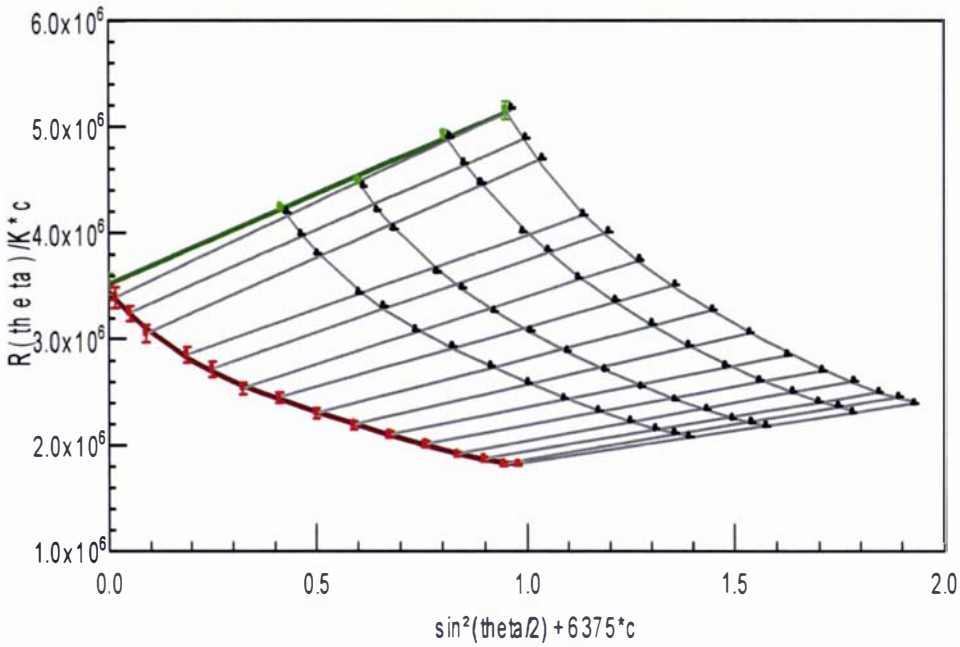

Figure 7.17 Berry Plot for Na-LT100 in water at 25°C (filtered through 0.2µm and held for 30 min before sample loading) at 4th order detector fit angle. Concentrations were 6.75, 8.96 x 10^{-5} and 1.15, 1.25 x 10^{-4} g/mL.

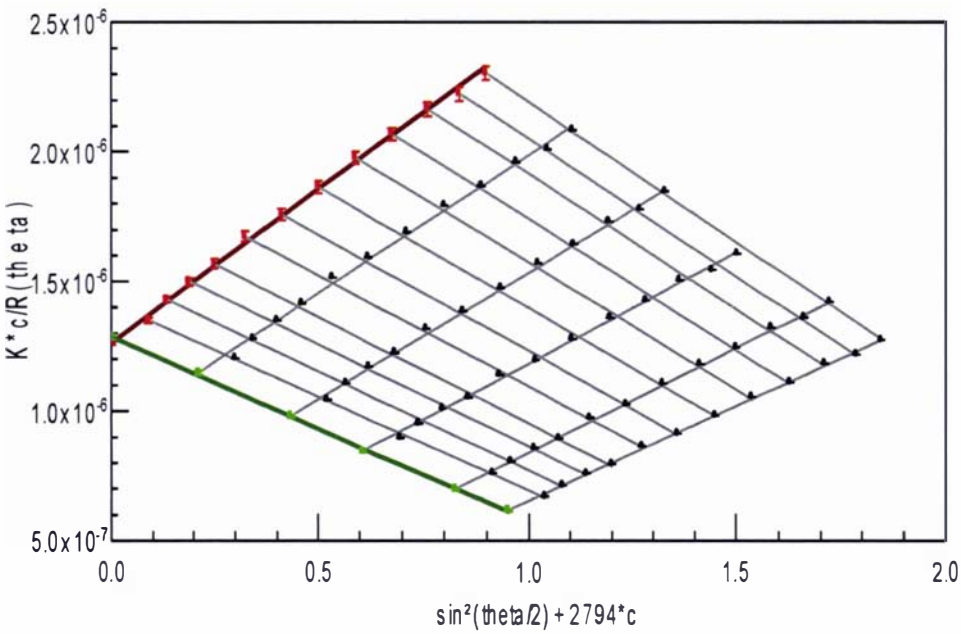

Figure 7.18 Zimm Plot for Na-LT100 in water at 25°C (filtered through 0.2µm during injection). Concentrations were 7.54 x 10^{-5} and 1.55, 2.17, 2.95, 3.40 x 10^{-4} g/mL.

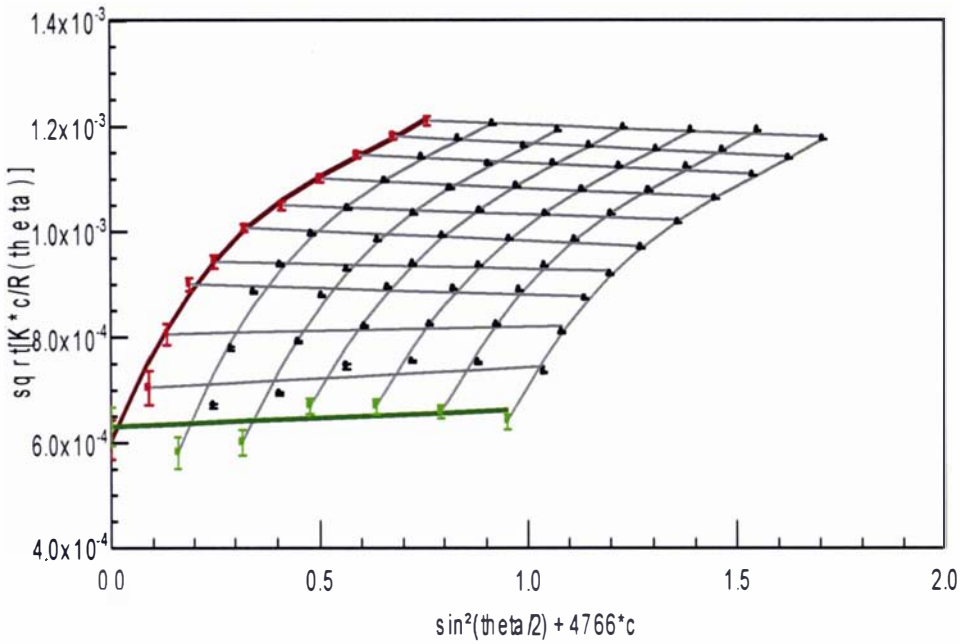

Figure 7.19 Berry Plot for Na-31461 in water at 25°C (filtered through 0.2µm and held for 30 min before sample loading) using 3rd order degree detector fit angle. Concentrations were 3.32, 6.64, 9.97 x 10^{-5} and 1.33, 1.66, 1.99 x 10^{-4} g/mL.

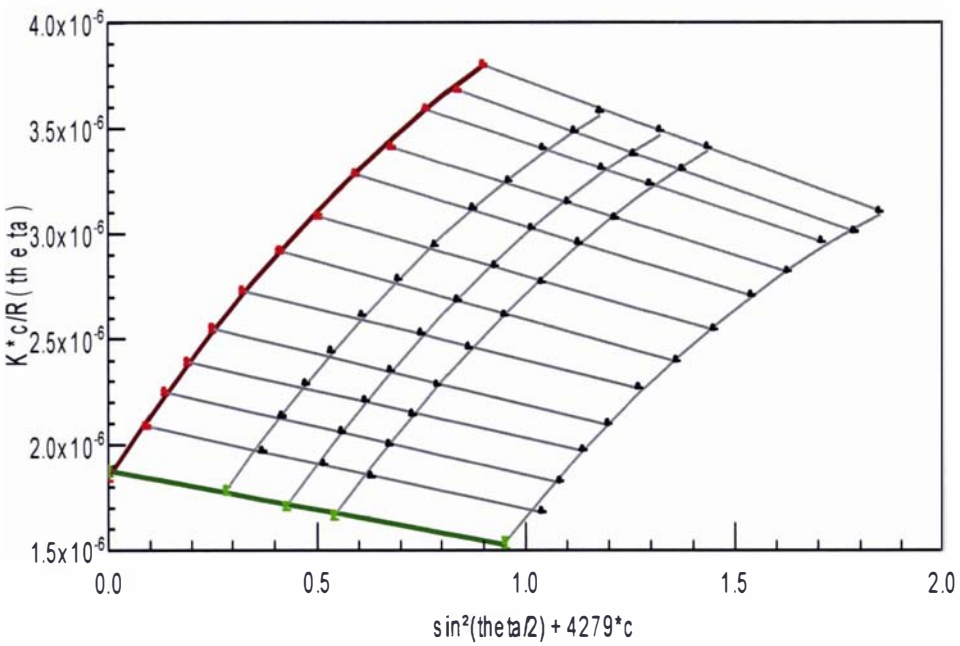

Figure 7.20 Zimm Plot for Na-31461 in water at 25°C (filtered through 0.2µm during injection) at 2rd order detector fit angle. Concentrations were 6.63, 9.95 x 10^{-5} and 1.26, 2.22 x 10^{-4} g/mL.

Table 7.5 Molecular parameters of Na-gellan.

Samples	M_w (Da)	$(r_g^2)_z^{1/2}$ (nm)	A_2 (mol mL/g^2)	Fit Model	Order of Fit
Na-LT100	7.84 ± 0.08 x 10^5	63.4 ± 0.6	-9.89 ± 0.17x 10^{-4}	Zimm	1
Na-LT100 (Filtered and held for 30 min before sample loading)	3.49 ± 0.13 x 10^6	74.9 ± 8.1	-4.36 ± 0.51x 10^{-4}	Berry	4
Na-31461	5.36 ± 0.09x 10^5	82.3 ± 1.3	-7.89 ± 0.96x 10^{-4}	Zimm	2
Na-31461 (Filtered and held for 30 min before sample loading)	2.31 ± 0.20 x 10^6	150.9 ± 11.7	-7.52 ± 21.65x 10^{-5}	Berry	3

Reliable sample preparation procedure for gellan solutions was crucial when carrying out light scattering experiments. It was found that when Na-LT100 or Na-31461 gellan sample was left to stand for 30 min after filtration, a substantial increase in M_w was observed compared to the sample that was analysed immediately after filtration. This large difference in M_w was probably due to progressive aggregation of the gellan molecules when left to stand for a certain period. The negative A_2 values for both Na-gellan samples could imply that polymer-solvent interactions were less favoured compared to polymer-polymer interactions, hence, the likely occurrence of aggregation among the Na-gellan molecules in water.

The filtration step during sample preparation has been shown by other researchers to be a crucial factor influencing the light scattering data. For instance, Gunning and Morris (1990) reported a M_w of 1.06 x 10^5 Da and a $(r_g^2)_z^{1/2}$ of 72nm for TMA-gellan when filtered through a 0.45µm. However, when the same sample was filtered using a 3µm filter, M_w and $(r_g^2)_z^{1/2}$ values obtained were 4.5 x 10^6 Da and 159nm respectively. It is reasonable to assume that the larger aggregates of Na-gellan molecules were removed and/or disrupted (due to shear) during filtration. However, as soon as the samples were left unperturbed, aggregation could occur progressively over time. This was indicated

by increases in the M_w of Na-LT100 and Na-31461 samples held for 30 min after filtration (Table 7.5). Analysing the sample immediately after filtration seemed to bring the M_w values closer to reported values ranging from 2.5-5 x 10^5 Da (Milas, Shi & Rinaudo, 1990). It is reasonable to expect that some re-aggregation inevitably took place instantaneously after filtration and during analysis. The tendency of gellan molecules to form aggregates has certainly made molecular weight determination by light scattering difficult (Brownsey, Chilvers, Anson & Morris, 1984; Dreveton, Monot, Lecourtier, Ballerini & Choplin, 1996; Walter & Jacon, 1994). Hence, it is not surprising that the reported molecular weights for gellan molecules vary widely among researchers. Interpretation of the results has to be dealt with much care.

7.3.5.2 Gel-filtration Chromatography combined with Multi-angle Laser Light Scattering (GFC-MALLS)

The superimposed signals (UV, DRI and light scattering intensity at 90°) for Na-LT100 and Na-31461 samples are shown in Figure 7.21 The UV signals, particularly in Na-LT100 sample, appeared to be relatively high. This was probably due to the carry-over of small amounts of protein components from the growth medium and/or cellular materials, which were not removed during the purification step. Generally, the large molecular species (polysaccharides) were fairly well separated from the smaller molecular species using the Shodex SB 806 HQ column.

For the two Na-gellan samples, the Zimm fit method was used. The data (outliers) from the higher angles (above 90°) were occasionally omitted to allow for a better fit using first order polynomials. The molecular parameters are summarized in Table 7.6.

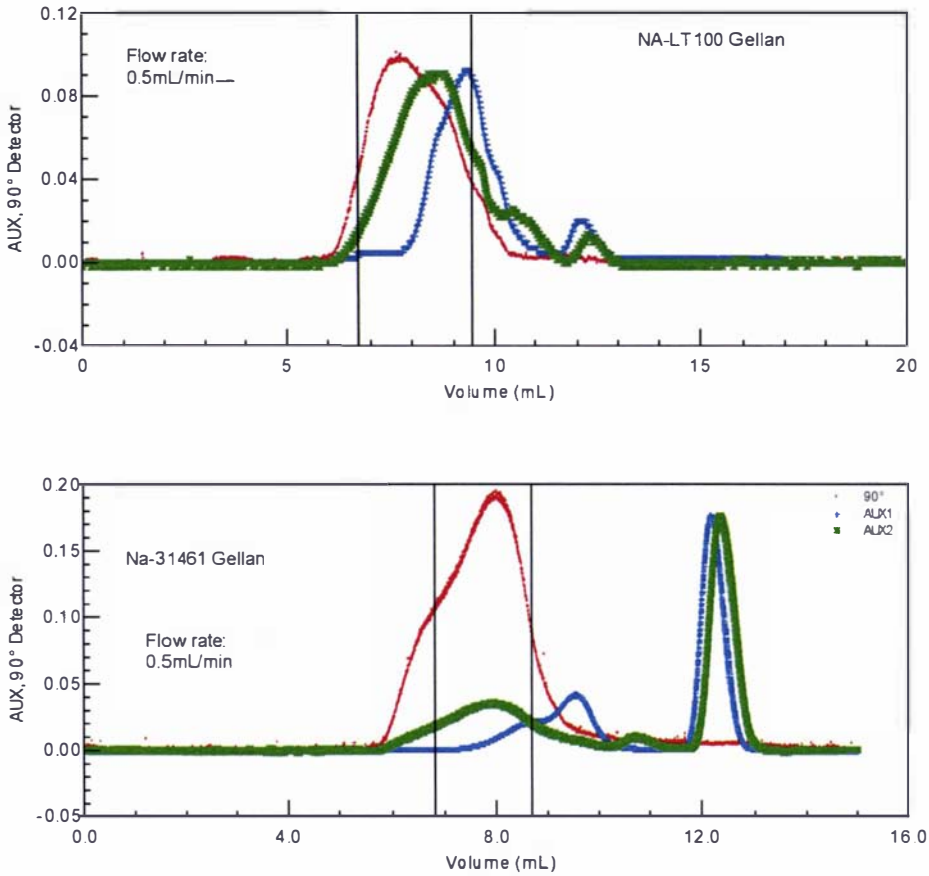

Figure 7.21 Light scattering (red), DRI (green) and UV(blue) signals from (a) Na-LT100 and (b) Na-31461 samples using Shodex SB-806 HQ column. The light scattering signal was traced for the detector at 90° angle. Scaling factor for DRI and UV signals is 0.9. The two vertical lines indicate the boundaries of peak and represent the area of the chromatograms selected for molecular weight determination by the ASTRA software.

7.3.5.3 Molecular weight distribution

The molecular weight distributions of the first eluted fraction from Na-LT100 and Na-31461 are shown in Figure 7.22. The molecular weight distributions of both Na-LT100 and Na-31461 fractions indicated moderately good separation of the molecular species by the GFC column.

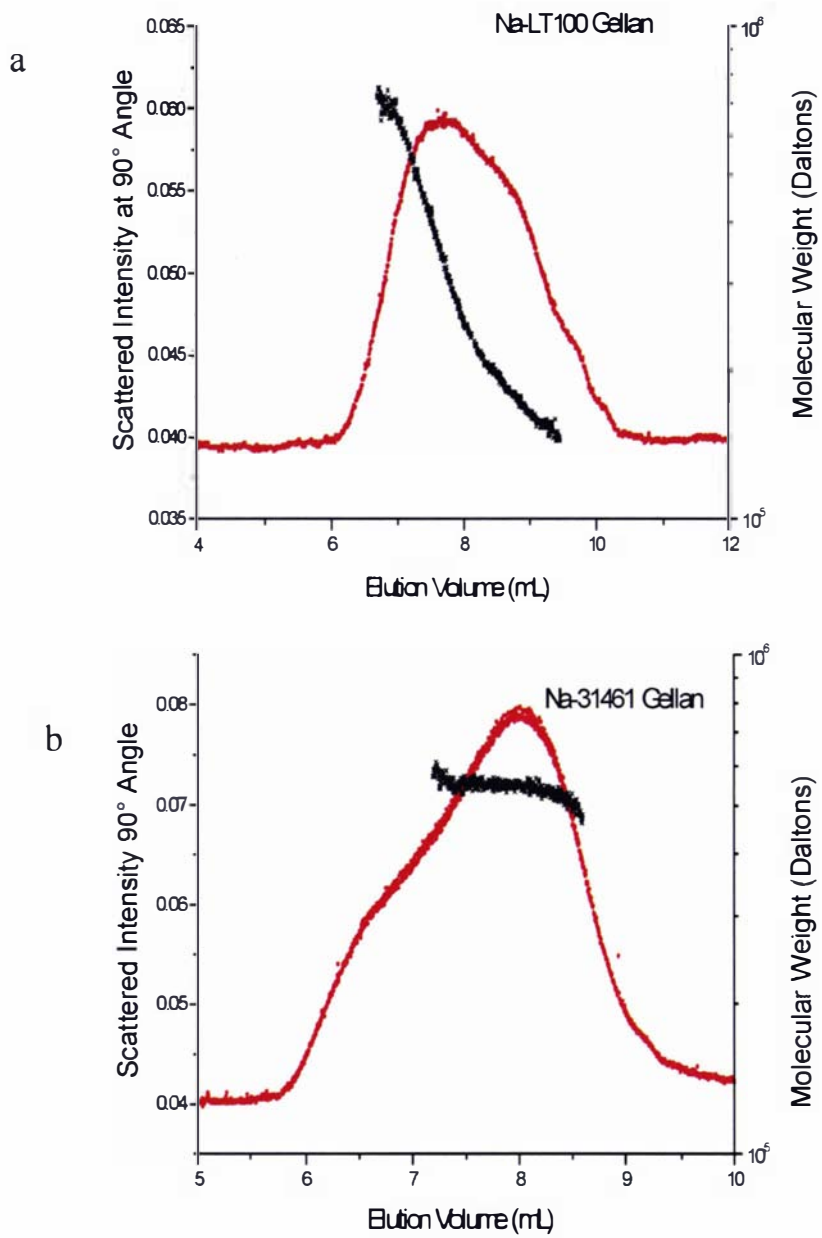

Figure 7.22 Light scattering signal at 90° (red) and molecular weight distribution (black) as a function of elution volume for (a) Na-LT100 gellan and (b) Na-31461 gellan.

Table 7.6 Molecular parameters of polysaccharide samples obtained from GFC-MALLS.

Molecular Parameters	Na-LT100	Na-31461
Molecular Weight (Da)		
M_n	$2.26 \pm 0.11 \times 10^5$	$4.57 \pm 0.68 \times 10^5$
M_w	$2.71 \pm 0.14 \times 10^5$	$5.23 \pm 0.69 \times 10^5$
M_z	$3.45 \pm 0.40 \times 10^5$	$5.60 \pm 1.64 \times 10^5$
Root Mean Square Radius (nm)		
$(r_g^2)_n^{1/2}$	45.8 ± 4.0	45.4 ± 10.2
$(r_g^2)_w^{1/2}$	48.7 ± 3.9	44.9 ± 9.5
$(r_g^2)_z^{1/2}$	52.9 ± 3.8	44.9 ± 9.1
Polydispersity		
M_w/M_n	1.20 ± 0.08	1.14 ± 0.23
M_z/M_n	1.53 ± 0.19	1.23 ± 0.40
Fit method		
Model	Zimm	Zimm
Order of polynomial	1	1

In the chromatography mode, the chances of molecular re-aggregation are probably reduced because of the shear caused by the flow of the sample through the column and the high dilution of the gellan samples. The M_w obtained by GFC-MALLS may hence be considered to be more reliable than that determined by the batch mode.

Based on the results of the chromatography mode, the M_w of Na-31461 ($M_w \sim 5.2 \times 10^5$) is approximately twice that of Na-LT100($M_w \sim 2.7 \times 10^5$). The results could suggest that Na-LT100 gellan molecules were present in the single-stranded state whereas Na-31461 gellan molecules occurred in the double-stranded form. The values obtained in this study are in good agreement with Milas, Shi and Rinaudo (1990), who reported M_w of 2.5×10^5 Da and 4.9×10^5 for TMA-gellan[1] in its single-stranded form (36°C) and double-stranded form (24°C) respectively. Dentini, Coviello, Burchard & Crescenzi (1988) also reported a very similar value of gellan molecules in the double-stranded form ($M_w = 4.34 \times 10^5$ Da) in dilute aqueous salt solution. The transition from an

[1] TMA-gellan is prepared by replacing cations with tetramethyl ammonium ions (TMA^+). The bulky TMA^+ ion has a large molecular volume which deters aggregation and gelation of gellan (Okamoto, Kubota & Kuwahara, 1993).

ordered state (double-stranded) to a disordered state (single-stranded) has been demonstrated for gellan gum by subjecting the sample to a temperature above the transition temperature of ~36°C (Ogawa, 1996). In the present study, it was shown that Na-gellan samples at ambient temperature (~20°C) could exist in the single-stranded state, at very low ionic concentration, below its transition temperature.

While the results of the present study agree with several researchers as mentioned, there was also disagreement with a few others. For example, the M_w of the purified TMA-gellan at 25°C (ordered state) and 40°C (disordered state) were reported to be 2.17 x 10^5 and 9.47 x 10^4 Da, respectively (Akutu, Kubota & Nakamura, 1999; Takahashi, Akutu, Kubota & Nakamura, 1999). Brownsey et al. (1984) reported M_w of ~1.3 x 10^6 Da for the deacylated and acylated gellan while Ogawa (1993) reported yet a different M_w of 3.6 x 10^5 Da for the single-stranded gellan molecule, measured at 40°C. The differences in the results are possibly due to different ionic concentrations, sample preparation procedures as well as analytical techniques used.

The $(r_g^2)_z^{1/2}$ value of Na-31461 (~45nm) obtained by GFC-MALLS was very similar to Na-LT100 (~49nm). The $(r_g^2)_z^{1/2}$ value of Na-31461 was lower than the reported values of 96nm (Takahashi et al., 1999) and 127nm (Milas et al., 1990) for gellan molecules in the double-stranded state. However, the $(r_g^2)_z^{1/2}$ value of Na-31461 obtained by the batch mode (82nm, see Table 7.5) was closer to the reported values. As for Na-LT100, the $(r_g^2)_z^{1/2}$ values obtained by the batch (~63nm) and chromatography mode (~53nm) were within the reported values of 46nm (Takahashi et al., 1999) and 69.5nm (Milas et al., 1990) for gellan molecules in single-stranded form. The polydispersity indices (M_w/M_n) of both samples were low.

The M_w of Na-31461 gellan obtained by the batch and chromatography modes are very similar (see Tables 7.5 and 7.6). This suggests that in the batch mode, the filtration step prior to sample analysis was effective in disrupting and/or removing any aggregates.

Besides, the double-stranded Na-31461 gellan molecules did not appear to re-aggregate as strongly as the Na-LT100 molecules.

Unlike Na-31461, Na-LT100 molecules showed different values of M_w between the batch mode (M_w~7.8x10^5 Da) and the chromatography mode (M_w~2.7x10^5 Da). The higher M_w of Na-LT100 sample obtained by the batch mode suggests that the Na-LT100 molecules have a high tendency to re-aggregate almost immediately after the filtration step.

Further evaluation was made based on the results obtained by the batch mode (Table 7.5). When both Na-LT100 and Na-31461 molecules were allowed to re-aggregate, the M_w and $\left(r_g^2\right)_z^{1/2}$ values were different. These suggest different modes of chain aggregation by the two Na-gellan samples. It seems probable that the Na-31461 gellan aggregates were formed by the aggregation of double-stranded molecules, whereas the Na-LT100 aggregates were formed by the aggregation of single-stranded molecules. The aggregates of Na-31461 molecules appeared to be loosely aggregated (hence, lower M_w~2.3x10^{6}Da but larger in size, $\left(r_g^2\right)_z^{1/2}$~151nm) than the more compact Na-LT100 aggregates (M_w~3.5x10^6 Da; $\left(r_g^2\right)_z^{1/2}$~75nm).

7.3.5.4 Molecular conformation

The conformations of the polysaccharide molecules could be predicted from a log-log plot of the $\left(r_g^2\right)_z^{1/2}$ versus M_w as shown in Figure 7.23. The slope of Na-LT100 sample (0.37) suggested that its molecular conformation was in-between a sphere and a random coil. This could be due to a short and flexible backbone of the Na-LT100 molecule, in which the macromolecule has the tendency to 'bend', hence, adopting a sphere-like conformation. In Na-31461 gellan, the exponent was much higher (>0.6) than the Na-LT100 counterpart, suggesting a stiffer conformation for Na-31461 molecules. A rigid, rod-like conformation for the double-stranded gellan molecule has previously been reported (Milas et al., 1990; Ogawa, 1993; Yuguchi et al., 1997). The above

approximation to predict the conformation of molecules was consistent with the implication that Na-LT100 and Na-31461 molecules were single-stranded and double-stranded, respectively.

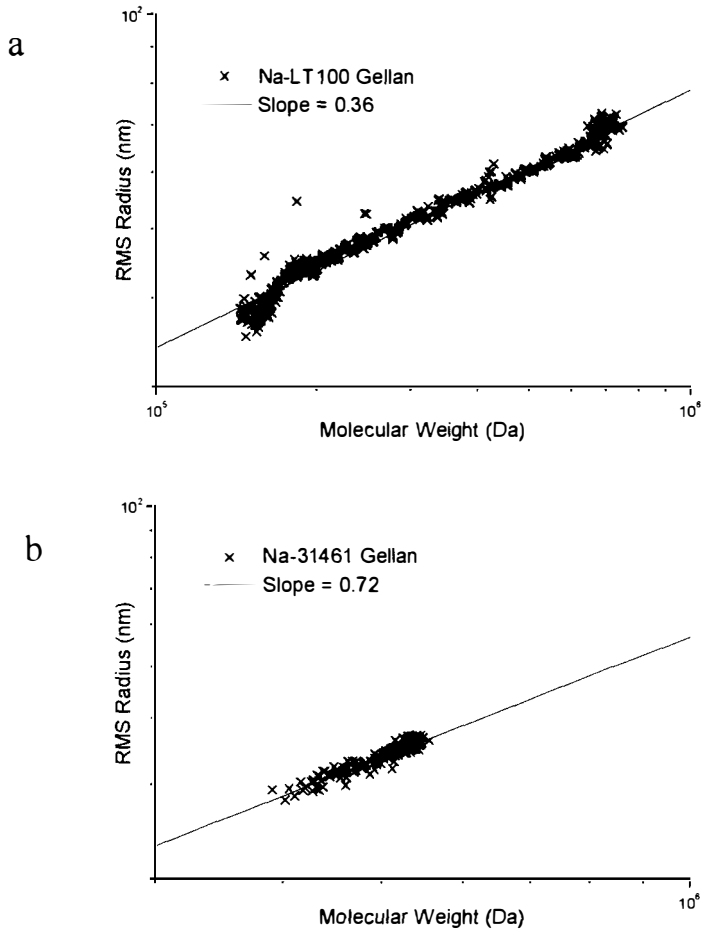

Figure 7.23 Weight-average molecular weight as a function of z-average RMS radius for (a) Na-LT100 and (b) Na-31461 gellan samples.

7.3.6 Viscoelastic properties

The viscoelastic behaviours of the Na-LT100, Na-31461 gellan and xanthan solutions were studied using dynamic oscillatory measurements.

7.3.6.1 Frequency sweep for Na-LT100, Na-31461 and xanthan

Frequency sweep tests performed on 0.42%, w/v, Na-LT100, Na-31461 and xanthan samples were carried out within the linear viscoelastic region (Figure 7.24).

a

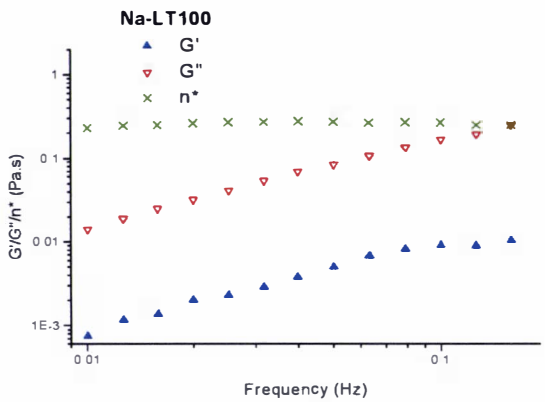

b

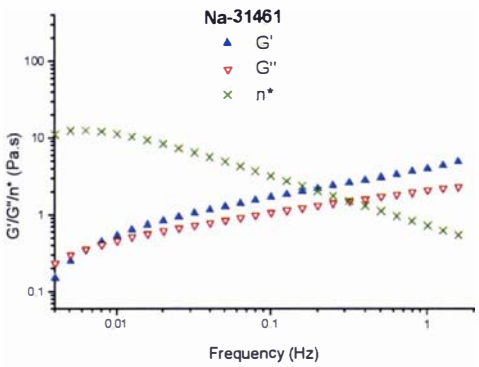

c

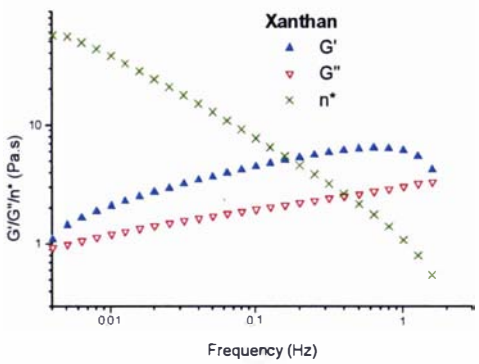

Figure 7.24 Dynamic frequency sweep tests performed on samples of 0.42% w/v (a) Na-LT100, (b) Na-31461 and (c) Xanthan in water at 20°C. *G'* (▲), *G"* (∇) and η^* (X).

At 0.42% (w/v) concentration, the mechanical spectra for Na-LT100 indicated that *G"* was higher than *G'* over the frequency range studied. The response was typical of a flexible chain polymer in dilute solution since the complex dynamic viscosity (η^*) showed Newtonian behaviour. The crossover frequency (where *G'=G"*) could not be reached as it was below the lower limit accessible by the rheometer.

The mechanical spectra for both Na-31461 (0.42% w/v) and xanthan (0.42%w/v) show relatively similar trends at frequency above 0.01 Hz, with *G'* dominating over *G"*. The results indicated that the rate of oscillation exceeded the rate of molecular rearrangement. This behaviour is typical of a weak gel structure and is believed to be contributed by chain stiffness of the double-helices and weak intermolecular interactions of both Na-31461 and xanthan molecules. The formation of weak junction zones among gellan double-helices has been proposed by Miyoshi et al. (1995). The crossover (i.e. *G'=G"*) of Na-31461 (~0.006 Hz) occurred at a higher frequency than xanthan (<0.004 Hz), indicating that xanthan has a longer relaxation time (junction lifetime) than Na-31461. The rigidity of the xanthan molecules, intermolecular interaction and higher molar mass were probably responsible for the longer relaxation time.

7.3.6.2 Effect of ionic strength on viscoelastic properties

7.3.6.2.1 Na-LT100 and 31461 solutions

Effects of ionic strength on the viscoelastic properties of Na-LT1000 and Na-31461 gellan samples (1% w/v) were determined. Both Na-LT100 and Na-31461 samples were dialysed overnight against water, 0.002M, 0.005M, 0.05M and 0.1M NaCl solutions. The percentage of ash and the concentration of Na^+ in the 1% (w/v) Na-gellan solutions are shown in Table 7.7.

The mechanical spectra (*G'*, *G"*) obtained by oscillatory measurements indicated that both Na-LT100 and Na-31461 (both at 1% w/v) underwent a gradual change in gel strength as the percentage of ash increased (Figure 7.25). For the Na-LT100 sample at ~17.0mM Na^+, the viscous modulus (*G"*) dominated over the elastic modulus (*G'*) at

low frequency. However, the entire spectra demonstrated a transition from a solution to a weak gel when *G'* crosses over *G"* (i.e. *G'=G"*) at ~0.13 Hz. The mechanical spectra of Na-LT100 resembled that of typical entangled random flexible chain polymers (Figure 7.25a).

Table 7.7 Percentage of ash and the concentration of Na^+ in 1% w/v Na-LT100 and Na-31461 solution dialysed against water or different concentrations of NaCl solutions.

Samples	Ash(% w/w)	Na^+ Concentration (mM)
Na-LT100		
Water	0.039	17.0
0.002M NaCl	0.043	18.7
0.005M NaCl	0.049	21.3
0.05 NaCl	0.069	30.0
0.1 NaCl	0.13	56.5
Na-31461		
Water	0.047	20.4
0.002M NaCl	0.051	22.2
0.005M NaCl	0.056	24.3
0.05 NaCl	0.103	44.8
0.1 NaCl	0.253	110.0

As the concentration of Na^+ increased from ~17.0 to ~18.7mM, a shift towards a lower crossover frequency (~0.02 Hz) was observed (Figure 7.25b). In terms of relaxation time for Na-LT100, there was an increase from 1.2 s to 8 s, indicating decreasing chain mobility due to increasing chain-chain interactions. At a slightly higher Na^+ concentration (~21.3mM), *G'* clearly dominated over *G"* and both showed strong frequency dependence, typical of very soft gels (Figure 7.25c). With a further increment in Na^+ concentration to 30mM, the mechanical spectra showed a relatively strong gel with *G'* showing no frequency dependence. This implies the presence of a large population of permanent bonds which form the three-dimensional gel network structure (Figure 7.25d). The gel was relatively firm (as *G'* and *G"* differed approximately by a decade) and elastic (as shown by its low frequency dependence of *G"*). At ~56mM Na^+ concentration, a further increase in gel elasticity (*G'*) was observed (Figure 7.25e).

The Na-31461 gellan at ~20.4mM Na^+ concentration exhibited the behaviour of a weak gel as indicated by a higher *G'* compared to *G"* (Figure 7.25f). Both spectra were highly dependent on frequency indicating a weak gel structure. These mechanical spectra were very similar to that of xanthan. As the percentage of Na^+ concentration increased to ~24.3mM, the difference between *G'* and *G"* continued to increase and a decrease in frequency dependence of the mechanical spectra was observed (Figure 7.25g & h). At ~45mM Na^+ concentration, a strong gel was formed with *G'* and *G"* differed by slightly more than a decade and the mechanical spectra showed no frequency dependence (Figure 7.25i). A further increase of Na^+ concentration to ~110mM resulted in a strong gel with high elastic modulus (Figure 7.25j).

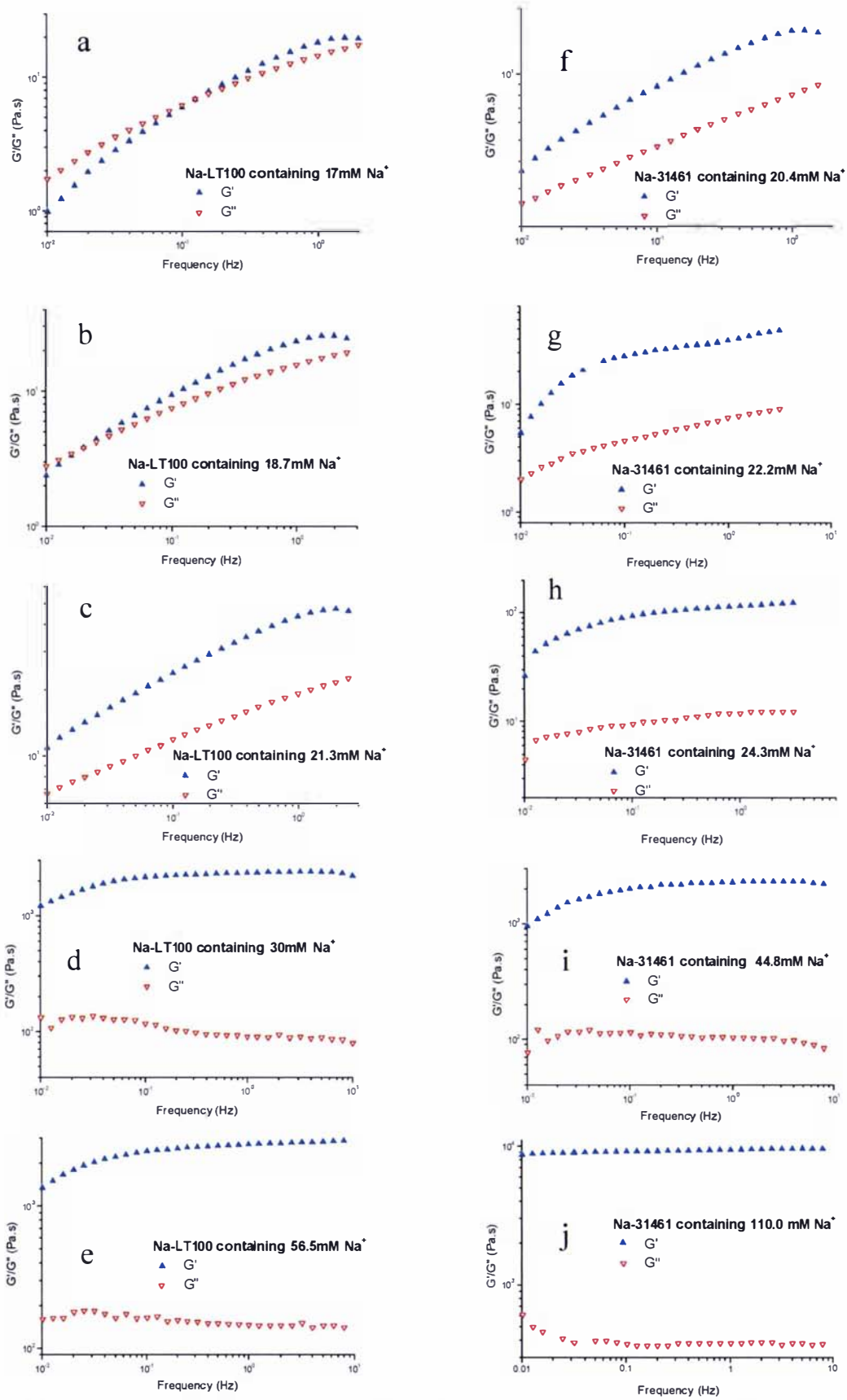

Figure 7.25 Dynamic frequency sweep tests performed on samples of (a – e) 1% w/v Na-LT100 (left column) and (f –j) 1% w/v Na-31461 (right column) containing different Na^+ concentrations. *G'* (▲) and *G"* (▽).

Comparison between the complex moduli (G^*) of Na-LT100 and Na-31461 was made based on the plot of G^* as a function of Na^+ concentration (Figure 7.26). The complex moduli of both Na-31461 and Na-LT100 showed an initial rapid increase with an increase in Na^+ concentration up to ~44mM. A further increase in Na^+ concentration had less effect on G^*. The overall trend shows that G^* of Na-31461 and Na-LT100 closely superimposed each other, indicating that both gellan samples gave similar gel strengths under similar Na^+ concentrations.

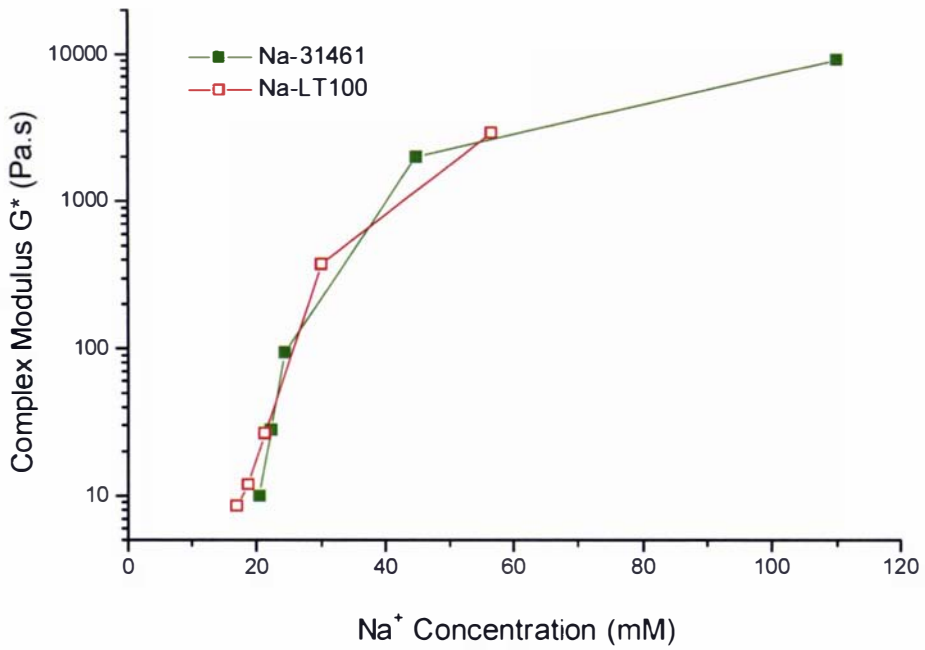

Figure 7.26 Complex Modulus (G^*) as a function of Na^+ concentration obtained from dynamic frequency sweep tests at 0.1 Hz for Na-LT100 (□), and Na-31461(■).

7.3.6.2.2 Xanthan solution (1% w/v)

The mechanical spectra of a 1% w/v xanthan in different salt concentrations (0, 0.005, 0.02, 0.05, 0.1, 0.5, 1M) are shown in Figure 7.27

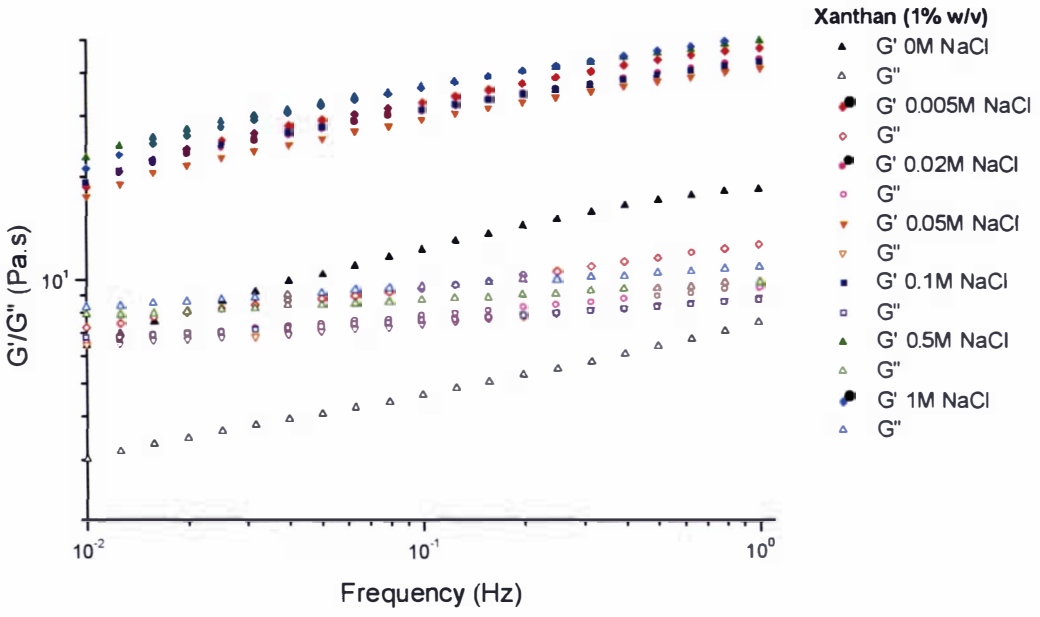

Figure 7.27. Dynamic frequency sweep of a 1% w/v xanthan solution at 20°C under different ionic strength. *G'* are represented by closed symbols and *G"* by open symbols.

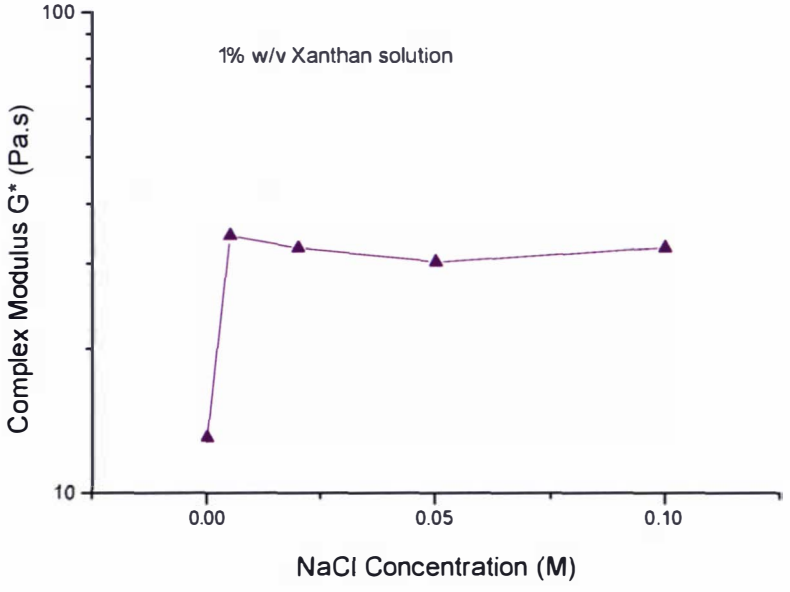

Figure 7.28 Complex Modulus (*G) as a function of NaCl concentration obtained from dynamic frequency sweep tests at 0.1 Hz.**

The mechanical spectra of xanthan solutions at all ionic strengths showed G' dominating over G'', typical of a 'weak gel' characteristic, contributed by rigid conformation of the polymers.

The values of G' and G'' increased by almost half a decade for xanthan in salt solutions. The increase in G' and G'' of xanthan solutions with the addition of salt indicated that the solutions had become more elastic and viscous, probably resulting from increased intermolecular interactions. This observation agrees with the results obtained by Lim, Uhl & Prudhomme (1984). Among the xanthan samples in different salt solutions (0.002M to 1M NaCl), no clear trend for G' and G'' was noted (Figure 7.27). However, when the complex modulus (G^*) was plotted as a function of salt concentration (Figure 7.28), it was noted that the complex modulus (G^*) increased initially with the addition of salt but remained constant from salt concentrations of 0.005M to 0.1M. This agrees with the results reported previously by Rochefort & Middleman (1987). The presence of Na^+ could reduce the electrostatic barrier, hence, allowing weak intermolecular interactions among the xanthan molecules. Several researchers have suggested that the rigid molecules form weak three-dimensional network by non-covalent interactions of double-stranded conformation (Hember & Morris, 1995; Richardson, Morris, Ross-Murphy, Taylor & Dea, 1989).

7.3.7 Cox-Merz plot

Many polymer solutions, particularly those of flexible random coil conformation, are found to obey Cox-Merz superposition (Cox & Merz 1958; Graessley, 1974), where the frequency dependence of dynamic complex viscosity (η^*) and the shear rate dependence of η, superimpose at the same numerical values of ω and $\dot{\gamma}$. The Cox-Merz plots for Na-LT100, Na-31461 and xanthan solutions are shown in Figure 7.29.

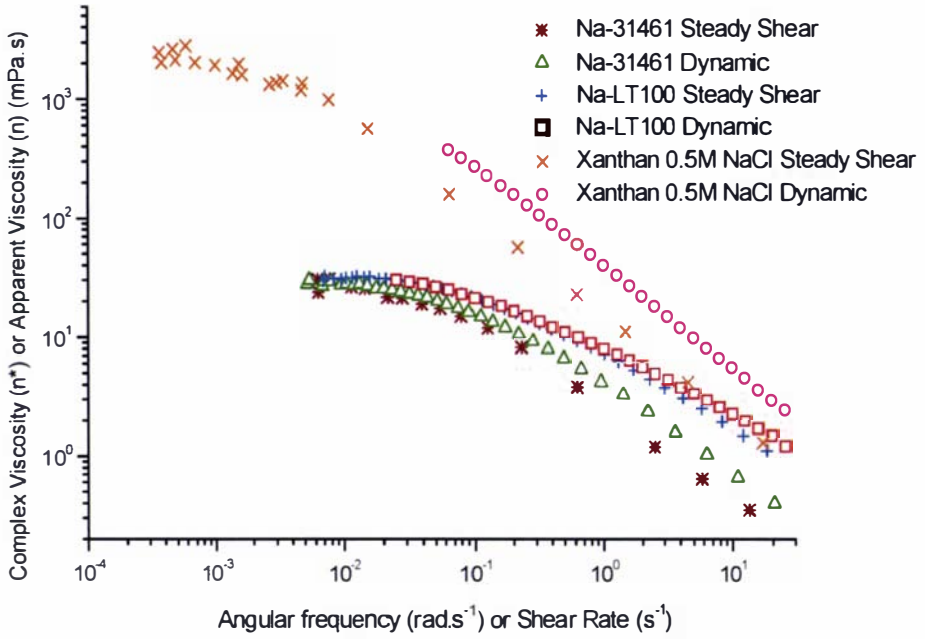

Figure 7.29 The 'Cox-Merz Plot' of complex dynamic viscosity, η^* (□△o) and apparent viscosity, η (* + x) as a function of angular frequency (rad/s) and shear rate (1/s) for 1.1% w/v Na-LT100 (+ □), 0.6% w/v Na-31461 (* △) solution in water and 1% w/v xanthan (x o) in 0.5M NaCl solution at 20°C.

The Cox-Merz plot for xanthan shows that η^* values, obtained by low amplitude oscillatory measurements, were higher than the values of steady-shear viscosity (η) obtained by steady flow measurements. The deviation from Cox-Merz rule suggests that the polymer chains do not interact solely by topological entanglements (Cox & Merz 1958). Instead, Cox-Merz violation can be attributed to specific interactions among chain segments, such as hydrogen bonds (Eteshola, Karpasas, Arad & Gottlieb, 1998; Pal, 1995; Richardson & Ross-Murphy, 1987; Yamakawa & Yoshizaki, 1980), in addition to topological constraints caused by the stiff molecular conformation. The intermolecular interactions were not disrupted by low amplitude oscillatory strains in the linear viscoelastic region. However, intermolecular interactions were reversibly disrupted above the critical shear rates during steady-shear viscosity measurement.

For both Na-LT100 and Na-31461, superposition of $\eta^*(\omega)$ and $\eta(\dot{\gamma})$ curves occurred only at low frequencies and low shear rates because interactions between chain segments were not disrupted by low amplitude oscillatory strains nor in the zero-shear viscosity region, respectively. However, at high frequencies and high shear rates, the curves deviate from each other ($\eta^*(\omega) > \eta(\dot{\gamma})$), probably due to the disruption of interactions between chain segments apart from topological constraints. Therefore, under small deformation, a weak gel structure was apparent but under large-deformation, the weak gel structure was temporarily disrupted. The indication of intermolecular interactions in both Na-gellan samples based on Cox-Merz plot is consistent with the rheological and light scattering results discussed earlier.

7.3.8 Proposed model for the conformational changes of sodium gellan molecules

From the rheological and light scattering data obtained in this study, it appears that Na-LT100 molecules adopted the conformation of a random flexible chain (exponent value based on the Cross-type model ~0.76; M_w ~2.7x10^5 Da) and its mechanical spectra obtained by oscillatory measurements (G' & G'') demonstrated the characteristic of a typical viscous solution (Fig 7.25a). On the other hand, the Na-31461 molecule was found to adopt a stiffer conformation (exponent value based on the Cross-type model ~0.82) with M_w (~5.2x10^5 Da) approximately twice that of Na-LT100 molecules, implying a double-stranded molecule. The mechanical spectra of Na-31461 solution demonstrated the characteristic of a weak gel.

However, from the plot of the complex modulus versus Na^+ concentration (Fig 7.26), it is apparent that both Na-LT100 and Na-31461 curves closely superimposed, suggesting that the different characteristics of the two Na-gellan samples were due to differences in the Na^+ concentrations. The following describes the proposed model for the conformational changes of Na-gellan molecules in different Na^+ concentrations:

At low Na^+ concentrations (~19Mm or ~4.5% w/w), the flow properties of the Na-gellan were typical of random coil polymers. The M_w obtained (for Na-LT100), which was approximately half that of Na-31461, could imply that Na-LT100 molecules were

single-stranded molecules. Figure 7.30a illustrates the proposed conformation of single flexible, random Na-gellan molecules. As the Na^+ concentration was increased slightly (~19-24mM or ~4.5%-5.6% w/w), the flow properties were characteristic of a polymer solution where the molecules adopt semi-stiff conformations. The increase in the stiffness of Na-gellan molecules was proposed to be due to the formation of double-stranded helices (disordered to ordered transition), as the electrostatic repulsions among molecules were screened by an increase in NaCl concentration (Figure 7.30b). A further increase in the Na^+ concentration (>24.3mM) led to formation of a gel network. The formation of a gel could be explained by a further increase in electrostatic screening effects such that the overall charge density is significantly reduced. This promotes the association of the double-stranded molecules mainly due to carboxylate-Na^+-water-Na^+-carboxylate interactions (Chandrasekaran & Radha, 1995). The interactions will eventually lead to the formation of a three dimensional gel network at sufficiently high polymer concentrations. Morris, Richardson & Whittaker (1999) suggested the association of double-helices in the gel network, which causes the formation of a large number of heterogeneous clusters, and a resulting increase in gel strength. The increase in gel strength with increasing concentration of salt was clearly shown by the results obtained in this study. Figure 7.30c illustrates the association of the double-helices forming a three-dimensional gel network.

It is also interesting to note that under zero-shear condition, the Na-gellan molecules under the conditions shown in Figures 7.30a and 7.30b, both single-stranded and double stranded molecules have the tendency to form aggregates, although the type and extent of aggregation may differ. The aggregates of single-stranded molecules had higher M_w (~3.5x10^6 Da) but were smaller in size ($[\eta]$~2360mL/g; $\left(r_g^2\right)_z^2$~63-75nm) as compared to the aggregates formed from the double-stranded molecules (M_w ~2.3x10^6 Da; $[\eta]$~3953mL/g; $\left(r_g^2\right)_z^2$~151nm). The formation of aggregates could contribute to the high gradient values obtained in the concentrated domains ($\eta_{spo} \propto c^{5-6}$) The intermolecular interactions among the single-stranded and double-stranded chains were considered weak and transient based on the light scattering data and Cox-Merz plot. However, of the two Na-gellan samples, the intermolecular interaction between the

double-stranded aggregates also appeared to be weaker than that of the single-stranded aggregates as indicated by the difference in the Cox Merz plot (where the deviation between η^* and η was greater in double-stranded Na-31461 solution as compared to the single-stranded Na-LT100 solution). This is consistent with the light scattering data which showed that filtering the double-stranded Na-31461 solution immediately prior to analysis was sufficient to disrupt the aggregates.

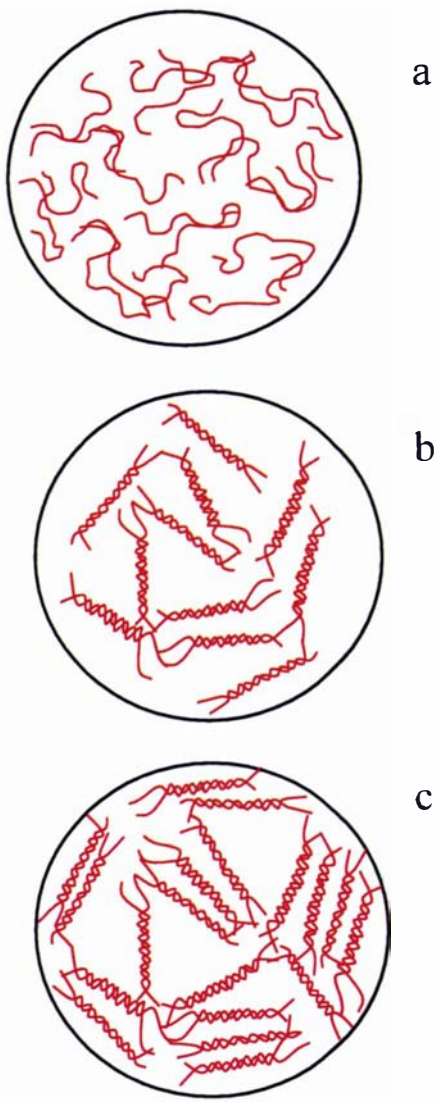

Figure 7.30 Diagrammatic representation of gel formation by gellan macromolecules with increasing Na^+ concentrations. (a) Na-gellan as single-stranded molecules at low Na^+ concentration (<19mM) as in Na-LT100 in water; (b) Na-gellan formed double-stranded molecules with a slight increase in Na^+ concentration (~20-24mM) as in Na-31461 in water (c) Association of double-stranded molecules with the formation of a gel at Na^+ concentration >24mM.

The aggregation of the single-stranded gellan molecules as micro-aggregates (instead of single chains) have been reported by Dentini et al. (1988). However, aggregation of double-stranded Na-gellan has not been reported before. The exact mechanism of the aggregation of double-stranded gellan molecules under the existing ionic condition is currently unknown and may be trigged by non-specific interactions. The overall results of the present study on both Na-LT100 and Na-31461 gellan showed that the conformation and rheological properties of Na-gellan were highly dependent on the concentration of Na^+.

7.4 CONCLUSIONS

The gellan produced by *Sphingomonas elodea* ATCC 31461 grown in a milk permeate-based medium was isolated. Along with a commercial high acyl gellan, both gellan samples were purified and converted to Na-gellan using cation ion exchange resins. The purified gellan samples (Na-LT100 and Na-31461) dispersed in water had slightly different Na^+ concentrations based on their ash contents. The Na-gellan solutions were then characterised using static light scattering and rheological measurements.

From the light scattering and rheological measurements, it was found that the conformation of Na-gellan molecules was dependent on the Na^+ concentrations. At Na^+ concentrations (<19mM) as was in the case of Na-LT100, the Na-gellan molecules were single-stranded and adopted random coil conformation (M_w ~2.5 x 10^5 Da , exponent value based on the Cross-type model ~0.76). The single-stranded Na-gellan molecules became double-stranded at slightly higher Na^+ concentrations (~19-24mM) as also observed in the Na-31461 gellan. The double-stranded molecules had a M_w ~5.2 x 10^5 Da and adopted a stiffer conformation (exponent value based on the Cross-type model ~0.82). The double-stranded conformation was shown by weak gel characteristics based on the mechanical spectra (G', G'') of dynamic viscosity plot. A further increase the Na^+ concentration (>24mM) resulted in a strong and elastic gel. The formation of a three-dimensional network could be explained by strong double-helix associations through the formation of water-bridges between the sodium ion bound to the carboxyl group on each gellan molecule.

When Na-gellan molecules occurred either as single-stranded or double-stranded molecules at low Na^+ concentration (<24mM), the molecules had a tendency to form aggregates. The aggregates formed by the single chain molecules appeared to be more compact (stronger interactions) as shown by the higher molar mass and smaller size ($\left(r_g^2\right)^{1/2}$, $[\eta]$) than those formed by the double-stranded molecules. The formation of aggregates was considered to contribute to the high gradient values obtained in the concentrated domains ($\eta_{spo} \propto c^{5-6}$) in both gellan samples. However, the interactions of

the molecules forming the aggregates appeared to be weak and transient according to the Cox-Merz plot and the light scattering data with Na-LT100 showing stronger intermolecular interactions than the Na-31461 molecules.

For xanthan solutions, the rheological measurements were rather different from that of Na-gellan. Stiff conformations of xanthan molecules were verified in this study as indicated by the strong shear-thinning behaviour with the exponent value of the Cross-type model of ~8.9 and a relatively low Smidsrod Parameter B giving a value of 0.013. Xanthan molecules did not form true gels in the presence of added salt but the mechanical spectra demonstrated 'weak gel' characteristics. In the dilute domain, the addition of salt caused a decrease in zero-shear viscosity due to a reduction in hydrodynamic volume as indicated by the decrease in intrinsic viscosities. However, in the concentrated domain, the zero-shear viscosity of xanthan solution was enhanced by salt addition. The concentration dependence of zero-shear viscosity exponent showed a linear increase with salt concentration. This could be explained by interactions among chain segments as demonstrated by the violation of the Cox-Merz rule.

Chapter 8

OVERALL CONCLUSIONS AND RECOMMENDATIONS

8.1 OVERALL CONCLUSIONS

The research set out to study the physico-chemical characteristics of two EPSs produced by *Lactobacillus delbrueckii* subsp. *bulgaricus* NCFB 2483 and *Sphingomonas elodea* ATCC 31461. In both instances, the EPSs were produced by fermentation using milk permeate as a base medium. A large part of this research focused on the EPS produced by *Lactobacillus delbrueckii* subsp. *bulgaricus* NCFB 2483. This included microscopy examination of EPS *in situ*; improvement of EPS assay; isolation and purification of EPS; and physico-chemical characterisation of 2483 using viscometric and static light scattering techniques. In the case of the fermented culture of *Sphingomnas elodea* ATCC 31461, the EPS was isolated and purified. Together with a commercial high-acyl gellan, the two polysaccharides were studied using rheological and light scattering techniques. Other commercial polysaccharides, which included dextran, λ-carrageenan, and xanthan, were also included in the studies for comparative purposes.

The examination of 2483 EPS in culture media was successfully accomplished using CLSM in combination with SBA lectin Alexa Fluor conjugate as the fluorescent stain. The SBA lectin Alexa Fluor conjugate was selected on the basis of its specificity for galactopyranosyl residues which are present in EPSs produced by many LAB strains. The 2483 EPS appeared randomly distributed as aggregates in milk permeate-based media. The use of CLSM provided an excellent view of the location of EPS *in situ* at magnifications typical of light microscopes. The technique involved minimal sample preparation, and hence avoided the introduction of possible artefacts which could interfere with image interpretation. At high magnifications using SEM, the EPS aggregates appeared as web structures. In the fermented milk system, EPS filled the interstices and channels of the protein aggregates. The web EPS structures seen in the SEM micrographs were due to concentration of EPS during the critical drying process. From both CLSM and SEM micrographs, it was observed that the 2483 EPS aggregates remained intact at neutral or low pH (~3.9). However, the 2483 EPS was highly

susceptible to alkaline pH conditions. Increasing the pH from 8 to 10 disrupted the EPS structure and caused a loss in its 'ropy' characteristics. The examination of EPS using TEM was unsuccessful despite the use of electron dense ruthenium red to stain the EPS to increase image contrast. The sample preparation procedures used were probably either too harsh, disrupting the EPS aggregates or the ruthenium red did not effectively stain the EPS.

Many EPS assay procedures reported to date do not adequately consider the interference from non-EPS components present, which can make the analysis inaccurate and non-reproducible. In the development of an improved EPS assay, each of the processing steps was examined so that the EPS component could be isolated and quantified with greater accuracy. Improvements include hydrolysing the milk proteins using Flavourzyme; using 70% ethanol for optimum EPS precipitation so as to allow the lactose present to remain soluble; implementing an optimum centrifugation regime at 27,000*g* for 40 min at 4°C for effective isolation of precipitated EPS; and using a small sample volume of 0.1mL so that total sugar determination by phenol-sulphuric acid method could be performed rapidly without further sample dilution. These revised procedures yielded reproducible results (5% coefficient of variation) with improved accuracy.

The isolation of 2483 EPS from milk-based media was found to be difficult because of interference from the coagulated proteins. Heating the culture medium or subjecting the medium to alkaline conditions (pH $\geq$ 8) were found to be detrimental to the EPS. An effective method which provided greater ease in isolating the EPS was developed. This method involved using a protein hydrolysed milk medium, which was ultrafiltered to remove molecular species larger than 2.5 x 10^5 Da. This growth medium was found to be a suitable for the bacteria producing ~400mg/L EPS. The EPS produced was easily isolated. This was achieved by removing the bacterial cells followed by the precipitation of EPS using ethanol. The use of the ultrafiltered hydrolysed milk medium allowed maximum recovery of EPS from the culture medium and could be adapted for industrial scale-up operation. The recovered EPS contained a soluble and an insoluble fraction. The soluble fraction was purified using a series of ethanol precipitations to achieve a relatively pure fraction (~98%). Elemental analysis showed that the soluble

EPS fraction comprised of 39.1%, 6.2%, 50.3% and 2.8% of carbon, hydrogen, oxygen and nitrogen respectively. The presence of nitrogen could be due to the interaction of some peptides with the EPS. The polysaccharide fraction comprised of galactose, glucose, rhamnose and mannose residues in the ratio of approximately 5:1:0.6:0.5. Traces of glucosamine were also found in the fraction.

Physical characterisation of the purified 2483 EPS was carried out using light scattering and viscometric techniques. From the static light scattering data, the M_w and $(r_g^2)_z^{1/2}$ of 2483 EPS were ~2 x 10^6 Da and 165nm respectively. The 2483 EPS had an unusually low polydispersity (M_w/M_n ~1.15). The flow properties of 2483 EPS solutions were consistent with a neutral non-gelling polysaccharide with shear-thinning behaviour and an intrinsic viscosity of ~2013 mL/g. Both the shear rate dependence of viscosity curve (which reflected an exponent value based on the Cross-type model of 0.76) and the concentration dependence of viscosity plot (with gradients of ~1 and ~3.3 in the dilute and semi-dilute to concentrated domains respectively), suggested that the 2483 EPS behaved like typical random flexible coil polymers such as dextran and λ-carrageenan. The graph of $(r_g^2)_z^{1/2}$ versus M_w, which showed a gradient of ~0.5 also suggested a random coil conformation adopted by the 2483 EPS.

The second part of the thesis involved studies on gellan gum (a GRAS-listed gelling EPS). The EPS was obtained from the aerobic fermentation of *Sphingomonas elodea* ATCC 31461 using a milk permeate-based medium. The EPS was isolated and along with a commercial high-acyl gellan, were converted to Na-gellan using cation exchange resins. Both Na-gellan samples (Na-31461 and Na-LT100) were purified to ~96% purity (based on the total sugar content) using centrifugation and ethanol precipitations. The two Na-gellan samples, which remained as viscous solutions allowed viscometric and static light scattering measurements to be carried out at ambient temperature. The purified Na-LT100 solution had a lower Na^+ concentration (~19mM) than Na-31461 solution (~24mM). It was observed that increasing salt concentration would cause the solutions to form gels. Based on the results of oscillatory measurements, it was found that the complex moduli of Na-LT100 and Na-31461 superimposed closely at all Na^+

concentrations. The results suggest that both Na-gellan samples possess similar viscoelastic properties which are highly dependent on Na^+ concentration. A model for the conformational changes of Na-gellan molecules from solution to gel is proposed. At very low Na^+ concentrations (<19mM, in the case of Na-LT100), the Na-gellan molecules are single-stranded and adopt a random coil conformation. This is indicated by the exponent value based on the Cross-type model of ~0.76 and a M_w ~2.5 x 10^5 Da. The single-stranded Na-gellan molecules change from a disordered to an ordered conformation at slightly higher Na^+ concentrations (~19-24mM) as observed in the Na-31461 gellan. This leads to an approximately two-fold increase in M_w ~5.2 x 10^5 Da. The double-stranded molecule appears to be stiffer than its single-stranded counterpart as indicated by the higher exponent value of the Cross-type model (0.82). The ordered conformation shows 'weak gel' characteristics based on the mechanical spectra (G', G'') of dynamic viscosity plot. A further increase the Na^+ concentration (>24mM) results in the formation of a gel network. When Na-gellan molecules occur either as single-stranded or double-stranded molecules at low Na^+ concentration (<24mM), the molecules have a tendency to form aggregates. The aggregates formed by the single chain molecules are more compact (stronger interactions) as shown by the higher molar mass (~3.5x10^6 Da vs 2.3x10^6 Da) and smaller size ($\left(r_g^2\right)_z^{1/2}$ ~75nm vs ~151nm; $[\eta]$~2360mL/g vs ~3950mL/g), than those formed by the double-stranded molecules. The interactions of the molecules forming the aggregates in both cases are considered weak and transient although Na-LT100 shows stronger intermolecular interactions than the Na-31461 molecules, according to the Cox-Merz plot and the light scattering data.

For xanthan solutions, the rheological data differ from that of Na-gellan. The stiff conformation of xanthan molecules is indicated by the strong shear-thinning behaviour, with the exponent value of the Cross-type model (~8.9) and a relatively low Smidsrod Parameter B (~0.013). Xanthan molecules do not form a true gel in the presence of added salt but the mechanical spectra demonstrate 'weak gel' characteristics. In the dilute domain, the addition of salt causes a decrease in zero-shear viscosity due to a reduction in hydrodynamic volume as indicated by the decrease in intrinsic viscosities. However, in the concentrated domain, the zero-shear viscosity of xanthan solution is enhanced by salt addition. The exponent values of the concentration dependence of

zero-shear viscosity show a linear increase with salt concentration. This can be explained by interactions among chain segments demonstrated by the violation of the Cox-Merz rule.

From the work presented in this thesis, it is evident that the conformations adopted by the individual polysaccharide molecules, the intermolecular interactions involved, and the solvent conditions have major influences on the physico-chemical properties of a polysaccharide system. The conformation adopted by polysaccharide molecules and their interactions are in turn dependent on the primary sequence structure and the presence or absence of charged groups. Polysaccharides from different sources possess diverse molecular structures, and can be expected to possess unique physico-chemical properties. In food systems, novel polysaccharides will continue to play a major role in imparting useful functional properties and modifying the sensory characteristics to meet changes in consumer demand. An effective avenue for obtaining novel polysaccharides with unique characteristics is via microbial fermentation under controlled conditions. The methodologies developed in this work can be applied to the examination, quantification, isolation, purification and characterisation of a diverse range of polysaccharides from various sources. The concept of using an untrafiltered hydrolysed milk medium rather than a semi-defined medium in LAB fermentation is novel but simple. This approach not only provides a good nutrient source for LAB fermentation (hence, higher EPS), but also allows rapid and effective isolation of the EPS. Researchers in LAB EPS are likely to favour this approach if their objective is to isolate the EPS for further work.

A significant outcome arising from this research is that the milk permeate proved to be a useful medium for bacterial fermentation producing gellan gum and 2483 EPS. It could potentially be extended to other microbial fermentations to obtain other polysaccharides. Milk permeate is currently treated as a waste stream in the dairy industry, and in New Zealand, often disposed of by irrigation in the paddocks where the dairy cows graze. The utilisation of the milk permeate as a base medium will not only reduce environmental pollutions but will also add value to the dairy industry. At present, the isolation of LAB EPSs is hindered mainly by the low yield, making production uneconomical. If this issue can be resolved, great opportunity awaits the

application of EPS in food systems. It is envisaged that high EPS producing strains of LAB will be isolated and used to produce a new generation of polysaccharides which can deliver desired sensory attributes, improved functionality in food products and enhance human health.

The importance of polysaccharides in human nutrition has escaped the attention of health professionals. With a greater understanding and awareness of glycemic loading in foods, polysaccharide may be due to take its place as an important functional component. Novel EPS such as those from LAB can be safely incorporated in diets to reduce calorie intake and improve satiety if resistance to the digestive enzymes is validated. These polysaccharides may then possibly function as prebiotics to improve gut health; act as soluble fibres, or influence the rate of absorption of food containing large quantities of digestible carbohydrates.

With the gellan polysaccharide, understanding the conformational changes of the Na-gellan molecules means that the sol-gel transition of Na-gellan can be controlled by manipulating salt concentration at ambient temperature. Although a similar system exists for alginate where gels are formed in the presence of calcium chloride, the Na-gellan gels are likely to demonstrate different textural and viscoelastic properties. Controlled gelation of Na-gellan may be used for the microencapsulation of unstable materials including flavours, micronutrients, probiotic bacteria, etc, to facilitate effective delivery of ingredients including nutriceuticals to consumers.

8.2 RECOMMENDATIONS

The recommendations for further research on 2483 EPS are as follows:

- Interactions of EPS with milk proteins

  In this research, the culture medium was observed to be much thicker than the purified EPS solutions, indicating some interactions between the EPS and the milk proteins. Such interaction of EPS with proteins is poorly understood. Investigation of how EPS influences the functional properties of acidified and non-acidified milk systems would lead to new applications in food systems.

- Structures and synergistic effects with other polysaccharides

Bacterial polysaccharides are diverse in their molecular structures, but the relationship between structure and functionality is not completely understood. Modification of the EPS structure may uncover other useful functional properties in foods. Another area that remains to be explored is the determination of synergistic effects of the EPS with other polysaccharides.

- Biological activity and health

As polysaccharides are diverse in structure, EPSs from LAB have great potential in the area of nutriceuticals. Some recent studies have indicated that the EPSs produced by certain strains possess antitumour activity. This research is in its infancy and merits further investigation.

- Applications of EPS in food systems

Applications of EPS, whether *in situ* or in purified form to improve sensory and functional attributes, have not been thoroughly explored in different food systems. Some examples include the reduction of syneresis in yoghurt; reducing meltdown in ice cream; increasing moisture retention in bread; and replacing milk solids in dairy beverages, etc. The effects of EPS in sourdough fermentation has recently been investigated (Tieking, Korakli, Ehrmann, Ganzle, & Vogel, 2003).

Recommendations for further study on gellan include:

- Properties characteristic of Na-gellan gels

The chemical and physical characteristics of Na-gellan gels are currently not well established. These include gel porosity, melting temperature, water-holding capacity, sensory attributes, etc. The ability to control the gelation at ambient temperature is a unique attribute of Na-gellan. Understanding the properties of Na-gellan gels will enable researchers to maximise its usage in food and non-food applications.

- Interaction of Na-gellan molecules with other polysaccharides

Disordered Na-gellan molecules can be used in conjunction with other polysaccharide molecules and may achieve unique viscoelastic properties. This synergistic interaction between polysaccharide systems has not been explored and may provide new opportunities to engineer gels with unique properties.

REFERENCES

Abbad-Andaloussi, S., Talbaoui, H., Marczak, R., & Bonaly, R. (1995). Isolation and characterization of exocellular polysaccharides produced by *Bifidobacterium longum*. *Applied Microbiology & Biotechnology, 43*(6), 995-1000.

Akutu, M., Kubota, K., & Nakamura, K. (1999). Light scattering, sound velocity and viscoelastic behavior of aqueous gellan solutions. *Progress in Colloid & Polymer Science, 114*, 56-61.

Allan-Wojtas, P., & Kalab, M. (1984a). Milk gel structure. XIV. Fixation of fat globules in whole milk yoghurt for electron microscopy. *Milchwissenschaft, 39*, 323-327.

Allan-Wojtas, P., & Kalab, M. (1984b). A simple procedure for the preparation of stirred yoghurt for SEM. *Food Microstructure, 3*, 197-198.

Anthonsen, M. W., Varum, K. M., Hermansson, A. M., Smidsrod, O., & Brant, D. A. (1994). Aggregates in acidic solutions of chitosans detected by static laser light scattering. *Carbohydrate Polymers, 25*(1), 13-23.

Arendt, O., & Kulicke, W. M. (1998). Determination of the viscoelastic properties of a homologous series of the fermentation polymer xanthan gum. *Angewandte Makromolekulare Chemie, 259*, 61-67.

Ariga, H., Urashima, T., Michihata, E., Ito, M., Morizono, N., Kimura, T., et al. (1992). Extracellular polysaccharide from encapsulated *Streptococcus salivarius* subsp *thermophilus* OR-901 isolated from commercial yogurt. *Journal of Food Science, 57*(3), 625-628.

Azeredo, J., & Oliveira, R. (1996). A new method for precipitating bacterial exopolysaccharides. *Biotechnology Techniques, 10*(5), 341-344.

Baird, J. K., & Smith, W. W. (1989). An analytical procedure for gellan gum in food gels. *Food Hydrocolloids, 3*(5), 407-411.

Bergmaier, D., Champagne, C. P., & Lacroix, C. (2003). Exopolysaccharide production during batch cultures with free and immobilized *Lactobacillus rhamnosus* RW-9595M. *Journal of Applied Microbiology, 95*(5), 1049-1057.

Berry, G. C. (1966). Thermodynamic and conformational properties of polystrrene 1. Light-scattering studies on dilute solutions of linear polystyrenes. *Journal of Chemical Physics, 44*, 4550-4564.

Bohdanecky, M., & Kovar, J. (1982). *Viscosity of polymer solutions.* The Netherlands: Elsevier Scientific Publishing Company.

Bottazzi, V., & Bianchi, F. (1986). Types of microcolonies of lactic acid bacteria, formation of void spaces and polysaccharides in yoghurt. *Scienza E Tecnica Lattiero Casearia, 37*(4), 297-315.

Bouzar, F., Cerning, J., & Desmazeaud, M. (1996). Exopolysaccharide production in milk by *Lactobacillus delbrueckii* ssp. *bulgaricus* CNRZ 1187 and by two colonial variants. *Journal of Dairy Science, 79*(2), 205-211.

Brant, D. A. (1999). Novel approaches to the analysis of polysaccharide structures. *Current Opinion in Structural Biology, 9*(5), 556-562.

Broadbent, J. R., McMahon, D. J., Welker, D. L., Oberg, C. J., & Moineau, S. (2003). Biochemistry, genetics, and applications of exopolysaccharide production in *Streptococcus thermophilus*: A review. *Journal of Dairy Science, 86*(2), 407-423.

Brooker, B. E. (1976). Cytochemical observations on the extracellular carbohydrate produced by *Streptococcus cremoris*. *Journal of Dairy Research, 43*, 283-290.

Brooker, B. E. (1979). Electron microscopy of the dextrans produced by lactic acid bacteria. In R. C. W. Berkeley, Gooday, G.W., and Ellwood, D.C. (Ed.), *Microbial polysaccharides and polysaccharases* (pp. 85-115). London: Academic Press.

Brooker, B. E. (1995). Imaging food systems by confocal laser scanning microscopy. In E. Dickson (Ed.), *New physico-chemical techniques for the characterization of complex food systems*. (pp. 53-68). United Kingdom: Blackie Academic & Professional.

Brown, M. J., & Lester, J. N. (1980). Comparison of bacterial extracellular polymer extraction methods. *Applied & Environmental Microbiology, 40*, 179-185.

Brownsey, G. J., Chilvers, G. R., Anson, K. I., & Morris, V. J. (1984). Some observations or problems on the characterization of gellan gum solutions. *International Journal of Biological Macromolecules, 6*(4), 211-214.

Bubb, W. A., Urashima, T., Fujiwara, R., Shinnai, T., & Ariga, H. (1997). Structural characterisation of the exocellular polysaccharide produced by *Streptococcus thermophilus* OR 901. *Carbohydrate Research, 301*(1-2), 41-50.

Buchheim, W. (1982). Aspects of sample preparation for freeze fracture/ freeze-etch studies of proteins and lipids in food systems. A review. *Food Microstructure, 1*, 189-208.

Bueche, F. (1962). *Physical properties of polymers*. New York: Interscience.

Bueche, F., & Harding , S. W. (1958). A new absolute molecular weight method for linear polymers. *Journal of Polymer Science, XXXII*, 177-186.

Burchard, W. (1994a). Light scattering techniques. In S. B. Ross-Murphy (Ed.), *Physical techniques for the study of food biopolymers* (pp. 151-213). United Kingdom: Chapman & Hall.

Burchard, W. (1994b). Light-Scattering-Studies on Polysaccharide Solutions. *Papier, 48*(12), 755-764.

Cagle, G. D. (1975). Fine structure and distribution of extracellular polymer surrounding selected aerobic bacteria. *Canadian Journal of Microbiology, 21*, 395-408.

Capron, I., Grisel, M., & Muller, G. (1995). On-line size exclusion chromatograohy and multiangle laser light scattering of high-molecular-weight rigid polysaccharides. *International Journal of Polymer Analysios and Characterization, 2*, 9-20.

Carreau, P. J. (1972). Rheological equations from molecular network theories. *Transactions of the Society of Rheology, 16*(1), 99-127.

Cerning, J. , & Marshall, V. M. (1999). Exopolysaccharides produced by the dairy lactic acid bacteria. *Recent Research Developments in Microbiology, 3*(1), 195-209.

Cerning, J. (1990). Exocellular polysaccharides produced by lactic acid bacteria. *FEMS microbiology reviews, 7*(1-2), 113-130.

Cerning, J. (1995). Production of exopolysaccharides by lactic acid bacteria and dairy propionibacteria. *Lait, 75*(4/5), 463-472.

Cerning, J., Bouillanne, C., Desmazeaud, M. J., & Landon, M. (1986). Isolation and characterization of exocellular polysaccharide produced by *Lactobacillus bulgaricus*. *Biotechnology Letters, 8*(9), 625-628.

Cerning, J., Bouillanne, C., Desmazeaud, M. J., & Landon, M. (1988). Exocellular polysaccharide production by *Streptococcus thermophilus*. *Biotechnology Letters, 10*(4), 255-260.

Cerning, J., Bouillanne, C., Landon, M., & Desmazeaud, M. (1992). Isolation and characterization of exopolysaccharides from slime-forming mesophilic lactic acid bacteria. *Journal of Dairy Science, 75*(3), 692-699.

Cerning, J., Renard, C. M. G. C., Thibault, J. F., Bouillanne, C., Landon, M., Desmazeaud, M., et al. (1994). Carbon source requirements for exopolysaccharide production by *Lactobacillus casei* CG11 and partial structure analysis of the polymer. *Applied & Environmental Microbiology, 60*(11), 3914-3919.

Cesaro, A. (1994). The role of conformation on the thermodynamics and rheology of aqueous solutions of carbohydrate polymers. *Journal of Food Engineering, 22*(1-4), 27-42.

Chandrasekaran, R., & Radha, A. (1995). Molecular architectures and functional properties of gellan gum and related polysaccharides. *Trends in Food Science & Technology, 6*(5), 143-148.

Chandrasekaran, R., Radha, A., & Giacometti, A. (1995). Molecular modeling of substituted polysaccharides. *Carbohydrate Polymers, 28*(1), 49-59.

Chanliaud, E., Roger, P., Saulnier, L., & Thibault, J. F. (1996). Static and dynamic light scattering studies of heteroxylans from maize bran in aqueous solution. *Carbohydrate Polymers, 31*(1-2), 41-46.

Chapman, H. D., Morris, V. J., Selvendran, R. R., & O'Neill, M. A. (1987). Static and dynamic light scattering studies of pectic polysaccharides from the middle lamellae and primary cell walls of cider apples. *Carbohydrate Research, 165*(1), 53-68.

Christensen, B. E., & Characklis, W. G. (1990). *Physical and chemical properties of biofilms.* New York: Wiley.

Chronakis, I. S., Doublier, J. L., & Piculell, L. (2000). Viscoelastic properties for kappa- and iota-carrageenan in aqueous NaI from the liquid-like to the solid-like behaviour. *International Journal of Biological Macromolecules, 28*(1), 1-14.

Clark, A. H., & Farrer, D. B. (1995). Kinetics of biopolymer gelation - Implications of a cascade theory description for the concentration, molecular-weight, and temperature dependences of the shear modulus and gel time. *Journal of Rheology, 39*(6), 1429-1444.

Corstvet, R. E., Gentry, M. J., Newman, P. R., Confer, A. W., & Rummage, J. A. (1982). Demonstration of age-dependent capsular material on *Pasteurella haemolytica* serotype 1. *Journal of Clinical Microbiology, 16*(6), 1123-1126.

Cox , W. P., & Merz , E. H. (1958). Correlation of dynamic and steady flow viscosities. *Journal of Polymer Science., 28*, 619-622.

Crescenzi, V. (1995). Microbial polysaccharides of applied interest: ongoing research activities in Europe. *Biotechnology Progress, 11*(3), 251-259.

Cross, M. M. (1965). Rheology of non-Newtonain fluids: A new flow equation for pseudoplastic systems. *Journal of Colloid Science, 20*, 417-437.

Cuvelier, G., & Launay, B. (1986). Concentration regimes in xanthan gum solutions deduced from flow and viscoelastic properties. *Carbohydrate Polymers, 6*(5), 321-333.

De Gennes, P. G. (1971). Reptation of a polymer chain in the presence of fixed obstacles. *Journal of Chemical Physics, 55*(2), 572-579.

De Gennes, P. G. (1976). Dynamics of entangled polymer solutions. II. Inclusion of hydrodynamic interactions. *Macromolecules, 9*, 594-598.

De Gennes, P. G. (1979). *Scaling concepts in polymer physics.* Ithaca, New York: Cornell University Press.

De Gennes, P. G. (1983). Entangled polymers. *Physics Today, 6*, 33-39.

De Vuyst, L., De Vin, F., Vaningelgem, F., & Degeest, B. (2001). Recent developments in the biosynthesis and applications of heteropolysaccharides from lactic acid bacteria. *International Dairy Journal, 11*(9), 687-707.

De Vuyst, L., & Degeest, B. (1999a). Exopolysaccharides from lactic acid bacteria: Technological bottlenecks and practical solutions. *Macromolecular Symposia, 140*, 31-41.

De Vuyst, L., & Degeest, B. (1999b). Heteropolysaccharides from lactic acid bacteria [Review]. *FEMS Microbiology Reviews, 23*(2), 153-177.

De Vuyst, L., Vanderveken, F., Van de Ven, S., & Degeest, B. (1998). Production by and isolation exopolysaccharides from *Streptococcus thermophilus* grown in a milk medium and evidence for their growth-associated biosynthesis. *Journal of Applied Microbiology, 84*(6), 1059-1068.

Dea, I. C. M. (1993). Conformational origins of polysaccharide solution and gel properties. In R. L. Whistler & J. N. BeMiller (Eds.), *Industrial gums: Polysaccharides & their derevitives* (pp. 21-52). San Diego: Academic Press, Inc.

Debye, P. (1947). Molecular-weight determination by light scattering. *Journal of physical colloidal chemistry, 51*, 18-32.

Debye, P., & Bueche, A. M. (1948). Intrinsic viscosity, diffusion, and sedimentation rate of polymers in solution. *The Journal of Chemical Physics, 16*(6), 573-579.

Degeest, B., Mozzi, F., & De Vuyst, L. (2002). Effect of medium composition and temperature and pH changes on exopolysaccharide yields and stability during *Streptococcus thermophilus* LY03 fermentations. *International Journal of Food Microbiology, 79*(3), 161-174.

Degeest, B., & De Vuyst, L. (1999). Indication that the nitrogen source influences both amount and size of exopolysaccharides produced by *Streptococcus thermophilus* LY03 and modelling of the bacterial growth and exopolysaccharide production in a complex medium. *Applied & Environmental Microbiology, 65*(7), 2863-2870.

Degeest, B., Janssens, B., & De Vuyst, L. (2001). Exopolysaccharide (Eps) biosynthesis by *Lactobacillus sakei* 0-1: Production kinetics, enzyme activities and Eps yields. *Journal of Applied Microbiology, 91*(3), 470-477.

Dentini, M., Coviello, T., Burchard, W., & Crescenzi, V. (1988). Solution properties of exocellular microbial polysaccharides .3. Light-scattering from gellan and from the exocellular polysaccharide of *Rhizobium trifolii* (strain-TA-1) in the ordered state. *Macromolecules, 21*(11), 3312-3320.

Deveau, H., Van Calsteren, M. R., & Moineau, S. (2002). Effect of exopolysaccharides on phage-host interactions in *Lactococcus lactis. Applied and Environmental Microbiology, 68*(9), 4364-4369.

Ding, Q., Jiang, S., Zhang, L., & Wu, C. (1998). Laser light-scattering studies of pachyman. *Carbohydrate Research, 308*(3-4), 339-343.

Doco, T., Carcano, D., Ramos, P., Loones, A., & Fournet, B. (1991). Rapid isolation and estimation of polysaccharide from fermented skim milk with *Streptococcus salivarius* subsp. *thermophilus* by coupled anion exchange and gel-permeation high-performance liquid chromatography. *Journal of Dairy Research, 58*(1), 147-150.

Doco, T., Wieruszeski, J. M., & Fournet, B. (1990). Structure of an exocellular polysaccharide produced by *Streptococcus thermophilus. Carbohydrate Research, 198*(2), 313-322.

Dollinger,G, Cunico, B., Krunitani, M., Johnson, M., & Jones, R. (1992). Practical online determination of biopolymer molecular weights by high-performance liquid chromatography with classical light-scattering detection. *Journal of Chromatography, 592*, 215-228.

Doublier, J. L., & Cuvelier, G. (1996). Gums and hydrocolloids: functional aspects. In A. C. Eliasson (Ed.), *Carbohydrates in food.* (pp. 283-318). United States of America: Marcel Dekker, Inc.

Doublier, J. L., & Launay, B. (1981). Rheology of galactomannan solutions - comparative-study of guar gum and locust bean gum. *Journal of Texture Studies, 12*(2), 151-172.

Dreveton, E., Monot, F., Lecourtier, J., Ballerini, D., & Choplin, L. (1996). Influence of fermentation hydrodynamics on gellan gum physico-chemical characteristics. *Journal of Fermentation & Bioengineering, 82*(3), 272-276.

Duboc, P., & Mollet, B. (2001). Applications of exopolysaccharides in the dairy industry. *International Dairy Journal, 11*(9), 759-768.

Dubois, M., Gilles, J. K., Hamilton, P. A., Rebers, P. A., & Smith, F. (1956). Colorimteric method for determination of sugars and related substances. *Analytical Chemistry, 28*(3), 350-356.

Dunican, L. K., & Seeley, H. W. J. (1965). Extracellular polysaccharide synthesis by members of the genus *Lactobacillus:* conditions for formation and accumulation. *Journal of General Microbiology, 40*(3), 297-308.

Dupont, I., Roy, D., & Lapointe, G. (2000). Comparison of exopolysaccharide production by strains of *Lactobacillus rhamnosus* and *Lactobacillus paracasei* grown in chemically defined medium and milk. *Journal of Industrial Microbiology & Biotechnology, 24*(4), 251-255.

Durrani, C. M., & Donald, A. M. (2000). Shape, molecular weight distribution and viscosity of amylopectin in dilute solution. *Carbohydrate Polymers, 41*(2), 207-217.

Easson, D. D. J., Sinskey, A. J., & Peoples, O. P. (1987). Isolation of *Zoogloea ramigera* I-16-m exopolysaccharide biosynthetic genes and evidence for instability within this region. *Journal of Bacteriology, 169*(10), 4518-4524.

Einstein, A. (1906). A new determination of molecular dimensions. *Annalen der Physik, 19*, 271.

Einstein, A. (1911). A correction to my work. A new determination of molecular dimensions. *Annalen der Physik, 34*, 591-592.

Emerson, D., & Ghiorse, W. C. (1993). Role of disulphide bonds in maintaining the structure integrity of the sheath of *Leptothrix discophora* SP-6. *Journal of Bacteriology, 175*, 7819-7827.

Eteshola, E., Karpasas, M., Arad, S., & Gottlieb, M. (1998). Red microalga exopolysaccharides: 2. Study of the rheology, morphology and thermal gelation of aqueous preparations. *Acta Polymerica, 49*(10-11), 549-556.

Evans, J. M. (1972). Manipulation of light scattering data. In M. B. Huglin (Ed.), *Light scattering from polymer solutions* (pp. 89-164). London: Academic Press.

Faber, E. J., Zoon, P., Kamerling, J. P., & Vliegenthart, J. F. G. (1998). The exopolysaccharides produced by *Streptococcus thermophilus* Rs and Sts have the same repeating unit but differ in viscosity of their milk cultures. *Carbohydrate Research, 310*(4), 269-276.

Ferry, J. D. (1980). *Viscoelastic properties of polymers.* (3rd ed.). United States of America: John Wiley & Sons, Inc.

Figueroa, L. A., & Silverstein, J. A. (1989). Ruthenium red adsorption method for measurement of extracellular polysaccharides in sludge flocs. *Biotechnology & Bioengineering, 33*(8), 941-947.

Fishman, M. L., Cescutti, P., Fett, W. F., Osman, S. F., Hoagland, P. D., & Chau, H. K. (1997). Screening the physical properties of novel *Pseudomonas* exopolysaccharides by HPSEC with multi-angle light scattering and viscosity detection. *Carbohydrate Polymers, 32*, 213-221.

Fishman, M. L., Rodriguez, L., & Chau, H. K. (1996). Molar masses and sizes of starches by high-performance size-exclusion chromatography with on-Line multi-angle laser light scattering detection. *Journal of Agricultural and Food Chemistry, 44*(10), 3182-3188.

Fletcher, J. M., Greenfield, B. F., Hardy, C. J., Scargill, D., & Woodhead, J. L. (1961). Ruthenium red. *Journal of Chemical Society, 2*, 2000-2006.

Flory, P. J. (1953). Molecular weight determination. In *Principles of polymer chemistry.* (pp. 266-316). USA: Cornell University Press.

Flory, P. J., & Fox, T. G., Jr. (1951). Treatment of intrinsic viscosities. *Journal of the American Chemical Society, 73*, 1904-1908.

Frolund, B., Palmgren, R., Keiding, K., & Nielsen, P. H. (1996). Extraction of extracellular polymers from activated sludge using a cation exchange resin. *Water Research, 30*, 1749-1758.

Gamar-Nourani, L., Blondeau, K., & Simonet, J. M. (1997). Physiological approach to extracellular polysaccharide production by *Lactobacillus rhamnosus* strain C83. *Journal of Applied Microbiology, 83*(3), 281-287.

Gamar-Nourani, L., Blondeau, K., & Simonet, J. W. (1998). Influence of culture conditions on exopolysaccharide production by *Lactobacillus rhamnosus* strain C83. *Journal of Applied Microbiology, 85*(4), 664-672.

Gancel, F., & Novel, G. (1994). Exopolysaccharide production by *Streptococcus salivarius* ssp *thermophilus* cultures .1. Conditions of production. *Journal of Dairy Science, 77*(3), 685-688.

Garcia-Garibay, M., & Marshall, V. M. E. (1991). Polymer production by *Lactobacillus delbrueckii* ssp *bulgaricus*. *Journal of Applied Bacteriology, 70*(4), 325-328.

Gorret, N., Maubois, J. L., Ghoul, M., & Engasser, J. M. (2001). Exopolysaccharide production by *Propionibacterium acidi-propionici* on milk microfiltrate. *Journal of Applied Microbiology, 90*(5), 779-787.

Gorret, N., Renard, C. M. G. C., Famelart, M. H., Maubois, J. L., & Doublier, J. L. (2003). Rheological characterization of the EPS produced by *P. acidi-propionici* on milk microfiltrate. *Carbohydrate Polymers, 51*(2), 149-158.

Graessley, W. W. (1974). The entanglement concept in polymer rheology. *Advances in Polymer Science, 16*, 1-179.

Graessley, W. W. (1982). Entangled linear, branched and network polymer systems - molecular theories. *Advances in Polymer Science, 47*, 67-117.

Granath, K. A. (1958). Solution properties of branched dextrans. *Journal of Colloid Science, 13*, 308-328.

Grobben, G. J., Chin-Joe, I., Kitzen, V. A., Boels, I. C., Boer, F., Sikkema, J., et al. (1998). Enhancement of exopolysaccharide production by *Lactobacillus delbrueckii* subsp. *bulgaricus* NCFB 2772 with a simplified defined medium. *Applied & Environmental Microbiology, 64*(4), 1333-1337.

Grobben, G. J., Sikkema, J., Smith, M. R., & De Bont, J. A. M. (1995). Production of extracellular polysaccharides by *Lactobacillus delbrueckii* ssp. *bulgaricus* NCFB 2772 grown in a chemically defined medium. *Journal of Applied Bacteriology, 79*(1), 103-107.

Grobben, G. J., Smith, M. R., Sikkema, J., & De Bont, J. A. M. (1996). Influence of fructose and glucose on the production of exopolysaccharides and the activities of enzymes involved in the sugar metabolism and the synthesis of sugar nucleotides in *Lactobacillus delbrueckii* subsp. *bulgaricus* NCFB 2772. *Applied Microbiology & Biotechnology, 46*(3), 279-284.

Grobben, G. J., van Casteren, W. H. M., Schols, H. A., Oosterveld, A., Sala, G., Smith, M. R., et al. (1997). Analysis of the exopolysaccharides produced by *Lactobacillus delbrueckii* subsp. *bulgaricus* NCFB 2772 grown in continuous culture on glucose and fructose. *Applied Microbiology & Biotechnology, 48*(4), 516-521.

Gruter, M., Leeflang, B. R., Kuiper, J., Kamerling, J. P., & Vliegenthart, J. F. G. (1993). Structural characterisation of the exopolysaccharide produced by *Lactobacillus delbrueckii* ssp. *bulgaricus RR* grown in skimmed milk. *Carbohydrate Research, 239*(0), 209-226.

Gunning, A. P., & Morris, V. J. (1990). Light-scattering studies of tetramethyl ammonium gellan. *International Journal of Biological Macromolecules, 12*(6), 338-341.

Handley, P. S., Hargreaves, J., & Harty, D. W. S. (1988). Ruthenium red staining reveals surface fibrils and a layer external to the cell wall in *Streptococcus salivarius* HB and adhesion deficient mutants. *Journal of General Microbiology, 134*(12), 3165-3172.

Hanselmann, R., Burchard, W., Lemmes, R., & Schwengers, D. (1995). Characterization of DEAE-dextran by means of light scattering and combined size-exclusion chromatography/low-angle laser light scattering/viscometry. *Macromolecular Chemistry and Physics, 196*(7), 2259-2275.

Harding, S. E. (1995). Some recent developments in the analytical ultracentrifugation of food proteins. *Nahrung, 39*(5/6), 375-395.

Hassan, A. N., Frank, J. F., Farmer, M. A., Schmidt, K. A., & Shalabi, S. I. (1995a). Formation of yogurt microstructure and three-dimensional visualization as determined by confocal scanning laser microscopy. *Journal of Dairy Science, 78*(12), 2629-2636.

Hassan, A. N., Frank, J. F., Farmer, M. A., Schmidt, K. A., & Shalabi, S. I. (1995b). Observation of encapsulated lactic acid bacteria using confocal scanning laser microscopy. *Journal of Dairy Science, 78*(12), 2624-2628.

Hassan, A. N., Frank, J. F., & Qvist, K. B. (2002). Direct observation of bacterial exopolysaccharides in dairy products using confocal scanning laser microscopy. *Journal of Dairy Science, 85*(7), 1705-1708.

Haug, A., Larsen, B., & Smidsrod, O. (1967). Alkaline degradation of alginate. *Acta Chemica Scandinavica, 21*, 2859-2870.

Haugland, R. P. (1996). *Handbook of fluorescent probes and research chemicals.* (6th ed.). United States of America: Molecular Probes Inc.

Hebbar, K. P., Gueniot, B., Heyraud, A., Colin-Morel, P., Heulin, T., Blandreau, J., et al. (1992). Characterization of exopolysaccharides produced by rhizobacteria. *Applied Microbiology & Biotechnology, 38*, 248-253.

Hember, M. W. N., & Morris, E. R. (1995). Solubility, solution rheology and salt-induced gelation of welan polysaccharide in organic solvents. *Carbohydrate Polymers, 27*(1), 23-36.

Higashimura, M., Mulder-Bosman, B. W., Reich, R., Iwasaki, T., & Robijn, G. W. (2000). Solution properties of viilian, the exopolysaccharide from *Lactococcus lactis* subsp *cremoris* SBT 0495. *Biopolymers, 54*(2), 143-158.

Holzwarth, G., & Prestridge, E. B. (1977). Multistranded helix in xanthan polysaccharides. *Science, 197*, 757-759.

Hosono, M., Ishikawa, K., Mineki, R., Murayama, K., Numata, C., Ogawa, Y., et al. (1999). Tandem repeat structure of rhamnose-binding lectin from catfish (*Silurus asotus*) eggs. *Biochimica et Biophysica Acta, 1472*(3), 668-675.

Huglin, M. B. (1972). Specific refractive index increments. In M. B. Huglin (Ed.), *Light scattering from polymer solutions* (pp. 165-332). London: Academic Press.

Ioan, C. E., Aberle, T., & Burchard, W. (2001). Light scattering and viscosity behavior of dextran in semidilute solution. *Macromolecules, 34*(2), 326-336.

Jampen, S., Britt, I. J., & Tung, M. A. (2000). Gellan polymer solution properties: dilute and concentrated regimes. *Food Research International, 33*(7), 579-586.

Johnson, K., & Perry, M. B. (1976). Improved techniques for the preparation of bacterial lipopolysaccharides. *Canadian Journal of Microbiology, 22*, 29-34.

Kalab, M. (1979). Scanning electron microscopy of dairy products: an overview. *Scanning Electron Microscopy, 3*, 261-271.

Kalab, M. (1981). Electron microscopy of milk products: A review of techniques. *Scanning Electron Microscopy, 3*, 453-472.

Kalab, M., Allan-Wojtas, P., & Miller, S. S. (1995). Microscopy and other imaging techniques in food structure analysis. *Trends in Food Science & Technology, 6*(6), 177-186.

Kalab, M., Allan-Wojtas, P., & Phipps-Todd, B. E. (1983). Development of microstructure in set-style nonfat yoghurt - a review. *Food Microstructure, 2*, 51-65.

Kalab, M., & Harwalkar, V. R. (1973). Milk gel structure I. Application of scannomg electron microscopy to milk and other food gels. *Journal of Dairy Science, 56*(7), 835-842.

Kang, K. S., Veeder, G. T., & Cottrell, I. W. (1983). Some novel bacterial polysaccharides of recent development. *Progress in Industrial Microbiology, 18*, 231-253.

Karapanagiotis, N. K., Rudd, T., Sterritt, R. M., & Lester, J. N. (1989). Extraction and characterisation of extracellular polymers in digested sewage sludge. *Journal of Chemical Technology & Biotechnology, 44*, 107-120.

Kasaai, M. R., Charlet, G., & Arul, J. (2000). Master curve for concentration dependence of semi-dilute solution viscosity of chitosan homologues: the Martin equation. *Food Research International, 33*(1), 63-67.

Kavanagh, G. M., & Ross-Murphy, S. B. (1998). Rheological characterisation of polymer gels. *Progress in Polymer Science, 23*(3), 533-562.

Kimmel, S. A., & Roberts, R. F. (1998). Development of a growth medium suitable for exopolysaccharide production by *Lactobacillus delbrueckii* ssp. *bulgaricus* RR. *International Journal of Food Microbiology, 40*(1-2), 87-92.

Kimmel, S. A., Roberts, R. F., & Ziegler, G. R. (1998). Optimization of exopolysaccharide production by *Lactobacillus delbrueckii* subsp. *bulgaricus RR* grown in a semi-defined medium. *Applied & Environmental Microbiology, 64*(2), 659-664.

Kirby, A. R., Gunning, A. P., & Morris, V. J. (1995). Atomic force microscopy in food research: a new technique comes of age. *Trends in Food Science & Technology, 6*(11), 359-365.

Kirby, A. R., Gunning, P., Morris, V. J., & Ridout, M. J. (1995). Observation of the helical structure of the bacterial polysaccharide acetan by atomic force microscopy. *Biophysical Journal, 68*(1), 360-363.

Kojic, M., Vujcic, M., Banina, A., Cocconcelli, P., Cerning, J., & Topisirovic, L. (1992). Analysis of exopolysaccharide production by *Lactobacillus casei* CG11, isolated from cheese. *Applied & Environmental Microbiology, 58*(12), 4086-4088.

Lapasin, R., & Pricl, S. (1995). *Rheology of industrial polysaccharides: theory and applications.* Great Britain: Blackie Academic and Professional.

Launay, B. (1996). Rheological techniques. In G. Linden, L. translated by Dieter & J. W. editor for the English-language edition Hurst (Eds.), *Analytical techniques for foods and agricultural products* (pp. 195-227). United States of America: VCH Publishers, Inc.

Launay, B., Cuvelier, G., & Martinez-Reyes, S. (1997). Viscosity of locust bean, guar and xanthan gum solutions in the Newtonian domain: A critical examination of the log $[eta_{sp}]_o$-log C$[eta]_o$ master curves. *Carbohydrate Polymers, 34*(4), 385-395.

Launay, B., Doublier, J. L., & Cuvelier, G. (1986). Flow properties of aqueous solutionss and dispersions of polysaccharides. In J. R. Mitchell & D. A. Ledward (Eds.), *Functional properties of food macromolecules* (pp. 1-78). England: Elsievier Applied Science Publishers.

Launay, B., & Pasquet, E. (1982). Sucrose solutions with and without guar gum: rheological properties and relative sweetness intensity. In O. G. Philips, D. J. Wedlock & P. A. Williams (Eds.), *Gums and stabilisers for the food industry. Interactions of hydrocolloids.* (Vol. 6, pp. 247-258). Oxford: Pergamon Press.

Lemoine, J., Chirat, F., Wieruszeski, J.-M., Strecker, G., Favre, N., & Neeser, J.-R. (1997). Structural characterization of the exocellular polysaccharides produced by *Streptococcus thermophilus* SFi39 and SFi12. *Applied & Environmental Microbiology, 63*(9), 3512-3518.

Lim, T., Uhl, J. T., & Prudhomme, R. K. (1984). Rheology of self-associating concentrated xanthan solutions. *Journal of Rheology, 28*(4), 367-379.

Looijesteijn, P. J., & Hugenholtz, J. (1999). Uncoupling of growth and exopolysaccharide production by *Lactococcus lactis* subsp *cremoris* NIZO B40 and optimization of its synthesis. *Journal of Bioscience & Bioengineering, 88*(2), 178-182.

Looijesteijn, P. J., Trapet, L., De Vries, E., Abee, T., & Hugenholtz, J. (2001). Physiological function of exopolysaccharides produced by *Lactococcus Lactis. International Journal of Food Microbiology, 64*(1-2), 71-80.

Looijesteijn, P. J., van Casteren, W. H. M., Tuinier, R., Doeswijk-Voragen, C. H. L., & Hugenholtz, J. (2000). Influence of different substrate limitations on the yield, composition and molecular mass of exopolysaccharides produced by *Lactococcus lactis* subsp *cremoris* in continuous cultures. *Journal of Applied Microbiology, 89*, 116-122.

Lopes, L., Milas, M., & Rinaudo, M. (1994). Influence of the method of purification on some solution properties of welan gum. *International Journal of Biological Macromolecules, 16*(5), 253-258.

Low, D., Ahlgren, J. A., Horne, D., McMahon, D. J., Oberg, C. J., & Broadbent, J. R. (1998). Role of *Streptococcus thermophilus* MR-1C capsular exopolysaccharide in cheese moisture retention. *Applied & Environmental Microbiology, 64*(6), 2147-2151.

Ludbrook, K. A., Russell, C. M., & Greig, R. I. (1997). Exopolysaccharide production from lactic acid bacteria isolated from fermented foods. *Journal of Food Science, 62*(3), 597-600.

Luft, J. H. (1964). Electron microscopy of cell extraneous coats as revealed by rthenium red staining. *Journal of cell biology, 23*, 54A-55A.

Luft, J. H. (1971). Ruthenium red and ruthenium violet. I. Chemistry, purification, methods of use for electron microscopy and mechanism of action. *Anatomical Record, 171*, 347-368.

Maezawa, S., & Takagi, T. (1983). Monitoring of the elution from a high-performance gel chromatography column by a spectrophotometer, a low-angle laser light scattering photometer and a precision differential refractometer as a versatile way to determine protein molecular weight. *Journal of chromatography, 280*, 124-130.

Manca de Nadra, M. C., Strasser de Saad, A. M., Pesce de Ruiz Holgado, A. A., & Oliver, G. (1985). Extracellular polysaccharide production by *Lactobacillus bulgaricus* CRI-420. *Milchwissenschaft, 40*(7), 409-411.

Maneval, W. E. (1941). Staining bacteria and yeasts with acid dyes. *Stain Technology, 16*, 16-19.

Marshall, V. M., Cowie, E. N., & Moreton, R. S. (1995). Analysis and production of two exopolysaccharides from *Lactococcus lactis* subsp *cremoris* LC330. *Journal of Dairy Research, 62*(4), 621-628.

Martensson, O., Duenas-Chasco, M., Irastorza, A., Holst, O., Rudling, M., Norin, E., et al. (2002). Effects of fermented, ropy, non-dairy, oat-based products on serum lipids and the faecal excretion of cholesterol and short chain fatty acids in germfree and conventional rats. *Nutrition Research, 22*(12), 1461-1473.

McCurdy, R. D., Goff, H. D., Stanley, D. W., & Stone, A. P. (1994). Rheological properties of dextran related to food applications. *Food Hydrocolloids, 8*(6), 609-623.

Milas, M., Shi, X., & Rinaudo, M. (1990). On the physicochemical properties of gellan gum. *Biopolymers, 30*(3-4), 451-464.

Mitchell, J. R. (1979). Rheology of polysaccharide solutions and gels. In J. M. V. M. Blanshard, J.R. (Ed.), *Polysaccharides in food* (pp. 51-72). London: Butterworth.

Miyoshi, E., Takaya, T., & Nishinari, K. (1994). Gel-sol transition in gellan gum solutions. I. Rheological studies on the effects of salts. *Food Hydrocolloids, 8*(6), 505-527.

Miyoshi, E., Takaya, T., & Nishinari, K. (1995). Gel-sol transition in gellan aqueous solutions. *Macromolecular Symposia, 99*, 83-91.

Monsan, P., Bozonnet, S., Albenne, C., Joucla, G., Willemot, R. M., & Remaud-Simeon, M. (2001). Homopolysaccharides from lactic acid bacteria. *International Dairy Journal, 11*(9), 675-685.

Morris, E. R. (1986). Molecular origin of hydrocolloid functionality. In G. O. Phillips, D. J. Wedlock & P. A. Williams (Eds.), *Gums and stabilisers for the food industry 3* (pp. 3-16). Great Britain: Elsevier Applied Science Publishers Ltd.

Morris, E. R. (1989). Polysaccharide solution properties: origin, rheological characterization and implications for food systems. In R. P. Millane, J. N. BeMiller & R. Chandrasekaran (Eds.), *Frontiers in carbohydrate research, 1 : Food applications.* (pp. 132-163). London: Elsevier Applied Science.

Morris, E. R. (1990). Shear-thinning of random coil polysaccharides characterization by two parameters from a simple linear plot. *Carbohydrate Polymers, 13*(1), 85-96.

Morris, E. R. (1995). Polysaccharide rheology and in-mouth perception. In A. M. Stephen (Ed.), *Food polysaccharides and their applications* (pp. 517-546). New York: Marcel Dekker, Inc.

Morris, E. R., Cutler, A. N., Ross-Murphy, S. B., & Rees, D. A. (1981). Concentration and shear rate dependence of viscosity in random coil polysaccharide solutions. *Carbohydrate Polymers, 1*, 5-21.

Morris, E. R., Gothard, M. G. E., Hember, M. W. N., Manning, C. E., & Robinson, G. (1996). Conformational and rheological transitions of welan, rhamsan and acylated gellan. *Carbohydrate Polymers, 30*(2-3), 165-175.

Morris, E. R., Richardson, R. K., & Whittaker, L. E. (1999). Rheology and gelation of deacylated gellan polysaccharide with Na^+ as the sole counterion. *Progress in Colloid & Polymer Science, 114*, 109-115.

Morris, E. R., & Ross Murphy, S. B. (1981). Chain flexibility of polysaccharides and glycoproteins from viscosity measurements. *Techniques in Carbohydrate Metabolism, B310*, 1-46.

Morris, V. J., Gunning, A. P., Kirby, A. R., Round, A., Waldron, K., & Ng, A. (1997). Atomic force microscopy of plant cell walls, plant cell wall polysaccharides and gels. *International Journal of Biological Macromolecules, 21*(1-2), 61-66.

Mozzi, F., Graciela de Giori , S., Oliver, G., & Graciela de Valdez , F. (1996). Exopolysaccharide production by *Lactobacillus casei* under controlled pH. *Biotechnology Letters, 18*(4), 435-439.

Nakajima, H., Suzuki, Y., Kaizu, H., & Hirota, T. (1992). Cholesterol lowering activity of ropy fermented milk. *Journal of Food Science, 57*(6), 1327-1329.

Nakajima, H., Toyoda, S., Toba, T., Itoh, T., Mukai, T., Kitazawa, H., et al. (1990). A novel phosphopolysaccharide from slime-forming *lactococcus lactis* ssp *cremoris* SBT 0495. *Journal of Dairy Science, 73*(6), 1472-1477.

Nakamura, K., Harada, K., & Tanaka, Y. (1993). Viscoelastic properties of aqueous gellan solutions: the effects of concentration on gelation. *Food Hydrocolloids, 7*(5), 435-447.

Navarini, L., Abatangelo, A., Bertocchi, C., Conti, E., Bosco, M., & Picotti, F. (2001). Isolation and characterization of the exopolysaccharide produced by *Streptococcus thermophilus* SFi20. *International Journal of Biological Macromolecules, 28*(3), 219-226.

Navarini, L., Cesaro, A., & Ross-Murphy, S. B. (1992). Polysaccharides from cyanobacteria. 6. Viscoelastic properties of aqueous solutions of an exocellular polysaccharide from cyanobacteria. *Carbohydrate Polymers, 18*(4), 265-272.

Newlin, T. E., Lovell, S. E., Saunders, P. R., & Ferry, J. D. (1962). Mechanical properties of substances of high molecular weight. XXXVI. Long range intermolecular coupling in concentrated poly(butyl-methacrylate) solutions and its dependence on temperature and concentration. *Journal of Colloid Science, 17*, 10-25.

Nielsen, P. H., & Jahn, A. (1999). Extraction of EPS. In J. Wingender, T. R. Neu & H. C. Flemming (Eds.), *Microbial extracellular polymeric substances : Characterization, structure and function* (pp. 49-72). Verlag Berlin Heidelberg New York: Springer.

Nomura, H., Koda, S., & Hattori, F. (1990). Viscosity of aqueous solutions of polysaccharides and their carboxylate derivatives. *Journal of Applied Polymer Science, 41*(11-12), 2959-2969.

Oda, M., Hasegawa, H., Komatsu, S., Kambe, M., & Tsuchiya, F. (1983). Anti-tumor polysaccharide from *Lactobacillus* Sp. *Agricultural and Biological Chemistry, 47*(7), 1623-1625.

Ogawa, E. (1993). Osmotic pressure measurements for gellan gum aqueous solutions. *Food Hydrocolloids, 7*(5), 397-405.

Ogawa, E. (1996). Conformational transition of polysaccharide sodium-gellan gum in aqueous solutions. *Macromolecules, 29*(15), 5178-5182.

Ohshima, A., Kudo, H., Sato, T., & Teramoto, A. (1995). Entanglement effects in semiflexible polymer solutions .1. Zero-shear viscosity of poly(N-Hexyl Isocyanate) solutions. *Macromolecules, 28*(18), 6095-6099.

Okamoto, T., Kubota, K., & Kuwahara, N. (1993). Light scattering study of gellan gum. *Food Hydrocolloids, 7*(5), 363-371.

Ota, F., & Fukui, K. (1982). Scanning electron microscopy studies of the extracellular polysaccharides (EP) synthesized of EP and the effect of dextranase on them. *Microbiology Immunology, 26*(7), 623-628.

Overdahl, B. J., & Zottola, E. A. (1991). Relationship between bile tolerance and the presence of a ruthenium red staining layer on strains of *Lactobacillus acidophilus*. *Journal of Dairy Science, 74*(4), 1196-1200.

Pal, R. (1995). Oscillatory, creep and steady flow behavior of xanthan - thickened oil-in-water emulsions. *Aiche Journal, 41*(4), 783-794.

Pals, D. T., & Hermans, J. J. (1952). Sodium salts of pectin and of carboxymethylcellulose in aqueous sodium chloride. I. Viscosities. *Recueil des Travaux Chimiques des Pays-Bas et de la Belgique, 71*, 433-457.

Pelletier, E., Viebke, C., Meadows, J., & Williams, P. A. (2001). A rheological study of the order-disorder conformational transition of xanthan gum. *Biopolymers, 59*(5), 339-346.

Petry, S., Furlan, S., Crepeau, M., Cerning, J., & Desmazeaud, M. (2000). Factors affecting exocellular polysaccharide production by *Lactobacillus delbrueckii* subsp *bulgaricus* grown in a chemically defined medium. *Applied & Environmental Microbiology, 66*(8), 3427-3431.

Pidoux, M., Marshall, V. M., Zanoni, P., & Brooker, B. (1990). *Lactobacilli* isolated sugary kefir grains capable of polysaccharide production and minicell formation. *Journal of Applied Bacteriology, 69*(3), 311-320.

Podzimek, S. (1994). The use of GPC coupled with a multiangle laser-light scattering photometer for the characterization of polymers - on the determination of molecular-weight, size, and branching. *Journal of Applied Polymer Science, 54*(1), 91-103.

Racine, M., Dumont, J., Champagne, C. P., & Morin, A. (1991). Production and characterization of the polysaccharide from *Propionibacterium acidi propionici* on whey-based media. *Journal of Applied Bacteriology, 71*(3), 233-238.

Renardy, M. (1997). Qualitative correlation between viscometric and linear viscoelastic functions. *Journal of Non-Newtonian Fluid Mechanics, 68*(1), 133-135.

Ricciardi, A., Parente, E., Aquino, M., & Clementi, F. (1998). Use of desalting gel for the rapid separation of simple sugars from exopolysaccharides produced by lactic acid bacteria. *Biotechnology Techniques, 12*(9), 649-652.

Ricciardi, A., Parente, E., Crudele, M. A., Zanetti, F., Scolari, G., & Mannazzu, I. (2002). Exopolysaccharide production by *Streptococcus thermophilus* Sy: Production and preliminary characterization of the polymer. *Journal of Applied Microbiology, 92*(2), 297-306.

Richardson, R. K., Morris, E. R., Ross-Murphy, S. B., Taylor, L. J., & Dea, I. C. M. (1989). Characterization of the perceived texture of thickened systems by dynamic viscosity measurements. *Food Hydrocolloids, 3*(3), 175-192.

Richardson, R. K., & Ross-Murphy, S. B. (1987). Nonlinear viscoelasticity of polysaccharide solutions .1. Guar galactomannan solutions. *International Journal of Biological Macromolecules, 9*(5), 250-256.

Rinaudo, M., & Mils, M. (1978). Polyelectroyte behavior of a bacterial polysaccharide from *Xanthomonas campestris:* Comparison with carboxymethylcellulose. *Biopolymers, 17*(11), 2663-2678.

Roa, M. A. (1999). Measurement of flow and viscoelastic properties. In *Rheology of fluid and semisolid foods. Principles and applications* (pp. 59-151). United States of America: Aspen Publication, Inc.

Roberts, I. S. (1995). Bacterial polysaccharides in sickness and in health. *Microbiology, 141*(9), 2023-2031.

Robijn, G. W., Gutierrez, G. R., van den Berg, D. J. C., Haas, H., Kamerling, J. P., & Vliegenthart, J. F. G. (1996). Structural characterization of the exopolysaccharide produced by *Lactobacillus acidophilus* LMG9433. *Carbohydrate Research, 288*, 203-218.

Robijn, G. W., Imberty, A., van den Berg, D. J. C., Ledeboer, A. M., Kamerling, J. P., Vliegenthart, J. F. G., et al. (1996). Predicting helical structures of the exopolysaccharide produced by *Lactobacillus sake* 0-1. *Carbohydrate Research, 288*, 57-74.

Robinson, G., Manning, C. E., & Morris, E. R. (1991). Conformation and physical properties of the bacterial polysaccharides gellan, welan, and rhamsan. In E. Dickinson (Ed.), *Food polymers, gels and colloids.* (Vol. 82, pp. 22-33). Great Britain: Royal Society of Chemistry.

Robinson, G., Ross-Murphy, S. B., & Morris, E. R. (1982). Viscosity-molecular weight relationships, intrinsic chain flexibility and dynamic solution properties of guar galactomannan. *Carbohydrate Research, 107*(1), 17-32.

Rochefort, W. E., & Middleman, S. (1987). Rheology of xanthan gum - salt, temperature, and strain effects in oscillatory and steady shear experiments. *Journal of Rheology, 31*(4), 337-369.

Ross-Murphy, S. B. (1984). Rheological methods. In H. W. S. Chan (Ed.), *Biophysical methods in food research. Critical reports on applied chemistry vol 5* (pp. 138-199). Oxford: Blackwell Scientific Publication.

Ross-Murphy, S. B. (1992). Physical gelation of biopolymers. *ACS Symposium Series, 489*, 204-216.

Ross-Murphy, S. B. (1994). Rheological methods. In S. B. Ross-Murphy (Ed.), *Physical techniques for the study of food biopolymers* (pp. 343-392). United Kingdom: Chapman & Hall.

Ross-Murphy, S. B. (1995). Rheology of biopolymer solutions and gels. In E. Dickinson (Ed.), *New physico-chemical techniques for the characterization of complex food systems* (pp. 139-156). United Kingdom: Blackie Academic & Professional.

Ross-Murphy, S. B., Morris, V. J., & Morris, E. R. (1983). Molecular viscoelasticity of xanthan polysaccharide. *Faraday Symposia of the Chemical Society*(18), 115-129.

Rouse, P. E. (1953). A theory of the linear properties of dilute solutions of coiling polymers. *Journal of Chemical Physics, 21(7)*(1272-1280).

Ruas-Madiedo, P., Hugenholtz, J., & Zoon, P. (2002). An Overview of the functionality of exopolysaccharides produced by lactic acid bacteria. *International Dairy Journal, 12*(2-3), 163-171.

Ruas-Madiedo, P., Tuinier, R., Kanning, M., & Zoon, P. (2002). Role of exopolysaccharides produced by *Lactococcus lactis* subsp *cremoris* on the viscosity of fermented milks. *International Dairy Journal, 12*(8), 689-695.

Rudin, A. (1982a). Basic principles of polymer molecular weights. In *The elements of polymer science and engineering. An introductory text for engineers and chemists* (pp. 41-73). United States of America: Academic Press.

Rudin, A. (1982b). Practical aspects of molecular weight measurements. In *The elements of polymer science and engineering. An introductory text for engineers and chemists* (pp. 74-121). United States of America: Academic Press.

Sabatie, J., Choplin, L., Doublier, J. L., Arul, J., Paul, F., & Monsan, P. (1988). Rheology of native dextrans in relation to their primary structure. *Carbohydrate Polymers, 9*(4), 287-299.

Schellhaass, S. M., & Morris, H. A. (1985). Rheological and scanning electron microscopic examination of skim milk gels obtained by fermenting with ropy and non-ropy strains of lactic-acid bacteria. *Food Microstructure, 4*(2), 279-288.

Shatwell, K. P., Sutherland, I. W., & Ross-Murphy, S. B. (1990). Influence of acetyl and pyruvate substituents on the solution properties of xanthan polysaccharide. *International journal of biological macromolecules, 12*(2), 71-78.

Shimazaki, T., & Ogino, K. (1993). Viscoelastic properties of gellan gum aqueous solutions. *Food Hydrocolloids, 7*(5), 417-426.

Shortt, D. W. (1993). Differential molecular-weight distributions in high-performance size-exclusion chromatography. *Journal of Liquid Chromatography, 16*(16), 3371-3391.

Sidebotham, R. L. (1974). Dextrans. *Advances in Carbohydrate Chemistry & Biochemistry., 30*, 371-444.

Sikkema, J. , & Oba, T. (1998). Extracellular polysaccharides of lactic acid bacteria. *Snow Brand R&D Reports*(No. 107), 1-31.

Skriver, A., Buchheim, W., & Qvist, K. B. (1995). Electron microscopy of stirred yoghurt: Ability of three techniques to visualize exo-polysaccharides from ropy strains. *Milchwissenschaft, 50*(12), 683-686.

Smidsrod, O. (1970). Solution properties of alginate. *Carbohydrate Research, 13*, 359-372.

Smidsrod, O., & Haug, A. (1971). Estimatin of the relative stiffness of the molecular chain in polyelectrolytes from measurements of viscosity at different ionic strengths. *Biopolymers, 10*, 1213-1227.

Smidsroed, O., Andresen, I. L., Grasdalen, H., Larsen, B., & Painter, T. (1980). Evidence for a salt-promoted \"freeze-out\" of linkage conformations in carrageenans as a pre-requisite for gel-formation. *Carbohydrate Research, 80*(1), C11-C16.

Smith, I. H., & Pace, G. W. (1982). Recovery of microbial polysaccharides. *Journal of Chemical Technology & Biotechnology, 32*(1), 119-129.

Souw, P., & Demain, A. L. (1979). Nutritional studies on xanthan production by *Xanthomonas campestris* NRRL B1459. *Applied & Environmental Microbiology, 37*(6), 1186-1192.

Spurlin, H. M., Martin, A. F., & Tennent, H. G. (1946). Characterization of cellulose derivatives by solution properties: Plasticizers as solvents. *Journal of Polymer Science, 1*, 63-74.

Stingele, F., Vincent, S. J. F., Faber, E. J., Newell, J. W., Kamerling, J. P., & Neeser, J. R. (1999). Introduction of the exopolysaccharide gene cluster from *Streptococcus thermophilus* Sfi6 into *Lactococcus lactis* MG1363: production and characterization of an altered polysaccharide. *Molecular Microbiology, 32*(6), 1287-1295.

Sun, S. F. (1994). Chain configurations. In *Physical chemistry of macromolecules. Basic principles and issues* (pp. 98-128). United States of America: John Wiley & Sons, Inc.

Sutherland, I. W. (2001). Microbial polysaccharides from gram-negative bacteria. *International Dairy Journal, 11*(9), 663-674.

Takagi, T. (1990). Application of low-angle laser light scattering detection in the field of biochemistry. *Journal of chromatography, 506*, 409-416.

Takahashi, R., Akutu, M., Kubota, K., & Nakamura, K. (1999). Characterization of gellan gum in aqueous NaCl solution. *Progress in Colloid & Polymer Science, 114*, 1-7.

Theisen, A., Johann, C., Deacon, M. P., & Harding, S. E. (2000). *Refractive increment data-book for polymer and biomolecular scientists.* United Kingdom: Nottingham University Press.

Tieking, M., Korakli, M., Ehrmann, M. A., Ganzle, M. G., & Vogel, R. F. (2003). In situ production of exopolysaccharides during sourdough fermentation by cereal and intestinal isolates of lactic acid bacteria. *Applied and Environmental Microbiology, 69*(2), 945-952.

Tinland, B., & Rinaudo, M. (1989). Dependence of the stiffness of the xanthan chain on the external salt concentration. *Macromolecules, 22*(4), 1863-1865.

Tirtaatmadja, V., Dunstan, D. E., & Roger, D. V. (2001). Rheology of dextran solutions. *Journal of Non-Newtonian Fluid Mechanics, 97*(2-3), 295-301.

Toba, T., Nakajima, H., Tobitani, A., & Adachi, S. (1990). Scanning electron microscopic and texture studies on characteristic consistency of nordic ropy sour milk. *International Journal of Food Microbiology, 11*(3-4), 313-320.

Toba, T., Uemura, H., & Itoh, T. (1992). A new method for the quantitative determination of microbial extracellular polysaccharide production using a disposable ultrafilter membrane unit. *Letters in Applied Microbiology, 14*(2), 30-32.

Tobitani, A., & Ross Murphy, S. B. (1997). The intrinsic viscosity of polyelectrolytes revisited. *Polymer International, 44*(3), 338-347.

Torino, M. I., Taranto, M. P., & De Valdez, G. F. (2001). Mixed-acid fermentation and polysaccharide production by *Lactobacillus helveticus* in milk cultures. *Biotechnology Letters, 23*(21), 1799-1802.

Troch, P., Philip-Hollingworth, S., Orgambide, G., Dazzo, F. B., & Vanderleyden, J. (1992). Analysis of extracellular polysaccharides isolated from *Azospirillum brasilense* wild type and mutant strains. *Symbiosis, 13*, 229-241.

Tuinier, R., Zoon, P., Olieman, C., Stuart, M. A. C., Fleer, G. J., & De Kruif, C. G. (1999). Isolation and physical characterization of an exocellular polysaccharide. *Biopolymers, 49*(1), 1-9.

Tuinier, R., Zoon, P., Stuart, M. A. C., Fleer, G. J., & De Kruif, C. G. (1999). Concentration and shear-rate dependence of the viscosity of an exocellular polysaccharide. *Biopolymers, 50*(6), 641-646.

Uemura, J., Itoh, T., Kaneko, T., & Noda, K. (1998). Chemical characterization of exocellular polysaccharide from *Lactobacillus delbrueckii* subsp. *bulgaricus* OLL1073R-1. *Milchwissenschaft, 53*(8), 443-446.

Urashima, T., Ariga, H., Saito, T., Nakamura, T., Tanaka, S., & Arai, I. (1999). Exocellular polysaccharide produced by *Streptococcus thermophilus*. *Milchwissenschaft, 54*(4), 190-193.

van Calsteren, M. R., Pau-Roblot, C., Begin, A., & Roy, D. (2002). Structure determination of the exopolysaccharide produced by *Lactobacillus rhamnosus* strains RW-9595M and R. *Biochemical Journal, 363*, 7-17.

van Casteren, W. H. M., Dijkema, C., Schols, H. A., Beldman, G., & Voragen, A. G. J. (1998). Characterisation and modification of the exopolysaccharide produced by *Lactococcus lactis subsp. cremoris* B40. *Carbohydrate Polymers, 37*(2), 123-130.

van den Berg, D. J. C., Robijn, G. W., Janssen, A. C., Giuseppin, M. L. F., Vreeker, R., Kamerling, J. P., et al. (1995). Production of a novel extracellular polysaccharide by *Lactobacillus sake* O-1 and characterization of the polysaccharide. *Applied & Environmental Microbiology, 61*(8), 2840-2844.

van den Berg, D. J. C., Smits, A., Pot, B., Ledeboer, A. M., Kersters, K., Verbakel, J. M. A., et al. (1993). Isolation, screening and identification of lactic acid bacteria from traditional food fermentation processes and culture collections. *Food Biotechnology, 7*(3), 189-205.

van Geel-Schutten, G. H., Flesch, F. , ten Brink, B., Smith, M., R. , & Dijkhuizen, L. (1998). Screening and characterization of Lactobacillus strains producing large amounts of exopolysaccharides. *Applied Microbiology & Biotechnology, 50*(6), 697-703.

Vanhaverbeke, C., Bosso, C., Colin-Morel, P., Gey, C., Gamar-Nourani, L., Blondeau, K., et al. (1998). Structure of an extracellular polysaccharide produced by *Lactobacillus rhamnosus* strain C83. *Carbohydrate Research, 314*(3-4), 211-220.

Vaningelgem, F., Zamfir, M., Adriany, T., & De Vuyst, L. (2004). Fermentation conditions affecting the bacterial growth and exopolysaccharide production by *Streptococcus thermophilus* ST 111 in milk-based medium. *Journal of Applied Microbiology, 97*(6), 1257-1273.

Walter, R. H., & Jacon, S. A. (1994). Molecular weight approximations of ionic polysaccharides by pH determinations. *Food Hydrocolloids, 8*(5), 469-480.

Weaver, R. W., & Zibilske, L. (1975). Affinity of cellular constituents of two bacteria for fluorescent brighteners. *Applied Microbiology, 29*(2), 287-292.

Welman, A. D., Maddox, I. S., & Archer, R. H. (2003). Screening and selection of exopolysaccharide-producing strains of *Lactobacillus delbrueckii* subsp *bulgaricus*. *Journal of Applied Microbiology, 95*(6), 1200-1206.

Wen, J., Arakawa, T., & Philo, J. S. (1996). Size-exclusion chromatography with online light-scattering, absorbance, and refractive index detectors for studying proteins and their interactions. *Analytical Biochemistry, 240*(2), 155-166.

Whistler, R. I. (1993). Chitin. In R. L. Whistler & J. N. BeMiller (Eds.), *Industrial gums: Polysaccharides & their derevitives* (pp. 601-604). San Diego: Academic Press, Inc.

Wyatt, P. J. (1993). Light scattering and the absolute characterization of macromolecules. *Analytica Chimica Acta, 272*(1), 1-40.

Yamakawa, H., & Yoshizaki, T. (1980). Transport coefficients of helical wormlike chains. 3. Intrinsic viscosity. *Macromolecules, 13*, 633-643.

Yamamoto, Y., Murosaki, S., Yamauchi, R., Kato, K., & Sone, Y. (1994). Structural study on an exocellular polysaccharide produced by *Lactobacillus helveticus* TY1-2. *Carbohydrate Research, 261*(1), 67-78.

Yang, Z., Huttunen, E., Staaf, M., Widmalm, G., & Tenhu, H. (1999). Separation, purification and characterisation of extracellular polysaccharides produced by slime-forming *Lactococcus lactis* ssp. *cremoris* strains. *International Dairy Journal, 9*(9), 631-638.

Yiu, S. H. (1993). Food microscopy and the nutritional quality of cereal foods. *Food Structure, 12*, 123-133.

Yoo, S.H., & Jane, J.-l. (2002). Molecular weights and gyration radii of amylopectins determined by high-performance size-exclusion chromatography equipped with multi-angle laser-light scattering and refractive index detectors. *Carbohydrate Polymers, 49*(3), 307-314.

Yuguchi, Y., Urakawa, H., & Kajiwara, K. (1997). Structural characteristics of crosslinking domain in gellan gum gel. *Macromolecular Symposia, 120*, 77-89.

Zatz, J. L., & Knapp, S. (1984). Viscosity of xanthan gum solutions at low shear rates. *Journal of Pharmaceutical Sciences, 73*(4), 468-471.

Zayas, J. F. (1997). *Functionality of proteins in food.* Berlin Heidelberg New York.: Springer.

Zimm, B. H. (1948). Apparatus and methods for measurement and interpretation of the angular variations of light scattering; preliminary results on polystyrene solutions. *Journal of Chemical Physics, 16*(12), 1099-1116.

Zimm, B. H., Stein, R. S., & Doty, P. (1945). Classical theory of light scattering from solutions - a review. *Polymer Bulletine*, 90-119.

Appendix A

a. Light microscopy with Maneval stains

Two 'ropy' (2483 and 859) and two 'non-ropy' (1 and 30) strains of lactic acid bacteria were grown in 10% (w/w) milk medium for 24 hours at 37°C. The lactic acid bacteria strains used for the experiment are shown in Table A1.

Table A1 Lactic acid bacteria used the experiment

Strain	Remarks	Source
Lactobacillus delbrueckii subsp *bulgaricus* 2483	Ropy	NCIMB, UK
Streptococcus thermophilus 859	Ropy	NCIMB, UK
Streptococcus thermophilus 1	Non-Ropy (Control)	Fonterra Co-operative Ltd, New Zealand
Lactobacillus helveticus 30	Non-Ropy (Control)	

The staining solutions were prepared according to the method described by Corstvet *et al.* (1983). The preparation of the stains is shown in Table A2. A cell suspension was prepared in phosphate buffer at pH 7.2. Equal volumes of cell suspension and Stain I were mixed on a glass slide, spread to a thin film and allowed to air dry. It was counter-stained with Stain II for approximately 2mins, and then blotted dry with lint-free tissue paper.

Table A2 Composition of the Maneval capsule staining solutions

Solution	Components	Quantity
Stain I	1% (w/v) Congo red (Sigma)	20.0mL
Stain II	5% (w/w) aqueous phenol (Sigma) 20% (w/v) aqueous glacial acetic acid (Sigma) 30% (w/v) aqueous ferric chloride (BDH) 1% (w/v) aqueous acid fuchsin (BDH)	30.0mL 9.0mL 4.0mL 1.5mL
Phosphate buffer pH 7.2	36.0 ml of 0.2M Na_2HPO_4 (BDH) 14.0 ml 0.2M NaH_2PO_4 (BDH)	35.5nL

b. Probing EPS capsules using Maneval stains

Samples with bacteria 2483 and 859 were considered 'ropy' as the culture medium was seen adhering to the pipette tip during sample pipetting. On the other hand, the 'ropy' characteristic was not seen in the Control samples with cultures 1 and 30. With the Maneval staining method, specimens were examined under bright field light microscope at 1000x magnification under oil immersion. Capsules were seen in both the Samples 859 and 1 (*Streptococcus thermophilus*) but not in cultures 2483 and 30 (*Lactobacillus* species) after 24 hours of incubation period at 37°C in milk medium. Cells appeared red against a light blue background and the capsule appeared as a clear zone surrounding the cell. There was a subtle difference between culture 859 ('ropy') and culture 1 ('non-ropy'). The former appeared to have a thicker capsular layer compared to culture 1. Approximately 95% of bacterial cells in both cultures 859 and 1 showed the presence of capsules around the cell surfaces. The other 5% of the populations showed no capsular layer at all. A pictorial representation of the cultures in milk media with Maneval stains is shown in Figure A1.

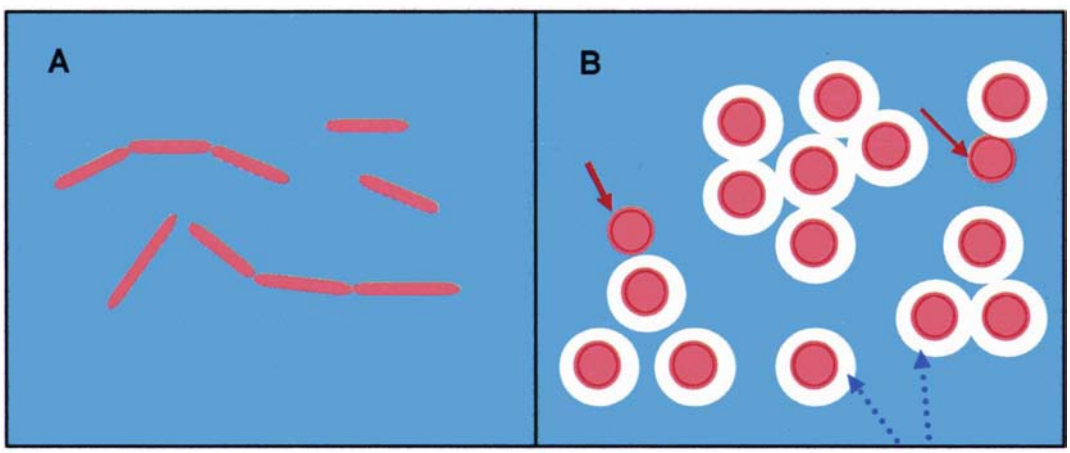

Figure A1 (A) represents cultures of 2483 and 30; (B) represents cultures of 859 and 1. The dotted arrows indicate the capsules surrounding the cells under light microscope while the filled arrows indicate cells without capsule.

It can be generally concluded that not all lactic acid bacteria that produced EPS with ropy characteristics had capsules or slim layers surrounding the cell surfaces. On the other hand, not all lactic acid bacteria with capsules or slime layers produced EPS with 'ropy' characteristics. These characteristics were independent of each other.

Appendix B

a. The *Acid Addition Method*

A sample of the fermented culture (10g) was transferred to a test tube and heated in boiling water for 10mins to inactivate the EPS degrading enzymes. The sample was cooled to room temperature and 100µL 5% (w/v) Pronase solution (EC 3.4.24.31, Sigma-Aldrich) was added followed by incubation at 37°C for 1h in a water bath shaker. The sample was mixed with 250µL of 80% (w/v) TCA (BDH), left for another 30mins at 4°C, and then centrifuged at 8000g for 20mins at 4°C (RC5C Sorvall centrifuge and SS-34 rotor, Kendro Laboratory Products GmbH, Langenselbold, Denmark) to remove the cells and proteins. The supernatant obtained (5mL) was transferred into a dialysis tubing of 6000-8000 Da molecular weight cut off (Biolab) and was dialysed for 48h in a 5L container filled with distilled water. Two changes of the distilled water were made everyday. The dialysed sample was analysed in duplicate for total carbohydrate using the phenol-sulphuric acid method. The amount of EPS was read against the glucose calibration curve. The processing steps for the *Acid Addition Method* shown in Figure B1 were carried out in duplicate.

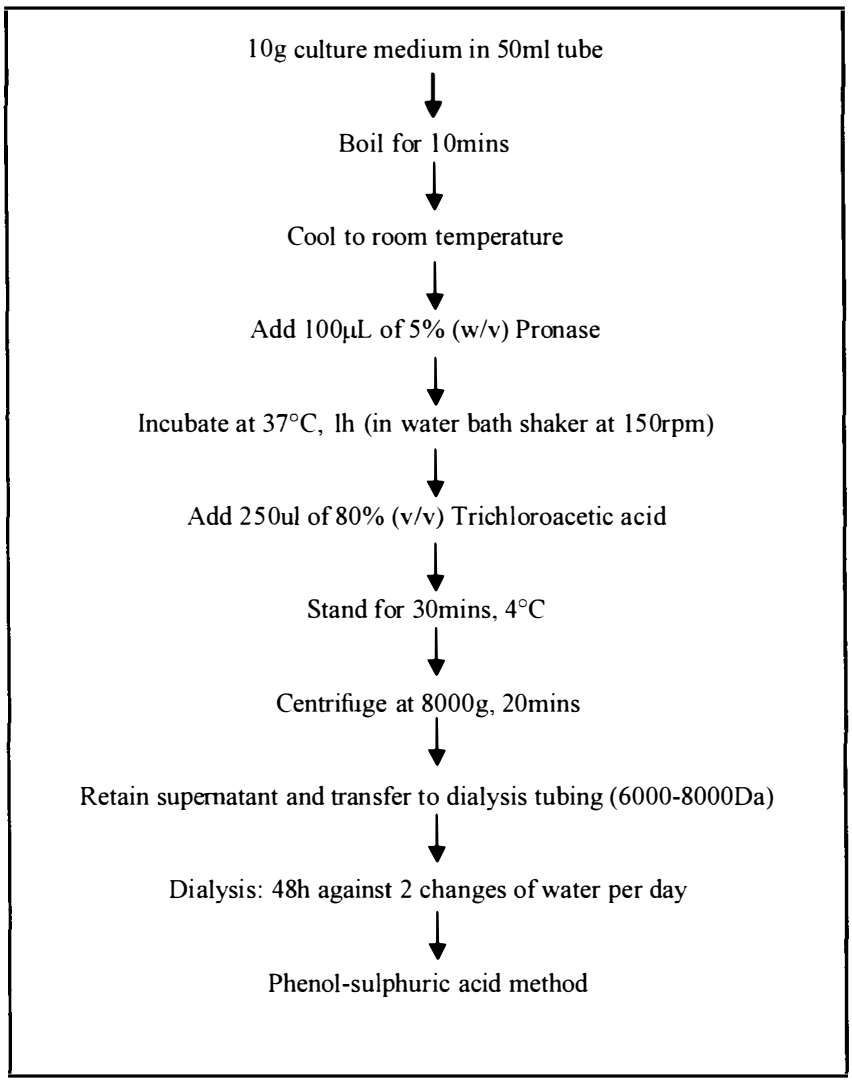

Figure B1 **The *Acid Addition Method* for EPS assay according to Kimmel, Roberts and Ziegler (1998).**

b. The *Ethanol Precipitation Method*

The *Ethanol Precipitation Method* adopted for this study had two additional steps compared to the method described by Cerning et al. (1994). This included a Pronase™ treatment step to digest the proteins and an additional 24h dialysis step. Another minor difference was that the dialysis tubing used for this investigation had a specification of 6,000-8,000 Da molecular weight cut off instead of 2,000-3,000 Da.

The culture medium (10g) was transferred to a test tube and heated in boiling water for 15mins to inactivate the EPS degrading enzymes. The sample was cooled to room temperature and 100µL 5% (w/v) Pronase™ solution was added followed by incubation at 37°C for 1h in a water bath shaker. The sample was centrifuged at 16,000g for 30mins at 4°C (RC5C Sorvall centrifuge and SS-34 rotor). The supernatant obtained was mixed with three volumes of chilled absolute ethanol (BDH) and left overnight at 4°C. The sample was then centrifuged at 12,000g for 20mins at 4°C. The pellet recovered was re-suspended in 10mL of distilled water. The re-suspended sample (5mL) was transferred into a dialysis tubing and dialysed against distilled water for 48h in a 5L container with continuous stirring at 4°C. The dialysis procedure included two changes of water everyday. The sample was analysed in duplicate for total carbohydrate using the phenol-sulphuric acid method. The amount of EPS was read against the glucose calibration curve. The processing steps for the *Ethanol Precipitation Method* shown in Figure B2 were carried out in duplicate.

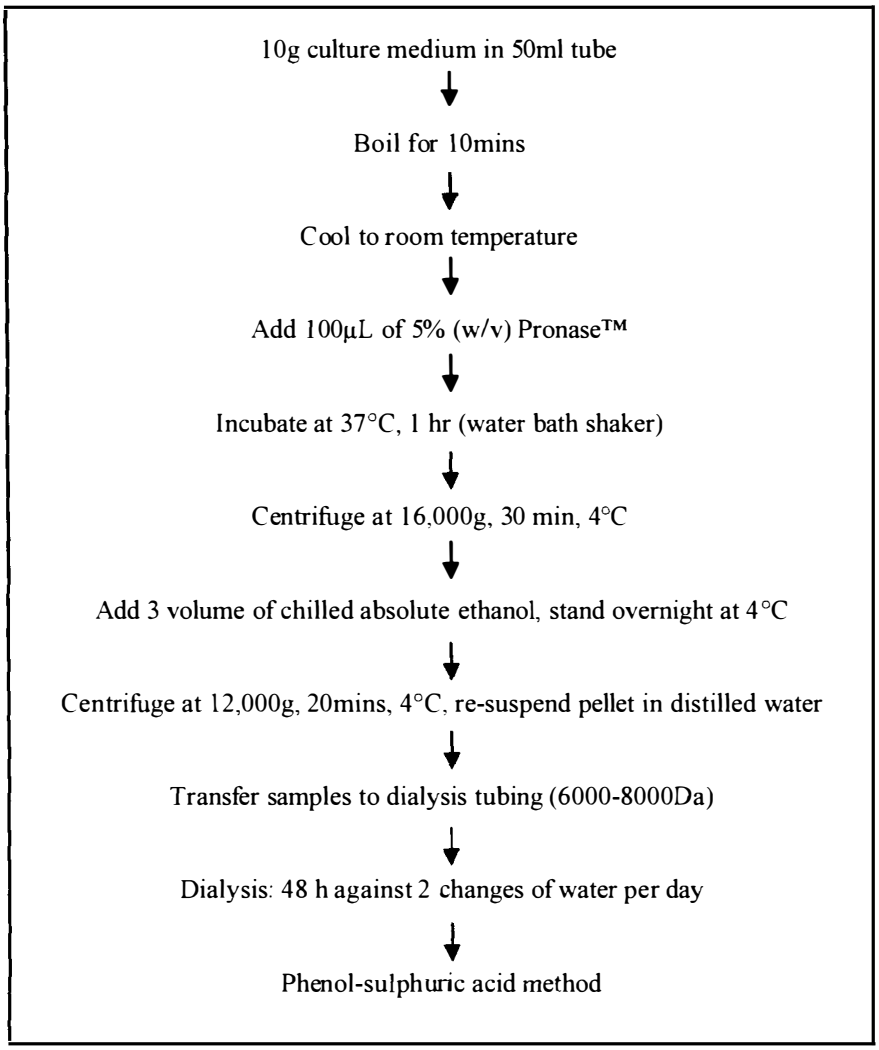

Figure B2 The *Ethanol Precipitation Method* for EPS assay adapted from Cerning *et al.*,(1994).

Appendix C

a. Sample preparation for transmission electron microscopy

A 5% (w/v) ruthenium red (Sigma) solution (20μL) was added to 50mL of culture medium. The sample was mixed with 3% (w/v) agarose solution at approximately 40°C to achieve a 1.5% (w/v) agarose concentration. The mixture was allowed to solidify at 4°C. The gel was then cut with a scalpel into tiny cubes of approximately $1 mm^3$.

b. Fixation, dehydration, polymerisation and sectioning

The sample cubes were fixed with 5mL of primary fixative for 1h. The primary fixative was made up of 3% (w/v) glutaraldehyde (Merck) and 0.1% (w/v) ruthenium red in 0.1M cacodylate buffer (pH 7.2). The samples were given two washes of cacodylate buffer at 15-min intervals. The buffer was replaced with a secondary fixative made of 1% (v/v) OsO_4 and 0.15% (v/v) ruthenium red in cacodylate buffer and the samples were left for 90min. The samples (which by then resembled pellets) were given another two washes of cacodylate buffer at 15-min intervals. After the fixation process, the pellets were dehydrated through a series of acetone solutions (25%, 50%, 75%, 95 and 100% v/v). Each dehydration step, except for the last step in which the pellets were placed in absolute acetone for 1h, lasted 15min. The dehydrated specimens were then immersed in a 1:1 mixture of absolute acetone and Procure 812 resin (ProSciTech, Queensland, Australia) and left overnight on a magnetic stirrer. The pellets were then transferred to a freshly prepared absolute resin and left for 8h to further infiltrate the specimen with the resin. Each pellet was finally transferred to a silicon rubber mould filled with fresh resin and allowed to polymerise at 60°C for 48h. Sections of ~90nm were cut using a diamond knife mounted on the Reichart-Jung Ultracut E Ultramicrotome. The sections were lifted onto copper grids. The grid-mounted sections were initially stained with saturated uranyl acetate (BDH) in 50% ethanol. This was followed by a lead citrate (BDH) stain prepared according to Venable and Coggeshall (1965). The samples were subsequently air dried and viewed using a Philips (Eindhoven, The Netherlands) 201C Transmission Electron Microscope.

Appendix D

a. Preparation of seed culture for the hydrolysed milk permeate-based medium

The growth medium for the seed culture was prepared using 10.0% (w/v) reconstituted SMP. It was first treated with 0.1% (w/v) Flavourzyme solution in a 50°C water bath with continuous agitation for 2 h. The medium was then centrifuged at 4,000*g* for 10mins to remove any insoluble material. The supernatant was filtered through a 0.45μm membrane filter (Millipore) and free-steamed for 10 min at 100°C. The 2483 culture, prepared in preservation beads, was inoculated in the medium (200mL). The fermentation of the seed culture was carried out at 37°C for 18 h and was ready to be inoculated (1% v/v) into the hydrolysed milk permeate medium.

b. Fermentation of 2483 in the hydrolysed Milk Permeate-based Culture Medium

Initial attempts to inoculate the hydrolysed milk permeate-based medium using 2483 bead inoculum did not result in any growth. Preparing a seed culture with an 'intermediate' growth medium was found to be an essential step. The hydrolysed milk medium used for the seed culture provided a bridging environment for the 2483 culture to adapt to the hydrolysed milk permeate-based medium. The reason for this has not been established although it could be attributed to the difference in the redox potential between the hydrolysed permeate-based medium and the milk medium (where the bead inoculum was prepared).

Another important aspect in ensuring good 2483 growth was that the hydrolysed milk permeate-based medium had a reduced oxygen level. Since 2483 grew best in a microaerophillic environment, the dissolved oxygen level was lowered by bubbling nitrogen through the medium for at least 15mins, prior to heat treatment.

A suitable heating regime for the hydrolysed permeate-based medium was 100°C for 10mins by free-steaming in an autoclave. Prolonging the holding time of heating (e.g. 15mins) or increasing the temperature (e.g. 121°C) resulted in a brownish coloured

medium due to Maillard reaction. The browning increased with an increase in time and/or temperature of heating, and had negative effects on the bacterial growth, hence, the levels of EPS produced. Other heat treatment methods, for example, high-temperature-short-time (HTST) using a plate-heat exchanger would be feasible for industrial scale operation and could provide a better environment for the growth of 2483.

Inoculation of the seed culture to the growth medium was carried out at room temperature. Although the use of the seed culture (1% v/v) as an inoculum would introduce some molecular species larger than 2.5 x 10^3 Da to the hydrolysed milk permeate-based medium, the amount was considered negligible. It was also observed that fermentation in a larger volume of growth medium, for example, in a 2L Duran bottle, the final pH of the culture broth reached pH of 3.9 and appeared more 'ropy' compared to a smaller volume of the same growth medium, for example, in a 200mL Duran bottle. This could be due to the reduced aerobic condition in the larger volume of ferment. During incubation, the bottle containing the culture medium was tightly capped to keep the environment microaerophilic. The culture medium was left without agitation throughout the incubation period. The average level of 2483 EPS obtained using this culture medium was approximately 400mg/L. The EPS level was lower than average EPS obtained in the unhydrolysed milk permeate-based medium containing SMP (~600mg/mL). However, the EPS levels were markedly higher than the milk permeate medium (~150mg/mL). Reported levels of EPS ranges from 50-550mg/L for *Streptococcus thermophilus* (Cerning *et al.*, 1988; Doco, Wieruszeski and Fournet, 1990 and de Vuyst *et al.*, 1998); 60-420mg/L for *Lactobacillus delbreuckii* subsp. *bulgaricus* (Cerning *et al*,., 1986; Toba, Uemura and Itoh, 1992; Garcia-Garibay and Marshall, 1991) and 30-600mg/L for *Lactococcus lactis* subsp. *cremoris* (Cerning *et al.*, 1992). Exceptionally high levels of EPS are rare but they have been reported for *Lactobacillus rhamnoses* ATCC 9595M (van Calsteren *et al.*, 2002) and *Lactobacillus sakei* 0-1 (Degeest, Janssens and de Vuyst, 2001) with EPS levels above 1000mg/L in both instances. Levels of EPS produced by some LAB are compiled in Table 5.3.

Appendix E

a. Procedures for elemental analysis of freeze-dried EPS using Carlo Erba Elemental Analyser EA 1108

The analytical method is based on the complete and instantaneous oxidation of the sample by "flash combustion" which converts all organic and inorganic substances into combustion products. The sample is held in a tin capsule and dropped into a vertical quartz tube, containing catalyst (tungstic oxide) and copper, which is maintained at a temperature of 102°C. The helium carrier gas is temporarily enriched with pure oxygen as the sample is dropped into the tube. The sample and its container melt and the tin promotes a violent reaction. Under these favourable conditions, even thermally resistant substances are completely oxidized. Quantitative combustion is then achieved by passing the mixture of gases over a catalyst layer, then through copper to remove excess oxygen and reduce nitrogen oxides to nitrogen. The resulting mixture is directed to the chromatographic column where the components (carbon dioxide, water, sulfur dioxide and nitrogen) are separated and detected by a thermal conductivity detector which gives an output signal proportional to the concentration of the individual components of the mixture. The information is fed into a work station and the percentages calculated using the weight of sample.

Note: The above procedures were obtained from Campbell Microanalytical Laboratory Chemistry Department, University of Otago, Dunedin, New Zealand

Appendix F

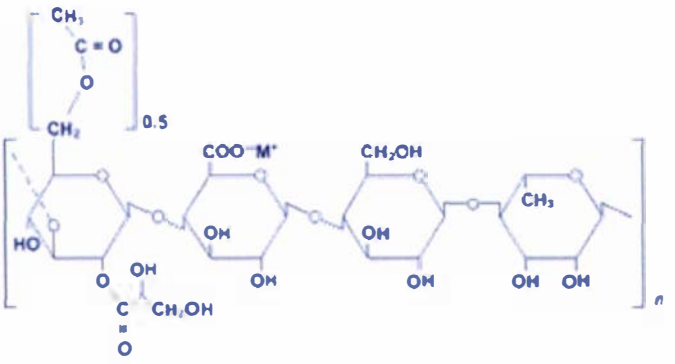

Figure F1 Structure of native or high acyl gellan (http://www.cpkelco.com, 20th January 2003).